

Variation in gout and urate-associated inflammation caused by genetics and epigenetic modifications Ildikó Orsolya Gaál

The work presented in this thesis received financial support from a Competitiveness Operational Programme grant of the Romanian Ministry of European Funds (P37 762, MySMIS 103587) and a grant of the Romanian Ministry of European Investments and Projects, PNRR-III-C9-2022-18, CF 85/15.11.2022.

The work presented in this thesis is performed at the Department of Medical Genetics, University Iuliu Hatieganu, Cluj-Napoca, Romania and the Radboud Institute for Molecular Life Sciences and the Department of Internal Medicine, Radboud University Center, Nijmegen, the Netherlands.

Variation in gout and urate-associated inflammation caused by genetics and epigenetic modifications

Ildikó Orsolya Gaál

Radboud Dissertation Series

ISSN: 2950-2772 (Online); 2950-2780 (Print)

Published by RADBOUD UNIVERSITY PRESS Postbus 9100, 6500 HA Nijmegen, The Netherlands www.radbouduniversitypress.nl

Design: Proefschrift AIO | Annelies Lips Cover: Proefschrift AIO | Guntra Laivacuma

Printing: DPN Rikken/Pumbo

ISBN: 9789465150567

DOI: 10.54195/9789465150567

Free download at: https://doi.org/10.54195/9789465150567

© 2025 Ildikó Orsolya Gaál

RADBOUD UNIVERSITY PRESS

This is an Open Access book published under the terms of Creative Commons Attribution-Noncommercial-NoDerivatives International license (CC BY-NC-ND 4.0). This license allows reusers to copy and distribute the material in any medium or format in unadapted form only, for noncommercial purposes only, and only so long as attribution is given to the creator, see http://creativecommons.org/licenses/by-nc-nd/4.0/.

Variation in gout and urate-associated inflammation caused by genetics and epigenetic modifications

Proefschrift ter verkrijging van de graad van doctor aan de Radboud Universiteit Nijmegen op gezag van de rector magnificus prof. dr. J.M. Sanders, volgens besluit van het college voor promoties

en

ter verkrijging van de graad van doctor aan de Universitatea de Medicină şi Farmacie "Iuliu Haţieganu" din Cluj-Napoca op gezag van de rector prof. dr. Anca Dana Buzoianu

> in het openbaar te verdedigen op dinsdag 25 maart 2025 om 14.30 uur precies

> > door

Ildikó Orsolya Gaál

geboren op 27 oktober 1992 te Zalău (Roemenië)

Promotoren:

Prof. dr. L.A.B. Joosten (Universitatea de Medicină și Farmacie "Iuliu Hațieganu" din Cluj-Napoca, Roemenië)

Prof. dr. M.G. Netea

Copromotor:

Dr. T.O. Crişan

Manuscriptcommissie:

Prof. dr. E.H.J. van den Bogaard Prof. dr. H.-.K. Ea (Université de Paris, Frankrijk) Dr. R. Duivenvoorden

Variation in gout and urate-associated inflammation caused by genetics and epigenetic modifications

Dissertation to obtain the degree of doctor from Radboud University Nijmegen on the authority of the Rector Magnificus prof. dr. J.M. Sanders, according to the decision of the Doctorate Board

and

to obtain the degree of doctor from Universitatea de Medicină și Farmacie "Iuliu Hațieganu" din Cluj-Napoca on the authority of the Rector prof. dr. Anca Dana Buzoianu

> to be defended in public on Tuesday, March 25, 2025 at 2.30 pm

> > by

Ildikó Orsolya Gaál

born on October 27, 1992 in Zalău (Romania)

PhD supervisors:

Prof. dr. L.A.B. Joosten (Universitatea de Medicină și Farmacie "Iuliu Hațieganu" din Cluj-Napoca, Romania)

Prof. dr. M.G. Netea

PhD co-supervisor:

Dr. T.O. Crişan

Manuscript Committee:

Prof. dr. E.H.J. van den Bogaard Prof. dr. H.-.K. Ea (Université de Paris, France) Dr. R. Duivenvoorden

To my parents, Ajánlom ezt a könyvet szüleimnek, Csabi és Gyöngyi

Table of contents

Chapter 1 General Introduction, aim and outline of the thesis	11
Chapter 2 Gout-associated SNP at the IL1RN-IL1F10 region is functionally linked to altered cytokine production in PBMCs of patients with gout and controls	31
Chapter 3 GWAS-identified hyperuricemia-associated IGF1R variant rs6598541 has a limited role in urate mediated inflammation in human mononuclear cells	57
Chapter 4 Interleukin 1 receptor type I variation in patients with gout and hyperuricemic individuals	77
Chapter 5 Hyperuricemia remodels the serum proteome toward a higher inflammatory state	93
Chapter 6 Urate – induced epigenetic modifications in myeloid cells	31
Chapter 7 Trained immunity and inflammation in rheumatic diseases	95
Chapter 8 Summary and general discussion	215
English Summary Research Data Management PhD portfolio List of publications Acknowledgements	2226 232 234 235 236 238



Chapter 1

General Introduction, aim and outline of the thesis

Gout and hyperuricemia – current status

Historical background

The history of gout can be traced back thousands of years and it has been documented since then. Gout was commonly known as the "disease of kings" or the "rich man's disease" due to its association with the consumption of foods and excessive alcohol which were primarily indulged in by the upper classes (1,2). The ancient Egyptians were among the civilizations to note down first the symptoms of gout as evident from texts dating back to 2600 BC.(2-5). Hippocrates, a physician widely regarded as the father of medicine also made noteworthy contributions to our understanding of gout. He described it as an ailment that predominantly affected men and recommended modifications and natural remedies to alleviate its symptoms(1). In the Middle Ages, it was widely prevalent among the European nobility, including preeminent figures such as King Henry VIII of England and Leonardo da Vinci(6).

Throughout history, a variety of factors, including diet, lifestyle, and genetics has been associated with gout (7). Scientific understanding of gout advanced in the 18th and 19th centuries. In 1797, the English physician Sir Alfred Baring Garrod identified uric acid as the vital cause of gout (3,8). His work established the foundation for the modern understanding of the disease. Although gout has been present throughout history, our understanding of the disease has significantly improved, allowing for better management and improved quality of life for individuals suffering from the disease. Alexander of Tralles, an Ancient Greek physician, was the first to advise the use of hermodactyl, this being derived from the plant Colchicum autumnale, the first long-lasting finding in the treatment of gout, in today's popular name, colchicine (2,9).

Also, over time, advances in medical research have provided further insights into the mechanisms of the disease and have led to the development of effective treatments and preventive measures. Today, gout is recognized as a chronic condition that requires long-term management (10). Moreover, lifestyle modifications, such as adopting a healthy diet low in purines, maintaining a healthy weight, limiting alcohol consumption, and staying hydrated, are recommended to help prevent gout attacks (11).

Hyperuricemia has a historical background closely related with the understanding and evolution of gout. The swedish chemist Carl Wilhelm Scheele, marked a pivotal moment in history being the first identifying uric acid in the urine (4). However, the link between high urate levels and health issues was not recognized from ancient times, as Alfred Garrod being the first scientist to prove the association between gout and elevated concentrations of uric acid (8). Moreover, the discovery of the enzyme xanthine oxidase, the one responsible for urate production, contributed to the understanding of the metabolic pathways involved (12). Normally, uric acid is dissolved in the blood then filtered by the kidneys and excreted in the urine (13). Hyperuricemia is diagnosed when the levels of serum urate are exceeding the approx. 6.8 mg/dl solubility limit, this resulting in the accumulation of serum in the kidneys and the joints (14). However, asymptomatic hyperuricemia often remains stable for many years without progressing.

Nowadays, research has expanded to explore the role of hyperuricemia beyond gout, being recognized as a key factor in other conditions as well, including cardiovascular diseases, kidney diseases and metabolic syndrome (15-17). Several clinical investigations have reported elevated serum urate levels as a predictive marker for cardiovascular outcomes (18). The mechanism which link hyperuricemia to cardiovascular events are represented by oxidative stress, inflammation and endothelial dysfunction (19).

Therefore, ongoing research continues to elucidate the complexities of hyperuricemia and its vast impact on health.

Epidemiology

Nowadays, gout, no longer is considered as a disease of the elite. The incidence of the disease has seen a rise prevalence and incidence in the last years, particularly in the older population and represents an important concern in terms of healthrelated quality of life (20,21). This increase is attributed to a series of risk factors, such as hyperuricemia, genetic factors, dietary habits, alcohol consumption, metabolic syndrome, hypertension, obesity, diuretic use, and chronic renal disease (20,21). Also, its prevalence can vary through different populations and it is influenced by factors such as age, sex, genetics and lifestyle (22,23). Gout is unusually common in indigenous Taiwanese and Polynesian people, including Māori (indigenous from New Zeeland), and Pacific people from Eastern and Western Polynesia, where the prevalence of gout is estimated at >8% of adults (22,24). Additionally, men are more likely to experience gout than women (25), as the prevalence of gout is uncommon in women before menopause (26). Moreover, women with gout are more likely to be presented together with comorbidities such as chronic kidney disease, hypertension and the use of diuretics (27). Thereafter, gout is a highly prevalent auto-inflammatory disease which affects cca. 4 % of the population within Europe (28) and 41 milion adults worldwide (29).

Clinical presentation

Gout is a common auto-inflammatory disease, caused by MSU crystal deposition and characterized by acute or chronic inflammation and damage to bone joints (30,31). Patients often describe it as a fiercely painful acute inflammatory arthritis (32). The progression of hyperuricemia and gout are believed to take place over four pathophysiological stages: onset of hyperuricemia, the deposition of MSU crystals, clinical presentation of gout flares due to the deposited MSU crystals and clinical presentation of advanced disease characterized by tophi (33).

Over the last few years, with the continuedresearch done on the field, more immune cells and inflammatory factors have been established as key factors in gouty inflammation. These studies has shown that neutrophil macrophages and T lymphocytes play significant roles in disease development, while releasing cytokines, such as IL-1\(\beta \), TNF, and IL-6 through the NLRP3 inflammasome pathway, activating an inflammatory cascade and the incidence of gout (23,34). Although, it is generally thought that hyperuricemia is the vital condition for gout, it is not sufficient for the development of clinically proven disease, as not everyone with elevated concentrations of serum urate will develop gout (35). Moreover, besides the high concentration of urate, low temperatures, physiological pH between 7 and 10, high concentrations of sodium ions and synovial and cartilage components are also necessary elements promoting monosodium urate cristallysation (36,37). Nevertheless, in deep-rooted gout and hyperuricemia, the MSU crystals may not be present only in the joint, but also in tophi, causing restriction to joint movements and joint deformity (10). Observational studies regarding joints of patients with gout reported that the normal cartilage architecture seems to be lost, presented with empty chondrocyte lacunaes (38).

In addition, this deposition of MSU crystals in the synovium leads to the release of reactive oxygen species (ROS) and reacitve nitrogen species in human fibroblasts which contributes to cell death (39). Thereafter, MSU crystals are not only capable of inducing direct cytotoxicity, but inflammation and inflammation-driven cell necrosis in the synovium as well (40). For a classification of gout, clinicians usually use either the criteria from the American College of Rheumatology (41), or the criteria from the European League Against Rheumatism (42). The diagnosis consists of the confirmation of the MSU crystalls in the synovial fluid or a presence of a clear clinical tophus (43). An online risk calculator (http://www.gp-training.net/rheum/ gout_calc.htm) can alternatively be used when no microscope is available. This tool uses sex, uric acid level along with five findings from the history and physical examination to predict the likelihood of an acute gout flare (44).

An overview of the disease progression from hyperuricemia to gout is shown in **Figure 1** (from (34)).

Treatment

Through the ages, the treatment of gout has focused mainly on dietary management (45), which in time has proven to have only a small role in the regulation of serum urate concentrations. As with the ongoing research, NSAIDs, colchicine and corticosteroids became the first-line treatment option for acute gout (41,43). However, in patients with other comorbidities, these treatments presented broad drug toxicities, as the presence of comorbidites resulted in contraindications for these drugs (46,47). Alternatively, studies have demonstrated that IL-1 inhibitors (such as canakinumab and anakinra) can be affective in an acute attack and should be considered for treatment (48). This option usually is used for patients who have extreme side effects or have contra-indications to first-line antiinflammatory therapy.

Based on current guidelines, the aim is to reduce serum urate concentration below 6 mg/dl, allowing the deposits of MSU crystals to dissolve (41,43). The urate lowering therapy (ULT) based on their mechanism of action can be a xanthine oxidase inhibitor (allopurinol, febuxostat), uricosurid drug (probenecid, lesinuard, benzbromarone), inhibiting the renal reabsorbtion of urate and with pegloticase function such as recombinant uricase. Xanthine oxidase inhibitors help to reduce the production of urate in the body by inhibiting the activity of the enzime xanthine oxidase (XO), which in the body is responsible for coverting hypoxanthine to xanthine and then to uric acid (49). XO is primarily found in the lungs, liver and serum where it can be also measured for diagnostic purposes. The ULT is to be continued as a long-term therapy, often requiring lifelong treatment (50).

Lately, histone deacetylases also got an important role in inflammation. Histone deacetylases (HDACs) are represented by a group of enzymes which remove acetyl groups from lysine residues on histones by changing the epigenetic landscape (51). In addition to this, this enzymes have widespread cellular effects besides chromatin remodeling, such as, RNA splicing, cell cycle regulation, nuclear transport and tubulin formation (52). The main observed effects of such enzymes in clinical reports were supression of cytokines along with nitric oxide production and inhibition of inflammatory transcription factors such as NF-kB and STAT (53). Also, decreased proliferation and differentiation of immune cells was recognized (53). Moreover, HDAC inhibitors, were shown to carry anti-rheumatic effects as well (54). The inhibition was associated with suppressed ex vivo inflammatory cytokine production in rheumatoid arthritis fibroblast-like synoviocytes and peripheral blood mononuclear cells (54-56). Thereafter, with the understanding of the molecular pathophysiology of the disease will lead to new therapy options in order to improve the medical management of gout.

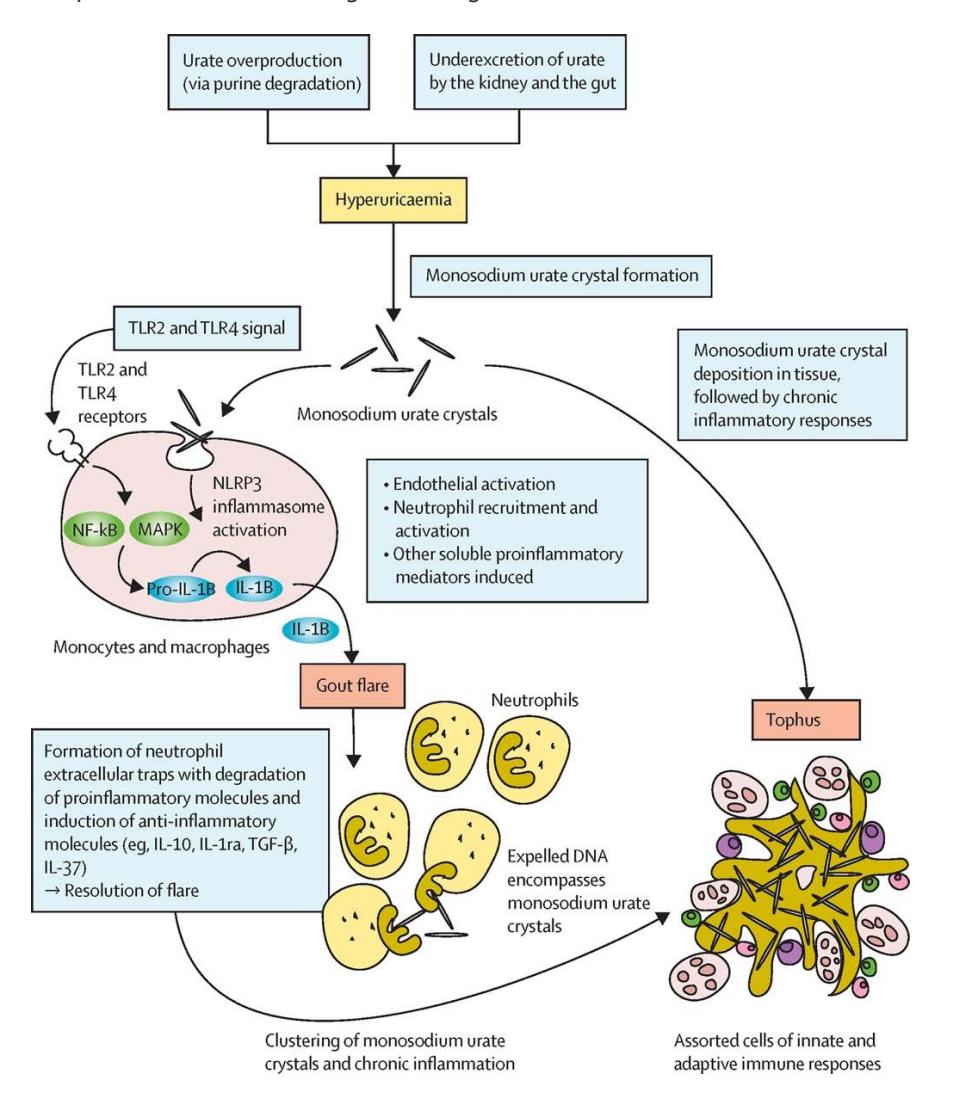


Figure 1 Progression of hyperuricaemia to gout. Urate overproduction or underexcretion leads to the development of hyperuricaemia, a state that facilitates the formation of monosodium urate crystals. These crystals can be phagocytosed by monocytes; an additional signal, through TLR2 and TLR4, is required to complete activation of the NLRP3 inflammasome and the production of proinflammatory IL-1β, which leads to acute flares of gouty arthritis. Flare resolution involves neutrophil extracellular traps that bind monosodium urate crystals. Aggregated neutrophil extracellular traps might also contribute to the formation of tophi. Figure from a recent review (34).

Urate metabolism

Hyperuricemia refers to abnormally high concentrations of urate in the blood, which can result from either increased production or reduced renal excretion (11). Elevated urate levels do not always cause symptoms, however they can contribute to the development of health issues, particularly gout (57,58).

Our understanding of urate metabolism has recently advanced with the ongoing research done on this field. With the exception of humans and other great apes, it is now generally acknowledged that urate metabolism engage a series of 3 enzymes (urate oxidase, 5-hydroxyisourate hydrolase, and 2-oxo-4-hydroxy-4carboxy-5-ureidoimidazoline decarboxylase) and transporters (59,60). In humans, uric acid is produced mainly in the liver, where its production is mainly influenced by dietary intake, endogenous purine synthesis and the breakdown of cellular nucleic acids (61). Once produced, this cannnot be further metabolized by human cells, so the removal happens through either renal or extra-renal eliminiation (61). During primate evolution, the gene encoding for urate oxidase suffered mutations that caused pseudogenization leading to the inability to metabolize urate to soluble allantoin (62). At the same time, alterations in the URAT1 transporter gene happened as well, leading to a lower capacity for the transport of uric acid (63). Therefore, our lack of ability to convert highly insoluble uric acid into a more soluble molecule makes us susceptible to diseases and other health complications (62).

When there is an overproduction of uric acid or the kidneys are unable to eliminate it efficiently, the urate levels in the blood become elevated, leading to hyperuricemia (64). Several factors can induce hyperuricemia, such as obesity, a diet high in purine-rich foods (red meat, seafood), excessive alcohol consumption, genetics and certain medical conditions and medications such as diuretics, lowdose aspirin, and certain anti-tuberculosis drugs (65,66). Understanding the mechanism that effects high urate concentrations is crucial for understanding the etiology of gout. Lately, GWAS studies tried to explain the variation in serum urate concentrations in the general population (67-70). These studies have identified multiple loci associated with serum urate variation, of which the strongest are localized in urate transporters (SLC22A12, SLC2A9, ABCG2) (71-73). Moreover, there is increasing evidence suggesting that it might have an important role in stimulating inflammation (57). Thereafter, understanding the urate metabolism is essential for a better recognition of conditions such as hyperuricemia and gout.

Urate induced inflammation

Urate is a byproduct of purine metabolism (74) and it has been associated with inflammation in various tissues. Additionally, it has been identified also, as a proinflammatory molecule released from dying cells, contributing to celldeath induced inflammatory responses in vivo (75). Moreover, lately it is linked to kidney disease, as it has a capacity to induce immune system activation while contributing to a proinflammatory state (76). Thereafter, with the multitudes of ongoing research, studies have broadened the knowledge of the biological effects of urate, other than being just the main cause of gout. It has an ability to activate the NLRP3 inflammasome in macrophages thus promoting inflammation and having the potential to be considered an inflammatory trigger along with MSU crystals (77). Furthermore, there is enough evidence suggesting a complex effect of urate on monocytes, illustrating that uric acid can have an affect on many different biological processes involving different cell phenotypes, primarily those involved in the immune responses, such as macrophages, neutrophils, monocytes, dentritic cells, synovial cells, chondrocytes, fibroblast and T cells. The pathways involved in this proinflammatory and prooxidative processes are related to oxidative stress, inflammatory signaling, autophagy and intracellular immunometabolic sensors (57). Moreover, in patients with hyperuricemia, white blood cells, CRP and cytokines such as IL-6, IL-1Ra, TNF or IL-18 were highly associated with high serum urate levels (78,79). Nevertheless, urate and hyperuricemia exposure has potential in altering the epigenetic programms of the immune cells while promoting a steady inflammatory state (57).

Urate, released in the human body, in conditions as hyperuricemia can crystallize and acts as a damage-associated mollecular-pattern (DAMP), contributing to sterile inflammation in conditions such as gout (80,81). Damps are endogenous molecules which are released or exposed by stressed, injured, or necrotic cells (81). The identification of DAMPs by pattern recognition receptors (PRRs) on immune cells, as long as Toll-like receptors (TLRs) and NOD-like receptors, take up a cascade of event which ends with the activation of the immune system while promoting inflammation.

Urate – induced innate immune memory

Trained immunity is a process involving the long-term modulation of the innate immune cells and it is characterized by the enhanced capacity of innate immune cells to increase responses to subsequent stimuli (82,83). Interleukin 6 (84), TNF- α (85) but also members of the IL-1 family such as interleukin 1 beta (IL-1 β) (86), are among the proinflammatory cytokines involved in the immune responses of trained cells. We can note an increase in cytokine production when human

monocytes are primed or trained in-vitro with microbial stimuli (such as betaglucan or BCG) (87), but also with endogenous molecules such as oxidized lowdensity lipoprotein(oxLDL) (88), oxidized phospholipids (oxPAPC) (89), or urate (79). These stimuli bind to Pattern Recognition Receptors (PRRs) on myeloid cells leading to the release of effector molecules and subsequent increased response to second stimulation (Figure 2.) (84). Although trained immunity suggest protective role againts infectious diseases, a dysregulated trained immunity might contribute to the pathogenesis of several autoimmune and autoinflammatory conditions.

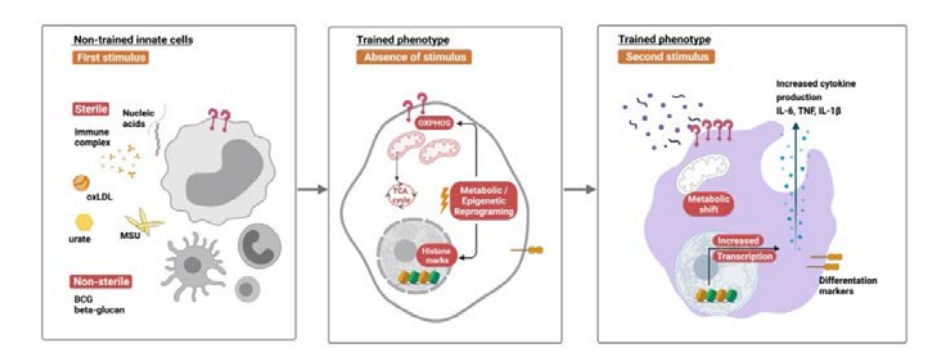


Figure 2 Schematic representation of innate immune memory development. Upon a first encounter of innate immune cells with a pathogen associated molecular pattern (e.g., BCG, beta-glucan)/or damage associated molecule pattern (e.g., urate, oxLDL, immune complexes), the down-stream signaling via pattern recognition receptors (PRRs) promotes metabolic changes (e.g., altered glycolysis or OXPHOS) and epigenetic modifications (e.g., histone modifications, DNA methylation) which persist after the initial triggers have been removed. Consequently, on a subsequent stimulation, the cells exhibit faster and stronger inflammatory responses facilitated by the pre-existent epigenetic marks which allow for increased gene expression, giving rise to hyper-inflammatory responses. The figure is used in Chapter 7 of this thesis as Figure 1.

In rheumatic and autoinflammatory diseases, this immune process is associated with changes in inflammatory mediators, cytokine production and immunometabolism (90). This approach is initiated in response to MSU crystals or soluble urate and it is increasingly shown to be important for urate-induced inflammation leading to elevated proinflammatory cytokines (90). Moreover, there is evidence suggesting that uric acid can induce immune memory formation, leading to enhanced non-specific immune responses and can mechanistically alter the inflammatory capacity of myeloid cells (91). High concentrations of urate on primary human peripheral mononuclear cells (PBMCs) and monocytes is linked with elevated IL-1b and concomitant with reduced IL-1Ra, described as a priming effect in the literature (92). In line with this, this process can also lead to abnormal programming and chronic inflammation, as seen in gout (91). Hyperuricemia can lead to hypomethylation of genes involved in inflammatory pathways, leading to increased expression while contributing to chronic inflammation.

These findings are interconnecting hyperuricemia with a large group of adult diseases, for which DAMP-mediated responses are of high relevance (92,93).

Regulation of IL-1

Interleukin-1 (IL-1) is a pro-inflammatory cytokine playing a central role in the regulation of the immune and inflammatory responses (93). It is part of the interleukin-1 family, which consists of 11 members of which IL-1α, IL-1β, IL-18, IL-33, IL-36α, IL-36β and IL-36γ are considered pro-inflammatory and IL-1Ra, IL-36Ra, IL-37 and IL-38 anti-inflammatory (94). The regulation of the IL-1 cytokine is driven by the proteolytic cleavage of its precursor by caspase-1, which is activated within inflammasomes (95). The cytokine is presented with a unique role in the pathogenesis of autoinflammatory diseases, especially in gout which is uniquely IL-1β mediated (96). The IL-1β signaling is currently considered an initiating event that triggers uric acid inflammation and promotes the recruitment of a large number of neutrophils to the inflammatory site (97).

Upon binding to its receptor IL-1R1, IL-1B activates several intracellular signaling pathways, including NF-κB and MAPK pathways, leading to the transcription of inflammatory genes (94). This cascade is resulting in the synthesis of pro-IL-1B, representing an inactive precursor which is thereafter cleaved by the caspase-1 in order to become a biologically active cytokine (95). The activity of the caspase-1 is firmly controlled by the activation of the inflammasome, particularly the so called NLRP3 inflammasome, which is capable of recognizing the danger signals and participating in inflammatory responses (98). The activation of the NLRP3 inflammasome is happening through a two-step process, namely, the first one is represented by **priming**, when the recognisition of the first signal by the Tolllike receptors is leading to the activation of NF-kB. Further, this will upregulate the expression of NLRP3, pro-IL-1β and pro-IL-18 (99). The second step is defined as activation and is represented by the second signal which is leading to the oligomerization of NLRP3 and activation of caspase-1. This series of events result in the cleavage of pro-IL-1\(\beta\) and pro-IL-18 into their active, mature form (99).

Dysregulation of the NLRP3 inflammasome is linked to numerous inflammatory and autoimmune diseases, including cryopyrin-associated periodic syndromes, Alzheimer's disease, atherosclerosis, type 2 diabetes, obesity and gout (100,101). Genetic mutations are one of the reasons leading to the malfunction of the inflammasome, resulting in the constitutive activation of it (102,103). Also, abberant activation by endogenous and exogenous stimuli, such as persistent exposure to uric acid crystals can lead to chornic activation and disruption of the NLRP3 inflammasome (104). Moreover, impaired regulatory mechanisms represent another cause for the dysfunction of the inflammasome (105). Autophagy is a crucial process for the cell fate regulation (105), thus dysfunction of this can result in hyperinflammation and excessive activation of the inflammasome. Furthermore, evidence is showing that elevated levels of Reactive Oxigen Species (ROS) can as well induce this event of activation (106).

The genetic basis of hyperuricemia and gout

The genetic basis of hyperuricemia and gout has been the focus of extensive research, especially through genome-wide association studies (GWAS). These studies have identified numerous genes involved in urate transport, metabolism, and inflammation, which together contribute to an individual's risk of developing hyperuricemia and gout.

More recently, genome-wide genetic and epigenetic studies have elucidated new pathways involved in the inflammatory processes in gout, including links between genetic factors and epigenetic regulators (107,108). Moreover, these studies have uncovered multiple loci (eq. SLC2A9, SLC22A12, ABCG2, SLC22A11, SLC17A1, SLC16A9, PDZK1, GCKR, INHBC, HNF4A, MAF), contributing to risk of gout via their implications for hyperuricemia (109). The genetic factors that contribute to both hyperuricemia and gout mostly include genes that encode transporters, transcriptional factors along with signaling receptors and enzymes, shedding light on the complex genetic landscape that underlies susceptibility to these inflammatory conditions. Such genetic studies shed light not only on the importance and involvement of pathways such as urate metabolism and transportation in the transition from hyperuricemia to clinically manifested gout, but on genes encoding innate immune cytokines and receptors as well. Furthermore, genomewide association studies of gout, assert the significance of epigenomic pathways, indicating that epigenetic reprogramming of innate immune cells by soluble urate heightens their sensitivity to monosodium urate crystals. The need remains for further exploration of the GWAS signals into molecular mechanisms and identifying new candidate molecules for therapeutic purposes.

Aim and Outline of the thesis

In the current thesis, we aimed to explore the variation in gout and urate-associated inflammation associated to genetic differences and epigenetic modifications. We have focused on possible gene variants that may be causative for the transition from hyperuricemia to gout and assessed inflammatory responses in the context of gout and hyperuricemia. In addition, we examined mechanism contributing to inflammation induced by hyperuricemia.

In Chapter 2, we conducted a functional assessment of the IL1RN/IL1F10 region in patients with gout and controls. We showed that this gout specific locus was associated with altered expression of IL1RN and IL1F10. Also, we present a SNP in IL1RN which confers predisposition to gout and results in an altered circulating IL1Ra production. In Chapter 3, we test the gout and urate-associated IGF1R rs6598541 polymorphism for association with the inflammatory capacity of mononuclear cells. In addition, we investigate the role of IGF-1/IGF1R signaling in the context of gouty inflammation. In Chapter 4, we identified the IL-1 receptor family member IL1R1 gene as being upregulated in hyperuricemic individuals. Also, the effect of the gout associated IL1R1 rs17767183 SNP was assessed in in vivo and in vitro setup. Chapter 5 provide evidence for inflammatory consequences of urate exposure in vivo, providing proof that asymptomatic hyperuricemia is marked by a strong systemic inflammatory signature. Next, in **Chapter 6**, we further investigated the epigenetic processes associated to this urate-mediated hyper-responsiveness and discovered that urate enhanced the inflammatory response in vitro in human cells and in vivo in mice, and broad-spectrum methylation inhibitors reversed this effect. Lastly, in Chapter 7, we summarized our current knowledge and tried to provide an overview of current data that describes features of trained immunity in rheumatic diseases, linking evidence on inflammatory mediators and cytokine production, immunometabolism and epigenetic regulation of immunological programs.

References

- KITTREDGE WE, DOWNS R. The role of gout in the formation of urinary calculi. J Urol. 1952:67(6):841-7.
- Nuki G, Simkin PA. A concise history of gout and hyperuricemia and their treatment. Arthritis Res 2. Ther. 2006;8(SUPPL. 1):1-5.
- 3. Bhattacharjee S. A brief history of gout. Int J Rheum Dis. 2009;12(1):61–3.
- 4. MacKenzie CR. Gout and Hyperuricemia: an Historical Perspective. Curr Treatm Opt Rheumatol. 2015;1(2):119-30.
- 5. Schwartz SA. Disease of distinction. Explore (NY). 2006;2(6):515–9.
- 6. Dittmar JM, Mitchell PD, Jones PM, Mulder B, Inskip SA, Cessford C, et al. Gout and "Podagra" in medieval Cambridge, England. Int J Paleopathol. 2021 Jun;33:170-81.
- 7. Dalbeth N, Merriman TR, Stamp LK. Seminar Gout. The Lancet. 2016;
- Galassi FM, Borghi C. A brief history of uric acid: From gout to cardiovascular risk factor. Vol. 26, 8. European journal of internal medicine. Netherlands; 2015. p. 373.
- 9 Degueker J. Gout: the patrician malady. BMJ. 1999 Jan;318(7175):64A.
- 10. Dalbeth N, Choi HK, Joosten LAB, Khanna PP, Matsuo H, Perez-Ruiz F, et al. Gout. Nat Rev Dis Primers. 2019 Sep;5(1):69.
- 11. Danve A, Sehra ST, Neogi T. Role of diet in hyperuricemia and gout. Best Pract Res Clin Rheumatol. 2021 Dec;35(4):101723.
- 12. Schwab M, editor. Xanthine Oxidase. In: Encyclopedia of Cancer. Berlin, Heidelberg: Springer Berlin Heidelberg; 2009. p. 3215.
- 13. Mandal AK, Mount DB. The molecular physiology of uric acid homeostasis. Annu Rev Physiol. 2015:77:323-45.
- 14. Mandell BF. Clinical manifestations of hyperuricemia and gout. Cleve Clin J Med. 2008 Jul;75 Suppl 5:S5-8.
- 15. Kivity S, Kopel E, Maor E, Abu-Bachar F, Segev S, Sidi Y, et al. Association of serum uric acid and cardiovascular disease in healthy adults. Am J Cardiol. 2013 Apr;111(8):1146–51.
- 16. Li X, Meng X, He Y, Spiliopoulou A, Timofeeva M, Wei WQ, et al. Genetically determined serum urate levels and cardiovascular and other diseases in UK Biobank cohort: A phenome-wide mendelian randomization study. PLoS Med. 2019;16(10):1-20.
- 17. Sandoval-Plata G, Nakafero G, Chakravorty M, Morgan K, Abhishek A. Association between serum urate, gout and comorbidities: a case-control study using data from the UK Biobank. Rheumatology (Oxford). 2021 Jul;60(7):3243-51.
- 18. Verdecchia P, Schillaci G, Reboldi G, Santeusanio F, Porcellati C, Brunetti P. Relation between serum uric acid and risk of cardiovascular disease in essential hypertension. The PIUMA study. Hypertension. 2000 Dec;36(6):1072-8.
- 19. Maruhashi T, Hisatome I, Kihara Y, Higashi Y. Hyperuricemia and endothelial function: From molecular background to clinical perspectives. Atherosclerosis. 2018 Nov;278:226–31.
- 20. Roddy E, Doherty M. Gout. Epidemiology of gout. Arthritis Res Ther. 2010;
- 21. Shields GE, Beard SM. A Systematic Review of the Economic and Humanistic Burden of Gout. Pharmacoeconomics. 2015 Oct;33(10):1029-47.
- 22. Kuo CF, Grainge MJ, Zhang W, Doherty M. Global epidemiology of gout: Prevalence, incidence and risk factors. Nature Reviews Rheumatology. 2015.

- 23. Dehlin M, Jacobsson L, Roddy E. Global epidemiology of gout: prevalence, incidence, treatment patterns and risk factors. Nat Rev Rheumatol. 2020 Jul;16(7):380-90.
- 24. Yokose C, McCormick N, Lu N, Tanikella S, Lin K, Joshi AD, et al. Trends in Prevalence of Gout Among US Asian Adults, 2011-2018. JAMA Netw Open. 2023 Apr;6(4):e239501.
- 25. Chen-Xu M, Yokose C, Rai SK, Pillinger MH, Choi HK, Contemporary Prevalence of Gout and Hyperuricemia in the United States and Decadal Trends: The National Health and Nutrition Examination Survey, 2007-2016. Arthritis Rheumatol. 2019 Jun;71(6):991-9.
- 26. Hak AE, Curhan GC, Grodstein F, Choi HK. Menopause, postmenopausal hormone use and risk of incident gout. Ann Rheum Dis. 2010 Jul;69(7):1305-9.
- 27. García-Méndez S, Beas-Ixtláhuac E, Hernández-Cuevas C, Mendoza-Torres JM, Melo-Centeno C, Rull-Gabayet M, et al. Female gout: age and duration of the disease determine clinical presentation. J Clin Rheumatol. 2012 Aug;18(5):242-5.
- 28. Te Kampe R, Jansen TL, van Durme C, Janssen M, Petersen G, Boonen A. Outcomes of Care Among Patients With Gout in Europe: A Cross-sectional Survey. J Rheumatol. 2022 Mar;49(3):312-9.
- 29. Global, regional, and national disability-adjusted life-years (DALYs) for 359 diseases and injuries and healthy life expectancy (HALE) for 195 countries and territories, 1990-2017: a systematic analysis for the Global Burden of Disease Study 2017. Lancet. 2018 Nov;392(10159):1859-922.
- 30. Dalbeth N, Merriman TR, Stamp LK. Gout. The Lancet. 2016.
- 31. Mikuls TR. Gout. N Engl J Med. 2022 Nov;387(20):1877-87.
- 32. Taylor WJ, Fransen J, Jansen TL, Dalbeth N, Schumacher HR, Brown M, et al. Study for Updated Gout Classification Criteria: Identification of Features to Classify Gout. Arthritis Care Res (Hoboken). 2015 Sep;67(9):1304-15.
- 33. Dalbeth N, Stamp L. Hyperuricaemia and gout: time for a new staging system? Ann Rheum Dis. 2014 Sep;73(9):1598-600.
- 34. Dalbeth N, Gosling AL, Gaffo A, Abhishek A. Gout. The Lancet. 2021;397(10287):1843–55.
- 35. Campion EW, Glynn RJ, DeLabry LO. Asymptomatic hyperuricemia. Risks and consequences in the Normative Aging Study. Am J Med. 1987 Mar;82(3):421-6.
- 36. Chhana A, Lee G, Dalbeth N. Factors influencing the crystallization of monosodium urate: a systematic literature review. BMC Musculoskelet Disord. 2015 Oct;16:296.
- 37. Chhana A, Pool B, Wei Y, Choi A, Gao R, Munro J, et al. Human Cartilage Homogenates Influence the Crystallization of Monosodium Urate and Inflammatory Response to Monosodium Urate Crystals: A Potential Link Between Osteoarthritis and Gout. Arthritis Rheumatol. 2019 Dec;71(12):2090-9.
- 38. Chhana A, Callon KE, Pool B, Naot D, Gamble GD, Drav M, et al. The effects of monosodium urate monohydrate crystals on chondrocyte viability and function: implications for development of cartilage damage in gout. J Rheumatol. 2013 Dec;40(12):2067-74.
- 39. Zamudio-Cuevas Y, Martínez-Flores K, Fernández-Torres J, Loissell-Baltazar YA, Medina-Luna D, López-Macay A, et al. Monosodium urate crystals induce oxidative stress in human synoviocytes. Arthritis Res Ther. 2016 May;18(1):117.
- 40. El-Zawawy H, Mandell BF. Update on Crystal-Induced Arthritides. Clin Geriatr Med. 2017 Feb;33(1):135-44.
- 41. FitzGerald JD, Dalbeth N, Mikuls T, Brignardello-Petersen R, Guyatt G, Abeles AM, et al. 2020 American College of Rheumatology Guideline for the Management of Gout. Arthritis Care Res (Hoboken). 2020 Jun;72(6):744-60.
- 42. Richette P, Doherty M, Pascual E, Barskova V, Becce F, Castaneda J, et al. 2018 updated European League against Rheumatism evidence-based recommendations for the diagnosis of gout. Ann Rheum Dis. 2020;79(1):31-8.

- 43. Richette P, Doherty M, Pascual E, Barskova V, Becce F, Castañeda-Sanabria J, et al. 2016 updated EULAR evidence-based recommendations for the management of gout. Ann Rheum Dis. 2017 Jan:76(1):29-42.
- 44. Janssens HJEM, Fransen J, van de Lisdonk EH, van Riel PLCM, van Weel C, Janssen M. A diagnostic rule for acute gouty arthritis in primary care without joint fluid analysis. Arch Intern Med. 2010 Jul:170(13):1120-6.
- 45. Porter R. Gout: framing and fantasizing disease. Bull Hist Med. 1994;68(1):1–28.
- 46. Bardin T, Richette P. Impact of comorbidities on gout and hyperuricaemia: an update on prevalence and treatment options. BMC Med. 2017 Jul;15(1):123.
- 47. Keenan RT, O'Brien WR, Lee KH, Crittenden DB, Fisher MC, Goldfarb DS, et al. Prevalence of contraindications and prescription of pharmacologic therapies for gout. Am J Med. 2011 Feb:124(2):155-63.
- 48. Dumusc A, So A. Interleukin-1 as a therapeutic target in gout. Curr Opin Rheumatol. 2015 Mar:27(2):156-63.
- 49. Hille R. Xanthine Oxidase-A Personal History. Molecules. 2023 Feb;28(4).
- 50. Janssens HJEM, Janssen M, van de Lisdonk EH, van Riel PLCM, van Weel C. Use of oral prednisolone or naproxen for the treatment of gout arthritis: a double-blind, randomised equivalence trial. Lancet. 2008 May;371(9627):1854-60.
- 51. Seto E, Yoshida M. Erasers of histone acetylation: the histone deacetylase enzymes. Cold Spring Harb Perspect Biol. 2014 Apr;6(4):a018713.
- 52. Choudhary C, Kumar C, Gnad F, Nielsen ML, Rehman M, Walther TC, et al. Lysine acetylation targets protein complexes and co-regulates major cellular functions. Science. 2009 Aug;325(5942):834–40.
- Blanchard F, Chipoy C. Histone deacetylase inhibitors: new drugs for the treatment of inflammatory diseases? Drug Discov Today. 2005 Feb;10(3):197-204.
- 54. Angiolilli C, Kabala PA, Grabiec AM, Van Baarsen IM, Ferguson BS, García S, et al. Histone deacetylase 3 regulates the inflammatory gene expression programme of rheumatoid arthritis fibroblast-like synoviocytes. Ann Rheum Dis. 2017 Jan;76(1):277-85.
- 55. Gillespie J, Savic S, Wong C, Hempshall A, Inman M, Emery P, et al. Histone deacetylases are dysregulated in rheumatoid arthritis and a novel histone deacetylase 3-selective inhibitor reduces interleukin-6 production by peripheral blood mononuclear cells from rheumatoid arthritis patients. Arthritis Rheum. 2012 Feb;64(2):418-22.
- 56. Grabiec AM, Krausz S, de Jager W, Burakowski T, Groot D, Sanders ME, et al. Histone deacetylase inhibitors suppress inflammatory activation of rheumatoid arthritis patient synovial macrophages and tissue. J Immunol. 2010 Mar;184(5):2718-28.
- 57. Joosten LAB, Crişan TO, Bjornstad P, Johnson RJ. Asymptomatic hyperuricaemia: a silent activator of the innate immune system. Nat Rev Rheumatol. 2020;16(2):75-86.
- 58. Yip K, Cohen RE, Pillinger MH. Asymptomatic hyperuricemia: is it really asymptomatic? Curr Opin Rheumatol. 2020 Jan;32(1):71-9.
- 59. Tipton PA. Urate to allantoin, specifically (S)-allantoin. Vol. 2, Nature chemical biology. United States; 2006. p. 124-5.
- 60. Turner R, Brennan SO, Ashby L V., Dickerhof N, Hamzah MR, Pearson JF, et al. Conjugation of urate-derived electrophiles to proteins during normal metabolism and inflammation. Journal of Biological Chemistry. 2018;293(51):19886-98.
- 61. Hyndman D, Liu S, Miner JN. Urate Handling in the Human Body. Vol. 18, Current Rheumatology Reports. 2016.

- 62. Kratzer JT, Lanaspa MA, Murphy MN, Cicerchi C, Graves CL, Tipton PA, et al. Evolutionary history and metabolic insights of ancient mammalian uricases. Proc Natl Acad Sci U S A. 2014:111(10):3763-8.
- 63. Tan PK, Farrar JE, Gaucher EA, Miner JN. Coevolution of URAT1 and Uricase during Primate Evolution: Implications for Serum Urate Homeostasis and Gout. Mol Biol Evol. 2016;33(9):2193-200.
- 64. Bardin T, Richette P. Definition of hyperuricemia and gouty conditions. Vol. 26, Current Opinion in Rheumatology, 2014.
- 65. Moriwaki Y. Effects on uric acid metabolism of the drugs except the antihyperuricemics. J Bioequivalence Bioavailab. 2014;6(1):10-7.
- 66. Leung N, Yip K, Pillinger MH, Toprover M. Lowering and Raising Serum Urate Levels: Off-Label Effects of Commonly Used Medications. Mayo Clin Proc. 2022;97(7):1345-62.
- 67. Köttgen A, Albrecht E, Teumer A, Vitart V, Krumsiek J, Hundertmark C, et al. Genome-wide association analyses identify 18 new loci associated with serum urate concentrations. Nat Genet. 2013;45(2):145-54.
- 68. Merriman T. Genomic Influences on Hyperuricemia and Gout. Rheumatic Disease Clinics of North America. 2017;43(3):389-99.
- 69. Major TJ, Dalbeth N, Stahl EA, Merriman TR. An update on the genetics of hyperuricaemia and gout. Nat Rev Rheumatol. 2018;14(6):351-3.
- 70. Lin CY, Chang YS, Liu TY, Huang CM, Chung CC, Chen YC, et al. Genetic contributions to female gout and hyperuricaemia using genome-wide association study and polygenic risk score analyses. Rheumatology. 2023 Feb 1;62(2):638–46.
- 71. Enomoto A, Kimura H, Chairoungdua A, Shigeta Y, Jutabha P, Cha SH, et al. Molecular identification of a renal urate-anion exchanger that regulates blood urate levels. Nature. 2002;417(6887):447–52.
- 72. Gunjaca G, Boban M, Pehlić M, Zemunik T, Budimir D, Kolcić I, et al. Predictive value of 8 genetic loci for serum uric acid concentration. Croat Med J. 2010 Feb;51(1):23-31.
- 73. Phipps-Green AJ, Merriman ME, Topless R, Altaf S, Montgomery GW, Franklin C, et al. Twenty-eight loci that influence serum urate levels: Analysis of association with gout. Ann Rheum Dis. 2016;
- 74. Mandel NS, Mandel GS. Monosodium Urate Monohydrate, the Gout Culprit. J Am Chem Soc. 1976;
- 75. Kono H, Chen CJ, Ontiveros F, Rock KL. Uric acid promotes an acute inflammatory response to sterile cell death in mice. Journal of Clinical Investigation. 2010;
- 76. Jung SW, Kim SM, Kim YG, Lee SH, Moon JY. Uric acid and inflammation in kidney disease. Am J Physiol Renal Physiol. 2020;318(6):F1327-40.
- 77. Kim SM, Lee SH, Kim YG, Kim SY, Seo JW, Choi YW, et al. Hyperuricemia-induced NLRP3 activation of macrophages contributes to the progression of diabetic nephropathy. Am J Physiol Renal Physiol. 2015 May;308(9):F993-1003.
- 78. Ruggiero C, Cherubini A, Ble A, Bos AJG, Maggio M, Dixit VD, et al. Uric acid and inflammatory markers. Eur Heart J. 2006;27(10):1174-81.
- 79. Badii M, Gaal Ol, Cleophas MC, Klück V, Davar R, Habibi E, et al. Urate-induced epigenetic modifications in myeloid cells. Arthritis Res Ther. 2021;23(1):1–11.
- 80. Braga TT, Forni MF, Correa-Costa M, Ramos RN, Barbuto JA, Branco P, et al. Soluble Uric Acid Activates the NLRP3 Inflammasome. Sci Rep. 2017;7(September 2016):1-14.
- 81. Rock KL, Kataoka H, Lai JJ. Uric acid as a danger signal in gout and its comorbidities. Nature Reviews Rheumatology. 2013.
- 82. Netea MG, Domínguez-Andrés J, Barreiro LB, Chavakis T, Divangahi M, Fuchs E, et al. Defining trained immunity and its role in health and disease. Nat Rev Immunol. 2020;20(6):375-88.

- 83. Nica V, Popp RA, Crisan TO, Joosten LAB. The future clinical implications of trained immunity. Expert Rev Clin Immunol. 2022 Nov;18(11):1125-34.
- 84. Netea MG, Domínguez-Andrés J, Barreiro LB, Chavakis T, Divangahi M, Fuchs E, et al. Defining trained immunity and its role in health and disease. Nat Rev Immunol. 2020 Jun;20(6):375-88.
- 85. Pérez-Hernández CA, Kern CC, Butkeviciute E, McCarthy E, Dockrell HM, Moreno-Altamirano MMB, et al. Mitochondrial Signature in Human Monocytes and Resistance to Infection in C. elegans During Fumarate-Induced Innate Immune Training. Front Immunol. 2020;11 (August).
- 86. Moorlag SJCFM, Röring RJ, Joosten LAB, Netea MG. The role of the interleukin-1 family in trained immunity. Immunol Rev. 2018;281(1):28-39.
- 87. Moorlag SJCFM, Khan N, Novakovic B, Kaufmann E, Jansen T, van Crevel R, et al. β-Glucan Induces Protective Trained Immunity against Mycobacterium tuberculosis Infection: A Key Role for IL-1. Cell Rep. 2020;31(7):107634.
- 88. Groh LA, Ferreira A V, Helder L, van der Heijden CDCC, Novakovic B, van de Westerlo E, et al. oxLDL-Induced Trained Immunity Is Dependent on Mitochondrial Metabolic Reprogramming. Immunometabolism. 2021;3(3):e210025.
- 89. Di Gioia M, Spreafico R, Springstead JR, Mendelson MM, Joehanes R, Levy D, et al. Endogenous oxidized phospholipids reprogram cellular metabolism and boost hyperinflammation. Nat Immunol. 2020:21(1):42-53.
- 90. Badii M, Gaal O, Popp RA, Crisan TO, Joosten LAB. Trained immunity and inflammation in rheumatic diseases. Joint Bone Spine. 2022;89(4).
- 91. Cabău G, Crisan TO, Klück V, Popp RA, Joosten LAB. Urate-induced immune programming: Consequences for gouty arthritis and hyperuricemia. Immunol Rev. 2020;294(1):92–105.
- 92. Crisan TO, Cleophas MCP, Oosting M, Lemmers H, Toenhake-Dijkstra H, Netea MG, et al. Soluble uric acid primes TLR-induced proinflammatory cytokine production by human primary cells via inhibition of IL-1Ra. Ann Rheum Dis. 2016:
- 93. Dinarello CA. Interleukin-1. Cytokine Growth Factor Rev. 1997 Dec;8(4):253-65.
- 94. Dinarello CA. Overview of the IL-1 family in innate inflammation and acquired immunity. Immunol Rev. 2018 Jan;281(1):8–27.
- 95. Guarda G, So A. Regulation of inflammasome activity. Immunology. 2010 Jul;130(3):329–36.
- 96. Dinarello CA. How interleukin-1ß induces gouty arthritis. Vol. 62, Arthritis and rheumatism. United States; 2010. p. 3140-4.
- 97. Klück V, Liu R, Joosten LAB. The role of interleukin-1 family members in hyperuricemia and gout. Joint Bone Spine. 2021;88(2).
- 98. Netea MG, Simon A, van de Veerdonk F, Kullberg BJ, Van der Meer JWM, Joosten LAB. IL-1beta processing in host defense: beyond the inflammasomes. PLoS Pathog. 2010 Feb;6(2):e1000661.
- 99. Swanson K V, Deng M, Ting JPY. The NLRP3 inflammasome: molecular activation and regulation to therapeutics. Nat Rev Immunol. 2019 Aug;19(8):477-89.
- 100. Xu J, Núñez G. The NLRP3 inflammasome: activation and regulation. Trends Biochem Sci. 2023 Apr;48(4):331-44.
- 101. Mangan MSJ, Olhava EJ, Roush WR, Seidel HM, Glick GD, Latz E. Targeting the NLRP3 inflammasome in inflammatory diseases. Nat Rev Drug Discov. 2018 Aug;17(8):588-606.
- 102. Booshehri LM, Hoffman HM. CAPS and NLRP3. J Clin Immunol. 2019 Apr;39(3):277-86.
- 103. Theodoropoulou K, Wittkowski H, Busso N, Von Scheven-Gête A, Moix I, Vanoni F, et al. Increased Prevalence of NLRP3 Q703K Variant Among Patients With Autoinflammatory Diseases: An International Multicentric Study. Front Immunol. 2020;11:877.

- 104. Wu H, Wang Y, Ren Z, Li Y, Huang J, Lin Z, et al. Overnutrition-induced gout: An immune response to NLRP3 inflammasome dysregulation by XOD activity increased in quail. Front Immunol. 2022;13:1074867.
- 105. Biasizzo M, Kopitar-Jerala N. Interplay Between NLRP3 Inflammasome and Autophagy. Front Immunol. 2020;11:591803.
- 106. Zhou R, Yazdi AS, Menu P, Tschopp J. A role for mitochondria in NLRP3 inflammasome activation. Nature. 2011 Jan;469(7329):221-5.
- 107. Major TJ, Dalbeth N, Stahl EA, Merriman TR. An update on the genetics of hyperuricaemia and gout. Vol. 14, Nature Reviews Rheumatology. 2018.
- 108. Leask MP, Crisan TO, Ji A, Matsuo H, Köttgen A, Merriman TR. The pathogenesis of gout: molecular insights from genetic, epigenomic and transcriptomic studies. Nat Rev Rheumatol. 2024 Aug;20(8):510-23.
- 109. Okada Y, Sim X, Go MJ, Wu JY, Gu D, Takeuchi F, et al. Meta-analysis identifies multiple loci associated with kidney function-related traits in east Asian populations. Nat Genet. 2012 Jul;44(8):904-9.



Chapter 2

Gout-associated SNP at the IL1RN-IL1F10 region is functionally linked to altered cytokine production in PBMCs of patients with gout and controls

Orsolya I. Gaal, Megan Leask, Valentin Nica, Georgiana Cabău, Medeea Badii, Ioana Hotea, HINT Consortium, Dennis M de Graaf, Zhenhua Zhang, Yang Li, Cristina Pamfil, Simona Rednic, Tony R. Merriman, Tania O. Crisan*, Leo A.B. Joosten*

*These authors share senior authorship

Abstract

Objectives

Gout is caused by the response of the innate immune system to monosodium urate (MSU) crystals. A recent gout GWAS identified a signal of genetic association at a locus encompassing IL1RN-IL1F10. Colocalisation analysis using Genotype Tissue Expression Database (GTEx) eQTL data showed that the signal overlaps with genetic control of IL1RN/IL1F10 gene expression. We assess the functional implications of IL1RN rs9973741, the lead gout-associated variant.

Methods

We conducted functional validation of IL1RN rs9973741 in patients with gout and controls. The transcription level of IL1RN/IL1F10 was investigated in unstimulated or MSU-crystal co-stimulated PBMCs. Ex vivo functional assays were performed in PBMCs stimulated with C16+MSU crystals or LPS for 24h. Cytokine levels were assessed by ELISA.

Results

In unstimulated PBMCs, no association of IL1RN rs9973741 (gout risk allele G) to IL1RN expression was observed while IL-1F10 was hindered by low expression at both transcriptional and protein levels. However, G allele carriers showed lower IL1RN expression in PBMCs stimulated with C16/MSU crystal and lower concentrations of circulating IL-1Ra in both controls and gout patients. PBMCs depicted less spontaneous IL-1Ra release in GG homozygous controls and lower IL-1Ra production in response to C16+MSU crystal costimulation in patients with gout. The G allele was associated with elevated IL-1β cytokine production in response to C16+MSU crystal stimulation in controls.

Conclusions

The gout risk allele G associates with lower circulating IL-1Ra, lower IL-1Ra production in PBMC assays and elevated IL-1β production in PBMCs challenged with C16+MSU crystals but not in unchallenged cells. Our data indicate that the genetic signal that associates with gout at IL1RN-IL1F10 region functions to alter expression of IL-1Ra when stimulated by MSU crystals.

Introduction

Gout is a common inflammatory disorder affecting approximately 41 million adults worldwide (1-3). The neccesary prerequisite for gout is the deposition of monosodium urate (MSU) crystals in the joints and other tissues as a result of elevated serum urate concentrations (4.5).

Interleukin IL-1\(\beta\) is the crucial inflammatory cytokine in gout, which is antagonized by IL-1 Receptor antagonist (IL-1Ra), both of which are known to be modulated in gout and urate-driven inflammation (6). IL-1Ra operates as an acute-phase protein, its expression being strongly induced by LPS, IL-1a and IL-1B, and interferon (IFN)- β (7.8). The balance between IL-1 and IL-1Ra is critical for the development of adaptive immune responses and for the regulation of innate immunity (9). IL-1F10 (IL-38) is another anti-inflammatory member of the IL-1 family that shares 41% sequence homology with IL-1Ra (10) and is known to suppress inflammation (11).

Although the indispensable cause of gout (MSU crystal exposure) is well described in the literature (12-14), the genetic contribution to the progression from hyperuricemia to gout is still relatively poorly understood. Genomewide association studies (GWAS) in gout using individuals with asymptomatic hyperuricemia as controls have mostly identified variants in urate transporters (ABCG2, SLC2A9, SLC22A11) as predictors of the transition to clinically evident gout (15–17). These studies, however, need to be interpreted with caution, as higher urate levels measured once in hyperuricemic patients do not represent strong evidence for association of genetic variants in the transition from hyperuricemia to gout (18). Recently, a large gout GWAS has identified variants near genes in inflammatory pathways, such as genetic variation at the IL1RN-IL1F10 region, with possible roles in the inflammatory aspects of transition from asymptomatic hyperuricemia to gout (19).

Our group previously described that soluble urate primes cells via epigenetic programming towards a higher inflammatory state along with downregulating the transcription of IL1RN (20). High concentrations of urate facilitate IL-1β production in PBMCs along with downregulation of IL-1Ra, causing a shift in the IL-1B/IL-1Ra balance (21). In addition, IL-1Ra has been shown to inhibit MSU crystal induced inflammation, being an important therapeutic target in gouty inflammation (6). These findings implicate the IL1RN-IL1F10 loci in gout, representing well characterized molecules directly connected to IL-1β induced inflammation.

Therefore, in the present study, we tested for functional impact of genetic variation at the IL1RN-IL1F10 region in gout. Also, we assessed the association of the rs9973741 with IL1RN-IL1F10 expression in circulating mononuclear cells and cytokine production capacity in patients with gout and controls.

Materials and methods

Genetic analyses

Summary GWAS statistics for the UKBB blood cell traits were downloaded from https://ftp.sanger.ac.uk/pub/project/humgen/summary statistics/UKBB blood cell traits/. Plots were generated using LocusZoom (22) and for gout from Major et al.(19). Correlated traits for the lead gout SNP were identified using LDtrait and LD was calculated using 1000 genomes in LDlink (23,24).

Participants

The participants in this study consisted of patients with gout (n=246) and asymptomatic controls (n=443) recruited at the Rheumatology Department of the "Iuliu Hatieganu" University of Medicine and Pharmacy, Clui-Napoca, Romania for the HINT Project. (Hyperuricemia-induced Inflammation: Targeting the central role of uric acid in rheumatic and cardiovascular diseases, ID P 37 762; MySMIS 103587) implemented in Clui-Napoca Romania at the Iuliu Hatieganu University of Medicine and Pharmacy. Subjects were enrolled after written informed consent. Peripheral blood was drawn from the cubital vein into EDTA tubes under sterile conditions. Experiments were conducted according to the principles expressed in the Declaration of Helsinki. The patient study was approved by the Ethical Committee of the "Iuliu Hatieganu" University of Medicine and Pharmacy, Cluj-Napoca (approval no. 425/2016). All study participants in the gout group were included based on ACR/EULAR 2015 classification criteria with a minimum score of 8 and controls had negative history of gout attacks. The described groups were similar in age and BMI. The gender distribution shows a higher number of men in the gout study group, consistent with the higher prevalence of gout in males.

PBMC isolation and stimulation

Isolation and stimulation of human peripheral blood mononuclear cells (PBMCs) was assessed as described previously (21). PBMCs were separated using Ficoll-Pague and resuspended in RPMI culture medium with Dutch modification (Gibco), supplemented with human pooled serum. Cells were incubated for 24 hours with culture medium as negative control or palmitate with MSU crystals (C16.0+MSU)

(gout relevant costimulation cocktail for TLR2 binding and NLRP3 inflammasome activation), or LPS (TLR4 ligand). Cells were incubated at 37 °C 5% CO2. Cytokine levels were measured in culture supernatants.

Cytokine measurements

Cytokine concentrations were determined in cell culture supernatants using specific sandwich ELISA kits for IL-1B, IL-1Ra, IL-6 (R&D Systems, Minneapolis). The lowest range of detection was 39 pg/ml for IL-1β; 390 pg/ml for IL-1Ra and 94 pg/ml for IL-6. Samples were diluted before assay 10-fold for IL-1β and IL-1Ra and 20-fold for IL-6.

Genotyping for IL1RN rs9973741

Two independent groups were genotyped (gout group N=246 and control group N=443). Genomic DNA was isolated from whole blood (Promega) and genotyping was performed on an Illumina Infinium HD assay platform using The Infinium Global Screening Array-24 v3.0 BeadChip. Quality control for genotyping data was performed Using Illumina's GenomeStudio. The SNPs with <95% call rate were excluded and all the remaining SNPs were verified and manually re-clustered or removed when necessary. The data were exported to PLINK format and further filters were applied: minor allele frequency > 0.01; Hardy-Weinberg equilibrium test p value > 10⁻⁶; samples with heterozygosity rate of +/-3 standard deviations and related individuals were excluded. For the final step, the strands were flipped and all the data was verified to align to the GRCh37 hg19 build.

Transcriptomics

Freshly isolated PBMCs were frozen in TRIzol Reagent (Invitrogen) and stored at -80°C until bulk RNA-Sequencing analysis (outsourced to Beijing Genomics Institute, BGI, Denmark). The integrity of extracted RNA was assessed using the Agilent 2100 Bioanalyzer. Oligo dT magnetic beads were used to capture mRNA from total RNA. Fragmented target RNA was reverse transcribed to cDNA using random N6 primers followed by end-repair and A tailing for adaptor ligation. Purified ligation products were enriched using PCR amplification followed by denaturation and cyclization of ssDNA by splint oligos and DNA ligase generating DNA nanoballs (DNBs). Sequencing of DNBs was performed on DNBseq platform. Raw data were generated by removing reads mapped to rRNAs. Clean reads were generated using the SOAPnuke software (v.1.5.2) by removing reads with adaptors, reads with unknown bases >10% and low-quality reads. These were later defined as reads with a quality score less than 15 in over 50% bases. Clean reads were mapped to UniGenes and read counts were estimated using Bowtie2 and RSEM (v.1.2.12). Normalization, quality control and identification of differentially expressed genes (DEGs) was performed using the Bioconductor package DESeg2 (Version: DESeg2 1.24.0). Quality control at this stage consisted of removal of samples with highly abnormal values (PCA: ± 3 Standard Deviations on PC1 or PC2). The samples were sequenced in two different batches and the resulting effect was corrected using the limma package. The resulting variance stabilized (VS) counts were used for the target genes for statistical analysis.

Statistical methods

Statistical analysis was performed using GraphPad version 10.0.0 (GraphPad Software, La Jolla California USA) and R software. Comparisons were performed using One-Way ANOVA or Kruskal-Wallis when testing for at least 3 groups, and Student t-test or Mann-Whitney, when comparing 2 groups, Values of P < 0.05 were considered statistically significant.

Results

GWAS identified gout-associated IL1RN rs9973741 variant is an expression quantitative trait locus (eQTL) for IL1RN and IL1F10

As previously reported (19) the gout GWAS signal at the IL1RN locus colocalised with signals of genetic control of expression of both the IL1RN and IL1F10 genes (Figure 1 A-F). The index SNP with the lowest p-value at the IL1RN-IL1F10 region was rs9973741, for which the minor allele G significantly associated with IL-1ß response to MSU crystal stimulation [$\beta = 0.34$, P = 3.6×10^{-4}] (19). The GWAS signal colocalises ((posterior probability of colocalisation > 0.8) with a signal of genetic control of expression (i.e. an expression quantitative trait locus (eQTL)) for each of IL1RN and IL1F10 (19). The gout risk allele, G, was associated to discordant expression patterns in the GTEx data (lower IL1RN expression in adipose tissue versus higher IL1RN expression in testis), suggesting context-specific control of IL1RN expression, while IL1F10 (IL38) showed decreased expression in G allele carriers (19) in skin tissue samples, in both sun exposed and not exposed. Here we show that, in addition to the association of IL1RN rs9973741 with available GTEx data(25) (for IL1RN in subcutaneous adipose tissue and testis (Figure 1C and 1E), and for IL1F10 in skin (Figure 1D and 1F)) the rs9973741 variant is also an eQTL for IL1RN in whole blood according to eQTLGen data (Figure 1B) (Table 1). However, in whole blood data, the variant represents a minor signal, possibly due to the existence of different cell-types in different states of activation (26) (Figure 1B). The gout variant rs9973741 allele G in the eQTLGen dataset is negatively associated with the expression of the IL1RN gene (Z-score -6,715, p= 1,88×10⁻¹¹), consistent with a role for IL-1Ra in suppressing gout.

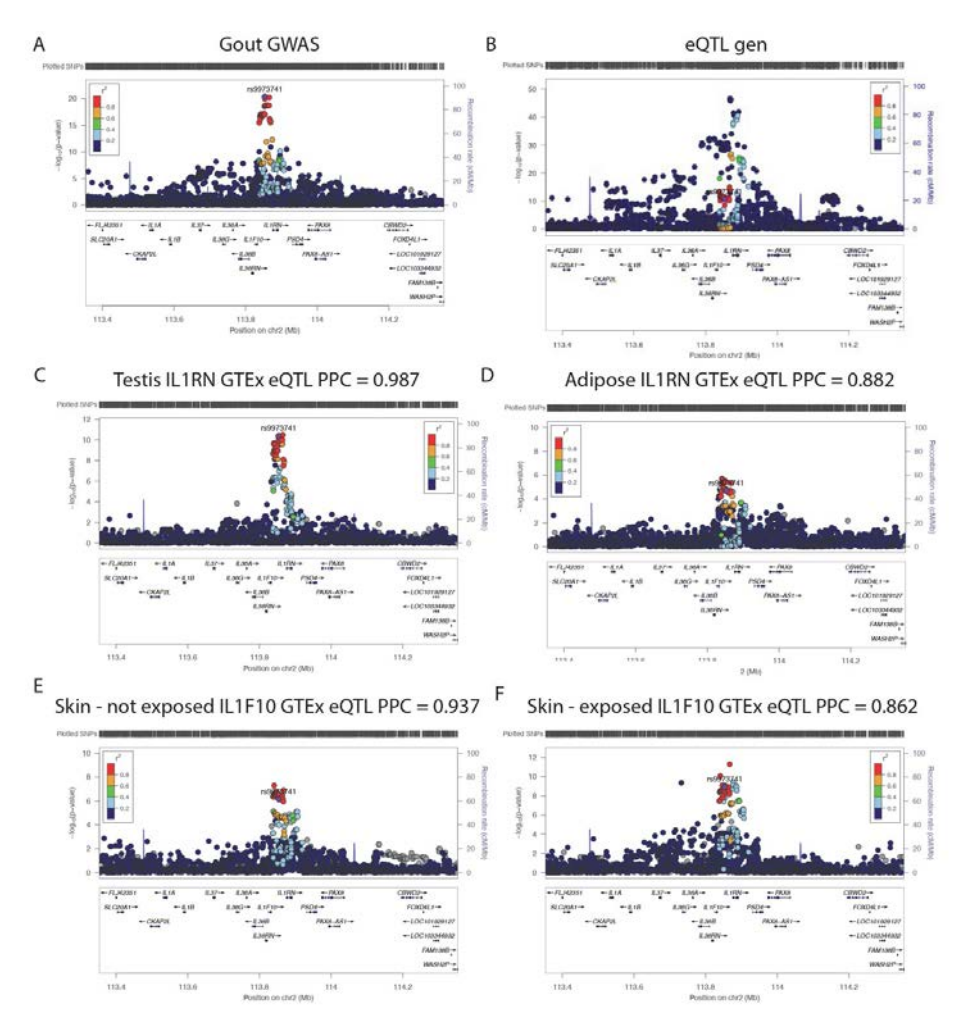


Figure 1 Locus Zoom plots of IL1RN locus in Euroean Gout GWAS, GTEx and eQTLGen dataset (whole blood). The IL1RN rs9973741 SNP is labeled in purple. Each dot represents an individual SNP with the colour representing the LD with the most associated (lead) SNP in the panel. The vertical axis represents -log10 (p value) for assessment of the association of the SNP with IL1RN expression. The genes within the region are annotated, and the direction of the transcripts is shown by arrows. The plot was generated using LocusZoom (22). Values for posterior probability of colocalisation (PPC) are included in the panels.

Moreover, IL-1Ra was identified in a proteome-wide association study (PWAS) of serum urate and gout, showing that genetically-controlled higher IL-1Ra concentrations exhibit protection from gout (27). The IL1RN-IL1F10 region has been found to be associated with different types of markers of systemic inflammation, including Interleukin-1 receptor antagonist protein (IL-1Ra), Interleukin-1 receptor type 1 (IL-1R1), Fibrinogen alpha chain (FGA), Complement factor H-related protein 5 (CFHR5), Interleukin-6 (IL-6) with the lead variant rs55709272 in these studies is in LD with the gout variant rs9973741 (R²=0.83). In addition, the lead gout variant at IL1RN rs9973741 is also amongst the maximally associated variants for several blood cell traits identified in previous GWAS studies (28,29) (Supplementary Figure 1).

Table 1. Association of IL1RN rs9973741 with gene expression in GTEx and eQTLGen datasets, where the assessed allele is "G".

eOTL Tissue P-value Normalized Z-score- Source										
eQTL Gene	Tissue	P-value	Normalized EffectSize-GTEx	2-score- eQTLGen	Source					
IL1F10	Skin - Sun Exposed (Lower leg)	1.10E-09	-0.18	-	GTEx Analysis Release V14					
IL1F10	Skin - Not Sun Exposed (Suprapubic)	6.90E-07	-0.16	-	GTEx Analysis Release V15					
IL1RN	Testis	4.00E-11	0.29	-	GTEx Analysis Release V16					
IL1RN	Skin - Not Sun Exposed (Suprapubic)	1.70E-08	0.13	-	GTEx Analysis Release V17					
IL1RN	Thyroid	8.30E-07	-0.18	-	GTEx Analysis Release V18					
IL1RN	Skin - Sun Exposed (Lower leg)	0.0000069	0.091	-	GTEx Analysis Release V19					
IL1RN	Adipose - Subcutaneous	0.00002	-0.13	-	GTEx Analysis Release V20					
PSD4	Lung	0.0000074	-0.15	-	GTEx Analysis Release V21					
PSD4	Nerve - Tibial	0.000022	-0.16	-	GTEx Analysis Release V22					
PSD4	Blood sample	1.12E-17	-	-8,5603	eQTLGen-2019- 12-25-release					
IL1RN	Blood sample	1.88E-11	-	-6,715	eQTLGen-2019- 12-26-release					
SLC20A1	Blood sample	2.71E-10	-	-6,3146	eQTLGen-2019- 12-27-release					

Basal expression and protein concentrations for IL-1Ra and IL-38 in rs9973741 carriers

We further examined the basal expression level of IL1RN in freshly isolated unstimulated PBMCs from patients with gout or controls (Figure 2A). No association of rs9973741 with IL1RN read counts was observed. Variation in IL1F10 expression could not be assessed due to low expression levels of IL1F10 in PBMCs. We next assessed the basal protein concentration in the plasma of patients with gout and controls. We observed that the gout risk allele is associated with decreasing concentrations of circulating IL-1Ra, consistent with the gene expression data (Figure 2B). For IL-38 protein concentrations, despite many samples being below the detection level (16 pg/ml), a significant association of rs9973741 could still be observed in the control group (AA genotype carriers produced more IL-38 in comparison with the AG genotype, p=0,0073).

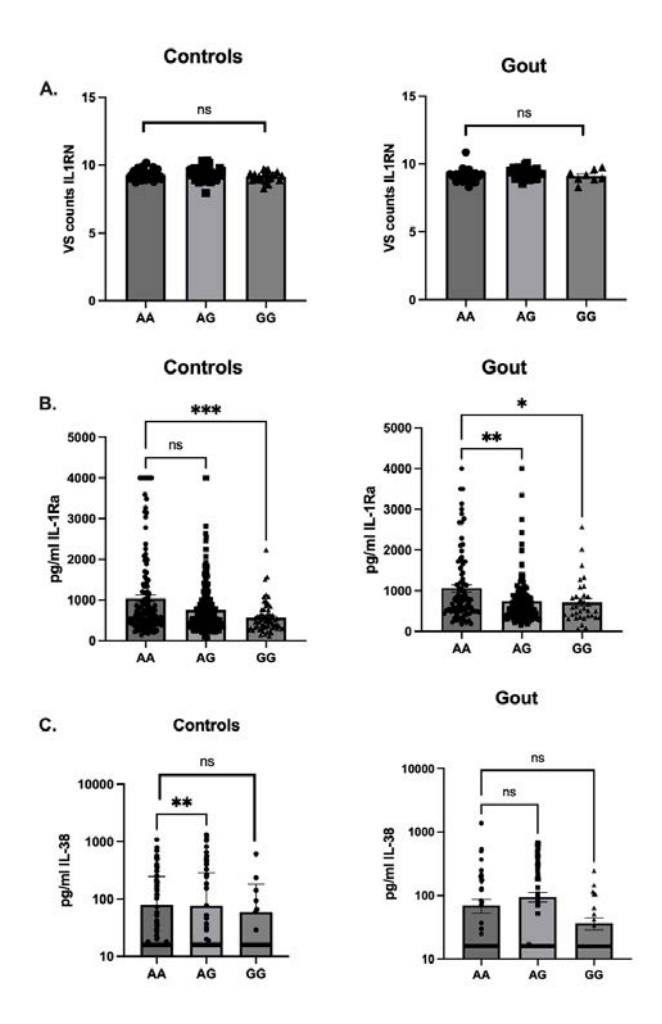


Figure 2 Correlation of the GWAS SNP rs9973741 with IL1RN and IL38 expression levels A. mRNA expression of the two genes in freshly isolated PBMCs originating from gout patients (n=64) and asymptomatic controls (n=128). The data is represented as variance stabilized (VS) counts. B. Circulating IL-1Ra plasma concentrations in n= 443 controls and n=246 gout patients. C. Circulating IL38 concentrations measured in the serum of controls (n=330) and gout patients (n=238). Graphs depict means+/-SEM. Kruskal-Wallis and post-hoc analysis p<0,05

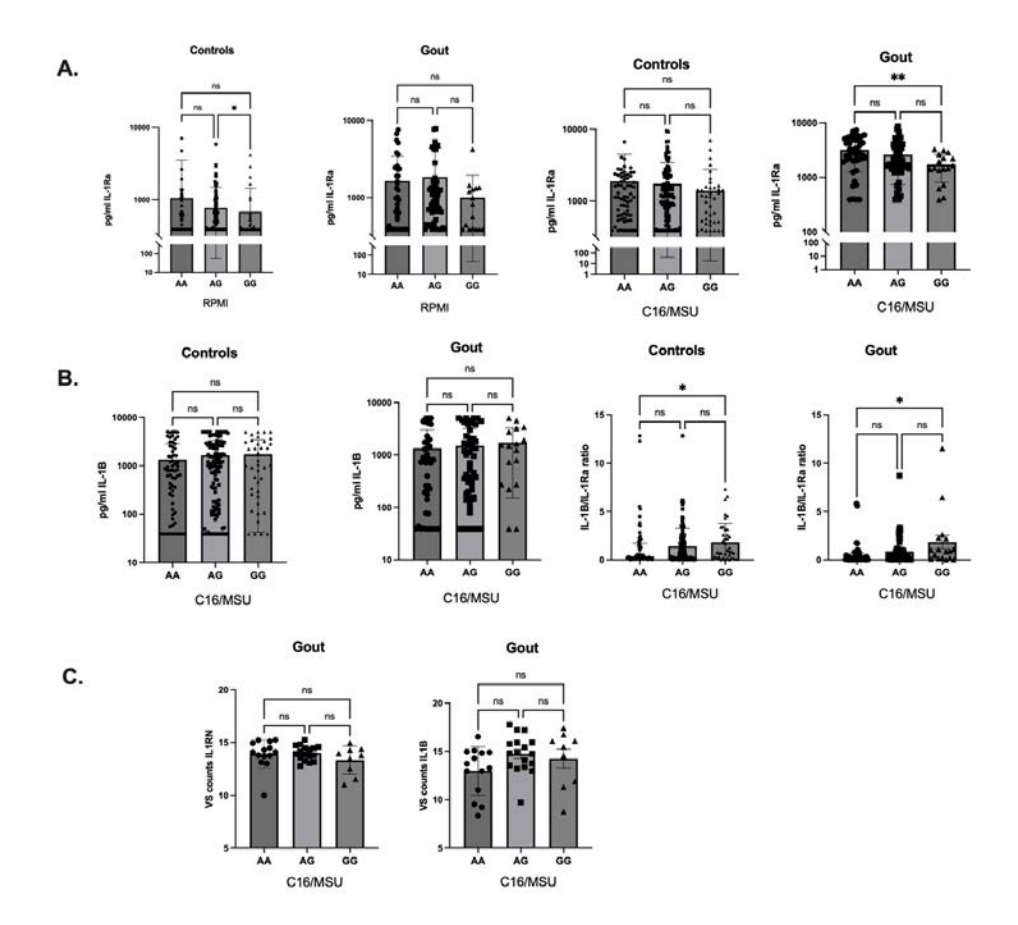


Figure 3 Association of the rs9973741 SNP with *ex vivo* cytokine production **A.** Freshly isolated PBMCs originating from gout patients (n=113) and controls (n=218) stimulated with RPMI, C16 50uM+MSU 300ug/ml and LPS 100ng/ml for 24h. After 24h the supernatants were collected and IL-1Ra (R&D Systems, Minneapolis) was measured. **B.** Concentration of IL-1 β measured in the supernatants of PBMCs after stimulation for 24h. Ratio of IL-1 β and IL-1Ra production in controls and gout patients upon C16/MSU stimulation. The lowest range of detection was 78 pg/ml for IL-1 β ; 390 pg/ml for IL-1Ra. **C.** mRNA expression level of *IL1RN* and *IL1B* in PBMCs stimulated with C16+MSU 300 ug/mL for 24h. Graphs depict mean with SD. Kruskal-Wallis and post-hoc analysis p<0,05

Assessment of *ex vivo* cytokine production capacity in PBMCs of *IL1RN* rs9973741 carriers validates lower IL-1Ra release upon C16 and MSU crystal stimulation in patients with gout.

Next, we performed *ex vivo* functional assays on PBMCs originating from patients with gout and controls, which were stimulated with C16 and MSU crystal for 24h. Cells originating from the control group depicted less unstimulated IL-1Ra release in GG genotype carriers (Figure 3A) but no differences were observed in patients

with gout. However, a significantly lower IL-1Ra production was observed in patients with gout carrying the G allele in response to C16+MSU crystal stimulation (p=0,005) (Figure 3A) and LPS 100 ng (p=0.04) (Supplementary Figure 2C), while no differences were present in the control group. IL-1ß production in response to C16+MSU crystal in cells of patients with gout were not significantly associated with genotype, however the IL-1β/IL-1Ra ratio showed significant differences (Figure 3B). No other statistically significant differences were present in the studied samples (Supplementary Figure 2A, B). Possibly due to lower numbers or due to a less optimal time point of 24h, no significant difference in mRNA levels of the IL1RN and IL1B genes was detected in PBMCs of patients with gout exposed for 24h with the C16+MSU crystal condition (Figure 3C).

Functional validation of elevated IL-1ß release associated to IL1RN rs9973741 in response to C16 + MSU crystal stimulation

As a confirmation of the results presented in our cohort, we investigated the data revealed in the Major et al. study (19) regarding the IL1RN rs9973741 SNP and cytokine production of PBMCs of healthy subjects. For this we used the Human Functional Genomes Project (http://www.humanfunctionalgenomics.org/), where data from 316 healthy controls originating from the Netherlands (included in the 500FG cohort (30)) were used to test association of the rs9973741 SNP with cytokine production. The IL1RN rs9973741 G allele was associated with higher IL-1β in response to C16+MSU crystal (Figure 4A). This effect was specific for C16+MSU crystal as this association was not observed for other stimuli, e.g. LPS or heat killed Candida albicans (Figure 4 B,C).

Discerning regulatory mechanisms of *IL1RN* rs9973741

To further elucidate the functional role of our SNP of interest IL1RN rs9973741, we attempted to identify candidate causal variants using haploreg (version 4.2) and regulomeDB and determined that the genetic variants in linkage equilibrium (LD $R^2 > 0.90$) with IL1RN rs9973741 (19) overlap candidate regions of regulatory function (Supplementary Table 1). These elements include DNA accessibility signatures in blood and transcription factor binding sites in blood cell lines (K652 and GM12878) including important immune cell transcription factors IRF1, CEBPB, MTIF, TFE3 and MAFG. Therefore it is possible that the causal variant could be altering the accesibility or transcriptional regulation of the IL1F10 and/or IL1RN, however these candidate variants remain to be functionally tested.

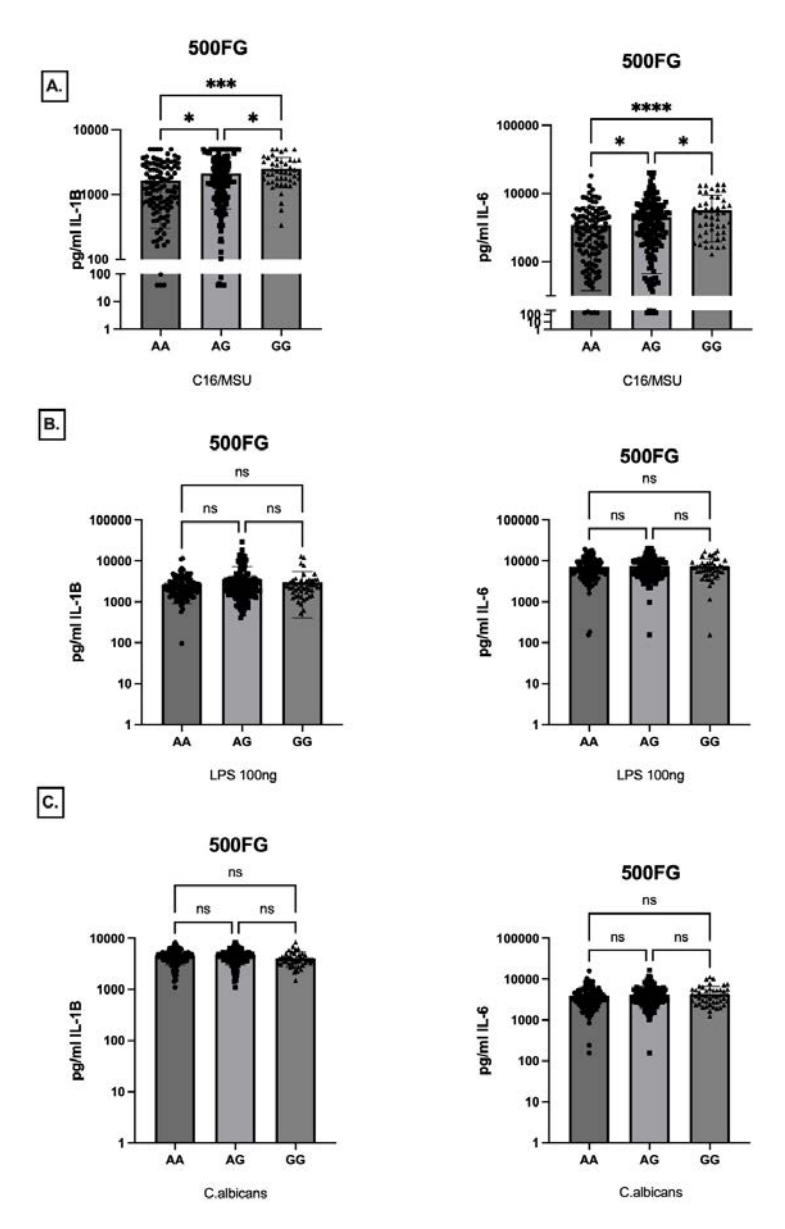


Figure 4 IL-1 β and IL-6 production after 24h stimulation of PBMCs *in vitro*. **A**. Freshly isolated PBMCs originating from healthy controls (n=316) stimulated with C16/MSU crystal 300ug/ml for 24h. After 24h the supernatants were collected and IL-1 β and IL-6 (R&D Systems, Minneapolis) was measured. **B**. Freshly isolated PBMCs originating from healthy controls (n=316) stimulated with LPS 100ng for 24h. After 24h the supernatants were collected and IL-1 β and IL-6 was measured. **C**. Freshly isolated PBMCs originating from healthy controls (n=316) stimulated with Candida albicans conidia for 24h. After 24h the supernatants were collected and IL-1 β and IL-6 was measured. The lowest range of detection was 78 pg/ml for IL-1 β ; 312 pg/ml for IL-6. Graphs depict means with SD. Kruskal-Wallis and post-hoc analysis p<0,05

Discussion

Both genetic and environmental factors are known to account for the development of gout (31-34). For instance, more than 200 urate-associated loci have been identified by genome-wide association studies (35–37). Genes within the identified loci have been causally implicated in urate homeostasis and transport (e.g. SLC2A9, SLC22A12, ABCG2, SLC22A11, SLC17A1, SLC16A9, PDZK1, GCKR, INHBC, HNF4A, MAF), contributing to risk of gout via their implications for hyperuricemia (17.38.39). Recently, 376 loci were associated to gout (19) and a subset of these genes that mapped under these loci were prioritised to be functionally linked to inflammation in gout. Notably, the signal at the IL1RN-IL1F10 region (encoding for the IL-1Ra and IL-38 proteins) was found to be associated to gout and to altered expression of IL1RN and IL1F10.

Both IL-1Ra and IL-38 are anti-inflammatory cytokines of the IL-1 family. IL-1Ra is a natural antagonist of IL-1 signaling, mainly produced by hepatic cells, though monocytes and macrophages also represent an important source. IL-1B is an important inducer of IL-1Ra production along with being one of the essential upstream inducer of many inflammatory cascades (40). The balance between IL-1Ra and IL-1B plays an important role in preventing inflammation-related tissue damage (41). Gout is often described as an IL-1 disease (1,4), in which IL-1Ra is playing an important inhibitory function, by counterbalancing MSU crystal-induced inflammation (42). IL-1F10 (IL-38) has a significant role in the immune responses, suppressing inflammatory conditions (43).

Major et al showed discordant patterns of association for IL1RN expression in different tissues (gout risk allele G associated with increasing expression of IL1RN in testis and decreasing expression in adipose tissue) (19). Further, the identified signal was not associated with urate levels, emphasising a role in inflammatory regulation in gout and not the control of urate levels. The possible mechanism of how the risk variant at this locus could contribute to progression from asymptomatic hyperuricemia to gout pathogenesis needs further assessment. It is conceivable that epigenetic regulatory mechanisms could be at play to explain the control of gene expression observed in association to this genetic signal, given its position within regulatory elements.

Querying the eQTLGen expression data associated the rs9973741 SNP with altered IL1RN expression also in whole blood. This suggests that circulating blood cells are a relevant system to study this SNP and inflammatory consequences. Furthermore, the IL1RN-IL1F10 region has also been found to associate with circulating markers of inflammation, including IL-1Ra and IL-6 protein levels, in previous GWAS (27–29). The lead SNP in these GWAS is in LD with the lead gout SNP presented in this paper (IL1RN rs9974741) suggesting that these signals of association "gout, IL-1Ra and IL6" are shared.

In our study, when assessing IL1RN gene expression in unstimulated freshly isolated PBMCs from patients with gout or controls we did not observe an association with the IL1RN rs9973741 SNP. Importantly however, the gout risk allele G was associated to significantly lower concentrations of circulating IL-1Ra in both controls and patients with gout. This is consistent with the other associations for blood cell traits from the UKBB centered on the gout SNP rs9974741 at the IL1RN-IL1F10 region which include monocyte count and monocyte percentage suggesting that IL1RN expression in these alternative tissues alters the composition of monocytes in blood which could contribute to levels of circulating IL-1Ra.

Ex vivo cytokine secretion by freshly isolated PBMCs revealed significantly lower IL-1Ra production in response to C16+MSU crystal costimulation in patients with gout. In line with the lower IL-1Ra in G allele carriers, the SNP was associated with significantly elevated IL-1 β /IL-1Ra ratio in gout patients and in controls. The significant rise in IL-1β cytokine production in response to C16+MSU crystals was also replicated in G-allele carriers among the healthy controls of the 500FG cohort. Our data indicate that the IL1RN rs9973741 variant is associated with differential cytokine production in blood mononuclear cells with possible implications for inflammatory risk in gout progression: the decrease in IL-1Ra circulating protein production in addition to an altered cytokine profile could contribute to elevated IL-1β production by myeloid cells when activated with MSU crystals and synergizing stimuli. This can subsequently mediate the autoinflammatory events characteristic to symptomatic gout.

On the one hand, the downregulation of IL-1Ra in the context of gout was already reported in the literature(44,45). On the other hand, in other rheumatic disorders, such as systemic lupus erythematosus (SLE) high IL-1Ra production by monocytes was observed when comparing to controls(46). Moreover, elevated systemic IL-1Ra concentrations are described in individuals with cardiometabolic risk factors, such as obesity, insulin resistance and type 2 diabetes mellitus (47-49). These findings show that IL-1Ra is a marker of inflammation (being induced in inflammatory conditions), as well as a potent inhibitor of IL-1R1 signaling. Nevertheless, the severe deficit of IL-1Ra results in life-theatening autoinflammatory disease (50),

therefore the association of the rs9973741 SNP with reduced IL-1Ra production is extremely relevant and might contribute to the inflammatory state in gout.

The model of IL-1B/IL-1Ra dysregulation in the pathogenesis of gout has also been evoked in other studies. In PBMCs from healthy donors, urate influences inflammatory responses by causing a shift in the IL-1\beta/IL-1Ra balance, decreasing IL-1Ra concentrations at both the transcriptional and protein levels, contributing to more robust inflammatory responses upon subsequent stimulation in vitro (20,21). Importantly, in a recent proteome-wide association study of serum urate and gout an association between genetically higher levels of IL1Ra and lower odds of gout was observed (27), supporting the results presented in this study.

Some limitations of our research need mentioning. First, the participants involved in the study were all of European descent, which restricts the generalisation of these findings to other ancestries. Another limitation is the cross-sectional design, making causal interpretations of association between IL1RN rs9973741 and inflammation difficult – this variant, while the strongest associated at the locus, could be in linkage disequilibrium with the causal variant. Furthermore, the high inter-individual variability in cytokine data coming from primary cells precludes robust conclusions in some comparisons with moderate sample sizes, and it is obvious that larger cohorts are needed. Nevertheless, this study has the strength of assessing the association of the SNP of interest with cytokine production at several layers: transcription data together with circulating proteins and ex vivo cytokine measurements in stimulated primary PBMCs of a relatively large number of patients with gout and controls.

In conclusion, using two independent study cohorts and the lead gout SNP, we show that the G allele of the IL1RN rs9973741 variant associates with lower circulating concentrations of IL-1Ra, lower IL-1Ra production in PBMC assays and elevated IL-1β production in PBMCs challenged with C16+MSU crystals. Our data indicate that the genetic signal that associates with gout at IL1RN-IL1F10 region (or locus) revealed to alter the expression of both IL1RN and IL1F10 resulting in modified cytokine profiles, leading to elevated bioactive IL-1\u00e3.

References

- 1. Dalbeth N, Gosling AL, Gaffo A, Abhishek A. Gout. Lancet. 2021;397(10287):1843-55.
- 2. Mattiuzzi C, Lippi G. Recent updates on worldwide gout epidemiology. 2019;(Icd):10-2.
- Kuo CF, Grainge MJ, Zhang W, Doherty M. Global epidemiology of gout: Prevalence, incidence 3. and risk factors. Nature Reviews Rheumatology. 2015.
- Dalbeth N, Choi HK, Joosten LAB, Khanna PP, Matsuo H, Perez-Ruiz F, et al. Gout. Nat Rev Dis Prim. 4. 2019;5(1).
- 5. Narang RK, Dalbeth N. Pathophysiology of Gout. Semin Nephrol. 2020 Nov;40(6):550–63.
- Klück V, Liu R, Joosten LAB. The role of interleukin-1 family members in hyperuricemia and gout. 6. Jt Bone Spine. 2021;88(2).
- Arena WP, Malyak M, Guthridge CJ, Gabay C. Interleukin-1 receptor antagonist: Role in biology. 7. Annu Rev Immunol. 1998:16:27-55.
- 8. Frühbeck G, Catalán V, Ramírez B, Valentí V, Becerril S, Rodríguez A, et al. Serum Levels of IL-1 RA Increase with Obesity and Type 2 Diabetes in Relation to Adipose Tissue Dysfunction and are Reduced After Bariatric Surgery in Parallel to Adiposity. J Inflamm Res. 2022;15(February):1331-45.
- Mantovani A, Dinarello CA, Molgora M, Garlanda C. IL-1 and related cytokines in innate and adaptive immunity in health and disease. Immunity [Internet]. 2019;50(4):778. Available from: / pmc/articles/PMC7174020/%0A/pmc/articles/PMC7174020/?report=abstract%0Ahttps://www. ncbi.nlm.nih.gov/pmc/articles/PMC7174020/
- 10. Bensen JT, Dawson PA, Mychaleckyj JC, Bowden DW. Identification of a novel human cytokine gene in the interleukin gene cluster on chromosome 2g12-14. J Interf Cytokine Res. 2001;21(11):899-904.
- 11. Xu WD, Huang AF. Role of interleukin-38 in chronic inflammatory diseases: A comprehensive review. Front Immunol. 2018;9(JUN).
- 12. Renaudin F, Orliaguet L, Castelli F, Fenaille F, Prignon A, Alzaid F, et al. Gout and pseudo-goutrelated crystals promote GLUT1-mediated glycolysis that governs NLRP3 and interleukin-1B activation on macrophages. Ann Rheum Dis. 2020;79(11):1506-14.
- 13. Vazirpanah N, Ottria A, Van Der Linden M, Wichers CGK, Schuiveling M, Van Lochem E, et al. MTOR inhibition by metformin impacts monosodium urate crystal-induced inflammation and cell death in gout: A prelude to a new add-on therapy? Ann Rheum Dis. 2019;78(5):663-71.
- 14. Martinon F, Pétrilli V, Mayor A, Tardivel A, Tschopp J. Gout-associated uric acid crystals activate the NALP3 inflammasome. Nature. 2006:
- 15. Sandoval-Plata G, Morgan K, Abhishek A. Variants in urate transporters, ADH1B, GCKR and MEPE genes associate with transition from asymptomatic hyperuricaemia to gout: Results of the first gout versus asymptomatic hyperuricaemia GWAS in Caucasians using data from the UK Biobank. Ann Rheum Dis. 2021;80(9):1220-6.
- 16. Lin C-Y, Chang Y-S, Liu T-Y, Huang C-M, Chung C-C, Chen Y-C, et al. Genetic contributions to female gout and hyperuricaemia using genome-wide association study and polygenic risk score analyses. Rheumatology [Internet]. 2023 Feb 1;62(2):638-46. Available from: https://doi. org/10.1093/rheumatology/keac369
- 17. Kawamura Y, Nakaoka H, Nakayama A, Okada Y, Yamamoto K, Higashino T, et al. Genome-wide association study revealed novel loci which aggravate asymptomatic hyperuricaemia into gout. Ann Rheum Dis. 2019;78(10).

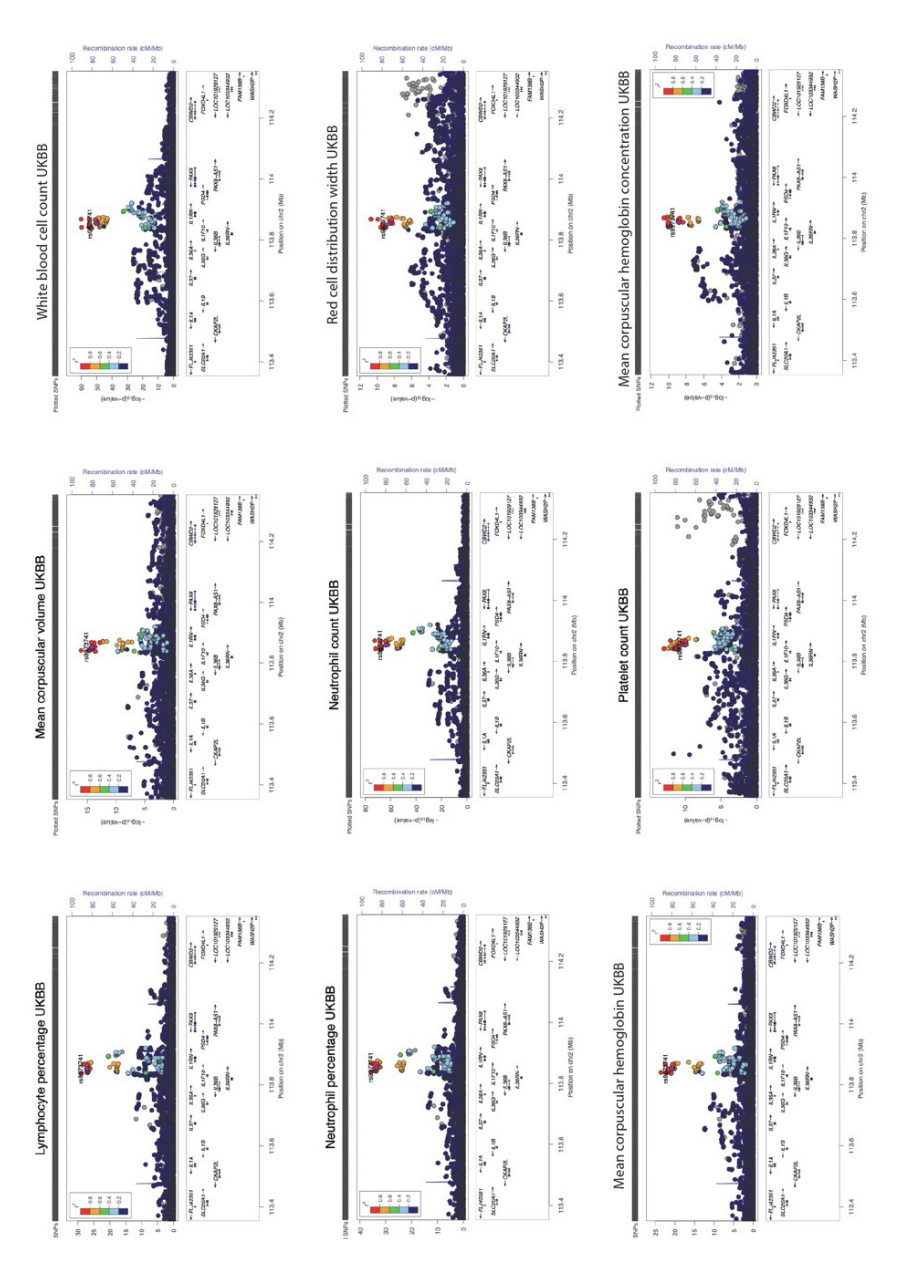
- 18. Sumpter NA, Takei R, Leask MP, Reynolds RJ, Merriman TR. Genetic association studies of the progression from hyperuricaemia to gout. Rheumatology (Oxford). 2022 May;61(6):e139-40.
- 19. Major TJ, Takei R, Matsuo H, Leask MP, Topless RK, Shirai Y, et al. A genome-wide association analysis of 2,622,830 individuals reveals new pathogenic pathways in gout. medRxiv [Internet]. 2022 Jan 1;2022.11.26.22281768. Available from: http://medrxiv.org/content/ early/2022/11/29/2022.11.26.22281768.abstract
- 20. Badii M, Gaal Ol, Cleophas MC, Klück V, Davar R, Habibi E, et al. Urate-induced epigenetic modifications in myeloid cells. Arthritis Res Ther. 2021;23(1):1-11.
- 21. Crisan TO, Cleophas MCP, Oosting M, Lemmers H, Toenhake-Diikstra H, Netea MG, et al. Soluble uric acid primes TLR-induced proinflammatory cytokine production by human primary cells via inhibition of IL-1Ra. Ann Rheum Dis. 2016;
- 22. Pruim RJ, Welch RP, Sanna S, Teslovich TM, Chines PS, Gliedt TP, et al. LocusZoom: Regional visualization of genome-wide association scan results. Bioinformatics. 2011;27(13):2336-7.
- 23. Lin S-H, Brown DW, Machiela MJ. LDtrait: An Online Tool for Identifying Published Phenotype Associations in Linkage Disequilibrium. Cancer Res. 2020 Aug;80(16):3443-6.
- 24. Machiela MJ, Chanock SJ. LDlink: a web-based application for exploring population-specific haplotype structure and linking correlated alleles of possible functional variants. Bioinformatics. 2015 Nov;31(21):3555-7.
- 25. Consortium G. The GTEx Consortium atlas of genetic regulatory effects across human tissues The GTEx Consortium* Downloaded from. 2021; Available from: http://science.sciencemag.org/
- 26. Võsa U, Claringbould A, Westra H-J, Bonder MJ, Deelen P, Zeng B, et al. Large-scale cis- and transeQTL analyses identify thousands of genetic loci and polygenic scores that regulate blood gene expression. Nat Genet [Internet]. 2021;53(9):1300-10. Available from: https://doi.org/10.1038/ s41588-021-00913-z
- 27. Zhang J, Dutta D, Köttgen A, Tin A, Schlosser P, Grams ME, et al. Plasma proteome analyses in individuals of European and African ancestry identify cis-pQTLs and models for proteome-wide association studies. Nat Genet. 2022;54(5):593-602.
- 28. Astle WJ, Elding H, Jiang T, Allen D, Ruklisa D, Mann AL, et al. The Allelic Landscape of Human Blood Cell Trait Variation and Links to Common Complex Disease. Cell. 2016;167(5):1415-1429.e19.
- 29. Tekola Ayele F, Doumatey A, Huang H, Zhou J, Charles B, Erdos M, et al. Genome-wide associated loci influencing interleukin (IL)-10, IL-1Ra, and IL-6 levels in African Americans. Immunogenetics [Internet]. 2012;64(5):351-9. Available from: https://doi.org/10.1007/s00251-011-0596-7
- 30. Ter Horst R, Jaeger M, Smeekens SP, Oosting M, Swertz MA, Li Y, et al. Host and Environmental Factors Influencing Individual Human Cytokine Responses. Cell. 2016 Nov;167(4):1111-1124.e13.
- 31. Matsuo H, Takada T, Ichida K, Nakamura T, Nakayama A, Ikebuchi Y, et al. Common defects of ABCG2, a high-capacity urate exporter, cause gout: a function-based genetic analysis in a Japanese population. Sci Transl Med. 2009 Nov;1(5):5ra11.
- 32. Li Z, Zhou Z, Hou X, Lu D, Yuan X, Lu J, et al. Replication of Gout/Urate Concentrations GWAS Susceptibility Loci Associated with Gout in a Han Chinese Population. Sci Rep. 2017 Jun;7(1):4094.
- 33. Boocock J, Leask M, Okada Y, Matsuo H, Kawamura Y, Shi Y, et al. Genomic dissection of 43 serum urate-associated loci provides multiple insights into molecular mechanisms of urate control. Hum Mol Genet. 2020;

- 34. Takei R, Sumpter NA, Phipps-Green A, Cadzow M, Topless RK, Reynolds RJ, et al. Correspondence on 'Variants in urate transporters, ADH1B, GCKR and MEPE genes associated with transition from asymptomatic hyperuricaemia to gout: results of the first gout versus asymptomatic hyperuricaemia GWAS in Caucasians using data from the UK Biob. Annals of the rheumatic diseases. England; 2021.
- 35. Köttgen A, Albrecht E, Teumer A, Vitart V, Krumsiek J, Hundertmark C, et al. Genome-wide association analyses identify 18 new loci associated with serum urate concentrations. Nat Genet. 2013;45(2):145-54.
- 36. Tin A, Marten J, Halperin Kuhns VL, Li Y, Wuttke M, Kirsten H, et al. Target genes, variants, tissues and transcriptional pathways influencing human serum urate levels. Nat Genet. 2019;
- 37. Major TJ, Dalbeth N, Stahl EA, Merriman TR. An update on the genetics of hyperuricaemia and gout. Vol. 14, Nature Reviews Rheumatology. 2018.
- 38. Matsuo H, Yamamoto K, Nakaoka H, Nakayama A, Sakiyama M, Chiba T, et al. Genome-wide association study of clinically defined Gout identifies multiple risk loci and its association with clinical subtypes. Ann Rheum Dis. 2016;75(4).
- 39. Nakayama A, Nakaoka H, Yamamoto K, Sakiyama M, Shaukat A, Toyoda Y, et al. GWAS of clinically defined gout and subtypes identifies multiple susceptibility loci that include urate transporter genes. Ann Rheum Dis. 2017;76(5).
- 40. Dinarello CA. Immunological and Inflammatory Functions of the Interleukin-1 Family. Annu Rev Immunol. 2009 Mar 20;27(1):519-50.
- 41. Arend WP, Gabay C. Physiologic role of interleukin-1 receptor antagonist. Arthritis Res. 2000;2(4):245-8.
- 42. ElSayed S, Jay GD, Cabezas R, Qadri M, Schmidt TA, Elsaid KA. Recombinant Human Proteoglycan 4 Regulates Phagocytic Activation of Monocytes and Reduces IL-1ß Secretion by Urate Crystal Stimulated Gout PBMCs. Front Immunol. 2021;12(December):1–17.
- 43. Graaf DM De, Jaeger M, Den ICL Van, Mercurio L, Madonna S, Rutten JHW, et al. Reduced concentrations of the B cell cytokine interleukin 38 are associated with cardiovascular disease risk in overweight subjects. 2021;662-71.
- 44. Roberge CJ, de Médicis R, Dayer JM, Rola-Pleszczynski M, Naccache PH, Poubelle PE. Crystalinduced neutrophil activation. V. Differential production of biologically active IL-1 and IL-1 receptor antagonist. J Immunol [Internet]. 1994 Jun 1;152(11):5485-94. Available from: https:// doi.org/10.4049/jimmunol.152.11.5485
- 45. Crişan TO, Cleophas MCP, Novakovic B, Erler K, Van De Veerdonk FL, Stunnenberg HG, et al. Uric acid priming in human monocytes is driven by the AKT-PRAS40 autophagy pathway. Proc Natl Acad Sci U S A. 2017;
- 46. Italiani P, Manca ML, Angelotti F, Melillo D, Pratesi F, Puxeddu I, et al. IL-1 family cytokines and soluble receptors in systemic lupus erythematosus. Arthritis Res Ther. 2018;20(1):1-10.
- 47. Meier CA, Bobbioni E, Gabay C, Assimacopoulos-Jeannet F, Golay A, Dayer JM. IL-1 receptor antagonist serum levels are increased in human obesity: A possible link to the resistance to leptin? J Clin Endocrinol Metab. 2002;87(3):1184-8.
- 48. Abdullah AR, Hasan HA, Raigangar VL. Analysis of the Relationship of Leptin, High-Sensitivity C-Reactive Protein, Adiponectin, Insulin, and Uric Acid to Metabolic Syndrome in Lean, Overweight, and Obese Young Females. Metab Syndr Relat Disord [Internet]. 2009;7(1):17-22. Available from: http://www.liebertonline.com/doi/abs/10.1089/met.2008.0045
- 49. Volarevic V, Al-Qahtani A, Arsenijevic N, Pajovic S, Lukic ML. Interleukin-1 receptor antagonist (IL-1Ra) and IL-1Ra producing mesenchymal stem cells as modulators of diabetogenesis. Autoimmunity. 2010;43(4):255-63.

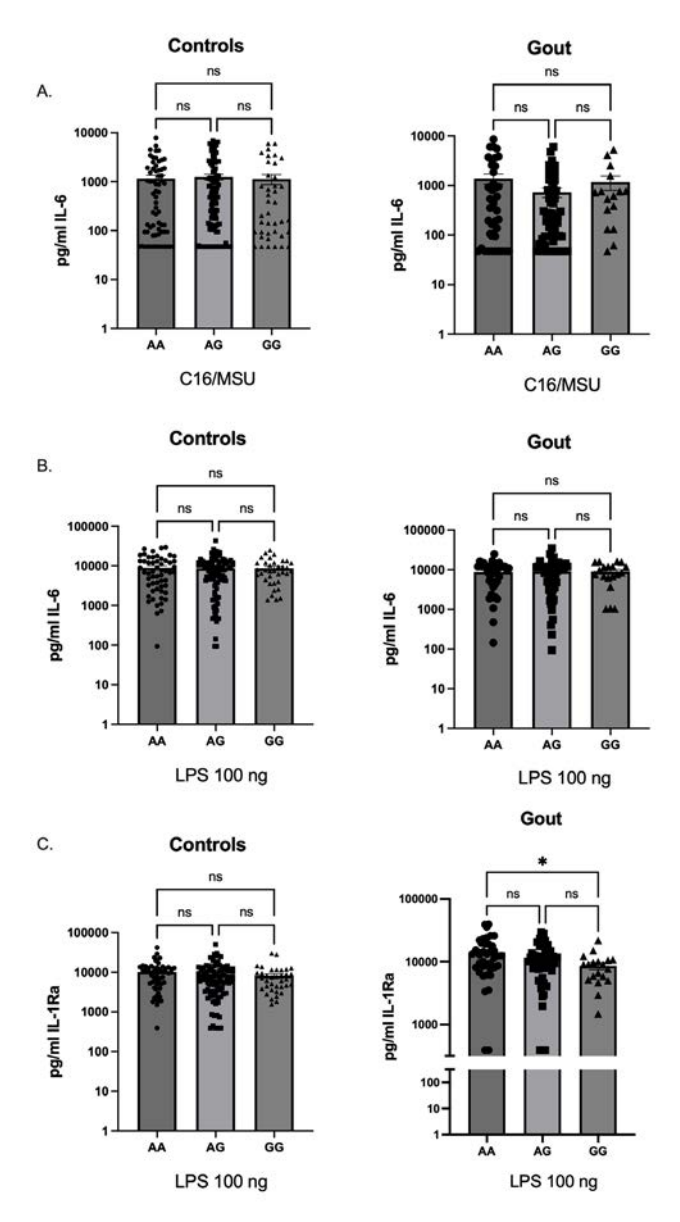
50. Aksentijevich I, Masters SL, Ferguson PJ, Dancey P, Frenkel J, van Royen-Kerkhoff A, et al. An autoinflammatory disease with deficiency of the interleukin-1-receptor antagonist. N Engl J Med. 2009 Jun;360(23):2426-37.

HINT consortium: Leo A. B. Joosten, Ioan V. Pop, Radu A. Popp, Simona Rednic, Cristina Pamfil, Tania O. Crisan, Marius Farcast, Dragos H. Marginean, Orsolya I. Gaal, Medeea O. Badii, Ioana Hotea, Loredana Peca, Andreea-Manuela Mirea, Georgiana Cabău, Valentin Nica, Doina Colcear, Mariana S. Pop, Ancuta Rus

Supplemental Data



Supplementary figure 1 Locus Zoom plots for blood cell traits centered on the gout rs9973741 SNP using the UKBB dataset. The IL1RN rs9973741 SNP is labeled in purple. The plot was generated using LocusZoom (22).



Supplementary figure 2 IL-6 and IL-1Ra production after 24h stimulation of PBMCs in vitro A. Freshly isolated PBMCs originating from gout patients (n=113) and controls (n=218) stimulated with C16/ MSU 300ug/ml for 24h. After 24h the supernatants were collected and IL-1β and IL-6 (R&D Systems, Minneapolis) was measured. B. Freshly isolated PBMCs originating from from gout patients (n=113) and controls (n=193) stimulated with LPS 100ng for 24h. After 24h the supernatants were collected and IL-6 was measured. C. Freshly isolated PBMCs originating from gout patients (n=113) and controls (n=218) stimulated with LPS 100ng for 24h. After 24h the supernatants were collected and IL-1Ra was measured. The lowest range of detection was 78 pg/ml for IL-1β; 312 pg/ml for IL-6. Graphs depict means+/-SEM. Kruskal-Wallis and post-hoc analysis p<0,01.

Supplementary Table 1. Annotations of potential regulatory SNPs in regulomeDB and Haploreg.

chr	pos (hg38)	LD	LD	variant	Ref	Alt	AFR	AMR	ASN	EUR	Promoter
		(r ²)	(D')	-			freq	freq	freq	freq	histone marks
2	113080525	0,88	0,94	rs13409360	G	Α	0,42	0,31	0,08	0,38	
2	113080568	0,89	0,94	rs13409371	G	Α	0,42	0,31	0,08	0,38	
2	113082481	0,92	0,97	rs6743171	G	С	0,21	0,3	0,08	0,38	
2	113082866	0,93	0,97	rs10188292	Α	Т	0,28	0,31	0,08	0,38	
		,	.,.				,	.,-	,,,,,,,,,,,,,,,,,,,,,,,,,,,,,,,,,,,,,,,	,,,,,,,,,,,,,,,,,,,,,,,,,,,,,,,,,,,,,,,	
2	113082998	0,93	0,97	rs10176274	C	G	0,3	0,31	0,08	0,38	
2	113083453	0,88	0,96	rs6734238	Α	G	0,48	0,32	0,08	0,39	
2	113083938	0,93	0,97	rs6722922	C	Т	0,31	0,31	0,08	0,38	
2	113083955	0,93	0,97	rs6750559	G	Α	0,34	0,31	0,08	0,38	
2	113084929	0,93	0,97	rs13398728	Т	C	0,31	0,31	0,08	0,38	
2	113085706	0,93	0,97	rs13410964	G	Α	0,28	0,31	0,08	0,38	
		,	•				•	•	•	,	
2	113086807	0,93	0,97	rs6741180	G	Α	0,34	0,31	0,08	0,38	
2	113086898	0,92	0,97	rs4496335	С	Т	0,21	0,3	0,08	0,38	
2	113089161	0,93	0,97	rs12328766	Α	G	0,43	0,31	0,08	0,38	
2	113089430	0,93	0,97	rs12329129	G	Α	0,34	0,31	0,08	0,38	
2	113089567	0,93	0,97	rs12328368	C	G	0,34	0,31	0,08	0,38	
2	113091384	0,93	0,97	rs6730516	C	Т	0,21	0,3	0,08	0,38	
2	113092685	0,93	0,97	rs7587033	C	G	0,34	0,31	0,08	0,38	
2	113093215	0,94	0,97	rs6738239	C	Α	0,34	0,31	0,08	0,38	
2	113093582	0,93	0,97	rs1446509	Α	Τ	0,34	0,31	0,08	0,38	
2	113093940	0,94	0,97	rs1446510	С	Т	0,34	0,31	0,08	0,38	
2	113094987	0,99	1	rs13424580	G	Α	0,21	0,29	0,08	0,38	
2	113095804	1	1	rs9973741	Α	G	0,35	0,31	0,08	0,38	
2	113095879	0,85	0,94	rs62158846	G	Т	0,33	0,33	0,11	0,39	
2	113096543	0,98	0,99	rs6746979	Т	Α	0,35	0,31	0,08	0,38	

Enhancer	DNAse	Proteins	Motifs	GENCODE
histone marks		bound	changed	genes
IPSC, FAT, BRST, SKIN, LIV, GI, MUS	BLD			4.7kb 3' of IL1F10
IPSC, FAT, BRST, SKIN, LIV, GI, MUS	BLD		CEBPB,CEBPD,Maf,p300	4.7kb 3' of IL1F10
				4.3kb 5' of U6
			ERalpha- a, Esr 2, PPAR, Pou 1f 1, RORalpha 1	3.9kb 5' of U6
			Evi-1,Hmbox1,Nkx2,Nkx3	3.8kb 5' of U6
BLD	BLD,BLD,BLD		Pbx3,RXRA	3.4kb 5' of U6
BLD			CACD,CTCF,SETDB1,SMC3,VDR	2.9kb 5' of U6
BLD			CCNT2,HNF1,Smad,TAL1	2.8kb 5' of U6
FAT, BRST, SKIN, GI				1.9kb 5' of U6
BRST, SKIN, GI, LIV	BRST,SKIN,PLCNT, BRST,SKIN		AP-1,PRDM1	1.1kb 5' of U6
				U6
				U6
LIV			Arid3a,Arid5a,Dbx1,Hlx1,Ho xd8,Lhx3,Ncx,Pax-6,Sox	2.2kb 3' of U6
BLD, LIV				2.5kb 3' of U6
BLD, LIV			FAC1	2.7kb 3' of U6
			Ets,Nanog,ZBTB33	4.5kb 3' of U6
MUS			Pax-4,TR4,Zic	5.8kb 3' of U6
MUS			STAT	6.3kb 3' of U6
MUS			AP-1,BCL,ERalpha- a,HNF4,NRSF,Sin3Ak-20,Smad	6.7kb 3' of U6
				7kb 3' of U6
			PLZF,Sox,TCF4	8.1kb 3' of U6
			Foxp1,HNF1,Maf,Pou2f2,TATA	8.9kb 3' of U6
			CDP,Cdx,Dbx1,Foxa,Foxd3,Foxf1,Foxi1, Foxj1,Foxj2,Foxk1,Foxl1,Foxo,HDAC2,H NF1,Hlx1,Hmx,Hoxb8,Hoxd8,Mef2,Ncx ,Pbx-1,Pou3f2,Pou3f4,Sox,TATA,Zfp105	9kb 3' of U6

Supplementary Table 1. Continued

chr	pos (hg38)	LD	LD	variant	Ref	Alt	AFR	AMR	ASN	EUR	Promoter
		(r²)	(D')	-			freq	freq	freq	freq	histone marks
2	113097266	0,97	0,99	rs7596350	Α	G	0,33	0,3	0,08	0,38	
2	113098058	0,97	0,99	rs55896126	G	C	0,21	0,29	0,08	0,38	BLD
2	113102184	0,98	0,99	rs7574159	G	Α	0,35	0,31	0,07	0,38	
2	113102461	0,97	0,99	rs7574427	G	Α	0,23	0,3	0,07	0,38	
2	113105959	0,98	0,99	rs13382561	Α	G	0,35	0,31	0,08	0,38	
2	113106433	0,97	0,99	rs17207494	Α	C	0,22	0,3	0,08	0,38	
2	113107837	0,97	0,99	rs28648961	G	Α	0,27	0,3	0,08	0,38	
2	113108257	0,91	0,99	rs10171849	Α	С	0,31	0,3	0,07	0,36	
2	113109277	0,87	0,98	rs7580634	G	Т	0,21	0,31	0,08	0,4	
2	113109711	0,83	0,98	rs55709272	Т	С	0,52	0,34	0,08	0,42	

Enhancer	DNAse	Proteins	Motifs	GENCODE genes	
histone marks		bound	changed		
				9.9kb 5' of IL1RN	
BLD, GI		MEF2A	AP-1,FXR,GATA,Obox3,SP1,TATA,p300	9.2kb 5' of IL1RN	
	SKIN			5kb 5' of IL1RN	
			DMRT7	4.8kb 5' of IL1RN	
				1.3kb 5' of IL1RN	
			Dobox4,Pax-5	780bp 5' of IL1RN	
			Elf5,Evi-1,Pax-4,Pou2f2	IL1RN	
			Cdx2,FXR,Glis2,HDAC2,HMG- IY,Hoxa9,Hoxc9,Mef2,Pax- 4,Pou6f1,TATA,Zfp105	IL1RN	
			Egr-1,Klf4,NRSF,RREB- 1,STAT,VDR,ZNF219,Zfp740	IL1RN	
			E4F1,Hmx,lsl2,Nkx2,Nkx3,Nrf- 2,TCF11::MafG	IL1RN	



Chapter 3

GWAS-identified hyperuricemiaassociated IGF1R variant rs6598541 has a limited role in urate mediated inflammation in human mononuclear cells

Orsolya I. Gaal, Ruiqi Liu, Dragoş Marginean, Medeea Badii, Georgiana Cabău, Ioana Hotea, Valentin Nica, Doina Colcear, HINT Consortium, Cristina Pamfil, Tony R. Merriman, Simona Rednic, Radu A.Popp, Tania O. Crişan*, Leo A.B Joosten*

#These authors share senior authorship

Abstract

Introduction

Gout is a common autoinflammatory joint diseases characterized by deposition of monosodium urate (MSU) crystals which trigger an innate immune response mediated by inflammatory cytokines. IGF1R is one of the loci associated with both urate levels and gout susceptibility in GWAS to date, and IGF-1-IGF-1R signaling is implicated in urate control.

Objectives

We investigate the role of IGF-1/IGF1R signaling in the context of gouty inflammation. Also, to test the gout and urate-associated IGF1R rs6598541 polymorphism for association with the inflammatory capacity of mononuclear cells.

Methods

Freshly isolated human peripheral blood mononuclear cells (PBMCs) were exposed to recombinant IGF-1 or anti-IGF1R neutralizing antibody in the presence or absence of solubilized urate, stimulated with LPS/MSU crystals. Association of rs6598541 with IGF1R and protein expression and with ex vivo cytokine production levels after stimulation with gout specific stimuli was tested.

Results

Urate exposure was not associated with IGF1R expression in vitro or in vivo. Modulation of IGF1R did not alter urate-induced inflammation. Developing urateinduced trained immunity in vitro was not influenced in cells challenged with IGF-1 recombinant protein. The IGF1R rs6598541 SNP was not associated with cytokine production.

Conclusions

Our results indicate that urate-induced inflammatory priming is not regulated by IGF-1/IGF1R signaling in vitro. IGF1R rs6598541 status was not asociated with IGF1R expression or cytokine production in primary human PBMCs. This suggests that the role of IGF1R in gout is tissue-specific and may be more relevant in the control of urate levels rather than in inflammatory signaling in gout.

Introduction

Gout is an important inflammatory disease with high prevalence in developed countries among men and postmenopausal women 1,2 with prevalence increasing worldwide3. The precondition for developing gout is the deposition of monosodium urate (MSU) crystals in the joint and other tissues as a result of elevated serum urate levels (hyperuricemia)⁴. While most research focuses on inflammation due to MSU crystal deposition 5-7, there is evidence that soluble urate also increases pro-inflammatory cytokine production⁸, associating hyperuricemia with a hyper-inflammatory state ^{9,10}, highlighting its pro-inflammatory effects within the intracellular setting together with an altered epigenetic landscape 11. Additionally, there exist indication on how soluble urate induce epigenetic modifications in myeloid cells, leading to an enhanced inflammatory response 12,13. Moreover, hyperuricemia may lead to innate immune memory, contributing to a persistently elevated inflammatory status 11,12,14. In conditions associated with chronic inflammation, such as metabolic syndrome, obesity and cardiovascular disease, there is an increased prevalence of hyperuricemia, suggesting that the link between hyperuricemia and inflammation is perhaps bidirectional. While inflammation itself may influence urate levels, alternatively elevated urate levels may add to an inflammatory state. The pathogenetic mechanism of gout at molecular level is not well established. Although, several treatment possibilities are already available such as colchicine, nonsteroidal anti-inflammatory drugs, urate lowering therapies, and anti-IL-1 therapies, their potential side effects are also worth noting. Such therapies have the potential to affect the immune system, raising the possibility of a secondary infection. Therefore, finding another category of modulators which are more effective and better tolerated would be a great benefit for gout patients.

IGF-1 is an important growth factor with signaling roles in numerous cell types, including monocytes 15, macrophages 16 and chondrocytes 17. The protein binds with high affinity to the Insulin Like Growth Factor 1 Receptor (IGF1R) 18. The activated receptor is engaged in cell growth and survival control, proliferation and is also known for being involved in metabolic regulation ^{19,20}. Previous genome-wide association studies on serum urate concentrations ^{21,22}, identified *IGF1R* as a genetic locus for serum urate levels. The index SNP with the lowest p-value at the IGF1R locus in the study performed by Köttgen et al. was rs6598541, of which the minor allele "A" was associated with increased urate levels (0.043 mg/dl increase [CI 0.031– 0.055], $P = 5 \times 10^{-15}$) ²¹. This variant also associated with urate control in a transancestral meta-analysis study in European and East Asian populations ²³. Moreover, this SNP also associated with gout in patients that met the American College of Rheumatology (ACR) classification criteria for gout 24.

The IGF-1 pathway was recently linked to innate immune memory and proinflammatory reprogramming induced by metabolic stimuli in human primary monocytes ²⁵. Stimulation via the IGF1R by mevalonate or by IGF-1 itself was able to induce trained immunity and epigenetic modifications in human primary monocytes and this contributed to enhanced proinflammatory responses to subsequent stimulation with LPS or Pam3Cys ²⁵. SNPs in *IGF1R* were significantly associated to cytokine production in response to training with BCG or ß-glucan in vitro ²⁵. Additional evidence shows IGF-1 as having pro-inflammatory effects upon 24h stimulation in primary human PBMCs, albeit these effects were only visible in synergy with TLR ligands such as LPS or Pam3Cys ²⁶. These effects were reported to be mediated via the MAPK pathway ²⁶. Other evidence shows that IGF-1 enhances chemotactic macrophage migration which leads to tissue inflammation ²⁷.

In the present study we address the hypothesis that signaling via the IGF1R is associated to inflammation in gout. We investigated whether soluble urate modulates IGF1R gene expression in human cells and whether the IGF-1 pathway has an effect on the proinflammatory priming elicited by soluble urate in vitro. Moreover, we assessed the association of the IGF1R rs6598541 SNP with IGF1R expression in circulating mononuclear cells and cytokine production capacity in patients with gout, asymptomatic hyperuricemia and normouricemic controls in an Eastern European population.

Materials and methods

Participants

The participants in this study consisted of patients with gout (n=116), hyperuricemic controls (n=78) and normouricemic volunteers (n=174), followed at the Rheumatology Department of the "Iuliu Hatieganu" University of Medicine and Pharmacy, Cluj-Napoca, Romania. Subjects were enrolled after written informed consent. Peripheral blood was drawn from the cubital vein on EDTA tubes under sterile conditions. The patient study was approved by the Ethical Committee of the "Iuliu Hatieganu" University of Medicine and Pharmacy, Cluj-Napoca (approval no. 425/2016) and all participants provided written informed consent. Experiments were conducted according to the principles expressed in the Declaration of Helsinki. All study participants in the gout group were included if they corresponded to the ACR/EULAR 2015 classification criteria with a score of 8. The cutoff for the asyptomatic hyperuricemia group was a serum urate concentration of 7 mg/dL and negative history of gout flares. The described groups were similar in age and BMI.

The gender distribution shows a higher number of men in the gout study group, consistent with the higher prevalence of gout in males.

PBMC isolation and stimulation

Isolation and stimulation of human peripheral blood mononuclear cells (PBMCs) was assessed as described previously8. Briefly, PBMCs were separated using Ficoll-Pague and resuspended in RPMI culture medium with Dutch modification (Gibco), supplemented with human pooled serum. Monocyte isolation was done using hyperosmotic Percoll® solution 28. Cells were incubated for 24 hours with culture medium as negative control, and urate in different concentrations. After priming, culture medium was removed, the remaining adherent cells were washed with warm PBS, then restimulated with medium or LPS with or without MSU crystals. IGF1R was induced by the addition of IGF-1 (R&D Systems, Abingdon, United Kingdom) in concentration of 5 µg/ml. In separate experiments IGF1R signalling was blocked with anti - IGF1R antibody (R&D Systems).

Cytokine measurements

Cytokine concentrations were determined in cell culture supernatants using specific sandwich ELISA kits for IL-1β, IL-1Ra, IL-6 (R&D Systems, Minneapolis).

Qantitative PCR for mRNA expression of IGF1R

PBMCs were incubated with the stimuli as mentioned above and after 24 hours of incubation at 37 °C in 5 % CO, The plates were centrifuged, the supernatant was collected and the cell pellets were lysed with 300 µl of TRIzol Reagent (Invitrogen). RNA purification was performed according to manufacturer's instructions. Subsequently, RNA concentrations were determined using NanoDrop software. Isolated RNA was subsequently transcribed into complementary DNA using High-Capacity cDNA Reverse Transcription Kit (Applied BioSystems) followed by quantitative PCR using the Sybr Green Method. The following primers were used in the reaction: IGF1R forward 5'-TCGACATCCGCAACGACTATC-3' and reverse 5'-TCGACATCCGCAACGACTATC-3' and 82-microglobulin forward 5'-ATGAGTATGCCTGCCGTGTG-3' and reverse 5'-CCAAATGCGGCATCTTCAAAC-3'. Results are shown as fold change in mRNA levels in stimulated samples compared to controls.

Genotyping for IGF1R rs6598541

Three independent groups were genotyped (gout group N=116; hyperuricemic group N=78 and healthy volunteers group N=174). Genomic DNA was isolated from whole blood(Promega) and genotyping was performed on an Illumina Infinium HD assay platform using The Infinium Global Screening Array-24 v3.0 BeadChip. The quality control protocol for genotyping data was performed Using Illumina's GenomeStudio. The SNPs with <95% call rate were excluded and all the SNPs with 95-98% call rate were verified and manually re-clustered or removed when necessary. The data was exported to PLINK format and further filters were applied: minor allele frequency > 0.01; hardy-weinberg equilibrium test p value > 10-6; samples with heterozygosity rate of +-3 standard deviations and related individuals were excluded. For the final step, the strands were flipped and all the data was verified to align to the GRCh37 hg19 build. The genotypes generated were checked using a predesigned TagMan SNP genotyping Assay (Applied Biosystems).

Transcriptomics

Freshly isolated PBMCs were frozen in TRIzol Reagent (Invitrogen) and stored at -80°C and were later used for commercial RNA-Seg analysis (Beijing Genomics Institute, BGI, Beijing, China). The integrity of extracted RNA was assessed using Agilent 2100 Bioanalyzer. Oligo dT magnetic beads were used to capture mRNA from total RNA. Purifed ligation products were enriched using PCR amplifcation followed by denaturation and cyclization of ssDNA by splint oligos and DNA ligase generating DNA nanoballs (DNBs). Sequencing of DNBs was performed on DNBseq platform.

Initial quality control was performed with SOAPnuke (v1.5.2). Clean reads were mapped to human transcriptome assembly GRCh37 (hg19) using bowtie2. Read counts were normalized using DESeg2 (Version: DESeg2 1.34.0) median of ratios method using R package (Version: R4.0.4.) and were used for downstream targeted gene expression statistical analysis.

Flow Cytometry Analysis

50 µl fresh EDTA whole blood and antibody solution were mixed by vortex for 4 seconds, and followed by 10 min incubation in room temperature avoiding light. Afterwards 1ml NH, Cl lysing solution (BD Pharm lyse, BD Biosciences) were added to the stained sample, and vortexed for 5 seconds. Then the solution was incubated at room temperature for 10 min without light. 300 µl of the lysed sample was used for flow cytometry measurement (Beckman Coulter). The antibody solution contained 5 antibodies, including IGF-1R (APC, Life Technologies), CD14 (FITC, Agilent technologies), CD16 (PE, eBioscience), CD45 (PECy7, Beckman Coulter), HLA-DR (PB, Beckman Coulter). Monocytes were first gated by forward scatter and side scatter, and then by CD45. The geometric mean of IGF-1R was used for t-test analysis.

Results

The effect of urate on the expression of IGF1R

To assess the effect of urate on the expression of IGF1R, mRNA was measured after stimulation of PBMCs of eight healthy donors with different concentrations of urate for 24 hours. No differences were observed in the expression of the receptor itself (Figure 1A). In addition, we assessed the mRNA level of the receptor in PBMCs from gout patients in the experimental setup of 24 hours urate priming followed by stimulation with LPS 10 ng/ml (TLR4 ligand) for another 24 hours. In line with the previous results, no differences regarding expression of IGF1R were observed after stimulation of the cells (Figure 1B). In contrast, we could observe an increased steady-state mRNA expression of IGF1R in unstimulated monocytes originating from gout patients compared to normouricemic controls (Figure 1C).

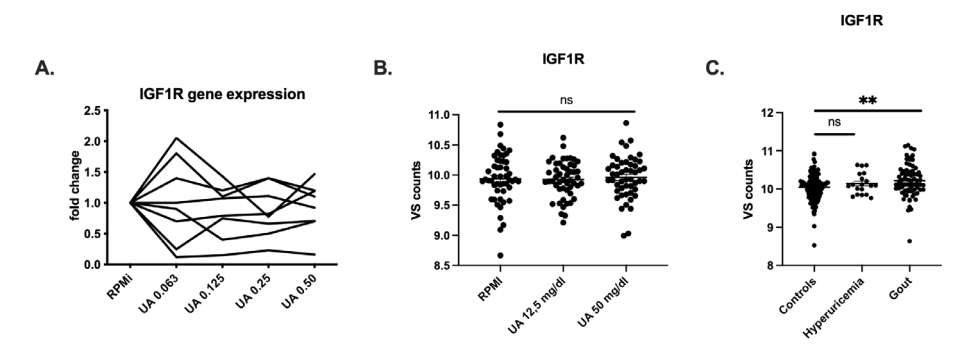


Figure 1 Urate effects on mRNA expression in vitro and basal expression of IGF1R of the studied groups A. mRNA expression of freshly isolated PBMCs originating from healthy donors (n=8) treated with different concentrations of uric acid (UA). B. mRNA expression of freshly isolated PBMCs originating from gout patients (n=50) treated with UA for 24h and restimulated with LPS 10ng/ml. Repeated Measurements oneway ANOVA and Tukey's multiple comparisons test, *p<0,05 C. mRNA expression of freshly isolated PBMCs originating from healthy controls (n=113), hyperuricemic patients (n=19) and gout patients (n=72). The data is represented as normalized counts. Brown -Forsythe and Welch ANOVA, *p<0,05

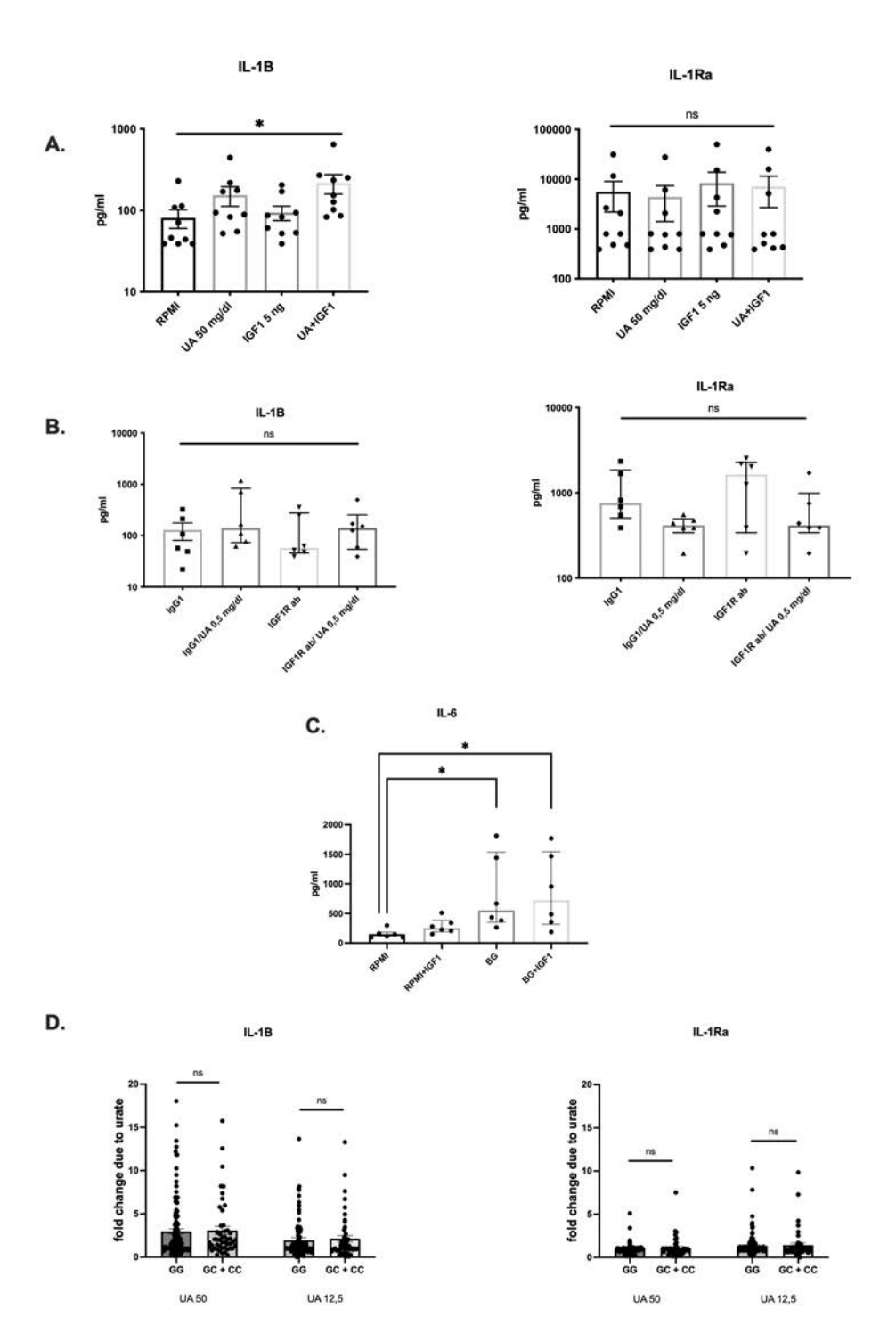
Activation or inhibition of IGF1R does not modify cytokine production in urate priming or trained immunity experiments

Next, we studied the possible contribution of IGF1R to inflammation in an experimental setup consisting of 24 hours exposure to recombinant IGF-1 protein (Figure 2A) (R&D Systems) or anti-IGF1R neutralizing antibody (Figure 2B) in the presence or absence of solubilized urate, followed by 24 hours stimulation with LPS and MSU crystals. Cells treated with solubilised urate (50mg/dl) together with the recombinant IGF-1 protein (5 ng) produced more IL-1β, but not IL-6 or IL-1Ra compared to control. The cytokine production was not modified by antiIGF1R neutralizing antibody. Further, we tested if IGF-1 could influence cytokine production in a trained immunity experimental design ^{29,30}, consisting of stimulation for 24h with IGF-1 or β-glucan (BG) as positive control, followed by washout and rest for 5 days and subsequent second stimulation with LPS (10 ng/mL). We did not observe an enhanced training effect by IGF1 (Fig 2C). Bekkering et al. reported SNPs in IGF1R (rs150571637, rs9672558, rs34428109, rs1573891) associated with trained immunity in response to Bacille Camette-Guerin (BCG) and beta-glucan isolated from C. albicans 31. Thereafter we assessed IGF1R rs1573891 in our study and found no association of this SNP to priming of PBMCs by soluble urate (Fig 2D).

IGF1R rs6598541 SNP and IGF1R expression levels in freshly isolated PBMCs

We further examined the IGF1R SNP rs6598541, previously associated with serum urate levels ^{21,23} and gout ²⁴, for association with *IGF1R* expression in patients with gout, hyperuricemia and normouricemic controls. The basal expression level of IGF1R in freshly isolated PBMCs from the three groups (Figure 3A-C) was not associated with rs6598541. Additionally, flow cytometric assessment of IGF1R surface expression on unstimulated PBMCs from healthy donors was also not association with IGF1R rs6598541 (Figure 3D).

Figure 2 Role of IGF1R in urate induced inflammation in vitro. A. Freshly isolated PBMCs isolated from healthy controls (n=9) were stimulated with RPMI, uric acid 50 mg/dl, IGF-1 recombinant protein (R&D Systems) 5ng for 24h. After 24h the cells were restimulated with LPS 10ng/ml together with MSU 300mg/dl. B. Freshly isolated Percoll enriched Monocytes (n=6) were treated with RPMI, IGF1R antibody (R&D Systems) or IgG1 isotype control and uric acid 50 mg/dl for 24h. After 24h monocytes were restimulated with LPS 10ng/ml with MSU 300mg/dl. C. Freshly isolated PBMCs (n=6) were trained in vitro with IGF-1 5ng and beta-glucan (BG) 1 ug/ml for 24h, subsequently washed, rested for 5 days, and at day 6 restimulated for 24 h with 10 ng/mL LPS. D. Freshly isolated PBMCs originating from healthy controls (n=174). Concentration IL-1β and IL-6 measured in the supernatants of PBMCs after stimulation with urate of conc. 50mg/dl and 12,5 mg/dl for 24h, followed by restimulation with LPS 10 ng/mL. IL-1β, and IL-1Ra (R&D Systems, Minneapolis) was measured in supernatant by ELISA. Graphs depict means+/-SEM. Friedman test, Dunn's multiple comparisons test, p*<0,05



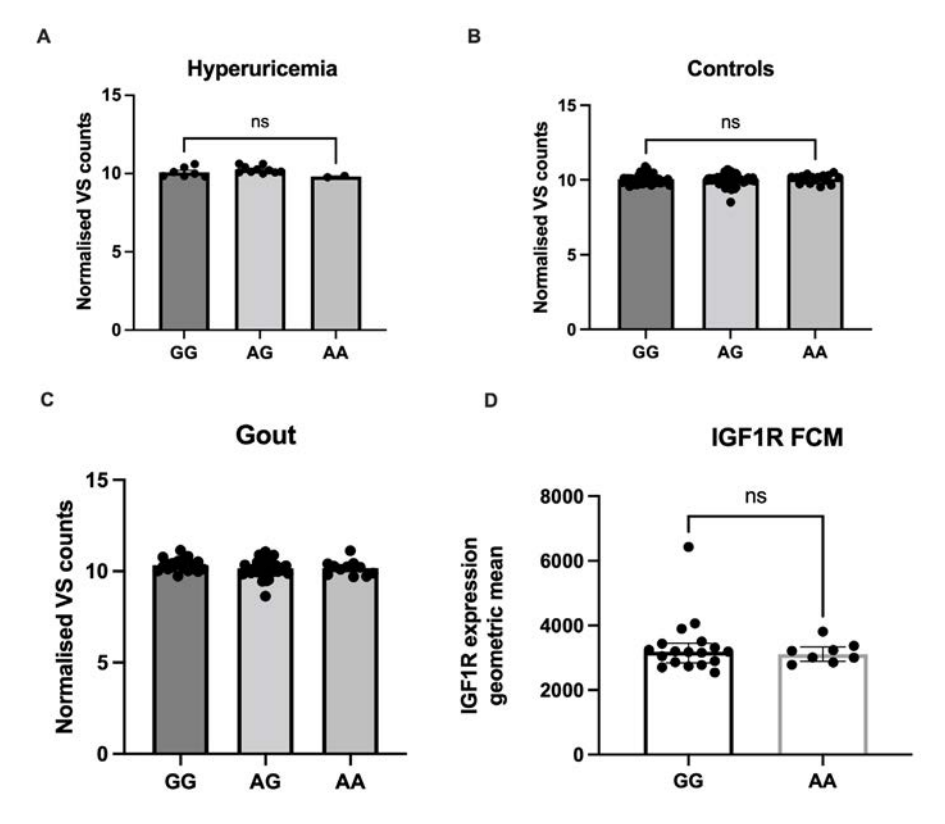


Figure 3 Corellation of the GWAS SNP rs6598541 with IGF1R expression levels. mRNA expression of freshly isolated PBMCs originating from **A**. hyperuricemic controls (n=19) **B.** normouricemic controls (n=105) and **C.** gout patients (n=68). The data is represented as normalized counts. **D.** IGF1R protein surface expression measurment by flow cytometric assay of unstimulated PBMCs originating from healthy donors (n=26). Brown -Forsythe and Welch ANOVA, *p<0,05

IGF1R rs6598541 SNP and cytokine production in stimulated PBMCS

To further study the possible implication of rs6598541 on inflammation, we assessed the *ex vivo* cytokine secretion by freshly isolated PBMCs challenged with various stimuli in association with the *IGF1R* rs6598541 genotypes: cytokine production in response to 24h stimulation with MSU, palmitate (C16.0) or the combination of MSU crystal with C16.0 (Figure 4A); urate priming for 24h and stimulation with LPS for 24h (Figure 4B); or 24h stimulation with LPS 100ng (Figure 4C). No significant association was found between the SNP and *ex vivo* cytokine production (IL-6, IL-1beta or IL-1Ra). The same analysis of data obtained following the same experiment carried out for the hyperuricemia individuals and for patients with gout(both active and non-active form) also showed no significant differences for these conditions between genotypes (supplementary figure 1,2 and 3).

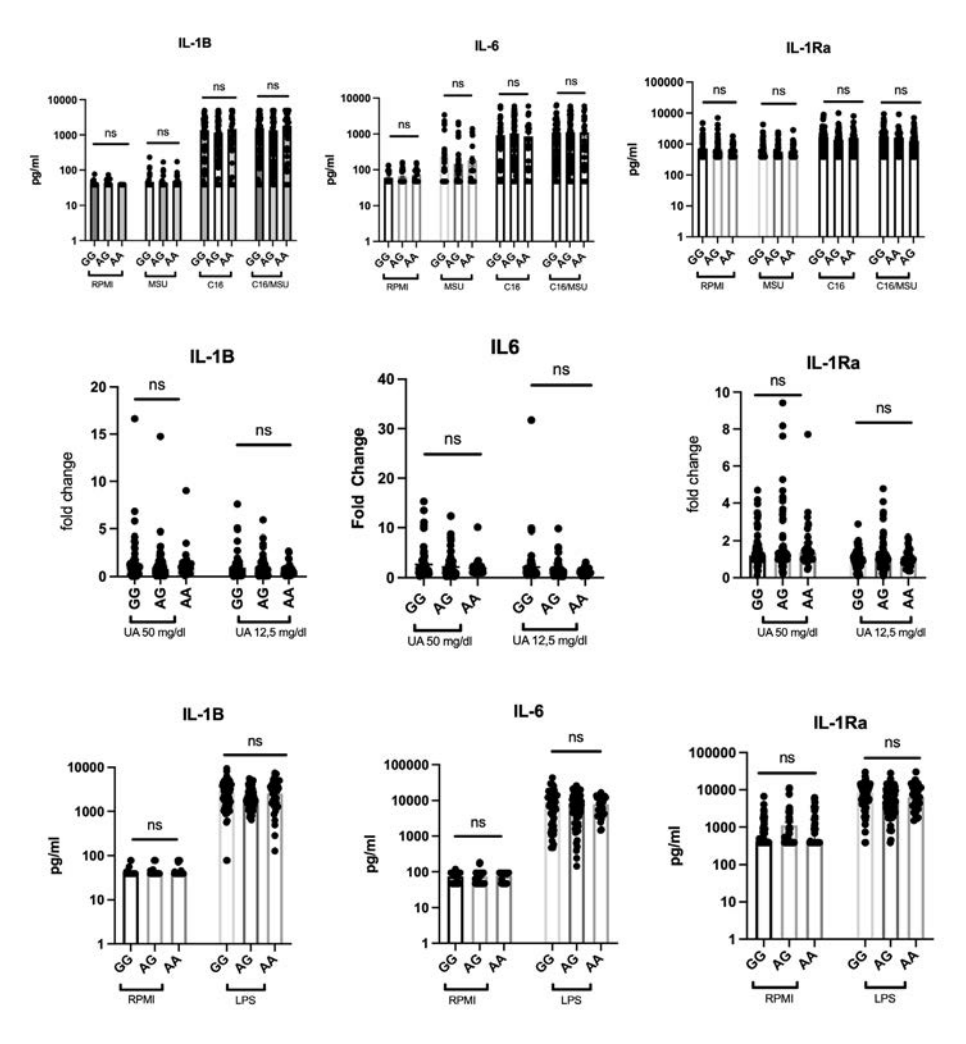


Figure 4 Correlation of the rs6598541 SNP with ex vivo cytokine production. A. Freshly isolated PBMCs originating from healthy controls (n=187) stimulated with RPMI, MSU 300mg/dl, C16, C16/MSU 300mg/dl for 24h. After 24h the supernatants were collected and IL-1β, IL-6 and IL-1Ra (R&D Systems, Minneapolis) was measured. B. Concentration IL-1β, IL-6 and IL-1Ra measured in the supernatants of PBMCs after stimulation with uric acid of conc. 50mg/dl and 12,5 mg/dl for 24h, followed by restimulation with LPS 10 ng/mL. C. IL-1β, IL-6 and IL-1Ra levels measured in the supernatants of PBMCs after stimulation with LPS 100ng for 24h. Graphs depict means+/-SEM.

Discussion

IGF-1 is known to have modulatory roles in human immune responses and a regulatory role in the activation of the peripheral monocytes ^{26,32}. Interestingly, IGF-1 has dual roles, being involved in inflammation in a context-dependent mode, presenting both pro- and anti-inflammatory properties. After myocardial infarction, IGF-1 acted like an anti-inflammatory cytokine on myeloid cells in vitro while negating the pro-inflammatory phenotype of neutrophils and macrophages in vivo 33. Also, several in vitro studies revealed anti-inflammatory properties of IGF-1 on astrocytes and microglia 34,35, whereas another study focused on it's role in decreasing the release of IL-1Ra and increasing IL-1 β ³⁶.

The IGF-1 pathway has recently been shown to be involved in the induction of trained immunity. Since innate immune memory is increasingly shown to be important for urate-induced inflammation, in the present study, we were interested in assessing IGF-1/IGF1R signalling in urate priming using primary PBMCs.

Our data indicate that IGF-1 does not contribute to urate-induced inflammation and blocking IGF1R did not influence the inflammatory responses triggered by urate. We show that urate does not modulate the expression of IGF1R itself in vitro in PBMCs from healthy donors nor in vivo in PBMCs from gout patients.

However, we noticed an increased steady-state mRNA expression of IGF1R in unstimulated PBMCs from gout patients. Increased expression of IGF1R was also seen in leukocytes of rheumatoid arthritis patients, which was associated with systemic inflammation and pain ³⁷. Interestingly, RA patients with high IGF1R gene expression values were found to have low IGF-1 serum levels ³⁷. In contrast, elevated circulating IGF-1 levels were reported in patients with gout and insulin resistance 38.

Bekkering et al. describe four SNPs in IGF1R associated with differential cytokine production in monocytes trained with β-glucan or BCG vaccine (Bacillus Calmette– Guérin)²⁵. We have also assessed one of these four SNPs with respect to urate priming and found no association of these variants to changes in cytokine profiles after urate exposure (Figure 2D). Therefore, our data provide no evidence for a role of IGF1R in urate-mediated inflammatory priming.

We explored association of the IGF1R rs6598541 SNP, identified as a genetic susceptibility variant for gout and serum urate levels ^{21,23,24}, with cytokine production in human PBMCs. IGF1R genetic variants are potentially functionally relevant in gout and hyperuricemia since the genetic control of urate levels and risk of gout at the IGF1R locus also colocalizes with genetic control of IGF1R expression data 23. For IGF1R rs6598541, the gout risk and elevated serum urate associated allele A is associated with lower IGF1R expression in heart tissue (left ventricle) ³⁹. In our study, when assessing freshly isolated PBMCs from patients with gout or controls we did not observe association of IGF1R gene expression with rs6598541. In addition, IGF1R surface expression evaluated by flow cytometry in monocytes of healthy donors also did not show modified IGF1R expression associated with rs6598541 genotype. In line with this, ex vivo cytokine secretion by freshly isolated PBMCs challenged with certain stimuli was also not associated with rs6598541. This indicates that this SNP may exert relevant functional roles in gouty inflammation, but they may be tissue specific and mononuclear cells do not show IGF1R expression patterns nor inflammatory cytokine production capacity in relationship to this SNP.

However, data on the role of IGF-1 on urate control give more mechanistic insight. A genetic variant associated with elevated IGF-1 levels (rs35767) correlated to diminished serum urate levels and higher uricosuria 40. Exposure of HEK293 human embryonic kidney cells to IGF1 resulted in a dose-dependent increase of secretory urate transporters MRP4, NPT1 and ABCG2 and a simultaneous reduction of GLUT9 expression at both the mRNA and protein levels 40. GLUT9a is the chief transporter for basolateral exit of reabsorbed urate into blood 41. As reported by Kottgen et al, the urate-associated IGF1R rs6598541 variant is also associated to lower fractional excretion of urate, supporting a role of the IGF1-IGF1R axis on urate transport. This is supported by data showing that, in Xenopus laevis oocytes expressing human IGF1R and urate transporters, IGF-1 promotes urate uptake via IGF1R ³⁹. Therefore *IGF1R* association to gout is most probably exerted via urate control rather than inflammatory mechanisms, via IGF1R, GLUT9 expression and activation, leading to urate reabsorbtion 42.

Another mechanism linking IGF1R rs6598541 to urate levels is insulin resistance. IGF1R rs6598541 was reported to be genome-wide associated with fasting glucose: people without diabetes carrying the A-allele have increased fasting glucose levels, suggesting an association with insulin resistance 43,44. It is known that hyperuricemia might be contributed to by the effect of insulin on decreasing renal urate clearance and sodium excretion in individuals^{42,45,46}.

In conclusion, our data do not support a role of IGF-1/IGF1R signalling in soluble urateinduced inflammation in primary PBMCs. Consistent with this, functional data associated to genetic variants in IGF1R shows no association with ex vivo cytokine production.

Therefore, these results suggest that a role of IGF1R in gout may be more relevant for the control of urate levels rather than on the inflammatory process.

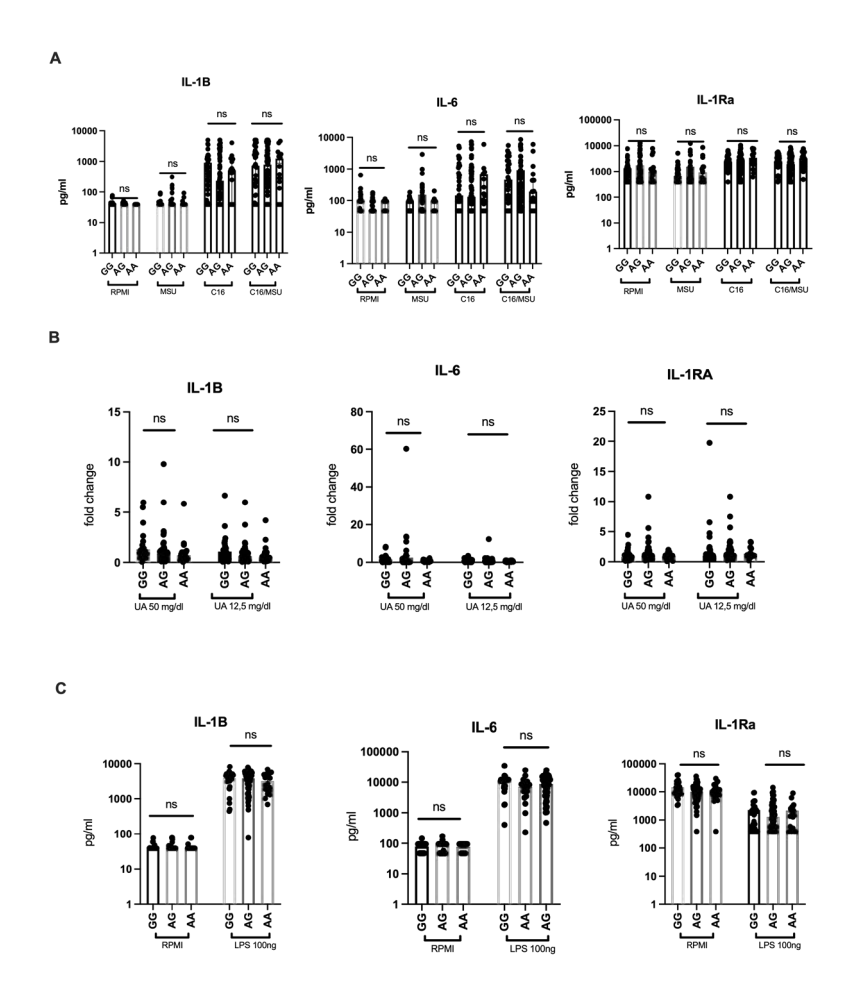
References

- 1 Bardin, T. & Richette, P. [The epidemiology and genetic of gout]. Presse Med. (2011). doi:10.1016/j. lpm.2011.04.012
- Roddy, E., Zhang, W. & Doherty, M. The changing epidemiology of gout. Nature Clinical Practice 2. Rheumatology (2007). doi:10.1038/ncprheum0556
- 3. Mattiuzzi, C. & Lippi, G. Recent updates on worldwide gout epidemiology. 10–12 (2019).
- Dalbeth, N. et al. Gout. Nat. Rev. Dis. Prim. 5, (2019). 4.
- 5. Renaudin, F. et al. Gout and pseudo-gout-related crystals promote GLUT1-mediated glycolysis that governs NLRP3 and interleukin-1β activation on macrophages. Ann. Rheum. Dis. 79, 1506-1514 (2020).
- Huang, Q. et al. HSP60 Regulates Monosodium Urate Crystal-Induced Inflammation by Activating the TLR4-NF- κ B-MyD88 Signaling Pathway and Disrupting Mitochondrial Function. Oxid. Med. Cell. Longev. 2020, (2020).
- Vazirpanah, N. et al. MTOR inhibition by metformin impacts monosodium urate crystal-induced inflammation and cell death in gout: A prelude to a new add-on therapy? Ann. Rheum. Dis. 78, 663-671 (2019).
- Crisan, T. O. et al. Soluble uric acid primes TLR-induced proinflammatory cytokine production by human primary cells via inhibition of IL-1Ra. Ann. Rheum. Dis. (2016). doi:10.1136/ annrheumdis-2014-206564
- Sah, O. S. P. & Qing, Y. X. Associations between hyperuricemia and chronic kidney disease: A review. Nephrourol. Mon. 7, (2015).
- 10. Stewart, D. J., Langlois, V. & Noone, D. Hyperuricemia and hypertension: Links and risks. Integr. Blood Press. Control 12, 43-62 (2019).
- 11. Badii, M. et al. Urate-induced epigenetic modifications in myeloid cells. Arthritis Res. Ther. 23, 1-11 (2021).
- 12. Cabău, G., Crișan, T. O., Klück, V., Popp, R. A. & Joosten, L. A. B. Urate-induced immune programming: Consequences for gouty arthritis and hyperuricemia. Immunol. Rev. 294, 92–105 (2020).
- 13. Badii, M., Gaal, O., Popp, R. A., Crişan, T. O. & Joosten, L. A. B. Trained immunity and inflammation in rheumatic diseases. Jt. Bone Spine 89, (2022).
- 14. Joosten, L. A. B., Crişan, T. O., Bjornstad, P. & Johnson, R. J. Asymptomatic hyperuricaemia: a silent activator of the innate immune system. Nat. Rev. Rheumatol. 16, 75-86 (2020).
- 15. Ge, R. T. et al. Insulin-like growth factor-1 endues monocytes with immune suppressive ability to inhibit inflammation in the intestine. Sci. Rep. 5, 1-7 (2015).
- 16. Gow, D. J., Sester, D. P. & Hume, D. A. CSF-1, IGF-1, and the control of postnatal growth and development. J. Leukoc. Biol. 88, 475-481 (2010).
- 17. Schalkwijk, J., Joosten, L. A. B., Van Den Berg, W. B., Van Wyk, J. J. & Van Putte, L. A. D. Insulinlike growth factor stimulation of chondrocyte proteoglycan synthesis by human synovial fluid. Arthritis Rheum. 32, 66-71 (1989).
- 18. Rosenzweig, S. A., Pharmacology, M. & Therapeutics, E. The Continuing Evolution of Insulin-like Growth Factor Signaling [version 1; peer review: 4 approved]. 9, 1–10 (2020).
- 19. Kineman, R. D., del Rio-Moreno, M. & Sarmento-Cabral, A. 40 years of IGF1: Understanding the tissue-specific roles of IGF1/IGF1R in regulating metabolism using the Cre/loxP system. Journal of Molecular Endocrinology (2018). doi:10.1530/JME-18-0076

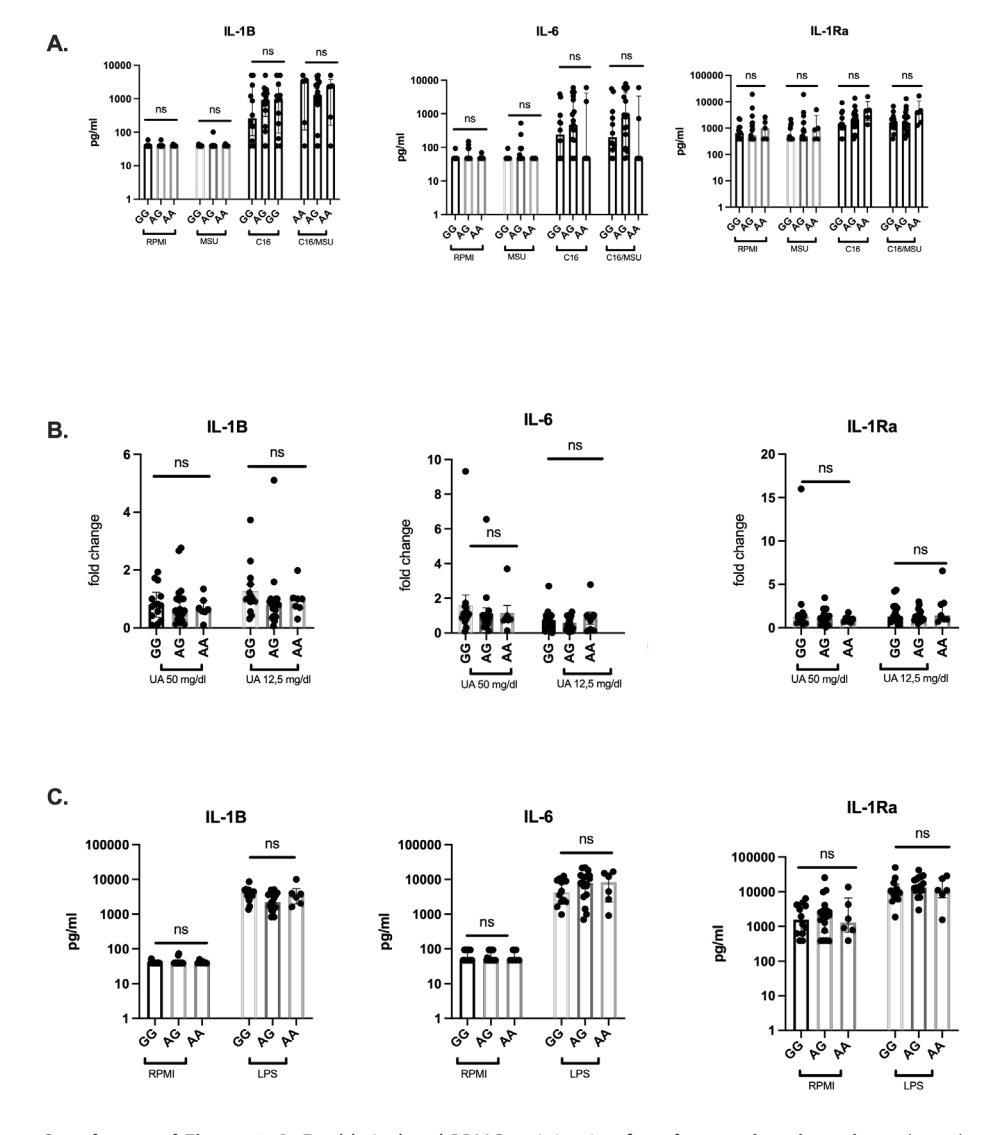
- 20. Xu, Y. et al. How ligand binds to the type 1 insulin-like growth factor receptor. Nat. Commun. 9, (2018).
- 21. Köttgen, A. et al. Genome-wide association analyses identify 18 new loci associated with serum urate concentrations. Nat. Genet. 45, 145-154 (2013).
- 22. Tin, A. et al. Target genes, variants, tissues and transcriptional pathways influencing human serum urate levels. Nat. Genet. (2019). doi:10.1038/s41588-019-0504-x
- 23. Boocock, J. et al. Genomic dissection of 43 serum urate-associated loci provides multiple insights into molecular mechanisms of urate control. Hum. Mol. Genet. (2020). doi:10.1093/hmg/ddaa013
- 24. Phipps-Green, A. J. et al. Twenty-eight loci that influence serum urate levels: Analysis of association with gout. Ann. Rheum. Dis. 75, 124-130 (2016).
- 25. Bekkering, S. et al. Metabolic Induction of Trained Immunity through the Mevalonate Pathway. Cell 172, 135-146.e9 (2018).
- 26. Wolters, T. L. C., Netea, M. G., Hermus, A. R. M. M., Smit, J. W. A. & Netea-Maier, R. T. IGF1 potentiates the pro-inflammatory response in human peripheral blood mononuclear cells via MAPK. J. Mol. Endocrinol. (2017), doi:10.1530/JME-17-0062
- 27. Furundzija, V. et al. IGF-1 increases macrophage motility via PKC/p38-dependent ανβ3-integrin inside-out signaling. Biochem. Biophys. Res. Commun. 394, 786-791 (2010).
- 28. Meital, L. T. et al. A simple and effective method for the isolation and culture of human monocytes from small volumes of peripheral blood. J. Immunol. Methods 472, 75-78 (2019).
- 29. Bekkering, S. et al. In Vitro experimental model of trained innate immunity in human primary monocytes. Clin. Vaccine Immunol. 23, 926-933 (2016).
- 30. Domínguez-Andrés, J. et al. In vitro induction of trained immunity in adherent human monocytes. STAR Protoc. 2, (2021).
- 31. Bekkering, S. et al. Metabolic Induction of Trained Immunity through the Mevalonate Pathway. Cell (2018). doi:10.1016/j.cell.2017.11.025
- 32. Higashi, Y. et al. Interaction between insulin-like growth factor-1 and atherosclerosis and vascular aging, in Cardiovascular Issues in Endocrinology (2014), doi:10.1159/000360571
- 33. Nederlof, R. et al. Insulin-Like Growth Factor 1 Attenuates the Pro-Inflammatory Phenotype of Neutrophils in Myocardial Infarction. Front. Immunol. 13, 1–16 (2022).
- 34. Bluthé, R. M., Kelley, K. W. & Dantzer, R. Effects of insulin-like growth factor-I on cytokine-induced sickness behavior in mice. Brain. Behav. Immun. 20, 57-63 (2006).
- 35. Palin, K. et al. TNFα-induced sickness behavior in mice with functional 55 kD TNF receptors is blocked by central IGF-I. J. Neuroimmunol. 187, 55-60 (2007).
- 36. Ueland, T. et al. Associations between body composition, circulating interleukin-1 receptor antagonist, osteocalcin, and insulin metabolism in active acromegaly. J. Clin. Endocrinol. Metab. **95**, 361–368 (2010).
- 37. Erlandsson, M. C. et al. IGF-1R signalling contributes to IL-6 production and T cell dependent inflammation in rheumatoid arthritis. Biochim. Biophys. Acta - Mol. Basis Dis. (2017). doi:10.1016/j. bbadis.2017.06.002
- 38. Kushnarenko, N., Medvedeva, T., Govorin, A. & Kushnarenko, K. Significance of growth factors (IGF-1, FGF-b, PDGF-AA), pro-inflammatory cytokines and cytokine soluble receptors in gouty patients with insulin resistance. Atherosclerosis 263, e111 (2017).

- 39. Mandal, A. K. et al. Genetic and Physiological Effects of Insulin-Like Growth Factor-1 (IGF-1) on Human Urate Homeostasis. J. Am. Soc. Nephrol. (2023). doi:10.1681/ASN.000000000000054
- 40. Mannino, G. C. et al. The polymorphism rs35767 at IGF1 locus is associated with serum urate levels. Sci. Rep. 8, 1-9 (2018).
- 41. Caulfield, M. J. et al. SLC2A9 is a high-capacity urate transporter in humans. PLoS Med. 5, 1509-1523 (2008).
- 42. Mandal, A. K. et al. Genetic and Physiological Effects of Insulin on Human Urate Homeostasis. Front. Physiol. 12, 1–17 (2021).
- 43. Lagou, V. et al. Sex-dimorphic genetic effects and novel loci for fasting glucose and insulin variability. Nat. Commun. 12, 1-18 (2021).
- 44. Chen, J. et al. The trans-ancestral genomic architecture of glycemic traits. Nat. Genet. 53, 840–860 (2021).
- 45. Ter Maaten, J. C. et al. Renal handling of urate and sodium during acute physiological hyperinsulinaemia in healthy subjects. Clin. Sci. 92, 51-58 (1997).
- 46. McCormick, N. et al. Assessing the Causal Relationships Between Insulin Resistance and Hyperuricemia and Gout Using Bidirectional Mendelian Randomization. Arthritis Rheumatol. 73, 2096-2104 (2021).

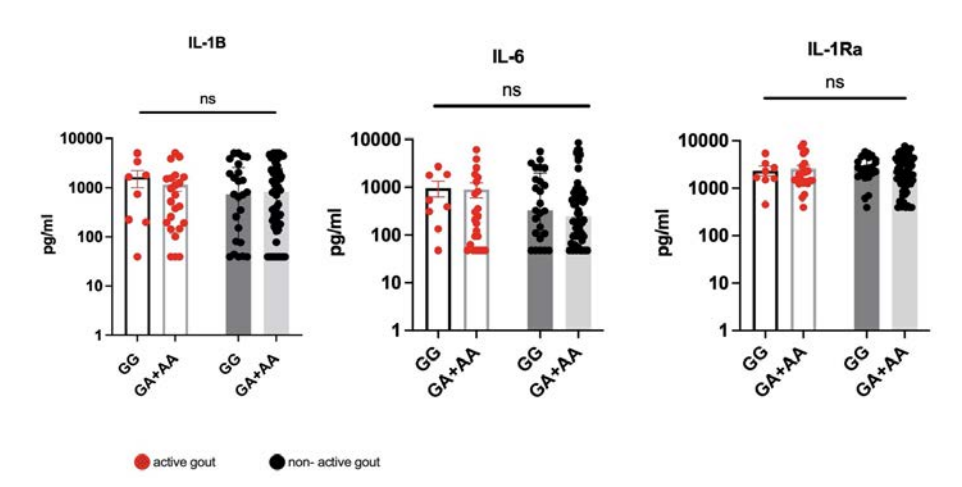
Supplemental information



Supplemental Figure 1. A. Freshly isolated PBMCs originating from gout patients (n=119) stimulated with RPMI, MSU 300mg/dl, C16, C16/MSU 300mg/dl for 24h. After 24h the supernatants were collected and IL-1β, IL-6 and IL-1Ra (R&D Systems, Minneapolis) was measured. **B**. Concentration IL-1β, IL-6 and IL-1Ra measured in the supernatants of PBMCs after stimulation with uric acid of conc. 50mg/ dl and 12,5 mg/dl for 24h, followed by restimulation with LPS 10 ng/mL. C. Concentration IL-1β, IL-6 and IL-1Ra measured in the supernatants of PBMCs after stimulation with LPS 100ng for 24h. The lowest range of detection was 78 pg/ml for IL-1β; 390 pg/ml for IL-1Ra and 188 pg/ml for IL-6. Graphs depict means+/-SEM.



Supplemental Figure 2. A. Freshly isolated PBMCs originating from hyperuricemic patients (n=40) stimulated with RPMI, MSU 300mg/dl, C16, C16/MSU 300mg/dl for 24h. After 24h the supernatants were collected and IL-1 β , IL6 and IL1Ra (R&D Systems, Minneapolis) was measured. B. Concentration IL-1 β , IL-6 and IL-1Ra measured in the supernatants of PBMCs after stimulation with uric acid of conc. 50mg/dl and 12,5 mg/dl for 24h, followed by restimulation with LPS 10 ng/mL C. Concentration IL-1 β , IL-6 and IL-1Ra measured in the supernatants of PBMCs after stimulation with LPS 100ng for 24h. The lowest range of detection was 78 pg/ml for IL-1 β ; 390 pg/ml for IL-1Ra and 188 pg/ml for IL-6. Graphs depict means+/—SEM.



Supplemental Figure 3. A. Freshly isolated PBMCs originating from gout patients (n=114 from which n=31 were patients with active gout,marked with red) were stimulated with C16/MSU 300mg/dl for 24h. After 24h the supernatants were collected and IL-1β, IL-6 and IL-1Ra (R&D Systems, Minneapolis) was measured. Graphs depict means+/-SEM.



Chapter 4

Interleukin 1 receptor type I variation in patients with gout and hyperuricemic individuals

Orsolya I. Gaal, Valentin Nica, Medeea Badii, Georgiana Cabău, Ioana Hotea, HINT Consortium, Cristina Pamfil, Megan Leask, Tony R. Merriman, Tania O. Crișan*, Leo A.B. Joosten*

#These authors share senior authorship

Abstract

Introduction

Gout is an important inflammatory disease with high prevalence in developed countries. Necessary for developing gout is the deposition of monosodium urate (MSU) crystals in the joint and other tissues as a result of elevated serum urate levels. Interleukin IL-1 β is the central inflammatory cytokine in gout and its effects are mediated through signalling via IL1 receptor type I (IL1R1). IL1R1 is a newly identified locus associated with gout in a recent GWAS and is a candidate gene for a role in the progression from hyperuricemia to gout. Differential expression of the IL1R1 gene was previously reported in monocytes exposed to lipopolysaccharide or MSU crystals. Here, we further assessed IL1R1 expression in gout and hyperuricemia. We also assessed the gout-associated IL1R1 rs17767183 variant for association with the cytokine production capacity of mononuclear cells.

Materials and methods

The study was performed in the HINT study groups (patients with gout and controls, Romania) and the 500FG (healthy volunteers, The Netherlands). RNA sequencing was used to assess the gene transcription in freshly isolated PBMCs from people with gout or with asymptomatic hyperuricemia or normouricemia. Circulating soluble IL1R1 and IL1R2 levels were measured in plasma. Genomic DNA was isolated from whole blood and genotyping was performed using the Illumina Infinium Global Screening Array. Ex vivo functional assays were performed, consisting of PBMC stimulations with C16+MSU (TLR2/NLRP3 inflammasome activator) or LPS (TLR4 ligand) for 24h. Cytokines were assessed by ELISA.

Results

IL1R1 was differentially expressed in PBMCs from gout patiens compared to controls. Serum soluble IL1R1 protein levels were very low and there were no differences in the studied groups. The IL1R1 rs17767183 SNP was not associated with changes in IL1R1 expression nor to cytokine production in the HINT study groups. However, the IL1R1 rs17767183 C (gout risk) allele was associated with significantly elevated IL-6 cytokine production in response to C16+MSU crystal in 500FG healthy controls.

Conclusions

Variation in expression of IL1R1 is observed in primary PBMCs of patients with gout and in hyperuricemic controls thus reinforcing data implicating these loci in gout and urate-related inflammation. Discordant results were observed for cytokine production levels in relationship to the IL1R1 rs17767183 SNP and further analysis into the possible regulatory effects of this SNP in inflammation is currently ongoing.

Introduction

Gout is a common form of arthritis, progressively becoming a global public health problem, given its high incidence rate (1,2) Elevated serum urate levels are the prerequisite, but not sufficient cause of developing gout (3,4). MSU crystals, formed at the event of supersaturation of urate, are deposited inside the joints provoking inflammation leading to tissue damage (5). Besides the already described intrinsic risk factors, such as age, sex and weight (6), it is also controlled by the moleculargenetic elements along with metabolic and environmental factors. Also, these elements are associated with altered serum urate concentrations as well, which later contributes to disease development (7).

Although, great progress is being achieved in this field, the progression from hyperuricemia to gout is still insufficiently understood. Interleukin IL-1\beta is the central inflammatory cytokine in gout (5,8) and its effects are mediated through signalling via IL1 receptor type I (IL1R1) (8). The IL1 receptor type II (IL1R2) is a defective receptor that functions as decoy and antagonizes IL-1ß signalling (9). Thereafter, proinflammatory cytokines represent key players in the pathogenesis and inflammatory responses seen in gout. The binding of IL-1β to IL1R1 prompts downstream signaling pathways which are then promoting inflammation by producing more cytokines, chemokines, and the recruitment of neutrophils to the site of inflammation (10).

So far, Genome Wide Association Studies (GWAS) studies assessing gout patients and controls have provided insight into the molecular mechanisms of urate control and establishing candidate pathways for the inflammatory events in gout. It is known that many individuals encountering high levels of urate do not necessarily develop gout, indicating that there is a sum of factors being responsible for developing symptomatic gout (7,11), therefore genetic variants in inflammatory genes might be among the aspects responsible for this shift.

IL1R1 is a newly identified locus associated with gout in therecent largest GWAS to date(12) and is a candidate gene for a role in the progression from hyperuricemia to gout(13). This locus is the first time being reported in gout- or urate-related GWAS studies. Moreover, it is being presented as part of a prioritization scheme described in the study conducted by Major et.al.(12) pinpointing its presence in both the European and trans-ancestry analyses (12). The GWAS overlaps a signal of genetic control of expression (an expression quantitative trait locus (eQTL)) for IL1R1 (12). The index SNP at the IL1R1 region was rs17767183, for which the major allele C, was associated to higher expression patterns in the GTEx data (higher IL1R1 expression in artery-aorta as well as pancreas tissue samples), likewise the same pattern observed in classical monocytes in the ImmuNexUT data (14). Moreover, differential expression of the IL1R1 gene was previously reported in monocytes exposed to lipopolysaccharide or MSU crystals (15).

In the present study, we tested for functional impact of genetic variation at the IL1R1 region in gout. Also, we assessed the association of the rs17767183 with IL1R1 expression in circulating mononuclear cells and cytokine production capacity in patients with gout and controls.

Materials and methods

Participants

The participants in this study consisted of patients with gout (n=161), hyperuricemia (n=123) and normouricemic samples (n=145) recruited at the Rheumatology Department of the "Iuliu Hatieganu" University of Medicine and Pharmacy, Cluj-Napoca, Romania. Subjects were enrolled after written informed consent. Peripheral blood was drawn from the cubital vein into EDTA tubes under sterile conditions. The patient study was approved by the Ethical Committee of the "Juliu Hatieganu" University of Medicine and Pharmacy, Cluj-Napoca (approval no. 425/2016). All study participants in the gout group were included based on ACR/EULAR 2015 classification criteria with a minimum score of 8 and controls had negative history of gout attacks.

PBMC isolation and stimulation

Isolation and stimulation of human peripheral blood mononuclear cells (PBMCs) was assessed as described previously (16). PBMCs were separated using Ficoll-Paque and resuspended in RPMI culture medium with Dutch modification (Gibco), supplemented with human pooled serum. Cells were incubated for 24 hours with culture medium as negative control or palmitate with MSU crystals (C16.0+MSU) (gout relevant costimulation cocktail for TLR2 binding and NLRP3 inflammasome activation). Cytokine levels were measured in culture supernatants.

Cytokine measurements

Cytokine concentrations were determined in cell culture supernatants using specific sandwich ELISA kits for IL-1R1, IL-1β, IL-1Ra, IL-6 (R&D Systems, Minneapolis). The lowest range of detection was 250 pg/ml for IL-1R1, 39 pg/ml for IL-1β; 390 pg/ml for IL-1Ra and 94 pg/ml for IL-6. Samples were diluted before assay 10-fold for IL-1B and IL-1Ra and 20-fold for IL-6.

Genotyping for IL1R1 rs17767183

Three independent groups were genotyped (gout group N=67, hyperuricemic group n=21 and control group N=105). Genomic DNA was isolated from whole blood (Promega) and genotyping was performed on an Illumina Infinium HD assay platform using The Infinium Global Screening Array-24 v3.0 BeadChip. Quality control for genotyping data was performed Using Illumina's GenomeStudio. The SNPs with <95% call rate were excluded and all the remaining SNPs were verified and manually re-clustered or removed when necessary. The data were exported to PLINK format and further filters were applied: minor allele frequency > 0.01: Hardy-Weinberg equilibrium test p value $> 10^{-6}$; samples with heterozygosity rate of $\pm 10^{-6}$ standard deviations and related individuals were excluded. For the final step, the strands were flipped and all the data was verified to align to the GRCh37 hg19 build.

Transcriptomics

Freshly isolated PBMCs were frozen in TRIzol Reagent (Invitrogen) and stored at -80°C until bulk RNA-Sequencing analysis (outsourced to Beijing Genomics Institute, BGI, Denmark). The integrity of extracted RNA was assessed using the Agilent 2100 Bioanalyzer. Oligo dT magnetic beads were used to capture mRNA from total RNA. Fragmented target RNA was reverse transcribed to cDNA using random N6 primers followed by end-repair and A tailing for adaptor ligation. Purified ligation products were enriched using PCR amplification followed by denaturation and cyclization of ssDNA by splint oligos and DNA ligase generating DNA nanoballs (DNBs). Sequencing of DNBs was performed on DNBseq platform. Raw data were generated by removing reads mapped to rRNAs. Clean reads were generated using the SOAPnuke software (v.1.5.2) by removing reads with adaptors, reads with unknown bases >10% and low-quality reads. These were later defined as reads with a quality score less than 15 in over 50% bases. Clean reads were mapped to UniGenes and read counts were estimated using Bowtie2 and RSEM (v.1.2.12). Normalization, quality control and identification of differentially expressed genes (DEGs) was performed using the Bioconductor package DESeq2 (Version: DESeq2_1.24.0). Quality control at this stage consisted of removal of samples with highly abnormal values (PCA: ± 3 Standard Deviations on PC1 or PC2). The samples were sequenced in two different batches and the resulting effect was corrected using the limma package. The resulting variance stabilized (VS) counts were used for the target genes for statistical analysis.

Statistical methods

Statistical analysis was performed using GraphPad version 10.0.0 (GraphPad Software, La Jolla California USA) and R software. Considering data distribution, statistical evaluation was performed using One-Way ANOVA or Kruskal-Wallis when testing for at least 3 groups, and Student t-test or Mann-Whitney, when comparing 2 groups. Values of P < 0.05 were considered statistically significant.

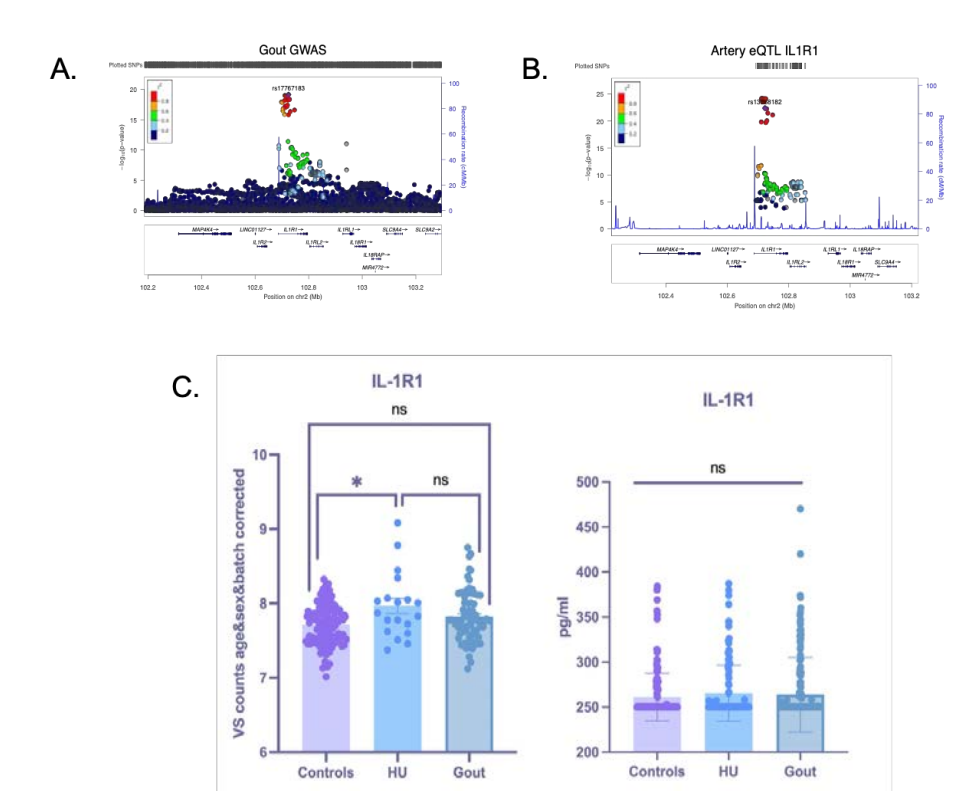


Figure 1 Locus Zoom plots of *IL1RN* locus in **A.** Gout GWAS and **B.** GTEx. The *IL1R1* rs17767183 SNP is labeled in purple. Each dot represents an individual SNP with the colour representing the LD with the most associated (lead) SNP in the panel. The vertical axis represents -log10 (p value) for assessment of the association of the SNP with *IL1R1* expression. The genes within the region are annotated, and the direction of the transcripts is shown by arrows. The plot was generated using LocusZoom (1). The Value for posterior probability of colocalisation (PPC) is included in the panel. **C.** mRNA expression level of IL1R1 in PBMCs originating from gout patients (n=72), hyperuricemic samples (19) and controls (n=113). **D.** Circulating IL1R1 plasma concentrations in n= 161 gout patients, n=123 hyperuricemic patients and n=145 healthy controls. Graph depicts means+/–SD. Kruskal-Wallis and post-hoc analysis p<0,05

Results

IL1R1 gene upregulated in hyperuricemic individuals

To evaluate the steady-state mRNA expression of the gout-associated *IL1R1* gene (12) we analyzed the expression in patients with gout (n=72), hyperuricemic samples (n=19) and normouricemic controls (n=113), where we could observe a higher expression of the IL1R1 gene in the samples of hyperuricemic people in comparison with the normouricemic controls (Figure 1 A). In contrast, no differences were observed in the gout group. Further, we assessed the basal circulating protein concentration of IL1R1 of the same individuals. Serum soluble IL1R1 protein levels depicted very low concentrations and there were no differences in the studied groups (Figure 1 B).

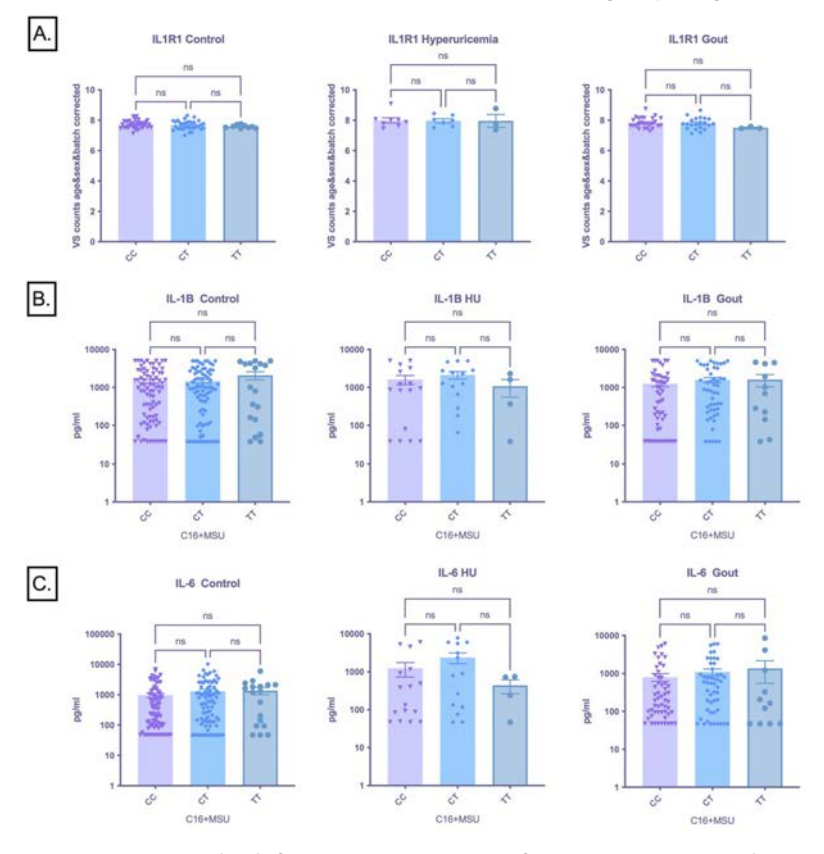


Figure 2. A. mRNA expression level of IL1R1 in PBMCs originating from gout patients (n=67), hyperuricemic samples (21) and controls (n=105). The data is represented as normalized counts age and sex corrected. B. Freshly isolated PBMCs originating from gout patients (n=97), hyperuricemic samples (n=91) and controls (n=150) stimulated with C16/MSU 300mg/dl for 24h. After 24h the supernatants were collected and IL-1 β (R&D Systems, Minneapolis) was measured. **C**. Concentration IL-6 measured in the supernatants of PBMCs after stimulation for 24h. The lowest range of detection was 78 pg/ml for IL-1β; 94 pg/ml for IL-6 Graph depicts means+/-SEM. Kruskal-Wallis and post-hoc analysis p<0,05

Basal expression and ex vivo cytokine production capacity in PBMCs of IL1R1 rs17767183 carriers show no difference in cvtokine production

Next, we studied the IL1R1 rs17767183 SNP previously associated with gout (12,13) for association with IL1R1 rs17767183 in patients with gout, hyperuricemia and normouricemic controls. The basal expression level of IL1R1 in freshly isolated PBMCs from the three studied groups (Figure 2A) was not associated with rs17767183. To further elucidate the possible implications of IL1R1 rs17767183 on inflammation, we assessed the ex vivo cytokine release of freshly isolated PBMCs exposed to different stimuli in association with the IL1R1 rs17767183 genotype: cytokine production in response to 24 h stimulation with the combination of MSU crystal with palmitate (C16.0). No significant association was found between the SNP and ex vivo cytokine production of IL-1\(\beta\) and IL-6 (Figure 2B-C) or IL-1Ra (Suppl. Fig 1) in any of the gout, hyperuricemia and normouricemic groups

Elevated IL-6 release upon C16+MSU crystal stimulation in the 500FG cohort

To assess the potential involvement of the IL1R1 rs17767183 SNP on inflammation in another cohort of samples, we took advantage of the Human Functional Genomics Project (http://www.humanfunctionalgenomics.org), where data from 316 healthy controls originating from the Netherlands (included in the 500FG cohort (17)) were used to test association of the rs17767183 SNP with cytokine production. The freshly isolated PBMCs were treated for 24h with various stimuli such as LPS 100ng, heat killed Candida albicans or the combination of C16.0 with MSU crystal 300mg/ dl. The IL1R1 rs17767183 C (gout risk) allele was associated with significantly elevated IL-6 cytokine production in response to C16+MSU crystal (Figure 3A). This effect was specific for C16+MSU crystal as this association was not observed for other stimuli tested in this experiment.

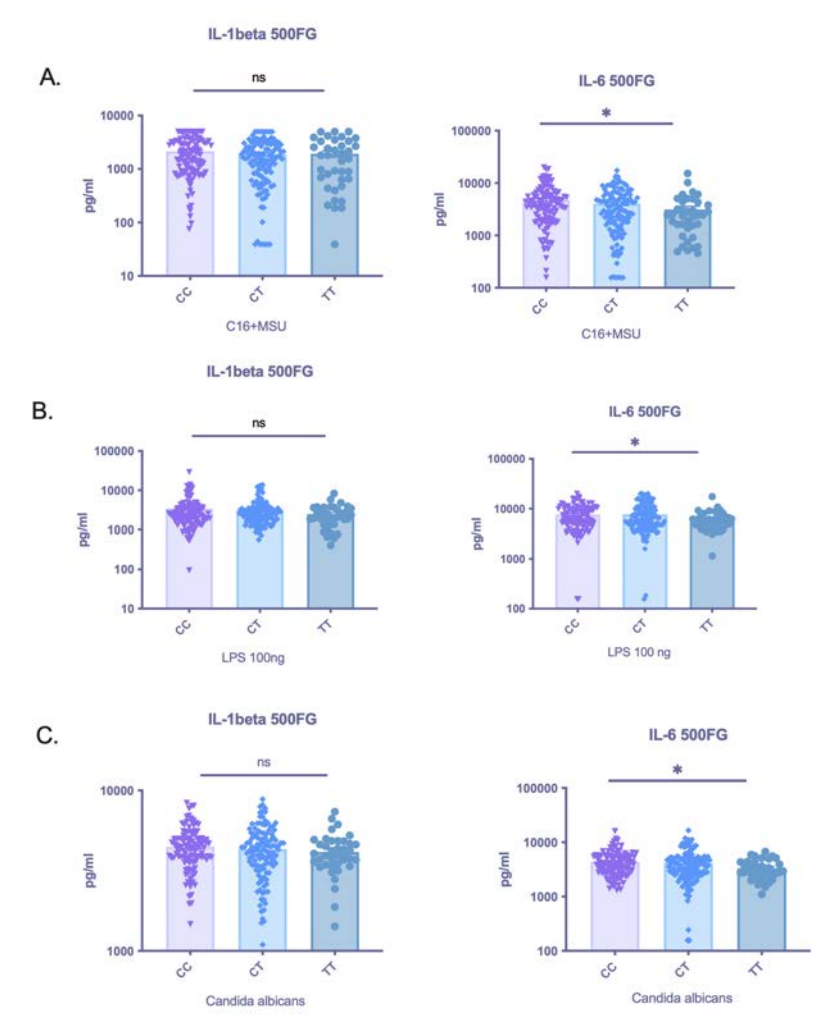


Figure 3 IL-1β and IL-6 production after 24h stimulation of PBMCs in vitro. A.Freshly isolated PBMCs originating from healthy controls (n=316) stimulated with C16/MSU 300mg/dl for 24h. After 24h the supernatants were collected and IL-1β and IL-6 (R&D Systems, Minneapolis) was measured. B. Freshly isolated PBMCs originating from healthy controls (n=316) stimulated with LPS 100ng for 24h. After 24h the supernatants were collected and IL-1β and IL-6 was measured. The lowest range of detection was 78 pg/ml for IL-1β; 312 pg/ml for IL-6. Graphs depict means+/–SEM. Kruskal-Wallis and post-hoc analysis p<0,05

Discussion

Despite the tremendous work on identifying genetic factors influencing the progression from hyperuricemia to gout, the specific molecular mechanisms involved in gout pathogenesis still need to be described. So far, Genome-wide association studies mostly revealed candidate genes associated with urate homeostasis and transport (SLC2A9, SLC22A12, ABCG2, MAF, HNF4A, PDZK1, GCKR) unveiling the kidney, the gut and liver as key points in urate regulation (18–20), therefore currently more than 200 urate-associated loci have been revealed (2,21). However, the focus on deciphering genetic factors that are associated to the inflammatory component in gout and that may contribute to the progression to clinical gout is a relatively new approach. The newest GWAS study conducted by Major et al. associated 377 loci to gout (12), where a subset of these genes were prioritized to their functional connection to inflammation in gout, Remarkably, the signal at the IL1R1 locus represents a novel finding, where a signal of association is being present in both traits (gout and urate) at a locus, but the signals do not overlap (12). Notably, the locus at the IL1R1 region was found to be associated to altered expression of IL1R1. with the gout association signal colocalizing with a signal of genetic control of expression (eQTL). The gout risk allele C was associated with increased expression of IL1R1 in various tissue types. Furthermore, the locus has been found to associate with white blood cell traits (12), these representing important markers of immune function and inflammation, thus potentially impacting an individual's immune response to different inflammatory processes. In line with this, studies in patients with hyperuricemia illustrated the association of elevated concentrations of serum urate with traits such as white blood cell counts (22).

IL1R1 is a key cytokine in mediating inflammatory and immune responses triggering an inflammatory cascade when binding to IL-1 (23). Also, it is being expressed on the surface of numerous immune cell types, such as macrophages, synovial cells and neutrophils (9,24). Not surprisingly, IL1R1 is linked to numerous inflammatory diseases, including rheumatoid arthritis (25), atherosclerosis (26,27), and lately gout (12,28). In accordance with this, similar studies in the literature emphasize the value of various IL1R1 genetic polymorphisms in inflammatory diseases such as rheumatoid arthritis in Chinese Han population (25), inflammatory bowel disease (29) or knee osteoarthritis (29) where the gene function may be altered, additionally influencing the onset and progression of the disease.

Hyperuricemia, described as elevated serum urate levels in the blood, represents the primary risk factor for gout (30). Several studies bring evidence on the proinflammatory role of urate (16,31,32), resulting in cytokine production differences and, especially, IL-1β increase. In our study, when assessing IL1R1 gene expression in unstimulated freshly isolated PBMCs from hyperuricemic individuals we noticed a higher expression in comparison with normouricemic controls, but this elevation was not observed in gout. Moreover, no differences could be detected

when measuring circulating IL1R1 protein concentrations in the same groups. A recent report described the IL1R1 gene as being one of the differentially expressed genes in monocytes in response to MSU crystal or LPS stimulation, suggesting its role in the inflammatory response to crystals, however, this was not mirrored in samples of patients with gout. In addition, when assessing IL1R1 gene expression in association with the rs17767183 SNP, no differences could be depicted.

Ex vivo cytokine production of freshly isolated PBMCs does not reveal any association of the IL1R1 rs17767183 SNP with cytokine production in the HINT Study group. Interestingly however, a significantly increased IL-6 cytokine production in response to C16+MSU crystals was observed in the C-allele carriers among the healthy controls of the 500FG cohort. This indicates that the variant associated with differential cytokine production in blood mononuclear cells, with possible implications for inflammatory risk. The observed discrepancy could be accedited to several factors, such as sample size and population specific differences, although the frequency of the studied SNP were similar in both of the cohorts. The "C" allele frequency of rs17767183 was 0,35 in the romanian normouricemic group, respectively 0,37 in the Dutch 500FG cohort. Another consideration is that neither the romanian nor the dutch cohorts met the Hardy-Weinberg Equilibrium (HWE) criteria.

Nevertheless, several limitations of our research deserve mention. First, the group sizes of subjects with hyperuricemia and gout are a limitation of the study. Secondly, the high inter-individual variability in cytokine data coming from primary cells, such as PBMCs, precludes robust conclusions in some comparisons with moderate sample sizes. Despite the limitations mentioned, our present research has the advantage of evaluating the association between the SNP of interest and cytokine production on multiple levels, including transcription data, circulating protein levels, and ex vivo cytokine measurements in stimulated primary PBMCs, using cohort coming from The HINT Study Cluj-Napoca, Romania and 500FG The Netherlands.

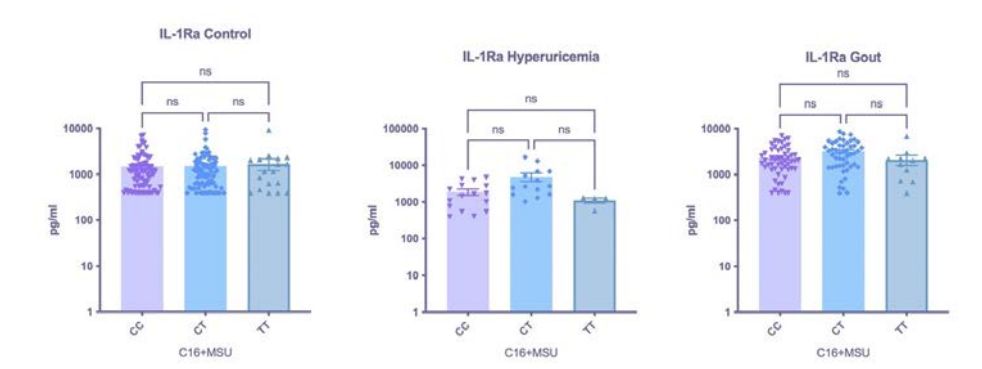
Finally, variation in expression of IL1R1 is observed in primary PBMCs of hyperuricemic individuals thus reinforcing data implicating these loci in gout and urate-related inflammation. However, discordant results were observed for cytokine production levels in relationship to the IL1R1 rs17767183 SNP. The possible mechanism of how the risk variant at this locus could contribute to progression from asymptomatic hyperuricemia to gout pathogenesis needs further assessment.

References

- Abhishek A, Roddy E, Doherty M. Gout a guide for the general and acute physicians. Clin Med. 2017 Feb;17(1):54-9.
- Robinson PC. Gout An update of aetiology, genetics, co-morbidities and management. 2. Maturitas. 2018 Dec;118:67-73.
- 3. Dalbeth N, Te Karu L, Stamp LK. Gout and its management. Intern Med J. 2024 May;54(5):716–23.
- 4. Dalbeth N, Gosling AL, Gaffo A, Abhishek A. Gout. Lancet (London, England). 2021 May;397(10287):1843-55.
- 5. Narang RK, Dalbeth N. Pathophysiology of Gout. Semin Nephrol. 2020 Nov;40(6):550-63.
- Robinson PC, Horsburgh S. Gout: joints and beyond, epidemiology, clinical features, treatment 6 and co-morbidities. Maturitas. 2014 Aug;78(4):245-51.
- 7. Dalbeth N, Phipps-Green A, Frampton C, Neogi T, Taylor WJ, Merriman TR. Relationship between serum urate concentration and clinically evident incident gout: An individual participant data analysis. Ann Rheum Dis. 2018;
- Klück V, Liu R, Joosten LAB. The role of interleukin-1 family members in hyperuricemia and gout. Jt Bone Spine. 2021;88(2).
- 9. Boraschi D, Italiani P, Weil S, Martin MU. The family of the interleukin-1 receptors. Immunol Rev. 2018 Jan;281(1):197-232.
- 10. Dinarello CA. How interleukin-1β induces gouty arthritis. Vol. 62, Arthritis and rheumatism. United States; 2010. p. 3140-4.
- 11. Dalbeth N, House ME, Aati O, Tan P, Franklin C, Horne A, et al. Urate crystal deposition in asymptomatic hyperuricaemia and symptomatic gout: a dual energy CT study. Ann Rheum Dis. 2015 May;74(5):908-11.
- 12. Major TJ, Takei R, Matsuo H, Leask MP, Topless RK, Shirai Y, et al. A genome-wide association analysis of 2,622,830 individuals reveals new pathogenic pathways in gout. medRxiv [Internet]. 2022 Jan 1;2022.11.26.22281768. Available from: http://medrxiv.org/content/ early/2022/11/29/2022.11.26.22281768.abstract
- 13. Takei R, Sumpter N, Merriman T. Genetic loci that affect urate levels but not gout risk-an apparent discordance between urate and gout genetics.
- 14. Ota M, Nagafuchi Y, Hatano H, Ishigaki K, Terao C, Takeshima Y, et al. Dynamic landscape of immune cell-specific gene regulation in immune-mediated diseases. Cell. 2021 May;184(11):3006-3021.e17.
- 15. Cobo I, Cheng A, Murillo-Saich J, Coras R, Torres A, Abe Y, et al. Monosodium urate crystals regulate a unique JNK-dependent macrophage metabolic and inflammatory response. Cell Rep. 2022 Mar;38(10):110489.
- 16. Crisan TO, Cleophas MCP, Oosting M, Lemmers H, Toenhake-Dijkstra H, Netea MG, et al. Soluble uric acid primes TLR-induced proinflammatory cytokine production by human primary cells via inhibition of IL-1Ra. Ann Rheum Dis. 2016;
- 17. Ter Horst R, Jaeger M, Smeekens SP, Oosting M, Swertz MA, Li Y, et al. Host and Environmental Factors Influencing Individual Human Cytokine Responses. Cell. 2016 Nov;167(4):1111-1124.e13.
- 18. Köttgen A, Albrecht E, Teumer A, Vitart V, Krumsiek J, Hundertmark C, et al. Genome-wide association analyses identify 18 new loci associated with serum urate concentrations. Nat Genet. 2013;45(2):145-54.

- 19. Matsuo H, Yamamoto K, Nakaoka H, Nakayama A, Sakiyama M, Chiba T, et al. Genome-wide association study of clinically defined Gout identifies multiple risk loci and its association with clinical subtypes. Ann Rheum Dis. 2016;75(4).
- 20. Phipps-Green AJ, Merriman ME, Topless R, Altaf S, Montgomery GW, Franklin C, et al. Twentyeight loci that influence serum urate levels: Analysis of association with gout. Ann Rheum Dis. 2016:75(1):124-30.
- 21. Tin A, Marten J, Halperin Kuhns VL, Li Y, Wuttke M, Kirsten H, et al. Target genes, variants, tissues and transcriptional pathways influencing human serum urate levels. Nat Genet. 2019;51(10):1459-74.
- 22. Ruggiero C, Cherubini A, Ble A, Bos AJG, Maggio M, Dixit VD, et al. Uric acid and inflammatory markers. Eur Heart J. 2006;27(10):1174-81.
- 23. Dinarello CA. Overview of the IL-1 family in innate inflammation and acquired immunity. Immunol Rev. 2018 Jan:281(1):8-27.
- 24. Mantovani A, Dinarello CA, Molgora M, Garlanda C. IL-1 and related cytokines in innate and adaptive immunity in health and disease. Immunity [Internet]. 2019;50(4):778. Available from: /pmc/articles/PMC7174020/%0A/pmc/articles/PMC7174020/?report=abstract%0Ahttps://www. ncbi.nlm.nih.gov/pmc/articles/PMC7174020/
- 25. Liu X, Peng L, Li D, He C, Xing S, Wang Y, et al. The Impacts of IL1R1 and IL1R2 Genetic Variants on Rheumatoid Arthritis Risk in the Chinese Han Population: A Case-Control Study. Int J Gen Med. 2021;14:2147-59.
- 26. Coppin E, Zhang X, Ohayon L, Johny E, Dasari A, Zheng KH, et al. Peripheral Ischemia Imprints Epigenetic Changes in Hematopoietic Stem Cells to Propagate Inflammation and Atherosclerosis. Arterioscler Thromb Vasc Biol. 2023 Jun;43(6):889-906.
- 27. Kidder E, Pea M, Cheng S, Koppada S-P, Visvanathan S, Henderson Q, et al. The interleukin-1 receptor type-1 in disturbed flow-induced endothelial mesenchymal activation. Front Cardiovasc Med. 2023:10:1190460.
- 28. de Lima JD, de Paula AGP, Yuasa BS, de Souza Smanioto CC, da Cruz Silva MC, Dos Santos PI, et al. Genetic and Epigenetic Regulation of the Innate Immune Response to Gout. Immunol Invest. 2023 Apr;52(3):364-97.
- 29. Latiano A, Palmieri O, Pastorelli L, Vecchi M, Pizarro TT, Bossa F, et al. Associations between genetic polymorphisms in IL-33, IL1R1 and risk for inflammatory bowel disease. PLoS One. 2013;8(4):e62144.
- 30. Joosten LAB, Crişan TO, Bjornstad P, Johnson RJ. Asymptomatic hyperuricaemia: a silent activator of the innate immune system. Nat Rev Rheumatol. 2020;16(2):75-86.
- 31. Badii M, Gaal Ol, Cleophas MC, Klück V, Davar R, Habibi E, et al. Urate-induced epigenetic modifications in myeloid cells. Arthritis Res Ther. 2021;23(1):1-11.
- 32. Badii M, Klück V, Gaal O, Cabău G, Hotea I, Nica V, et al. Regulation of SOCS3-STAT3 in urateinduced cytokine production in human myeloid cells. Jt bone spine. 2024 May;91(3):105698.

Supplemental information



Supplemental Figure 1 Freshly isolated PBMCs originating from gout patients (n=97), hyperuricemic samples (n=91) and controls (n=150) stimulated with C16/MSU 300mg/dl for 24h. After 24h the supernatants were collected and concentration IL-1Ra was measured. The lowest range of detection was 390 pg/ml for IL-1Ra. Graph depicts means+/—SEM. Kruskal-Wallis and post-hoc analysis p<0,05



Chapter 5

Hyperuricemia remodels the serum proteome toward a higher inflammatory state

Georgiana Cabău, Orsolya Gaal, Medeea Badii, Valentin Nica, Andreea-Manuela Mirea, Ioana Hotea, HINT-consortium, Cristina Pamfil, Radu A. Popp, Mihai G. Netea, Simona Rednic, Tania O. Crișan* and Leo A.B. Joosten*

^{*} Tania O. Crişan and Leo A.B. Joosten share senior authorship.

Abstract

Gout is an autoinflammatory disease triggered by a complex innate immune response to MSU crystals and inflammatory triggers. Whilst hyperuricemia is an obligatory risk factor for the development of gout, the majority of individuals with hyperuricemia never develop gout but have an increased risk of developing cardiometabolic disorders. Current management of gout aims at MSU crystal dissolution by lowering serum urate. We apply a targeted proteomic analysis, using Olink inflammation panel, to a large group of individuals with gout, asymptomatic hyperuricemia and normouricemic controls, and we show a uratedriven inflammatory signature. We add in vivo evidence of persistent immune activation linked to urate exposure and describe immune pathways involved in the pathogenesis of gout. Our results support a proinflammatory effect of asymptomatic hyperuricemia and pave the way for new research into targetable mechanisms in gout and cardiometabolic complications of asymptomatic hyperuricemia.

Introduction

Gout is the most common inflammatory arthritis with a rising prevalence in the majority of developed nations¹. Hyperuricemia, defined as elevated serum urate concentrations, is the main risk factor for developing gout. Abnormally elevated urate precipitates into MSU (monosodium urate) crystals which deposit within joints and surrounding tissues triggering inflammation, manifested by painful acute arthritis known as the gout flare². The initial manifestation typically self-resolves within two weeks, followed by an asymptomatic period before a subsequent flare develops³. Patients who have persistent hyperuricemia may experience chronic deposition of urate crystals in tophi and chronic joint inflammation, which can damage joints and impair articular motion⁴. The greater mortality rate reported in patients with gout is attributed to the association of gout with other comorbidities such as cardiovascular disease, hypertension, metabolic syndrome, kidney stones, and chronic kidney disease⁵.

The pathogenesis of gout begins with hyperuricemia, and the likelihood of developing gout is correlated with serum urate concentrations in a dose-dependent manner. Hyperuricemia can be caused by factors that stimulate the overproduction of urate, including high purine diets, myeloproliferative diseases, or other illnesses linked to a high rate of cellular turnover, as well as defects in excretion such as kidney dysfunction or certain diuretics. Cells of the innate immune system, primarily macrophages and monocytes, recognize MSU crystals as a damageassociated molecular pattern activating an inflammatory cascade resulting in the production of IL-1β through activation of the NLRP3 inflammasome, an intracellular danger signal sensor². Current treatment strategies in gout follow a treat-to-target approach using urate-lowering therapy aimed at the dissolution of MSU crystals, aiming for serum urate concentrations below 6 mg/dL as a treatment target⁶.

While this approach has supporting evidence in gout clinical trials, the treatment of asymptomatic hyperuricemia remains under debate⁷⁻⁹. On the one hand, hyperuricemia is a necessary, but insufficient risk factor for the onset of gout. In the United States of America, around 20 percent of the population presents with hyperuricemia, but the majority never develop gout¹⁰. Moreover, a significant percentage of individuals with hyperuricemia have asymptomatic crystal deposition^{11,12}. On the other hand however, in the absence of gout flares, asymptomatic hyperuricemia is linked to cardiovascular disease, coronary heart disease, heart failure, stroke, an increased risk of cardiovascular death, increased overall mortality, cancer, and accelerated aging 13-22. According to some prospective studies, hyperuricemia leads to refractory hypertension, chronic kidney disease, metabolic syndrome, and type 2 diabetes^{23–28}. Experimental research demonstrates that soluble urate exerts direct pro-inflammatory effects on human PBMCs (peripheral blood mononuclear cells) and PBMCs from patients with gout and hyperuricemia produce higher levels of pro-inflammatory cytokines^{29,30}. Soluble urate primes cells for higher induction of cytokines via epigenetic reprogramming and aside from transcriptional upregulation of pro-inflammatory genes, urate specifically downregulates the transcription of IL1RA, enhancing inflammation, as IL-1Ra serves as the main IL-1β antagonist³⁰. This results in a pro-inflammatory phenotype of soluble urate-exposed monocytes and macrophages, which can lead to persistent immune activation and chronic inflammation.

In the present study, we aimed to: 1) characterize and compare the inflammatory proteomic signatures of gout and asymptomatic hyperuricemia; 2) functionally characterize the identified FGF-21 biomarker in relation to cytokine production, and 3) monitor alterations in the proteomic profile of patients with gout following uratelowering therapy. Our study adds to the expanding body of evidence supporting the inflammatory role of urate and provides new insights into the pathophysiological mechanisms of gout and their potential use as therapeutic targets.

Experimental model and subject details

Patient recruitment and study design

Peripheral blood and serum were collected from patients with gout, asymptomatic hyperuricemia individuals and normouricemic controls recruited between 2016 and 2020 and attending the Rheumatology, Internal Medicine, Diabetes or Geriatrics clinics of the County Emergency Hospital of Cluj-Napoca, Romania. Ethical approval was obtained from the University of Medicine and Pharmacy of Cluj-Napoca, reference no. 425/2016. Informed consent was obtained from all individuals included. Participants were part of a larger study HINT, "Hyperuricaemia induced INflammation: Targeting the central role of uric acid in rheumatologic and cardiovascular diseases", P 37 762, MySMIS 103587, a multi-omics study aiming to assess whether soluble urate induces epigenetic and transcriptional reprogramming in cells of innate immune system, leading to a hyperinflammatory state. The present study included two independent groups, a larger cross-sectional cohort comprising of 193 patients with gout, 154 individuals with asymptomatic hyperuricemia and 215 normouricemic controls with sample and clinical data collected at baseline. Another independent group comprised of 25 "Treat-to-Target"

patients with gout following a longitudinal study design with sample, clinical and laboratory data collected at baseline, after 1 month and after 3 months of initiating urate-lowering therapy (ULT) using allopurinol in standard dosage of 100 to 300 milligrams (mg) per day at first and up to 400 mg after dosage stabilization.

Of note, the treat-to-target study was designed for a 12-month follow-up, but the sample collection was compromised due to the epidemiologic circumstances of the COVID-19 pandemic. For this reason, the data presented here only shows the evolution over three months.

Clinicopathologic assessment of cohorts

For the diagnosis of gout, patients fulfilled the 2015 American College of Rheumatology/European League Against Rheumatism (ACR/EULAR) criteria for the classification of gout, having a score of 8 or higher, or had crystal-proven gout with identification of MSU crystals in synovial fluid using compensated polarized light microscopy. For asymptomatic hyperuricemia, we defined hyperuricemia as serum urate concentration (sUA) greater or equal to 7 mg/dL in the absence, and without a history, of gout. For normouricemia, we included individuals with sUA below 7 mg/dL.

We collected participant information (reported in Figure 1) regarding age, sex, BMI, clinical chemistry including serum uric acid, total cholesterol (TC), triglycerides (TG), blood creatinine and medical history regarding cardiometabolic and renal comorbidities. Type 2 diabetes was based on repeated measurements of blood fasting glucose concentrations of 126 mg/dL or higher. Liver steatosis was evaluated by abdominal ultrasonography. Hypercholesterolemia (HyperTC) was defined as serum total cholesterol of 200 mg/dL or higher. Total triglyceride concentrations above 150 mg/dL were used as cut-off for hypertriglyceridemia (HyperTG). Repeated measurements of systolic blood pressure above 150 mmHg were used for diagnosing high blood pressure. Cardiovascular diseases (CVD) included myocardial infarction, stroke, transient ischemic attack and peripheral artery disease. Chronic kidney disease (CKD) was defined as reduced glomerular filtration rate for more than 3 months (GFR < 60 mL/min/ 1.73 m²). Chronic tophaceous gout diagnosis was determined by evaluating the extent and characteristics of the tophi, chronic arthropathy, joint inflammation and deforming features observed during the clinical examination and as previously described in the 2012 ACR guidelines for management of gout⁹⁶. The following parameters were clinically assessed: number of tophi, tophus drainage, tophus infection, extent of tissue destruction, size and growth rate, and joint inflammation. Mild disease was defined as simple chronic tophaceous gouty arthropathy limited to 1 joint and stable disease characterized by stable tophus size and slow growth, absence of drainage, low risk of infection, lack of aggressive tissue destruction and lack of severe chronic joint inflammation. Moderate disease was defined as simple chronic tophaceous gouty arthropathy affecting 2-4 joints and stable disease characterized by multiple, but stable and simple tophi as described above. Severe disease was defined as chronic tophaceous gouty arthropathy affecting more than 4 joints or more than 1 unstable, complicated tophus that presented drainage, a high risk of infection, accelerated growth, extensive tissue destruction and severe chronic tophaceous ioint inflammation.

Primary cell culture

Peripheral blood mononuclear cells (PBMCs) from participants recruited at the rheumatology clinic of Cluj-Napoca, were isolated from whole blood by density gradient centrifugation using FicoII-Pague PLUS (Sigma-Aldrich). For ex-vivo stimulation with FGF-21, PBMCs from 10 patients with gout (5 females and 5 males) and 11 sex and age matched controls (5 females and 6 males) recruited at the rheumatology clinic were seeded in 96-well round-bottom microplates (Greiner Bio-One) at a density of 5 x 10⁶ cells/mL in cell medium RPMI-1640 (Sigma-Aldrich) supplemented with 1 mM pyruvate, 50 µg/mL gentamicin (Sigma-Aldrich) and 2 mM GlutaMAX (ThermoFisher Scientific). The cells were stimulated with either 50uM C16:0 (palmitate) together with 300ug/mL MSU crystals with 2ug/mL rhFGF-21 (recombinant human FGF-21) (R&D Systems) or medium control. MSU crystals were prepared in-house by diluting crystalline uric acid in a solution of NaOH: 1.0 gram of crystalline uric acid was solubilized in 200 ml of sterile water containing 24 grams of NaOH. The pH was adjusted to 7.2 using HCl. The solution became pyrogen-free after heating for 6 hours at 120°C. The solution was left to cool at room 30 temperature and stored at 4°C. Crystals produced were 5–25 μm in length³⁰. Plates were incubated at 37°C and 5% CO₃ for 24h. After 24h incubation, plates were centrifuged, supernatants were removed and stored at -20°C until cytokine measurement was performed.

METHOD DETAILS

Proteomic analysis and data processing

Serum samples from normouricemic (NU), asymptomatic hyperuricemia individuals (AH) and patients with gout that were collected at enrolment or at every visit for the treat-to-target group and stored at -80°C, were thawed on ice mixed by pipetting and randomized before plating on 96-well PCR microplate. Serum

proteomic measurement was performed using Olink proximity extension assay, technology that uses gPCR for the simultaneous quantification of a pre-designed panel of proteins within a sample⁹⁷. For this study, we used the Olink® Target 96 inflammation panel98. Proteomic assay, data normalization and quality control were performed at Olink Proteomics, Uppsala, Sweden. Briefly, the technology uses specific oligonucleotides-labelled antibodies against the target protein that upon binding come in proximity generating a PCR reporter sequence that allows quantification of protein abundance by Real-Time PCR (qPCR). Using sample and plate controls, the resulting Ct-values were taken through multi-step quality control to correct for intra-assay and inter-assay technical variability generating normalized NPX (normalized protein expression) values. Following quality control, samples that did not pass OC (n=24) and proteins that had NPX values below the limit of detection in more than or equal to 20% of samples (n=19) were filtered out and excluded from further analysis. A total of 73 proteins were included in the subsequent analysis. The NPX units are on a log2 scale, with 1 NPX difference equivalating to a 2-fold change in protein expression.

Cytokine measurements

IL-1β, IL-1Ra and IL-6 concentrations were determined using commercial ELISA kits (R&D Systems) in harvested supernatants from PBMCs treated with FGF-21 and C16+MSU or RPMI control for 24h. Absorbance was measured on Bio Tek Synergy HTX reader

QUANTIFICATION AND STATISTICAL ANALYSIS

Median and interquartile range (IQR) are used to present continuous variables. Categorical variables such as sex and presence or absence of comorbidities are presented as absolute frequencies and percent of individuals. Percentages are expressed as relative frequency of that variable based on the available data for the subgroup. Non-parametric variables age, BMI, blood creatinine, and sUA concentrations in three or more groups were tested using Kruskal-Wallis test with Dunn's correction for multiple testing. Wilcoxon matched pairs signed rank test was used to test for differences in cytokine production between two paired groups. Categorical variables for sex and comorbidities were evaluated using a Chi-squared test. All proteomics data was corrected for age and sex using a linear regression model with age and sex as covariates. Analysis was performed using the R software and 'stats' package. Adjusted NPX values were retrieved and used in all downstream analyses. Untargeted group comparison analyses were performed using multiple t-test with Welch correction and two-stage step-up method of Benjamini, Krieger and Yekutieli for controlling the false-discovery rate (FDR, Q = 5%). Associations with Q <0.05 were considered significant. Targeted analysis of individual proteins for two groups comparisons was performed using Welch's t test and Welch's ANOVA for three groups comparison with Dunnett's T3 test for multiple testing correction when sample size n < 50 and Games-Howell for multiple testing correction when sample size was n > 50. All tests were two-tailed, and the statistical significance cut-off was P < 0.05. All analyses were performed using GraphPad Prism (v.9.5.1) or R software⁹⁶ (v.4.2.1).

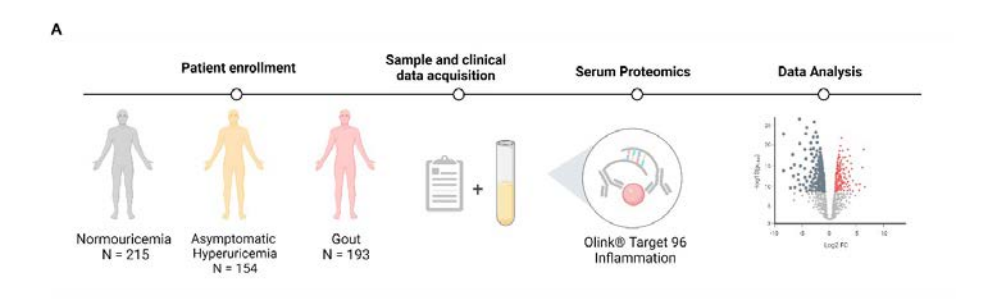
DATA AND CODE AVAILABILITY

The Olink proteomics dataset reported in this paper has been deposited to Mendeley Data (DOI: 10.17632/rhn9vsgk45.1) Any additional information required to reanalyze the data reported in this paper is available upon request from the lead contact.

Results

Baseline clinical and laboratory characteristics of the study groups.

We sought to characterize the inflammatory signatures of gout and asymptomatic hyperuricemia (AH) using patients and control sera. We included 193 patients with gout, 154 individuals with asymptomatic hyperuricemia and 215 normouricemic controls (NU). Biological sample collection and baseline laboratory analysis were conducted at inclusion in the study (Figure 1A) (Cf. Methods). Differences between groups were found for age and sex. Male sex representation was higher in gout, 81.3% compared to 42.8% in AH and 26.6% in the NU group (Figure 1B). Patients with gout tended to be slightly younger (median 62 years, IQR 53.0-67.5) than NU controls (median 64 years, IQR 58.0-70.0), with no difference compared to AH (median 64 years, IQR 57.0-71.0) (Figure 1C). AH individuals had slightly higher BMI (median 29.4, IQR 27.1-35.1) compared to NU controls (median 28.5, IQR 26.4-31.7), with no difference compared to gout (median 29.6, IQR 26.8-33.1) (Figure 1D). Blood creatinine was significantly higher in gout (median 0.93 IQR 0.8-1.1) and AH (median 0.98, IQR 0.8- 1.2) compared to NU controls (median 0.8, IQR 0.7-0.9) (Figure 1E). Baseline serum urate concentrations ranged from 2.4 to 6.9 with a median of 5.1 mg/dL in the NU controls groups, 7.0 to 13.9, with a median of 8.1 mg/dL for hyperuricemic individuals, and 1.8 to 14.2 with a median of 7.2 mg/dL for patients with gout (Figure 1F). There were significant differences in the prevalence of comorbidities, with AH and gout having higher occurrences of high blood pressure, hypertriglyceridemia, cardiovascular disease, type 2 diabetes mellitus, steatosis, and chronic kidney disease (Figure 1G, Table S1).



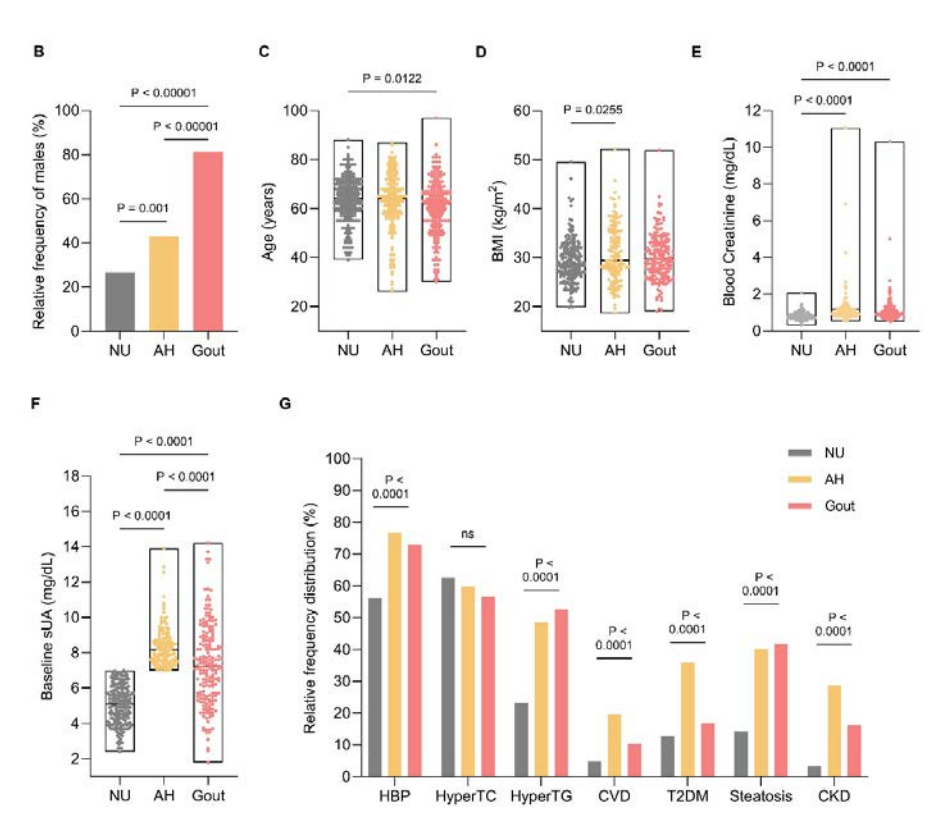


Figure 1 Baseline clinical and laboratory characteristics of the study groups (A) Study design. The image was created with BioRender.com. (B-F) Differences in (B) sex distribution, (C) age, (D) body mass index (BMI), (E) blood creatinine, (F) serum uric acid, (G) comorbidities distribution among nomoruricemic, hyperuricemic individuals and patients with gout. Floating bars (C-F) represent the range of values with line at median. Bars (B, G) represent percentages. Kruskal-Wallis test was performed for (C-F) with Dunn's test for multiple comparisons and the chi-squared test was used to test for differences in observed frequencies (B, G). Significance is reported as two-tailed P values (See also Table S1). Abbreviations: NU normouricemia; AH asymptomatic hyperuricemia, HBP high blood pressure, HyperTC hypercholesterolemia, HyperTG hypertriglyceridemia, CVD cardiovascular disease, T2DM type 2 diabetes mellitus, CKD chronic kidney disease.

Serum proteomic signatures of gout and hyperuricemia

To determine the serum inflammatory proteomic signature of our study groups, targeted proteomic analysis was performed using the Olink® Target 96 inflammation panel. We first investigated the proteomic profile difference between patients with gout and all controls (comprising both AH and NU individuals). Across the 73 proteins, we found no differentially expressed biomarkers between the two groups (Figure 2A). However, when we investigated the serum proteome profiles of AH versus NU individuals, we identified a marked inflammatory signature in the AH group, consisting of 58 significantly differentially expressed proteins (Figure 2B and Table S2).

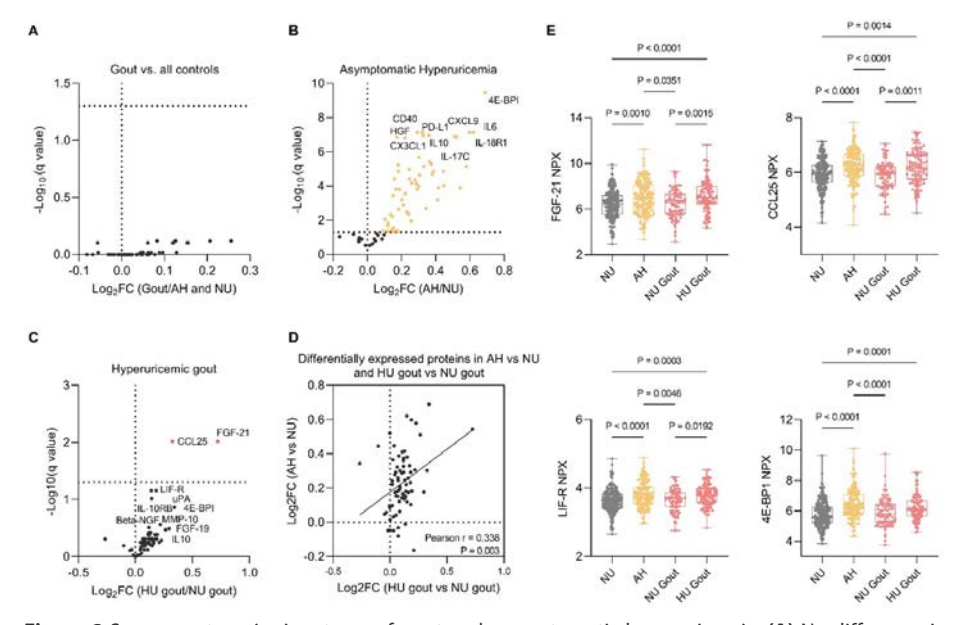


Figure 2 Serum proteomic signatures of gout and asymptomatic hyperuricemia. **(A)** No difference in protein expression between gout versus all controls (NU and AH individuals). **(B)** Volcano plot showing proteins upregulated in AH compared to NU controls. **(C)** Proteins upregulated in hyperuricemic patients with gout compared to normouricemic patients with gout. Top 10 proteins are labeled **(D)** Correlation of differences between AH vs NU and HU gout vs NU gout. (E) Targeted analysis of the two proteins upregulated in HU gout compared to NU gout, FGF-21, CCL25 and two nominally significant proteins, LIF-R and 4E-BP1. Volcano plots for (A-C) are shown. Associations with q values < 0.05 were considered significant, Welch multiple t-test, FDR 5%. Box plots (E) show line at median and the 75th and 25th percentiles, whiskers show the range of values. Welch's ANOVA with Games-Howell's multiple comparisons test was used to test for differences between groups (See also Figure S1 and Table S2). Abbreviations: NU normouricemia; AH asymptomatic hyperuricemia.

The most upregulated protein in the AH group was the mTOR effector 4E-BP1, followed by IL-18R1. The concentrations of IL-6 and other members of the IL-6 family of cytokines such as LIF-R (leukemia inhibitory factor receptor) and OSM (oncostatin M)

were also upregulated in the AH group. Other upregulated proteins were the immunomodulatory IL-10 cytokine and its receptor subunit IL-10RB, which together act as a negative regulator to dampen the inflammatory response³¹; the TNF cytokine family and its receptors: the pleiotropic TNF cytokine, TNFSF14, the receptors CD40, TNFRSF9, and OPG (osteoprotegerin); and to a lesser extent the pro-inflammatory Lymphotoxin (formerly known as TNF-β)³². Among other cytokines upregulated in AH we found IFN-y, IL-17A and IL-17C, IL-12B, and the receptor subunit IL-15RA. The proteomic signature of hyperuricemia was also comprised of a wide array of chemokines both inflammatory and homeostatic, as well as dual chemokines. They were represented by the inflammatory CC chemokines, monocyte chemoattractant proteins MCP-1, MCP-2, MCP-3, MCP-4, the homeostatic CCL19, CCL25, CCL28 and the dual chemokines CCL11, CCL20, as well as the platelet chemokine CCL23³³. The upregulated CXC chemokines comprised the neutrophil chemoattractants CXCL1, CXCL6, CXCL8, and the IFN-y (interferon-gamma)-inducible CXCL9, CXCL10 and CXCL11 axis, the latter involved in immune cell differentiation, migration and activation³⁴. The novel CX3CL1, fractalkine, described to have anti-apoptotic effects on immune cells and other cell types³⁵ was induced in the AH group. Another group of inflammatory proteins we screened for were growth factors, among which HGF was one of the top 10 most upregulated proteins, followed by CSF-1, TGF- α , β -NGF, VEGFA, FGF-21, LAP TGF-beta, NT-3 and FGF-19. Other immunoregulatory proteins overexpressed in AH were PDL-1 (programmed death-ligand 1), CD8 antigen, S100A12, CDCP1, the T-cell marker CD5, SLAMF1, STAMBP, SIRT2, CASP8, CST5, uPA (urokinase) and the proteinases MMP-1 and MMP-10.

Next, we wanted to test if the proteomic profile of AH is recapitulated in gout. We stratified gout samples based on sUA concentrations equal to 7mg/dL or higher, here called hyperuricemic gout (HU gout) n = 104 and below 7 mg/dL, here called normouricemic gout (NU gout) n = 81. We found two proteins FGF-21 (fibroblast growth factor 21) and CCL25 significantly overexpressed in HU patients with gout compared to NU gout and another 8 nominally significant (Figure 2C). We further tested whether the lack of significance was due to the smaller number of patients included in the analysis and we looked for the directionality of differences, assessed as log2-fold-changes, resulting from the comparison of the AH group versus NU and HU gout versus NU gout group (Figure 2D). We observed a convergent directionality with most protein differences correlating between the two groups (Pearson r = 0.338, p = 0.003). This was also recapitulated when we looked at FGF-21 and CCL25 which were significantly increased, while LIF-R and 4E-BP1 were nominally significant in HU gout: we observed significantly higher concentrations of these proteins in HU gout compared to NU or NU gout, but no difference was observed in HU gout compared to AH, nor in NU gout compared to normouricemia (Figure 2E). The lack of differences between gout and the total control group could be thus explained by the high concentrations of inflammatory markers associated with hyperuricemia, masking the effect of gout when we compared gout against all controls. This is also supported by analyzing the gout group against normouricemic controls, which revealed 39 differentially expressed inflammatory markers, of which 36 overlapped with the markers associated to AH (Figure S1A-B). Comparison of AH to gout revealed 14 markers that had higher levels in AH samples than in gout (Figure S1C).

The hepatokine FGF-21 modulates gout-related inflammation

The most significantly upregulated protein in the hyperuricemic gout samples compared to normouricemic gout, was the hepatokine FGF-21, which also correlated with sUA concentrations (r = 0.29, P < 0.0001) (Figure 2C and Figure S1D). Previous studies showed FGF-21 to be a pleiotropic stress-inducible hormone with tissue and organ-specific immunometabolic benefits^{36,37}.

We hypothesized that FGF-21 may be an adaptive regulator in hyperuricemia and gout-related inflammation. To assess a functional role, primary PBMCs from 21 volunteers were stimulated *ex vivo* with palmitate (C16) together with MSU, which mimic fatty acid accumulation that may result from metabolic changes, hypothesized to initiate the gout flare (cf. Methods section)².

We found that in C16 and MSU co-stimulated cells, treatment with rhFGF-21 decreased the production of IL-1 β (P = 0.0049) and IL-1Ra (P = 0.0080), while it had no significant effect on IL-6 production (P = 0.2402) (Figure 3).

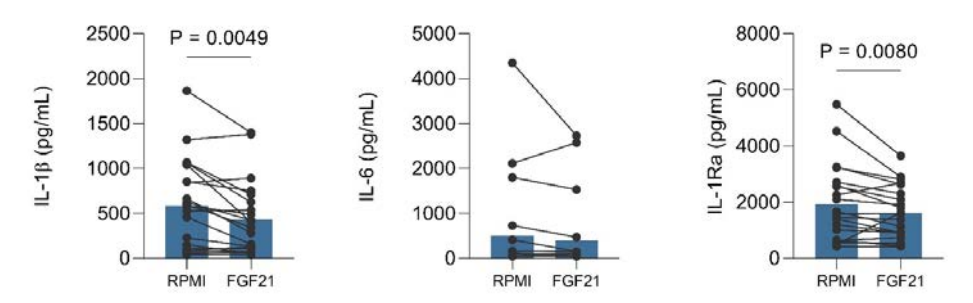


Figure 3 The hepatokine FGF-21 modulates gout-related inflammation. Production of IL-1 β , IL-1Ra and IL-6 in response to stimulation with C16+MSU in the presence or absence of rhFGF-21 treatment. Data is representative for 21 individual samples, comprising of patients with gout (n=10) labelled in red, and sex and age matched controls (n=11). Four independent experiments were performed. Dots and lines represent the paired samples under different conditions. Bars show means. Differences were tested using Wilcoxon matched pairs signed rank test.

Association of serum protein levels with gout flares and tophaceous gout

To better understand the mechanisms and molecular triggers of gout flares, we looked at whether there were any differences in the serum proteome of individuals who were experiencing flares. Out of the 193 patients with gout, 65 individuals presented and had serum collected during a flare. Out of the 65 patients, 27 presented with monoarticular disease, affecting the metatarsophalangeal (MTP) joint, while another 27 had larger joints involved, such as the ankle, knee, or elbow, and 11 patients exhibited polyarticular disease (Figure 4A). Six significantly distinct proteins were identified in the serum proteomic profile of gout flares, these patients having elevated circulating concentrations of MMP-1, IL-6, VEGFA (vascular endothelial growth factor A), and CCL23 and decreased DNER (Delta and Notch-like epidermal growth factor-related receptor) and CD6 levels (Figure 4B and Figure S2A). Among the 10 proteins which were nominally significant before multiple testing correction, 8 proteins (LAP-TGF-beta, S100A12, HGF (hepatocyte growth factor), CXCL1, CXCL11, MCP-3, IL-17A and SCF (stem cell factor) showed significant differences in a targeted analysis between flaring patients and non-flaring patients, with the latter showing decreased levels (Figure S2B). We next looked at whether these markers correlated with the extent of joint involvement. IL-6, CCL23, VEGFA, MMP-1, S100A12, and DNER were strongly associated (P < 0.0001) (Table S3), and IL-6, CCL23, S100A12 also had higher concentrations in polyarticular flares or when larger joints were affected compared to small joints (Figure S3).

The main source of joint injury, bone erosion, and pathological tissue remodeling in gout is thought to be the tophi, which arise as a result of repeated cycles of joint inflammation and resolution ^{2,38}. We divided patients with gout into groups according to whether they had tophi (n = 42) or not (n = 151) to determine whether there was a proteomic signature associated with chronic tophaceous gout. Among the 42 patients diagnosed with chronic tophaceous gout, 10 exhibited mild disease, 19 had moderate disease, and 13 presented with severe chronic tophaceous gout (Figure 4A) (Cf. Methods). Nominally significant differences were observed for 7 proteins: TRAIL (TNF-related apoptosis-inducing ligand), DNER, IL-10, and CCL3 were reduced, and IL-6, RANKL (Receptor activator of nuclear factor kappa-B ligand), and MCP-3 were elevated in samples of patients with tophaceous gout (Figure 4C-D). RANKL levels strongly correlated with disease severity (r=0.37, p<0.0001) (Table S4) and were higher in patients with severe tophaceous gout compared to mild and moderate disease (Figure 4E).

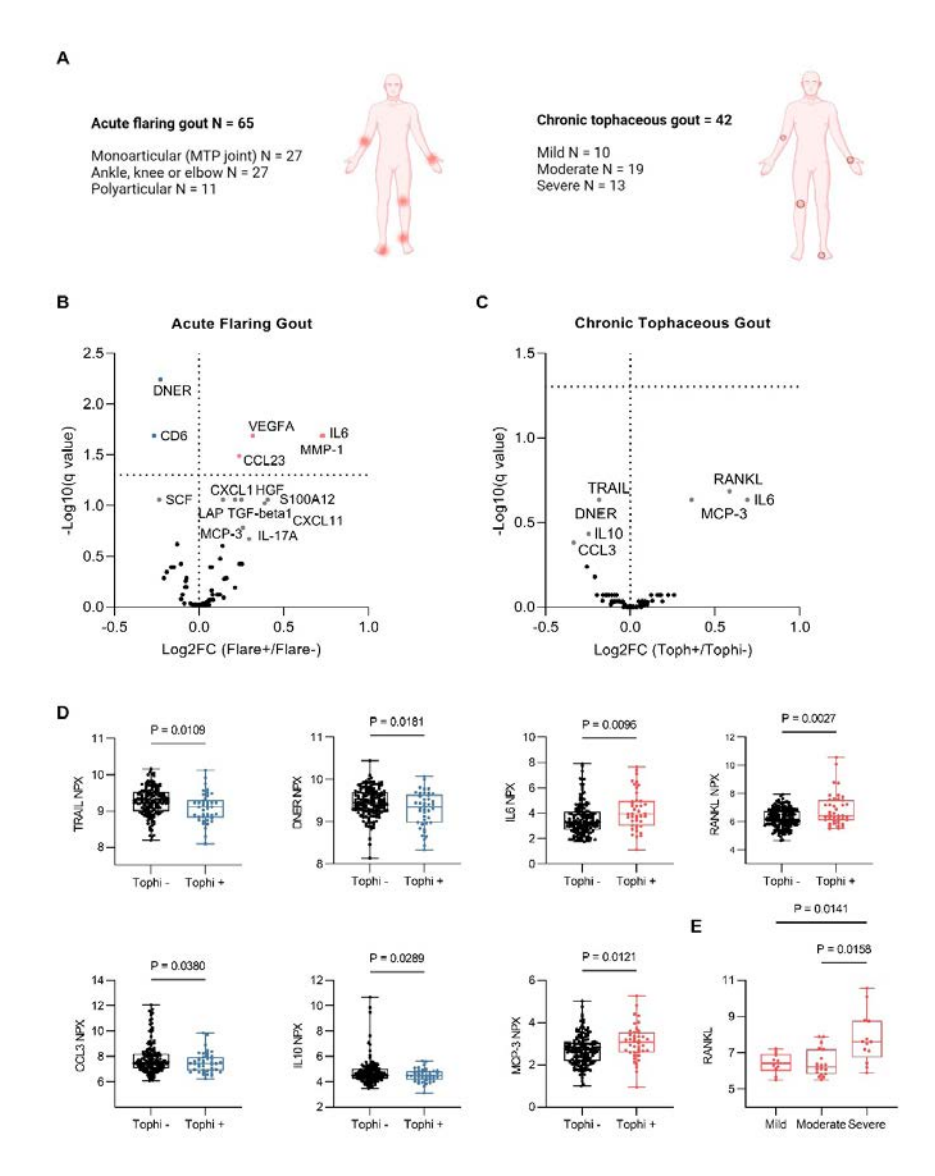


Figure 4 Association of serum protein levels with disease status in gout. **(A)** Number of patients included in the analysis and their disease characteristics. The image was created with BioRender.com. Volcano plots show differentially expressed proteins in acute flaring patients with gout compared to non-flaring patients **(B)** and chronic tophaceous gout compared to patients without tophi **(C)**. Marked in red represent significantly increased proteins, marked in blue represent significantly decreased proteins, labeled and marked in gray represent nominally significant proteins. Associations with q values < 0.05 were considered significant, Welch multiple t-test, FDR 5%. **(D)** Targeted analysis of the nominally significant proteins in tophaceous gout. **(E)** RANKL NPX levels in mild, moderate and severe tophaceous gout. Box plots show line at median and the 75th and 25th percentiles, whiskers show the range of values. Welch's t-test was used for two groups comparisons **(D)** and Welch's ANOVA with Dunnett T3 for multiple testing correction **(E)** (See also Figure S2-S3).

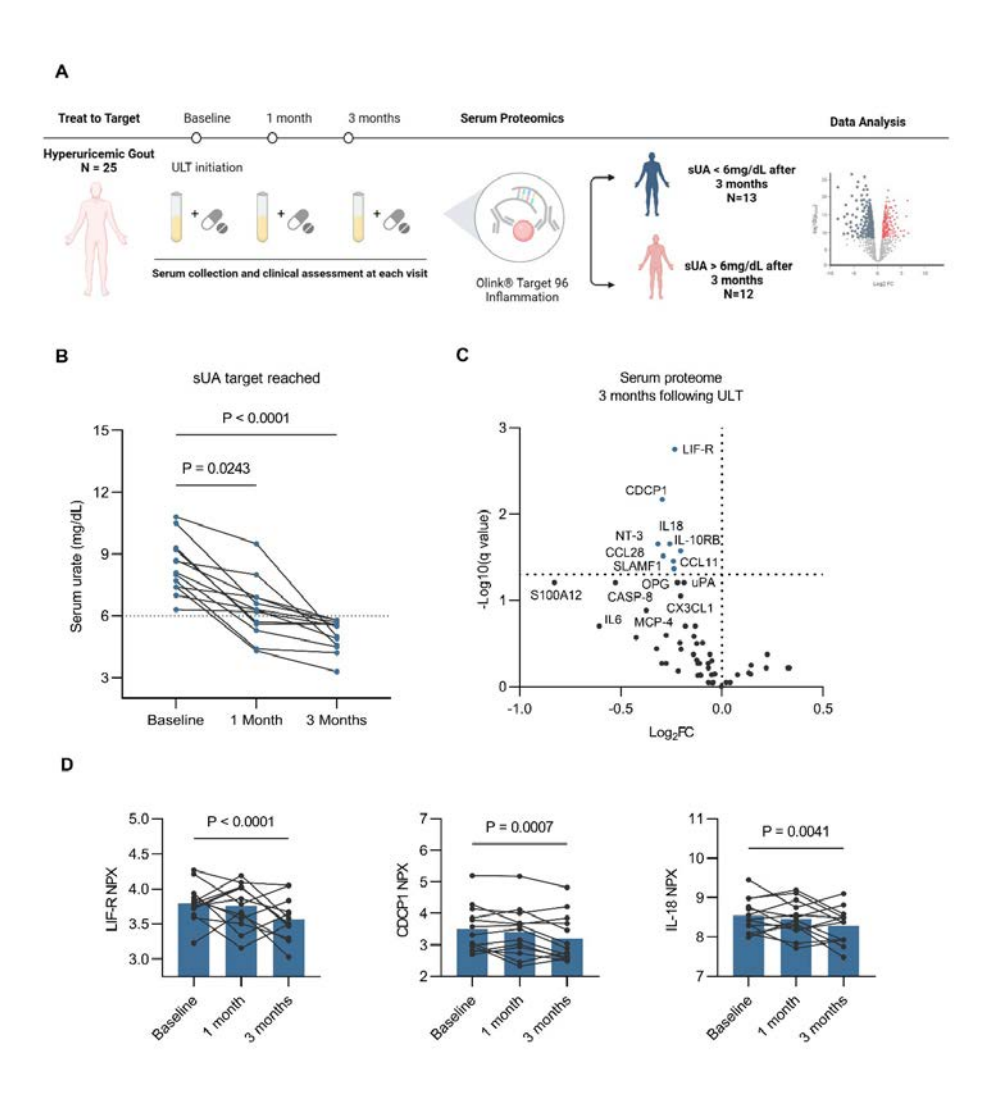


Figure 5 Dynamic changes in the inflammatory signature of hyperuricemic gout, following uratelowering therapy. (A) Study design. The image was created with BioRender.com. (B) serum urate concentrations at baseline, 1 month and 3 months following ULT in patients that reached sUA target at 3 months. Dots and lines represent the paired samples at different timepoints. (C) Volcano plot showing significantly decreased proteins after 3 months of ULT compared to baseline levels, Welch's multiple t-test, FDR 5%. Labeled proteins under the significance threshold represent proteins that have a nominally significant decrease. (D) Three examples of the downregulated proteins after 3 months of ULT compared to baseline. Dots and lines represent the same sample at different time points. Bars show means (See also Table S5).

Dynamic changes in the inflammatory signature of hyperuricemic gout, following urate-lowering therapy.

Lastly, we assessed whether the reduction of sUA concentrations can reverse the inflammatory profile observed in hyperuricemia. We included a separate group of 25 hyperuricemic patients with gout and collected serum and clinical chemistry data before, at one month and at 3 months following initiation of allopurinol therapy (Figure 5A).

Out of 25 patients included, only 13 patients reached the sUA target of 6 mg/dL after three months, while the rest did not reach the target and were excluded from further analysis (Figure 5B and Figure S4A). In the patients who achieved the sUA target, we compared the baseline urate concentration before ULT and three months later for the proteins that were differentially expressed in asymptomatic hyperuricemia. Eight proteins out of 58 had significantly lower levels after three months of ULT, with LIF-R (q = 0.0017), CDCP1, IL-18, NT-3, IL-10RB, CCL28, CCL11, and SLAMF1 being the most highly downregulated (g = 0.0017) (Figure 5C-D and Table S5). No difference was observed after only one month of urate-lowering therapy (Figure S4B).

Discussion

In this study, we performed targeted proteomics analysis to identify inflammatory proteins in large cohorts of patients with gout, individuals with asymptomatic hyperuricemia, and normouricemic individuals. We show a marked inflammatory signature in samples of individuals with AH compared to NU controls. Of high interest, no differentially expressed proteins were observed in samples of patients with gout versus all controls, which included asymptomatic hyperuricemia and normouricemic individuals. This could be explained by a urate-dependent effect which drives inflammation both in asymptomatic hyperuricemia as well as in gout. Indeed, we can observe a very similar inflammatory protein signature when stratifying patients with gout based on the presence of hyperuricemia. Although the mechanisms of immune activation and inflammation in gout are more established, asymptomatic hyperuricemia is less understood and still lacks an agreement concerning its pro-inflammatory effects and subsequent management. Here we show that the proteomic signature of asymptomatic hyperuricemia recapitulates previous findings in gout and in studies of soluble urate-driven inflammation, as will be discussed below. This report adds to the growing body of knowledge which suggests that AH may be pathogenetically linked to persistent immune activation, chronic inflammation, and to the subsequent increased prevalence of cardiometabolic comorbidities seen in hyperuricemic individuals.

The most upregulated protein identified in AH compared to NU, 4E-BP1, is a wellknown mTOR substrate with a crucial role in mTORC1 signaling, which was shown to reprogram macrophages towards a more pro-inflammatory phenotype by translational repression of anti-inflammatory proteins³⁹. In line with this, soluble urate priming of human monocytes was shown to activate mTOR leading to a higher inflammatory response⁴⁰. The IL-1 signaling member IL-18 and its receptor IL-18R1 and the IL-6 family of cytokines members IL-6, LIF-R and OSM were also elevated in AH, which is in line with major studies implicating IL-1-driven inflammation and IL-6 signaling in the pathogenesis of gout⁴¹. IL-18 signals by binding to its receptor IL-18R1 and has been shown to be secreted in an inflammasome-independent way, by caspase-8 cleavage⁴², with caspase-8 also being upregulated in AH sera in this study. IL-18 is reported to be elevated in patients with gout, associated with serum urate levels and postulated to contribute to the development of cardiovascular comorbidities⁴³. The TNF superfamily showed a strong upregulation in the AH group. In line with this, TNF production was shown to be induced by urate in rat vascular smooth muscle cells, an effect that was blocked by the addition of antioxidants, arguing for a pro-atherogenic effect of urate⁴⁴. TNF and TNFSF14 have also been shown to be induced by MSU crystals^{45,46}. A Th17 signature is also present in the urate inflammatory landscape identified in our study, characterized by elevated concentrations of the IL-17A, IL-17C, IL-12B cytokine and the associated chemokines CXCL1, CXCL2 and CXCL6. More recently Th17 responses have been described downstream of innate immune receptors signaling⁴⁷ and NLRP3 activation, with the production of IL-1 cytokines potentiating Th17 responses and bridging innate and adaptive immunity⁴⁸. Previous studies have shown that patients with gout have increased levels of circulating Th17 cells⁴⁹, and that urate crystals in combination with an NF-κB priming signal induce Th17 polarization in vitro⁵⁰. Moreover, in MSUinduced joint inflammation in mice, blocking IL-17 attenuated the recruitment and activation of immune cells, as well as joint inflammation⁵¹.

Another marker that was elevated in hyperuricemic individuals was FGF21. Due to the observation that this was also the most upregulated protein in hyperuricemic patients with gout compared to NU gout, we further assessed the functional consequences of rhFGF-21 addition in vitro stimulation experiments using primary human PBMCS. Our study indicates that rhFGF-21 dampened cytokine production (Figure 3) and we hypothesize that FGF-21 may play a role in limiting gouty inflammation by decreasing the inflammatory response of the gout-specific stimulus, C16.0 and MSU. FGF-21 beneficial effects on carbohydrate and lipid metabolism have been shown to be mediated by the fatty acid sensor peroxisome proliferator-activated receptor y (PPARy)⁵². PPARy is also expressed in immune cells and mediates its effect by a complex, ligand-dependent transrepression of inflammatory genes⁵³. Exposure to MSU crystals was shown to induce PPARγ in monocytes with authors arguing its implication in the resolution of flares⁵⁴. Elevated PPARγ expression was also demonstrated in synovial cells of acute patients with gout and gene variation in proliferator-activated receptor-γ coactivator 1β (PPARGC1B) was associated with IL-1β production in patients with gout⁵⁵. Even though FGF-21 analogues are currently undergoing clinical trials and that FGF-21 has emerged as a viable therapeutic target for metabolic disorders, particular consideration should be given to reported side effects in relation to a potential use in gouty arthritis³⁶. Skeletal system side effects are frequently documented, with FGF-21 shown to mediate the detrimental effects leading to bone loss by altering the RANKL/OPG ratio⁵⁶⁻⁵⁸. Whilst the mechanisms of bone erosion in gout are incompletely understood, most studies point towards the implication of the RANKL/OPG pathway dysregulation, which may present a limitation to the potential use of FGF-21 in gouty arthritis⁵⁹⁻⁶¹.

These observations are consistent with our findings on tophaceous gout (Figure 4C-E) where we found that patients with tophi have higher circulating concentrations of the pro-osteoclastogenic RANKL and those with severe disease have even higher levels compared to mild or moderate disease, suggesting that RANKL plays a key role in bone erosion in gout. Furthermore, our research revealed that patients with tophaceous gout have lower concentrations of circulating TRAIL. It has been known that TRAIL can induce osteoclast differentiation via a TRAF-6 dependent mechanism, but there is increasing evidence for a paradoxical role of TRAIL in inhibiting RANKL induced osteoclastogenesis by inhibition of lipid raft assembly required for TRAF-6 signaling^{62,63}. Osteoimmunological reports support a suppressive role of TRAIL in RANKL and M-CSF-induced osteoclast differentiation^{64,65}, with others showing the capacity of recombinant TRAIL to inhibit osteoclastogenesis and bone resorption via inhibition of RANKL signaling in a mouse model of collagen-induced arthritis⁶³. Other reports showed that recombinant TRAIL increased bone mass in an in vivo mouse model⁶⁶. It is noteworthy that dose-escalation urate-lowering therapy using allopurinol has been shown to prevent the progression of bone erosion in gout compared to conventional dosing, however, the reduction of bone loss was observed only after two years of treatment, with bone erosion initially progressing under treatment⁶. For reversal of bone erosion to be achieved, severe sUA lowering to undetectable levels was required^{8,67}. These results highlight the need for additional interventions, making RANKL and TRAIL attractive therapeutic targets that could be used in combination with ULT to prevent joint damage and possibly reverse bone erosion, as both RANKL inhibitors, as well as rhTRAIL and activating antibodies of its death receptors, DR4 and DR5, are already undergoing human clinical trials. TRAIL is mostly used as a therapeutic target in cancer due to its potent ability to selectively induce apoptosis of cancer cells⁶⁸ and RANKLneutralizing antibodies showed efficacy in preventing osteoporotic⁶⁹ and cancerrelated fractures⁷⁰.

The synovium during flares is characterized by infiltration of mononuclear cells, neutrophils, and lymphocytes. Following the phagocytosis of MSU crystals, monocytes become activated and release pro-inflammatory cytokines including IL-6 and IL-1 β^{71} . Our results show that flaring patients exhibited elevated concentrations of circulating proteins that reflected higher levels of inflammation, immune infiltration, tissue remodeling and angiogenesis (Figure 4B and Figure S2). VEGFA has been previously associated with serum urate concentrations in a human genome-wide association study (GWAS)⁷² as well as in a mouse model of gout⁷³. VEGFA is a pro-angiogenic factor produced by synovial monocytes and fibroblasts upon stimulation by IL-1β, TGF-β and other mediators⁷⁴ and which can also act as a chemoattractant for monocytes and neutrophils⁷⁵. VEGFA can induce MMP-1 and other MMPs which promote angiogenesis by degrading the extracellular matrix and allowing for the migration of new cells within the synovium and proliferation of new blood vessels⁷⁶. Another proangiogenic factor, HGF, was also enriched in the sera of flaring patients with gout. Previous studies showed its expression in the synovium of rheumatoid arthritis and osteoarthritis patients and that inhibition of HGF suppressed progression of arthritis and bone destruction in SKG mice⁷⁷. Another recent report in gout showed that the HGF/MET pathway blockade in a model of MSU-induced arthritis resolved articular inflammation, tissue damage and joint pain by enhancing neutrophilic apoptosis and reducing neutrophil infiltration, as well as decreasing CXCL178. CXCL1, a neutrophil attractant and activator of proteases, is a chemokine that was also found to be enriched in flaring patients in the present study. The interstitial collagenase MMP-1 has also been shown to be produced by synovial fibroblasts in response to MSU crystals⁷⁹. Previously TGF-β has been shown to have context-dependent pro-inflammatory and anti-inflammatory roles, mediating urate-induced inflammation⁸⁰, as well as limiting acute gouty inflammation when added exogenously in a synovium-like air pouch mouse model⁸¹. In a previous report investigating TGF-β in urate-induced inflammatory priming, we were not able to observe major differences in TGF-β or VEGFA levels during gout flares compared to inter-critical patients with gout⁸⁰. Possibly due to the different number of samples, in the present study we were able to observe significant differences for VEGFA and nominally significant increase in TGF- β – LAP. This is in line with other studies showing TGF- β increase over the course of gout

flares and potential involvement in the resolution of inflammation⁸². We also found higher levels of chemokine CCL23, a strong chemotactic molecule for resting T cells and monocytes⁸³;⁸⁴ CXCL11, chemotactic for activated T cells⁸⁴; and the monocyte chemotactic protein 3, MCP-3. IL-17A was also more elevated in our analysis of flaring versus inter-critical gout. IL-17A has been previously reported as a marker of acute gout, with $\gamma\delta T$ cell-derived IL-17A correlating with disease activity and IL-1 β levels ⁸⁵. Finally, the S100A12 protein was shown to be released by MSU-stimulated neutrophils⁸⁶ and was independently shown to induce mast cell recruitment and activation⁸⁷, which has been hypothesized to play a role in the inflammatory cascade of acute gout⁷¹.

Lastly, to assess whether serum urate reduction would have the potential to reverse the elevated levels of inflammatory biomarkers presented here, we investigated the effect of ULT on the inflammatory status of patients with gout. No change of the inflammatory proteome has been observed after 1 month of ULT, despite a slight reduction in serum urate levels already present at this time. After three months of ULT, in patients who reached the target urate level of 6 mg/dL, eight inflammatory markers were significantly decreased, and seven others showed a nominally significant reduction. This shows that, indeed, interventions aimed at reducing urate concentrations do, in the long-term, also reduce inflammatory profile of the patients. We show that both a reduction in sUA concentration and a longer duration of treatment plays a role in reversing the inflammatory status of patients with gout. It is tempting to speculate that further longer-term maintenance of urate concentrations within normouricemic limits would ultimately lead to further diminishment of systemic inflammation. Epigenetic mechanisms that could lead to the inflammatory reprogramming of myeloid cells have been implicated in gouty inflammation and in response to soluble urate^{88,89}. From other studies showing innate immune memory induced by sterile metabolic stimuli, such as ox-LDL particles, we know that it is possible for inflammatory phenotypes of reprogrammed cells to not disappear even despite normalization of the initial trigger as in the case of cholesterol normalization using statins⁹⁰. Therefore, the persistence of elevated concentrations of some inflammatory markers in hyperuricemic individuals even at the time of urate normalization could potentially be explained by other long-term epigenetic processes that maintain inflammation and that may take longer time to reverse.

Earlier reports that looked at urate-lowering therapy have addressed the effect of urate in mediating adverse cardiovascular and renal events in relation to high blood pressure and showed improvements attributed to sUA reduction in adolescents^{91,92} but not in adults,⁹³ while contrasting findings were also found for

CKD⁹⁴. An explanation for this discrepancy lies in the duration of treatment. For adolescents in the trials, the amount required for the benefit of ULT to be reached was 1 month and 2 months respectively. For the adults in which no improvement in systolic blood pressure was observed, the duration of treatment was 2 months. This could reflect the underlying biology of older individuals compared to younger individuals, but, as above, it could also be linked to urate-inducing long-term epigenetic modifications that imprint a pro-inflammatory phenotype on myeloid cells⁸⁸. Another explanation for the anti-inflammatory effect of allopurinol could lie in the inhibition of xanthine oxidoreductase (XOR), its therapeutic target, and the subsequent blocking of XO-derived reactive species of oxygen⁹⁵. Our data showing a long-term inflammatory potential of hyperuricemia in the absence of gout adds an important argument that high uric acid concentrations, rather than urate crystals alone, are an important risk factor for cardiometabolic complications, and needs to be addressed for the prevention of these life-reducing complications.

Some potential caveats of our research include the cross-sectional design for some of our sub-studies, which limits the ability to establish a causal relationship between serum urate levels, inflammation, and the development of cardiometabolic complications in AH and gout. Longitudinal studies could improve our understanding of these associations. By using a targeted proteomic approach, we may not have captured the inflammatory landscape in its entirety. Untargeted proteomic methods might offer a more comprehensive signature. Although we identified potentially targetable biomarkers in our study, further functional validations are needed to establish their role in the progression and resolution of the disease. While our study examines the impact of urate-lowering therapy on the inflammatory profile of gout, where we observed a decrease in inflammatory proteins paralleling a decrease in serum urate, other treatment-specific, urateindependent, anti-inflammatory mechanisms cannot be excluded. Lastly, our study did not account for all potential variables such as medication, BMI, lifestyle factors and comorbidities which might impact inflammation profiles, as this may lead to overcorrection of data since hyperuricemia might be an underlying driver.

In summary, here we provide evidence for inflammatory consequences of urate exposure in vivo. We describe a strong and broad inflammatory signature associated with asymptomatic hyperuricemia which correlated with differences observed in patients with gout and hyperuricemia compared to normouricemic gout. The proteins identified here were also associated to clinically relevant phenotypes in gout, such as presence and severity of flares or tophi. Importantly, the increased expression of these proteins is partially reversible upon urate-lowering therapy, which argues for the causal effect of urate in the significant enrichment observed for these proteins in hyperuricemic individuals. Our findings represent a foundation for future functional studies to examine mechanistic relationships of these inflammatory proteins in gout and hyperuricemia, to explore their potential to be used as clinically relevant disease biomarkers, and for the development of therapies targeting asymptomatic hyperuricemia as a strategy to prevent cardiometabolic diseases.

References

- Kuo CF, Grainge MJ, Zhang W, Doherty M. Global epidemiology of gout: Prevalence, incidence and risk factors. Nat Rev Rheumatol. 2015;11(11):649-662. doi:10.1038/nrrheum.2015.91
- Dalbeth N, Choi HK, Joosten LAB, et al. Gout. Nat Rev Dis Primers. 2019;5(1). doi:10.1038/s41572-2. 019-0115-v
- 3 Dalbeth N, Gosling AL, Gaffo A, Abhishek A. Gout. The Lancet. 2021;397(10287):1843-1855. doi:10.1016/S0140-6736(21)00569-9
- Chhana A, Dalbeth N. The Gouty Tophus: a Review. Curr Rheumatol Rep. 2015;17(3). doi:10.1007/ s11926-014-0492-x
- Joosten LAB, Crişan TO, Bjornstad P, Johnson RJ. Asymptomatic hyperuricaemia: a silent activator of the innate immune system. Nat Rev Rheumatol. 2020;16(2):75-86. doi:10.1038/s41584-019-0334-3
- 6. FitzGerald JD, Dalbeth N, Mikuls T, et al. 2020 American College of Rheumatology Guideline for the Management of Gout. Arthritis and Rheumatology. 2020;72(6):879-895. doi:10.1002/art.41247
- Doherty M, Jenkins W, Richardson H, et al. Efficacy and cost-effectiveness of nurse-led care 7. involving education and engagement of patients and a treat-to-target urate-lowering strategy versus usual care for gout: a randomised controlled trial. The Lancet. 2018;392(10156):1403-1412. doi:10.1016/S0140-6736(18)32158-5
- Dalbeth N, Billington K, Doyle A, et al. Effects of Allopurinol Dose Escalation on Bone Erosion and Urate Volume in Gout: A Dual-Energy Computed Tomography Imaging Study Within a Randomized, Controlled Trial. Arthritis and Rheumatology. 2019;71(10):1739-1746. doi:10.1002/art.40929
- Dincer HE, Dincer AP, Levinson DJ. Asymptomatic Hyperuricemia: To Treat or Not to Treat. Vol 69.; 2002. www.ccjm.org
- 10. Zhu Y, Pandya BJ, Choi HK. Prevalence of gout and hyperuricemia in the US general population: The National Health and Nutrition Examination Survey 2007-2008. Arthritis Rheum. 2011:63(10):3136-3141. doi:10.1002/art.30520
- 11. Perez-Ruiz F, Marimon E, Chinchilla SP. Hyperuricaemia with deposition: Latest evidence and therapeutic approach. Ther Adv Musculoskelet Dis. 2015;7(6):225-233. doi:10.1177/1759720X15599734
- 12. Dalbeth N, House ME, Aati O, et al. Urate crystal deposition in asymptomatic hyperuricaemia and symptomatic gout: A dual energy CT study. Ann Rheum Dis. 2015;74(5):908-911. doi:10.1136/ annrheumdis-2014-206397
- 13. Seo YK, Guevara JP, Kyoung MK, Hyon KC, Heitjan DF, Albert DA. Hyperuricemia and risk of stroke: A systematic review and meta-analysis. Arthritis Care Res (Hoboken). 2009;61(7):885-892. doi:10.1002/art.24612
- 14. Andrés M, Quintanilla MA, Sivera F, et al. Silent Monosodium Urate Crystal Deposits Are Associated with Severe Coronary Calcification in Asymptomatic Hyperuricemia: An Exploratory Study. Arthritis and Rheumatology. 2016;68(6):1531-1539. doi:10.1002/art.39581
- 15. Battelli MG, Bortolotti M, Bolognesi A, Polito L. Pro-aging effects of xanthine oxidoreductase products. Antioxidants. 2020;9(9):1-16. doi:10.3390/antiox9090839
- 16. Tamariz L, Hernandez F, Bush A, Palacio A, Hare JM. Association between serum uric acid and atrial fibrillation: A systematic review and meta-analysis. Heart Rhythm. 2014;11(7):1102-1108. doi:10.1016/j.hrthm.2014.04.003
- 17. Fini MA, Elias A, Johnson RJ, Wright RM. Contribution of Uric Acid to Cancer Risk, Recurrence, and Mortality.; 2012. http://www.clintransmed.com/content/1/1/16

- 18. Zhao G, Huang L, Song M, Song Y. Baseline serum uric acid level as a predictor of cardiovascular disease related mortality and all-cause mortality: A meta-analysis of prospective studies. *Atherosclerosis*. 2013;231(1):61-68. doi:10.1016/j.atherosclerosis.2013.08.023
- Xie Y, Xu P, Liu K, et al. Hyperuricemia and gout are associated with cancer incidence and mortality: A meta-analysis based on cohort studies. J Cell Physiol. 2019;234(8):14364-14376. doi:10.1002/jcp.28138
- Nozue T, Yamamoto S, Tohyama S, et al. Correlations between serum uric acid and coronary atherosclerosis before and during statin therapy. Coron Artery Dis. 2014;25(4):343-348. doi:10.1097/MCA.0000000000000084
- 21. Fini MA, Elias A, Johnson RJ, Wright RM. *Contribution of Uric Acid to Cancer Risk, Recurrence, and Mortality.*; 2012. http://www.clintransmed.com/content/1/1/16
- Yu J, Liu H, He S, et al. Negative Association of Serum Uric Acid with Peripheral Blood Cellular Aging Markers. *Journal of Nutrition, Health and Aging*. 2019;23(6):547-551. doi:10.1007/s12603-019-1200-3
- 23. Cicero AFG, Rosticci M, Fogacci F, Grandi E, D'Addato S, Borghi C. High serum uric acid is associated to poorly controlled blood pressure and higher arterial stiffness in hypertensive subjects. *Eur J Intern Med*. 2017;37:38-42. doi:10.1016/j.ejim.2016.07.026
- 24. Viazzi F, Rebora P, Giussani M, et al. Increased serum uric acid levels blunt the antihypertensive efficacy of lifestyle modifications in children at cardiovascular risk. *Hypertension*. 2016;67(5):934-940. doi:10.1161/HYPERTENSIONAHA.115.06852
- Grayson PC, Young Kim S, Lavalley M, Choi HK. Hyperuricemia and incident hypertension: A systematic review and meta-analysis. Arthritis Care Res (Hoboken). 2011;63(1):102-110. doi:10.1002/acr.20344
- Lv Q, Meng XF, He FF, et al. High Serum Uric Acid and Increased Risk of Type 2 Diabetes: A Systemic Review and Meta-Analysis of Prospective Cohort Studies. *PLoS One*. 2013;8(2). doi:10.1371/journal.pone.0056864
- 27. Yu TY, Jee JH, Bae JC, et al. Serum uric acid: A strong and independent predictor of metabolic syndrome after adjusting for body composition. *Metabolism*. 2016;65(4):432-440. doi:10.1016/j. metabol.2015.11.003
- 28. Li L, Yang C, Zhao Y, Zeng X, Liu F, Fu P. *Is Hyperuricemia an Independent Risk Factor for New-Onset Chronic Kidney Disease?: A Systematic Review and Meta-Analysis Based on Observational Cohort Studies.*; 2014. http://www.biomedcentral.com/1471-2369/15/122
- 29. Mylona EE, Mouktaroudi M, Crisan TO, et al. Enhanced interleukin-1β production of PBMCs from patients with gout after stimulation with Toll-like receptor-2 ligands and urate crystals. *Arthritis Res Ther*. 2012;14(4):R158. doi:10.1186/ar3898
- 30. Joosten LA, Netea MG, Mylona E, et al. Engagement of fatty acids with Toll-like receptor 2 drives interleukin-1β production via the ASC/caspase 1 pathway in monosodium urate monohydrate crystal-induced gouty arthritis. *Arthritis Rheum*. 2010;62(11):3237-3248. doi:10.1002/art.27667
- 31. Howes A, Gabryšová L, O'Garra A. Role of IL-10 and the IL-10 Receptor in Immune Responses. In: Reference Module in Biomedical Sciences. Elsevier; 2014. doi:10.1016/b978-0-12-801238-3.00014-3
- 32. Yasuda H, Shima N, Nakagawa N, et al. Osteoclast Differentiation Factor Is a Ligand for Osteoprotegerin Osteoclastogenesis-Inhibitory Factor and Is Identical to TRANCERANKL. Vol 95.; 1998. www.pnas.org.
- 33. Zlotnik A, Yoshie O. The Chemokine Superfamily Revisited. *Immunity*. 2012;36(5):705-716. doi:10.1016/j.immuni.2012.05.008

- 34. Metzemaekers M, Vanheule V, Janssens R, Struyf S, Proost P. Overview of the mechanisms that may contribute to the non-redundant activities of interferon-inducible CXC chemokine receptor 3 ligands. Front Immunol. 2018;8(JAN). doi:10.3389/fimmu.2017.01970
- 35. White GE, Greaves DR. Fractalkine: A survivor's guide chemokines as antiapoptotic mediators. Arterioscler Thromb Vasc Biol. 2012;32(3):589-594. doi:10.1161/ATVBAHA.111.237412
- 36. Geng L, Lam KSL, Xu A. The therapeutic potential of FGF21 in metabolic diseases: from bench to clinic. Nat Rev Endocrinol. 2020;16(11):654-667. doi:10.1038/s41574-020-0386-0
- 37. Major TJ, Takei R, Matsuo H, et al. Akiyoshi Nakayama 2,5, Tappei Takada 2,47, Masahiro Nakatochi 2,48, Seiko Shimizu 2,5, Yusuke Kawamura 2,5, Yu Toyoda 2,5, Hirofumi Nakaoka 49. Keitaro Matsuo. 50. doi:10.1101/2022.11.26.22281768
- 38. Dalbeth N, Clark B, Gregory K, et al. Mechanisms of bone erosion in gout: A quantitative analysis using plain radiography and computed tomography. Ann Rheum Dis. 2009;68(8):1290-1295. doi:10.1136/ard.2008.094201
- 39. William M, Leroux LP, Chaparro V, et al. eIF4E-Binding Proteins 1 and 2 Limit Macrophage Anti-Inflammatory Responses through Translational Repression of IL-10 and Cyclooxygenase-2. The Journal of Immunology. 2018;200(12):4102-4116. doi:10.4049/jimmunol.1701670
- 40. Crişan TO, Cleophas MCP, Novakovic B, et al. Uric acid priming in human monocytes is driven by the AKT-PRAS40 autophagy pathway. Proc Natl Acad Sci U S A. 2017;114(21):5485-5490. doi:10.1073/pnas.1620910114
- 41. So AK, Martinon F. Inflammation in gout: Mechanisms and therapeutic targets. Nat Rev Rheumatol. 2017;13(11):639-647. doi:10.1038/nrrheum.2017.155
- 42. Bossaller L, Chiang PI, Schmidt-Lauber C, et al. Cutting Edge: FAS (CD95) Mediates Noncanonical IL-1β and IL-18 Maturation via Caspase-8 in an RIP3-Independent Manner. The Journal of Immunology. 2012;189(12):5508-5512. doi:10.4049/jimmunol.1202121
- 43. Klück V, Liu R, Joosten LAB. The role of interleukin-1 family members in hyperuricemia and gout. Joint Bone Spine. 2021;88(2). doi:10.1016/j.jbspin.2020.105092
- 44. Tang L, Xu Y, Wei Y, He X. Uric acid induces the expression of TNF-α via the ROS-MAPK-NF-κΒ signaling pathway in rat vascular smooth muscle cells. Mol Med Rep. 2017;16(5):6928-6933. doi:10.3892/mmr.2017.7405
- 45. di Giovine FS, Malawista SE, Thornton E, Duff GW. Urate Crystals Stimulate Production of Tumor Necrosis Factor Alpha from Human Blood Monocytes and Synovial Cells Cytokine MRNA and Protein Kinetics, and Cellular Distribution.
- 46. Buisman SC, Haan G de. Epigenetic Changes as a Target in Aging Age-Related Malignancies. Cells. 2019:8(868):1-19.
- 47. Huang G, Wang Y, Chi H. Regulation of TH17 cell differentiation by innate immune signals. Cell Mol Immunol. 2012;9(4):287-295. doi:10.1038/cmi.2012.10
- 48. Joosten LAB. Excessive interleukin-1 signaling determines the development of Th1 and Th17 responses in chronic inflammation. Arthritis Rheum. 2010;62(2):320-322. doi:10.1002/art.27242
- 49. de Lima JD, de Paula AGP, Yuasa BS, et al. Genetic and Epigenetic Regulation of the Innate Immune Response to Gout. Immunol Invest. Published online 2023. doi:10.1080/08820139.2023.2168554
- 50. Conforti-Andreoni C, Spreafico R, Qian HL, et al. Uric Acid-Driven Th17 Differentiation Requires Inflammasome-Derived IL-1 and IL-18. The Journal of Immunology. 2011;187(11):5842-5850. doi:10.4049/jimmunol.1101408
- 51. Raucci F, Igbal AJ, Saviano A, et al. IL-17A neutralizing antibody regulates monosodium urate crystal-induced gouty inflammation. Pharmacol Res. 2019;147. doi:10.1016/j.phrs.2019.104351

- 52. Dutchak PA, Katafuchi T, Bookout AL, et al. Fibroblast growth factor-21 regulates PPARγ activity and the antidiabetic actions of thiazolidinediones. *Cell.* 2012;148(3):556-567. doi:10.1016/j. cell.2011.11.062
- 53. Varga T, Czimmerer Z, Nagy L. PPARs are a unique set of fatty acid regulated transcription factors controlling both lipid metabolism and inflammation. *Biochim Biophys Acta Mol Basis Dis*. 2011;1812(8):1007-1022. doi:10.1016/j.bbadis.2011.02.014
- 54. Akahoshi T, Namai R, Murakami Y, et al. Rapid induction of peroxisome proliferator-activated receptor γ expression in human monocytes by monosodium urate monohydrate crystals. *Arthritis Rheum*. 2003;48(1):231-239. doi:10.1002/art.10709
- 55. Chang WC, Wu YJJ, Chung WH, et al. Genetic variants of PPAR-gamma coactivator 1B augment NLRP3-mediated inflammation in gouty arthritis. *Rheumatology (United Kingdom)*. 2017;56(3):457-466. doi:10.1093/rheumatology/kew337
- 56. Wei W, Dutchak PA, Wang X, et al. Fibroblast growth factor 21 promotes bone loss by potentiating the effects of peroxisome proliferator-activated receptor γ. *Proc Natl Acad Sci U S A*. 2012;109(8):3143-3148. doi:10.1073/pnas.1200797109
- 57. Li H, Sun H, Qian B, et al. Increased Expression of FGF-21 Negatively Affects Bone Homeostasis in Dystrophin/Utrophin Double Knockout Mice. *Journal of Bone and Mineral Research*. 2020;35(4):738-752. doi:10.1002/jbmr.3932
- 58. Tang Y, Zhang M. Fibroblast growth factor 21 and bone homeostasis. *Biomed J. Published online* 2022. doi:10.1016/j.bj.2022.07.002
- Lee SJ, Nam K il, Jin HM, et al. Bone destruction by receptor activator of nuclear factor κB ligandexpressing T cells in chronic gouty arthritis. Arthritis Res Ther. 2011;13(5). doi:10.1186/ar3483
- 60. Chhana A, Aati O, Gamble GD, et al. Path analysis identifies receptor activator of nuclear factor-?b ligand, osteoprotegerin, and sclerostin as potential mediators of the tophus-bone erosion relationship in gout. *Journal of Rheumatology*. 2016;43(2):445-449. doi:10.3899/jrheum.150738
- 61. Dalbeth N, Smith T, Nicolson B, et al. Enhanced osteoclastogenesis in patients with tophaceous gout: Urate crystals promote osteoclast development through interactions with stromal cells. Arthritis Rheum. 2008;58(6):1854-1865. doi:10.1002/art.23488
- 62. Yen ML, Hsu PN, Liao HJ, Lee BH, Tsai HF. TRAF-6 dependent signaling pathway is essential for TNF-related apoptosis-inducing ligand (TRAIL) induces Osteoclast differentiation. *PLoS One*. 2012;7(6). doi:10.1371/journal.pone.0038048
- 63. Liao HJ, Tsai HF, Wu CS, Chyuan IT, Hsu PN. TRAIL inhibits RANK signaling and suppresses osteoclast activation via inhibiting lipid raft assembly and TRAF6 recruitment. *Cell Death Dis*. 2019;10(2). doi:10.1038/s41419-019-1353-3
- 64. Harper E, Rochfort KD, Forde H, Davenport C, Smith D, Cummins PM. TRAIL attenuates RANKL-mediated osteoblastic signalling in vascular cell monoculture and co-culture models. *PLoS One*. 2017;12(11). doi:10.1371/journal.pone.0188192
- Zauli G, Rimondi E, Nicolin V, Melloni E, Celeghini C, Secchiero P. TNF-related apoptosisinducing ligand (TRAIL) blocks osteoclastic differentiation induced by RANKL plus M-CSF. *Blood*. 2004;104(7):2044-2050. doi:10.1182/blood-2004-03-1196
- Zauli G, Rimondi E, Stea S, et al. TRAIL inhibits osteoclastic differentiation by counteracting RANKLdependent p27Kip1 accumulation in pre-osteoclast precursors. *J Cell Physiol*. 2008;214(1):117-125. doi:10.1002/jcp.21165
- 67. Dalbeth N, Doyle AJ, McQueen FM, Sundy J, Baraf HSB. Exploratory study of radiographic change in patients with tophaceous gout treated with intensive urate-lowering therapy. *Arthritis Care Res* (Hoboken). 2014;66(1):82-85. doi:10.1002/acr.22059

- 68. Montinaro A, Walczak H. Harnessing TRAIL-induced cell death for cancer therapy: a long walk with thrilling discoveries. Cell Death Differ. Published online February 1, 2022. doi:10.1038/ s41418-022-01059-z
- 69. Kendler Felicia Cosman Robert Kees Stad Serge Ferrari DL, Kendler DL, Cosman F, Stad RK, Ferrari S. Denosumab in the Treatment of Osteoporosis: 10 Years Later: A Narrative Review. Adv Ther. 1936;39. doi:10.6084/m9.figshare.16723372
- 70. Hegemann M, Bedke J, Stenzl A, Todenhöfer T. Denosumab treatment in the management of patients with advanced prostate cancer: Clinical evidence and experience. Ther Adv Urol. 2017;9(3-4):81-88. doi:10.1177/1756287216686018
- 71. Dalbeth N, Haskard DO. Mechanisms of inflammation in gout. Rheumatology. 2005;44(9):1090-1096. doi:10.1093/rheumatology/keh640
- 72. Köttgen A, Albrecht E, Teumer A, et al. Genome-wide association analyses identify 18 new loci associated with serum urate concentrations. Nat Genet. 2013;45(2):145-154. doi:10.1038/ng.2500
- 73. Fan Y, Yang J, Xie S, et al. Systematic analysis of inflammation and pain pathways in a mouse model of gout. Mol Pain. 2022;18. doi:10.1177/17448069221097760
- 74. Berse B, Hunt JA, Diegel RJ, et al. Hypoxia Augments Cytokine (Transforming Growth Factor-Beta (TGF-b) and IL-1)-Induced Vascular Endothelial Growth Factor Secretion by Human Synovial Fibroblasts.
- 75. Massena S, Christoffersson G, Seignez C, et al. Identification and characterization of VEGF-Aresponsive neutrophils expressing CD49d, VEGFR1, and CXCR4 in mice and humans. Published online 2015. doi:10.1182/blood-2015-03
- 76. Xiang Q, Sang A. MINIREVIEW Complex Role of Matrix Metalloproteinases in Angiogen-Esis. Vol 8.; 1998.
- 77. Tsunemi S, Iwasaki T, Kitano S, et al. Molecular targeting of hepatocyte growth factor by an antagonist, NK4, in the treatment of rheumatoid arthritis. Arthritis Res Ther. 2013;15(4). doi:10.1186/ar4252
- 78. Felix FB, Dias J, Vago JP, et al. Blocking the HGF-MET pathway induces resolution of neutrophilic inflammation by promoting neutrophil apoptosis and efferocytosis. Pharmacol Res. 2023;188. doi:10.1016/j.phrs.2022.106640
- 79. Johanson TM, Chan WF, Keenan CR, Allan RS. Genome organization in immune cells: unique challenges. Nat Rev Immunol. 2019;19(7):448-456. doi:10.1038/s41577-019-0155-2
- 80. Klück V, Cabău G, Mies L, et al. TGF-β is elevated in hyperuricemic individuals and mediates urate-induced hyperinflammatory phenotype in human mononuclear cells. Arthritis Res Ther. 2023;25(1):30. doi:10.1186/s13075-023-03001-1
- 81. Lioté F, Prudhommeaux F, Schiltz C, et al. Inhibition and prevention of monosodium urate monohydrate crystal- induced acute inflammation in vivo by transforming growth factor β1. Arthritis Rheum. 1996;39(7):1192-1198. doi:10.1002/art.1780390718
- 82. Scanu A, Oliviero F, Ramonda R, Frallonardo P, Dayer JM, Punzi L. Cytokine levels in human synovial fluid during the different stages of acute gout: Role of transforming growth factor \(\beta \) in the resolution phase. Ann Rheum Dis. 2012;71(4):621-624. doi:10.1136/annrheumdis-2011-200711
- 83. Arruda-Silva F, Bianchetto-Aquilera F, Gasperini S, et al. Human neutrophils produce CCL23 in response to various TLR-agonists and TNFα. Front Cell Infect Microbiol. 2017;7(MAY). doi:10.3389/ fcimb.2017.00176
- 84. Cole KE, Strick CA, Paradis TJ, et al. Interferon-Inducible T Cell Alpha Chemoattractant (I-TAC): A Novel Non-ELR CXC Chemokine with Potent Activity on Activated T Cells through Selective High Affinity Binding to CXCR3. Vol 187.; 1998. http://www.jem.org

- 85. Liu Y, Zhao Q, Yin Y, McNutt MA, Zhang T, Cao Y. Serum levels of IL-17 are elevated in patients with acute gouty arthritis. *Biochem Biophys Res Commun*. 2018;497(3):897-902. doi:10.1016/j. bbrc.2018.02.166
- Tardif MR, Chapeton-Montes JA, Posvandzic A, Pagé N, Gilbert C, Tessier PA. Secretion of S100A8, S100A9, and S100A12 by Neutrophils Involves Reactive Oxygen Species and Potassium Efflux. J Immunol Res. 2015;2015. doi:10.1155/2015/296149
- 87. Wei XY, Armishaw C, Goyette J, et al. Mast cell and monocyte recruitment by S100A12 and Its Hinge Domain. *Journal of Biological Chemistry*. 2008;283(19):13035-13043. doi:10.1074/jbc. M710388200
- 88. Badii M, Gaal OI, Cleophas MC, et al. Urate-induced epigenetic modifications in myeloid cells. Arthritis Res Ther. 2021;23(1). doi:10.1186/s13075-021-02580-1
- 89. Cabău G, Crișan TO, Klück V, Popp RA, Joosten LAB. Urate-induced immune programming: Consequences for gouty arthritis and hyperuricemia. *Immunol Rev.* 2020;294(1):92-105. doi:10.1111/imr.12833
- 90. Bekkering S, Stiekema LCA, Bernelot Moens S, et al. Treatment with Statins Does Not Revert Trained Immunity in Patients with Familial Hypercholesterolemia. *Cell Metab.* 2019;30(1):1-2. doi:10.1016/j.cmet.2019.05.014
- 91. Soletsky B, Feig DI. Uric acid reduction rectifies prehypertension in obese adolescents. *Hypertension*. 2012;60(5):1148-1156. doi:10.1161/HYPERTENSIONAHA.112.196980
- 92. Feig DI, Soletsky B, Johnson RJ. Effect of allopurinol on blood pressure of adolescents with newly diagnosed essential hypertension: A randomized trial. *JAMA*. 2008;300(8):924-932. doi:10.1001/jama.300.8.924
- 93. McMullan CJ, Borgi L, Fisher N, Curhan G, Forman J. Effect of uric acid lowering on reninangiotensin-system activation and ambulatory BP: A randomized controlled trial. *Clinical Journal of the American Society of Nephrology*. 2017;12(5):807-816. doi:10.2215/CJN.10771016
- 94. Richette P, Latourte A, Bardin T. Cardiac and renal protective effects of urate-lowering therapy. Rheumatology (Oxford). 2018;57(1):i47-i50. doi:10.1093/rheumatology/kex432
- 95. Ives A, Nomura J, Martinon F, et al. Xanthine oxidoreductase regulates macrophage IL1β secretion upon NLRP3 inflammasome activation. *Nat Commun*. 2015;6. doi:10.1038/ncomms7555
- 96. Khanna D, Fitzgerald JD, Khanna PP, et al. 2012 American college of rheumatology guidelines for management of gout. part 1: Systematic nonpharmacologic and pharmacologic therapeutic approaches to hyperuricemia. *Arthritis Care Res (Hoboken)*. 2012;64(10):1431-1446. doi:10.1002/acr.21772
- 97. Assarsson E, Lundberg M, Holmquist G, et al. Homogenous 96-plex PEA immunoassay exhibiting high sensitivity, specificity, and excellent scalability. *PLoS One*. 2014;9(4). doi:10.1371/journal. pone.0095192
- 98. Olink Target 96 Inflammation. https://olink.com/products-services/target/inflammation/

Supplemental information

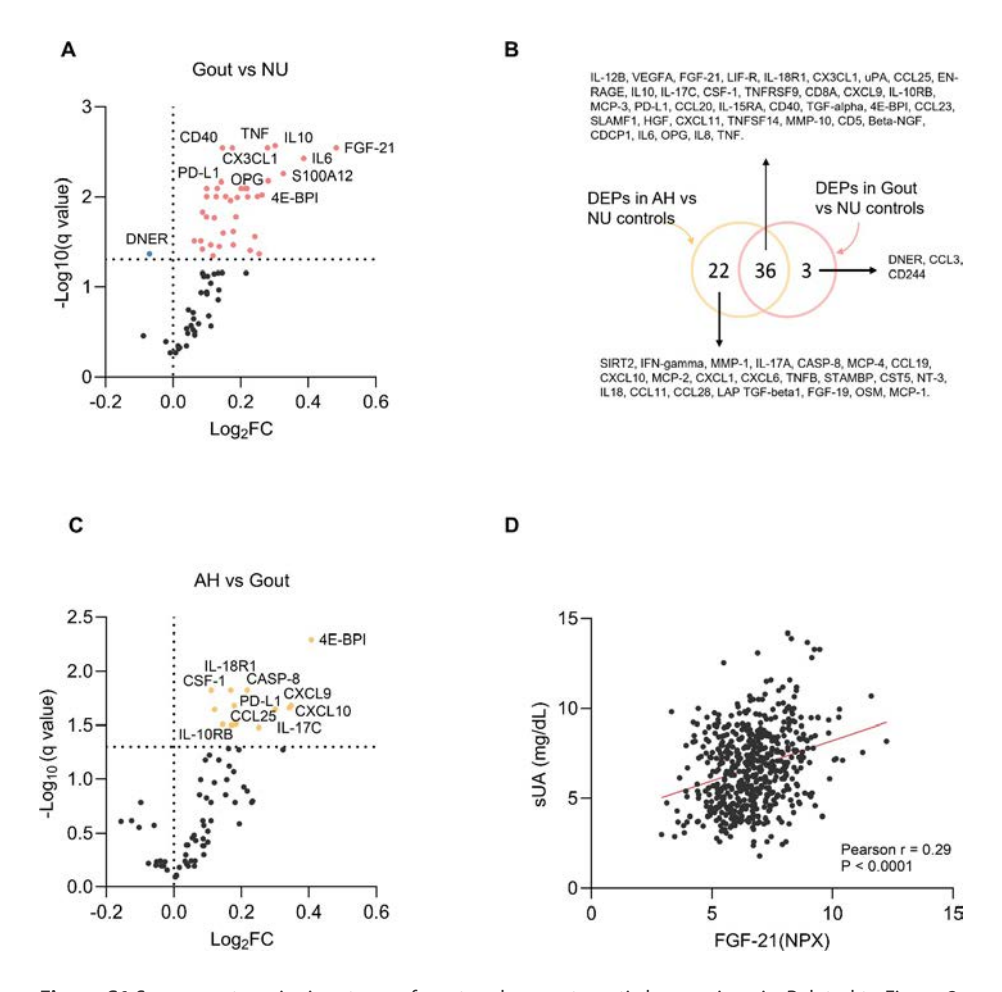
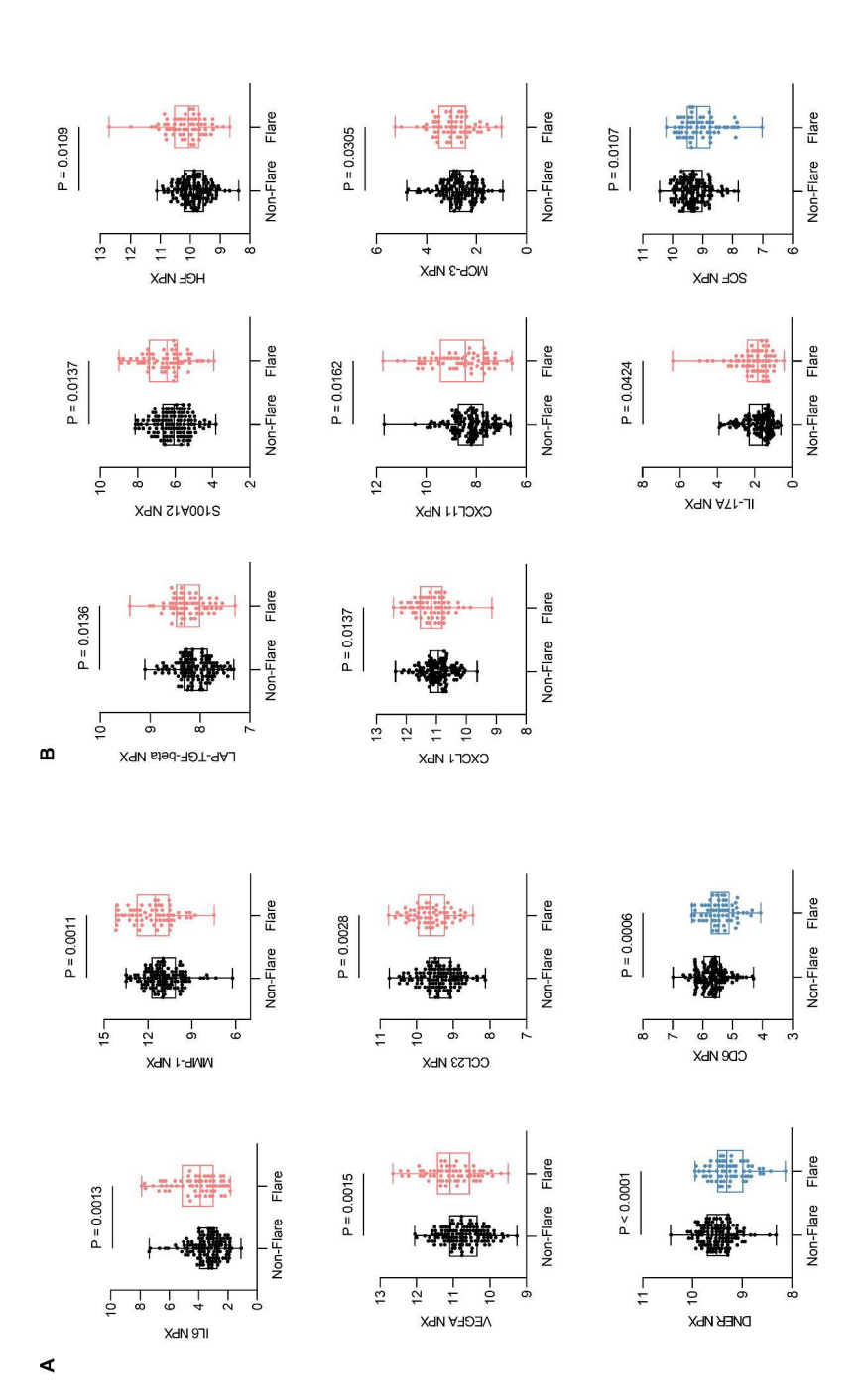
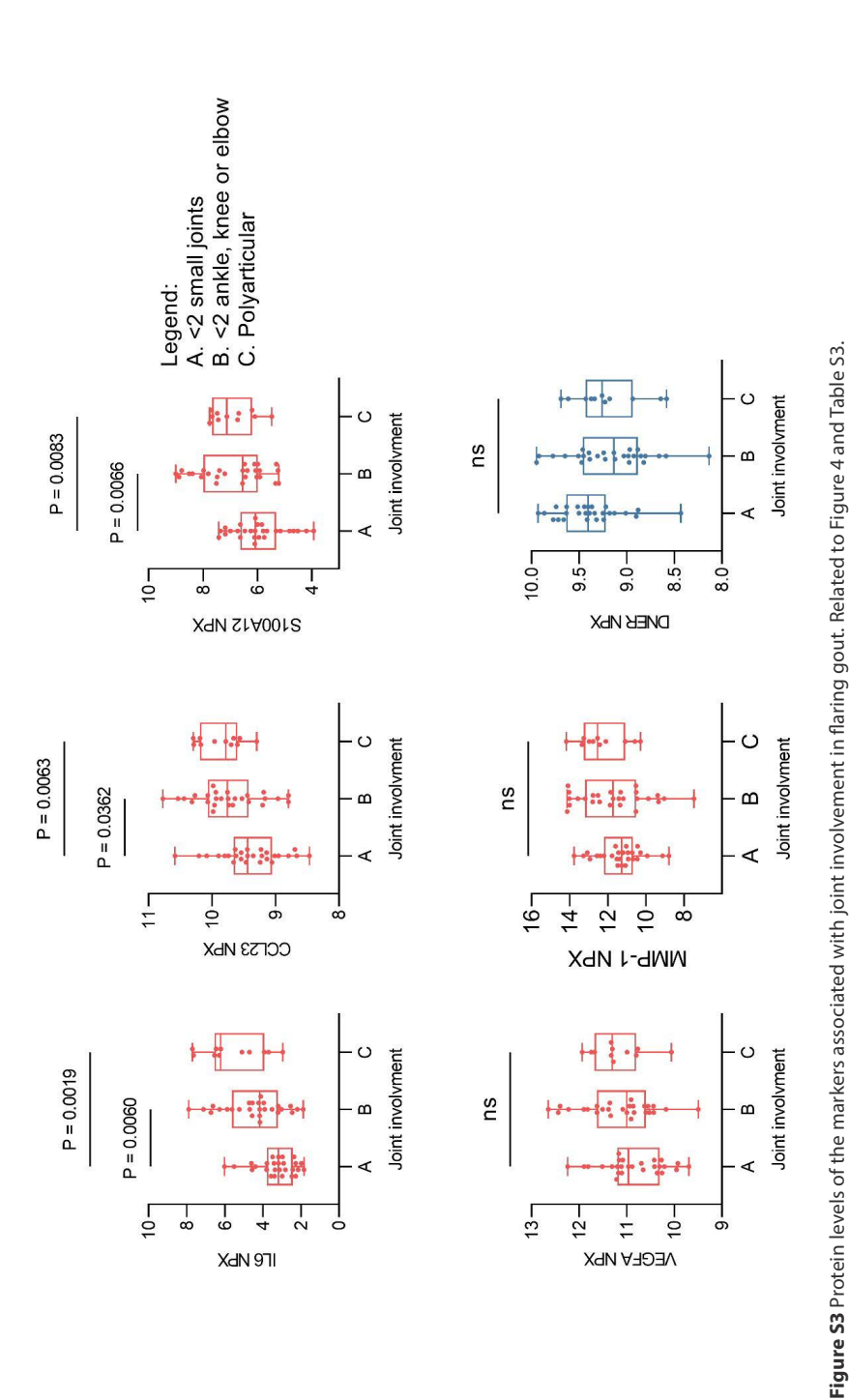


Figure S1 Serum proteomic signatures of gout and asymptomatic hyperuricemia. Related to Figure 2. Differentially expressed proteins (DEPs) in gout compared to normouricemic controls. (B) Venn diagram representing the overlap (36 proteins) between the DEPs in gout compared to NU controls (39 proteins) and asymptomatic hyperuricemia compared to NU controls (58 proteins). (C) Proteins upregulated in AH compared to gout. Volcano plots (A, C) show the top 10 proteins labeled. Associations with q values < 0.05 were considered significant, Welch multiple t-test, FDR 5%. (D) Pearson correlation between sUA levels and FGF-21 in all individuals included in the study.



Targeted analysis of the significantly differentially expressed proteins in flaring patients. (B) Targeted analysis of the nominally significant proteins in flaring patients. Box plots show median and the 75th and 25th percentiles, whiskers show the range of values. Welch's t-test was used to compare groups. (Seealso Figure 4B) Figure 52 Differentially expressed proteins in flaring gout compared to non-flaring gout samples. Related to Figure 4.



(A) IL-6, CCL23, S100A12 have significantly increased levels in polyarticular gout and when bigger joints were affected compared to smaller joints. Box plots show median and the 75th and 25th percentiles, whiskers show the range of values. Welch's ANOVA with Dunnett T3 for multiple testing correction was used to compare groups.

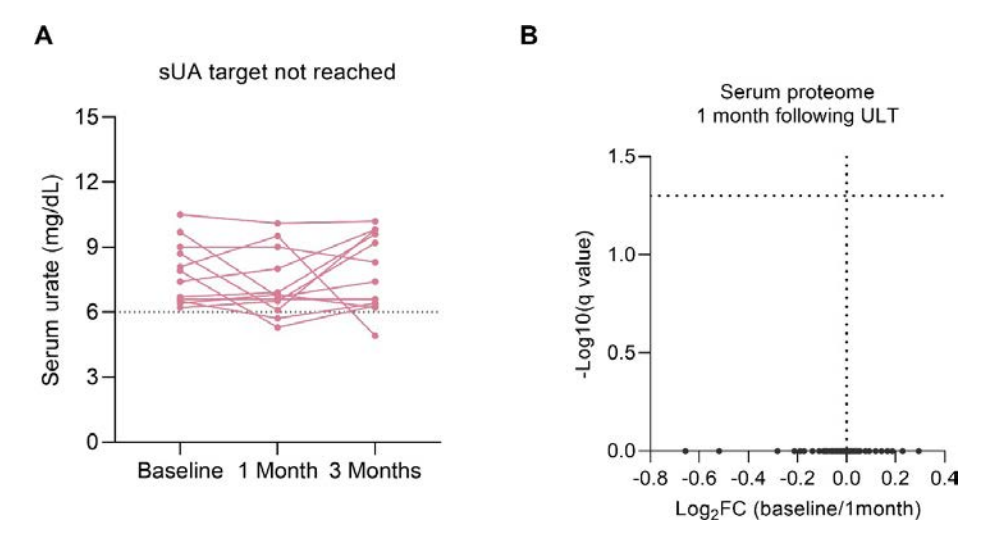


Figure S4 No early changes are observed in the proteome of patients with gout following ULT. Related to Figure 5.

(A) Patients that failed to reach sUA target (<6 mg/dL) at 1 month and 3 months compares to baseline. Dots and lines represent the paired samples at different timepoints. **(B)** Volcano plot showing no significant difference in proteins levels after only 1 month of ULT compared to baseline levels in patients that reached the target (sUA <6 mg/dL) after 3 months. Welch's multiple t-test, FDR 5%. (See also Figure 5).

Table S1. Prevalence of comorbidities in gout patients, hyperuricemic individuals and normouricemic controls. Related to Figure 1.

	T2DM+	T2DM-	CKD+	CKD-	CVD+	CVD-	HBP+
NU n (%)	27 (12.85)	183 (87.14)	7 (3.33)	203 (96.66)	10 (4.78)	199 (95.21)	119 (56.13)
AH n (%)	48 (35.82)	86 (64.17)	35 (28.68)	87 (71.31)	23 (19.65)	94 (80.34)	112 (76.71)
Gout n (%)	30 (16.85)	148 (83.14)	25 (16.23)	129 (83.76)	14 (10.29)	122 (89.70)	135 (72.97)

	HBP-	Steatosis+	Steatosis-	HyperCT+	HyperCT-	HyperTG+	HyperTG-
NU n (%)	93 (43.86)	30 (14.21)	181 (85.78)	132 (62.55)	79 (37.44)	49 (23.22)	162 (76.77)
AH n (%)	34 (23.28)	53 (40.15)	79 (59.84)	79 (59.84)	53 (40.15)	64 (48.48)	68 (51.51)
Goutn(%)	50 (27.02)	65 (41.66)	91 (58.33)	89 (56.68)	68 (43.31)	82 (52.56)	74 (47.43)

NU: normouricemia; AH: asymptomatic hyperuricemia; T2DM: type 2 diabetes; CKD: chronic kidney disease; CVD: cardiovascular disease; HBP: high blood pressure; HyperCT: hypercholesterolemia; HyperTG: hypertriglyceridemia;

Table S2: Comparison between asymptomatic hyperuricemia and normouricemic controls. Related to Figure 2.

Proteins	P value	Mean of Hyperuricemia	Mean of Normouricemia	Difference	q value
4E-BPI	<0.00001	6.464	5.775	0.689	<0.000001
IL6	<0.000001	3.917	3.297		<0.000001
				0.6205 0.2916	
IL-18R1	<0.000001	8.935	8.644		<0.000001
CD40	<0.000001	11.81	11.52	0.2912	<0.000001
CXCL9	<0.000001	6.466	5.868	0.5976	<0.000001
PD-L1	<0.000001	6.751	6.429	0.3221	<0.000001
HGF	<0.000001	10.16	9.832	0.3262	<0.000001
CX3CL1	<0.000001	6.319	5.959	0.3602	<0.000001
IL10	<0.000001	4.893	4.383	0.5099	<0.000001
IL-17C	<0.000001	2.007	1.487	0.5208	<0.000001
CSF-1	<0.000001	10.29	10.11	0.174	<0.000001
IL-10RB	<0.000001	6.185	5.964	0.2205	<0.000001
CCL25	0.000001	6.235	5.933	0.3016	0.000002
TGF-alpha	0.000002	6.384	6.02	0.3641	0.000004
MCP-3	0.000003	2.928	2.556	0.3727	0.000005
LIF-R	0.000004	3.81	3.631	0.1794	0.000006
TNFRSF9	0.000005	6.925	6.595	0.3303	0.000007
CCL20	0.000005	6.957	6.379	0.5783	0.000007
CCL23	0.000009	9.599	9.354	0.2451	0.000011
IL-15RA	0.000012	0.9253	0.7439	0.1814	0.000014
CXCL11	0.000013	8.556	8.111	0.4452	0.000014
OSM	0.000013	7.43	7.042	0.3874	0.000014
TNF	0.00002	3.718	3.338	0.3804	0.000021
MMP-10	0.000023	6.235	5.93	0.3055	0.000023
CST5	0.000042	5.397	5.152	0.2456	0.000039
Beta-NGF	0.000042	1.499	1.34	0.1585	0.000039
CASP-8	0.00005	3.229	2.95	0.2785	0.000045
VEGFA	0.000078	10.93	10.67	0.2596	0.000067
CXCL6	0.000089	9.844	9.558	0.2861	0.000074
CXCL10	0.000117	10.32	9.873	0.4477	0.000094
CD8A	0.000129	10.26	9.964	0.3012	0.000101
FGF-21	0.000171	6.936	6.392	0.5439	0.000127
EN-RAGE	0.000174	6.341	5.926	0.4154	0.000127
OPG	0.000219	9.587	9.42	0.1668	0.000152
CDCP1	0.000221	3.25	2.958	0.2914	0.000152
CD5	0.000234	4.706	4.517	0.1884	0.000157

Table S2: Continued

Proteins	P value	Mean of	Mean of	Difference	q value
		Hyperuricemia	Normouricemia	,	
CXCL1	0.000433	11.14	10.92	0.2224	0.00028
LAP TGF-beta1	0.000557	8.26	8.108	0.1514	0.00035
IFN-gamma	0.001064	7.055	6.643	0.4112	0.00065
MCP-1	0.001102	12.39	12.19	0.2012	0.00066
IL18	0.00215	8.608	8.398	0.2103	0.00126
MMP-1	0.00354	11.4	11.06	0.3428	0.00203
SLAMF1	0.004062	2.939	2.757	0.1819	0.00228
IL-17A	0.005957	1.989	1.757	0.2317	0.00327
IL-12B	0.008301	6.497	6.255	0.2415	0.00445
CCL11	0.008937	7.731	7.594	0.1369	0.00469
CCL28	0.011665	2.034	1.888	0.1457	0.00599
uPA	0.017784	9.552	9.449	0.1032	0.00894
CCL19	0.022426	9.966	9.708	0.2573	0.01105
NT-3	0.031017	2.544	2.422	0.1216	0.01498
STAMBP	0.044068	4.762	4.643	0.1188	0.02086
MCP-4	0.060707	14.65	14.49	0.152	0.02819
TNFSF14	0.08277	6.375	6.234	0.1416	0.03771
IL8	0.093323	7.791	7.616	0.1749	0.04173
TNFB	0.101639	5.08	4.984	0.09634	0.04462
SIRT2	0.104679	4.502	4.349	0.1528	0.04514
FGF-19	0.110302	8.027	7.85	0.1766	0.04627
MCP-2	0.111134	10.98	10.86	0.1196	0.04627
TRAIL	0.151578	9.27	9.214	0.05667	0.06204
CD6	0.165064	5.5	5.581	-0.08134	0.06643
AXIN1	0.181652	3.049	2.951	0.09781	0.07191
ADA	0.192156	4.39	4.328	0.06237	0.07484
ST1A1	0.244796	5.421	5.583	-0.1625	0.09383
TWEAK	0.276796	10.36	10.41	-0.04733	0.10444
CD244	0.346034	6.873	6.832	0.04072	0.12808
CCL3	0.350055	7.617	7.531	0.08607	0.12808
DNER	0.355604	9.456	9.488	-0.03252	0.12817
SCF	0.382909	9.193	9.241	-0.04863	0.13598
IL7	0.472552	4.486	4.44	0.04646	0.16539
RANKL	0.520677	6.253	6.302	-0.04939	0.17963
CCL4	0.683195	7.726	7.695	0.03088	0.23238
Flt3L	0.864213	9.302	9.313	-0.01094	0.28987
CXCL5	0.881287	12.59	12.57	0.01362	0.29154

Table S3: Correlation of joint involvement with differentially expressed and nominally significant proteins in flaring gout. Related to Figure 4 and Figure S3.

Protein	Pearson r	95% C.I.	R squared	P (two-tailed)
VEGFA	0.281	0.1451 to 0.4064	0.07894	<0.0001
MCP-3	0.2257	0.08691 to 0.3560	0.05096	0.0016
TGF-beta1	0.2327	0.09423 to 0.3624	0.05416	0.0012
IL6	0.3945	0.2679 to 0.5078	0.1557	<0.0001
IL-17A	0.147	0.005476 to 0.2827	0.0216	0.0419
CXCL11	0.1931	0.05289 to 0.3258	0.03727	0.0073
CXCL1	0.2315	0.09294 to 0.3613	0.05359	0.0012
CD6	-0.2168	-0.3477 to-0.07757	0.047	0.0025
SCF	-0.2073	-0.3390 to-0.06768	0.04297	0.0039
MMP-1	0.2864	0.1509 to 0.4113	0.08201	<0.0001
HGF	0.2408	0.1027 to 0.3698	0.05797	0.0008
CCL23	0.2858	0.1503 to 0.4108	0.08169	<0.0001
DNER	-0.3234	-0.4447 to-0.1905	0.1046	<0.0001
S100A12	0.2799	0.1440 to 0.4055	0.07836	<0.0001

Table S4: Correlation of disease severity with nominally significant proteins in tophaceous gout. Related to Figure 4.

Protein	Pearson r	95% C.I.	R squared	P (two-tailed)
RANKL	0.3761	0.2477 to 0.4915	0.1414	<0.0001
MCP-3	0.214	0.07465 to 0.3451	0.0458	0.0029
TRAIL	-0.1408	-0.2769 to 0.0007920	0.01983	0.0514
IL6	0.2052	0.06554 to 0.3371	0.04212	0.0043
IL10	-0.103	-0.2411 to 0.03913	0.01062	0.1549
DNER	-0.1974	-0.3298 to-0.05743	0.03898	0.0061
CCL3	-0.1123	-0.2499 to 0.02979	0.01261	0.121

Table S5: Differentially expressed proteins between baseline and 3 months following ULT. Related to Figure 5.

Protein	P value	Mean of 3 months	Mean of Baseline	Difference	q value
LIF-R	0.000031	3.565	3.799	-0.2332	0.001788
CDCP1	0.000233	3.2	3.496	-0.2953	0.006759
IL18	0.001381	8.287	8.544	-0.2576	0.022096
NT-3	0.001524	2.399	2.714	-0.3159	0.022096
IL-10RB	0.002319	5.879	6.084	-0.2043	0.026898
CCL28	0.003164	1.994	2.285	-0.2908	0.030587
CCL11	0.004242	7.584	7.822	-0.2389	0.035152
SLAMF1	0.005926	2.852	3.089	-0.2373	0.042961
EN-RAGE	0.009862	5.682	6.51	-0.8278	0.06235
OPG	0.013472	9.506	9.727	-0.2212	0.06235
CASP-8	0.013702	2.661	3.186	-0.5257	0.06235
CD5	0.013834	4.475	4.692	-0.2177	0.06235
uPA	0.013975	9.525	9.712	-0.187	0.06235
CX3CL1	0.021435	5.976	6.18	-0.2041	0.088801
MCP-4	0.033763	14.43	14.8	-0.3739	0.130552
L6	0.054818	3.356	3.963	-0.6062	0.198717
PD-L1	0.061516	6.441	6.622	-0.1809	0.198861
/EGFA	0.061716	10.69	10.83	-0.132	0.198861
MCP-3	0.083588	2.656	2.931	-0.2757	0.255163
L-18R1	0.090395	8.686	8.824	-0.1378	0.262146
4E-BPI	0.097573	5.932	6.356	-0.4243	0.269488
MCP-2	0.118293	10.85	11.05	-0.207	0.309205
CSF-1	0.122616	10.13	10.22	-0.09594	0.309205
CD40	0.130427	11.51	11.63	-0.1241	0.315199
GF-21	0.157138	6.415	6.737	-0.3228	0.364559
CXCL6	0.164819	9.577	9.778	-0.2019	0.367674
MMP-10	0.205606	5.935	6.076	-0.1404	0.422762
Beta-NGF	0.206315	1.535	1.595	-0.05947	0.422762
CCL20	0.211381	6.773	6.548	0.2246	0.422762
ΓNFB	0.254228	5.018	5.142	-0.1243	0.491507
L-15RA	0.266611	0.778	0.8276	-0.04954	0.498821
CXCL10	0.296433	10.09	10.37	-0.2759	0.537284
_AP-TGF-beta1	0.31972	8.101	8.169	-0.0675	0.537913

Table S5: Continued

Protein	P value	Mean of 3 months	Mean of Baseline	Difference	q value
MCP-1	0.319734	12.23	12.34	-0.1105	0.537913
CD8A	0.328796	9.826	9.938	-0.1122	0.537913
SIRT2	0.342677	4.221	4.517	-0.2965	0.537913
TNFRSF9	0.344722	6.577	6.696	-0.1184	0.537913
HGF	0.352426	9.954	10.07	-0.1137	0.537913
TGF-alpha	0.381685	6.302	6.157	0.1448	0.567635
IFN-gamma	0.442991	7.162	6.836	0.326	0.609246
IL-12B	0.449813	6.373	6.155	0.2187	0.609246
IL10	0.450437	5.071	4.738	0.3326	0.609246
CCL23	0.451682	9.374	9.44	-0.06681	0.609246
CXCL11	0.499828	8.371	8.587	-0.2158	0.658864
TNFSF14	0.534335	6.468	6.336	0.1324	0.688698
CCL25	0.563039	5.991	6.025	-0.03463	0.709919
OSM	0.577985	7.4	7.258	0.1427	0.713258
STAMBP	0.599821	4.601	4.708	-0.1064	0.724783
CST5	0.618974	5.044	5.095	-0.05063	0.726607
IL-17A	0.626385	1.651	1.573	0.07736	0.726607
TNF	0.659309	3.48	3.584	-0.1035	0.737372
CXCL9	0.661092	6.194	6.313	-0.1188	0.737372
MMP-1	0.836809	11.14	11.1	0.0412	0.894725
CCL19	0.839788	9.759	9.802	-0.04342	0.894725
FGF-19	0.863571	8.098	8.165	-0.06648	0.894725
CXCL1	0.863872	10.97	10.95	0.02096	0.894725



Chapter 6

Urate – induced epigenetic modifications in myeloid cells

Gaal OI*, Badii M*, Cleophas MC, Klück V, Davar R, Habibi E, Keating ST P, Novakovic B, Helsen MM, Dalbeth N, Stamp LK, Macartney-Coxson D 7, Phipps-Green AJ, Stunnenberg HG, Dinarello CA, Merriman TR, Netea MG MD, Crişan TO*, Joosten LAB*

*Contributed equally

Tania O. Crişan and Leo A.B. Joosten share senior authorship.

Abstract

Objectives

Hyperuricemia is a metabolic condition central to gout pathogenesis. Urate exposure primes human monocytes towards a higher capacity to produce and release IL-1 β . In this study we assessed the epigenetic processes associated to urate-mediated hyper-responsiveness.

Methods

Freshly isolated human peripheral blood mononuclear cells or enriched monocytes were pre-treated with solubilized urate and stimulated with LPS with or without monosodium urate (MSU) crystals. Cytokine production was determined by ELISA. Histone epigenetic marks were assessed by sequencing immunoprecepitated chromatin. Mice were injected intraarticularly with MSU crystals and palmitate after inhibition of uricase and urate administration in the presence or absence of methylthioadenosine. DNA methylation was assessed by methylation array in whole blood of 76 participants with normouricemia or hyperuricemia.

Results

High concentrations of urate enhanced the inflammatory response *in vitro* in human cells and *in vivo* in mice, and broad-spectrum methylation inhibitors reversed this effect. Assessment of histone 3 lysine 4 trimethylation (H3K4me3) and histone 3 lysine 27 acetylation (H3K27ac) revealed differences in urate-primed monocytes compared to controls. Differentially methylated regions (e.g. HLA-G, IFITM3, PRKAB2) were found in people with hyperuricemia compared to normouricemia in genes relevant for inflammatory cytokine signaling.

Conclusion

Urate alters the epigenetic landscape in selected human monocytes or whole blood of people with hyperuricemia compared to normouricemia. Both histone modifications and DNA methylation show differences depending on urate exposure. Subject to replication and validation, epigenetic changes in myeloid cells may be a therapeutic target in gout.

Introduction

Urate is the end-point metabolite in purine catabolism in humans and is regarded as an alarmin released from disintegrating cells at times of stress or cell death[1][2]. Higher urate concentration in the serum defines the condition of hyperuricemia, at which point monosodium urate (MSU) crystals can precipitate in peripheral tissues and cause an inflammatory response. Gout is caused by persistent hyperuricemia, a painful inflammatory arthritis caused by deposition of (MSU) crystals in the synovial cavity[3]. MSU crystals have been shown to induce IL-1B release through activation of the NLRP3 inflammasome[4]. They recruit ASC (Inflammasome Adaptor Protein Apoptosis-Associated Speck-Like Protein Containing CARD) at the inflammasome formation site through the polymerization of tubulin[5]. MSU crystals alone are insufficient for a gout flare and second signals are required to act in synergy with MSU crystals. Such second signals can be pathogen-related ligands such as lipopolysaccharide (LPS), [6]or Pam3Cys[7], or sterile stimuli such as fatty acids (e.g. stearate)[8], or the C5a component of the complement[9].

Despite a widely accepted pathogenesis model for gout stemming from long-lasting hyperuricemia that determines the formation of MSU crystals, many questions remain to address the clinical observations of urate-related inflammation[10]. The reasons why not all people with hyperuricemia develop gout, or why some people with MSU crystals in synovial fluid do not show signs of inflammation[11], remain unknown. Genome-wide association studies have identified hundreds of genomic loci associated with serum urate levels and gout [12][13][14][15] However, little progress has been made in understanding the genetic control of the progression from hyperuricemia to gout[16]. Large-scale genetic studies are likely to pinpoint additional factors that specifically lead to gout in people with hyperuricemia. Environmental factors (e.g. dietary triggers)[17] can also contribute to inflammation in people with hyperuricemia. Moreover, epidemiological studies suggest that MSU crystals and soluble urate itself also play a role in signaling danger in diseases other than gout: from the low-grade inflammation in aging[18], to common metabolic disorders[19], and cancer[20].

We previously described the priming effects of high concentrations of soluble urate on primary human peripheral blood mononuclear cells (PBMC)s and monocytes, where a shift in cytokine production towards elevated IL-1ß concomitant with reduced IL-1Ra could be observed [21]. In addition, we reported that PBMCs of individuals with hyperuricemia produce higher amounts of pro-inflammatory cytokines than normouricemic controls after ex vivo stimulation[21]. This can be reproduced in vitro by pre-treating cells with increasing urate doses followed by washout and re-stimulation with toll-like receptor ligands and MSU crystals. Interestingly, the high proinflammatory capacity coincided with a reduction in IL-1 receptor antagonist (IL-1Ra) production[21], which is at least in part mediated by AKT phosphorylation and autophagy repression in primary human monocytes[22]. Several stimuli exert long-term effects on innate immunity through epigenetic modifications (a process termed trained immunity)[23]. This persistent state of immunological memory can be induced by microbial stimuli such as Candida albicans or β-glucan (cell wall component of C. albicans)[24, 25], as well as sterile stimuli such as oxidized cholesterol or phospholipids[26, 27].

A recent study performed in patients with gout highlights several differentially methylated loci (DML) with relevance to inflammation (28). DMLs were found in known gout risk genes and candidate genes (eg.:SLC2A9, ABCC9), transcription factor genes (NFATC2 and MEF2C) and their regulated gene networks in leukocytes. Pathway analysis of DML suggests gout patients have altered DNA methylation levels of genes involved in both innate and adaptive immunity pathways, with a strong signature for Th17 differentiation and osteoclastogenesis[28].

In the present study, we hypothesize that urate drives persistent proinflammatory effects through epigenetically mediated innate immune memory and that hyperuricemic individuals could have altered epigenetic landscapes in immune cells compared to normouricemic people. We use complementary approaches aimed to establish the molecular basis of urate-mediated proinflammatory status of human monocytes. We show that exposure to urate can have persistent effects in vitro, which is consistent with previous data showing that monocytes of gout patients retain their capacity to produce more cytokines in the absence of hyperuricemia[7, 21]. We identify post-translational histone modifications and DNA methylation as molecular substrates for the effects of hyperuricemia.

Materials and methods

A detailed version of this section is provided in the Additional file 1.

Participants

Urate priming experiments were performed in 85 Dutch volunteers from the Human Functional Genomics Proiect (http://www.humanfunctionalgenomics.org)[29]. Experiments were approved by the Ethical Committee of Radboud University Nijmegen (nr. 42561.091.12). The DNA methylation study was performed in 76 individuals (Table S1) of New Zealand Māori ancestry and was approved by the New Zealand Lower South

Health and Disability Ethics Committee (MEC/05/10/130). Patients or the public were not involved in the design, or conduct, or reporting, or dissemination of our research.

PBMC and monocyte isolation

Human PBMCs were separated using FicoII-Paque (Pharmacia Biotech). Monocytes were enriched using hyperosmotic Percol solution[30], and were subsequently purified by negative selection using magnetic beads (Miltenyi Biotec).

Stimulation experiments

Experiments were performed in culture medium containing RPMI 1640, supplemented with 50 µg/ml gentamicin, 2 mM L-glutamine, 1 mM pyruvate and 10% human pooled serum following an in vitro urate priming protocol described extensively elsewhere[22].

Cytokine measurements

Cytokine concentrations were determined in cell culture supernatants using ELISA.

Animal model

Male 10-12 weeks old C57Bl/6J mice were purchased from Jackson Laboratories (Bar Harbor, Maine, USA). Uricase was inhibited using oxonic acid and urate was administered according to a previously described protocol[22].

ChIP sequencing preparation and analysis

DNA-histone crosslinking was performed using 1% formaldehyde followed by 1.25 mol/L glycine. Chromatin was sonicated using a Diagenode Bioruptor UCD-300 and immunoprecipitated using H3K27ac or H3K4me3 antibodies (Diagenode) and protein A/G magnetic beads. DNA was purified using QIAGEN Qiaquick MinElute PCR purification Kit. Illumina library preparation was done as previously described[31]. Sequencing was performed using Illumina HiSeq 2000.

DNA methylation analysis

Genomic DNA was isolated from the peripheral blood white cells of 76 individuals of Aotearoa New Zealand Māori ancestry with varying serum urate levels. Genome-wide methylation analysis was performed using Illumina InfiniumMethylationEPIC BeadChips[32].

Statistical analysis

Cytokine data were analyzed in GraphPad Prism version 8 using Friedmann or Wilcoxon signed rank test. ChIP sequencing and DNA methylation data were analyzed using R.

Results

Urate treatment of human PBMCs in vitro results in a specific and persistent cytokine production phenotype

We tested the effects of urate solubilized in culture medium at high concentration (50 mg/dL) or at concentrations similar to *in vivo* hyperuricemia (10 mg/dL). Both concentrations of soluble urate primed the cells to produce higher IL-1 β and lower IL-1Ra production (Figure1A-D). Next, we investigated whether these priming effects persisted beyond the 24h period of urate priming. Cells were incubated for 24h with urate, washed and thereafter subjected to increasing resting times (up to 5 days) in culture medium before stimulation with LPS (10 ng/mL) and MSU crystals (300 µg/mL). While IL-1 β production capacity was strongly diminished after 48h of culture (Figure2A-B – 24 h resting periods and onwards), persistent effects were observed for reduction of IL-1Ra (Figure2C-D) and for induction of IL-6 (Figure2E-F).

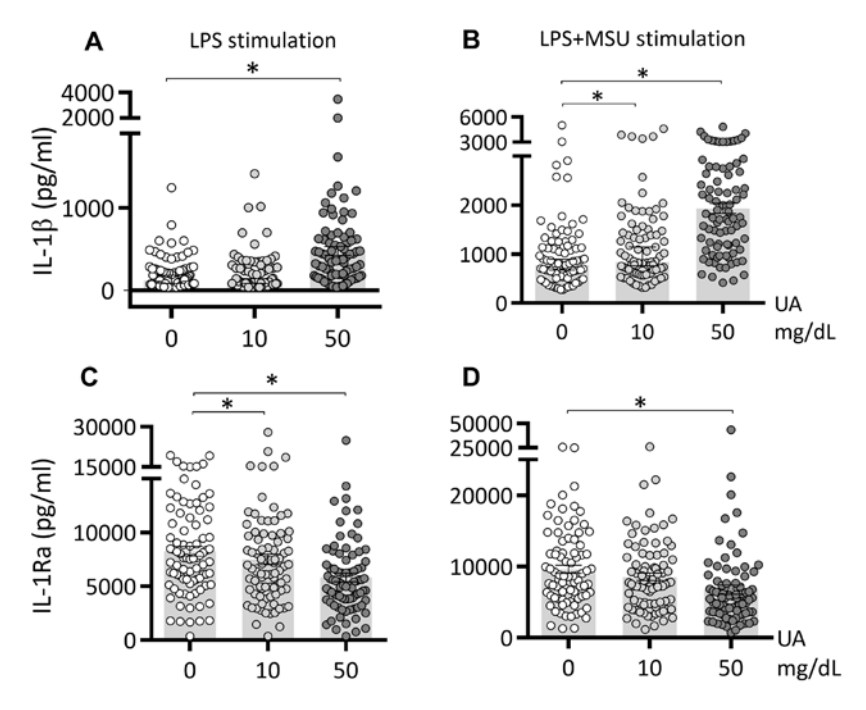


Figure 1 IL-1 β and IL-1Ra production after urate priming of PBMCs *in vitro*. Freshly isolated PBMCs from 85 healthy volunteers were exposed to culture medium (RPMI 1640 supplemented with 10% human pooled serum) in the presence or absence of urate (UA) 10 or 50 mg/dL. After 24 hours, urate was removed, and cells were stimulated with LPS 10 ng/mL in the presence or absence of MSU crystals (300 μ g/mL). IL-1 β (A-B) and IL-1Ra (C-D) were measured in the supernatants of cells, data are representative of 3 independent experiments using a total of 85 different healthy volunteers of the 200FG cohort, graphs depict means+/-SEM. UA, uric acid/urate. *, Friedman test and post-hoc analysis p<0.05.

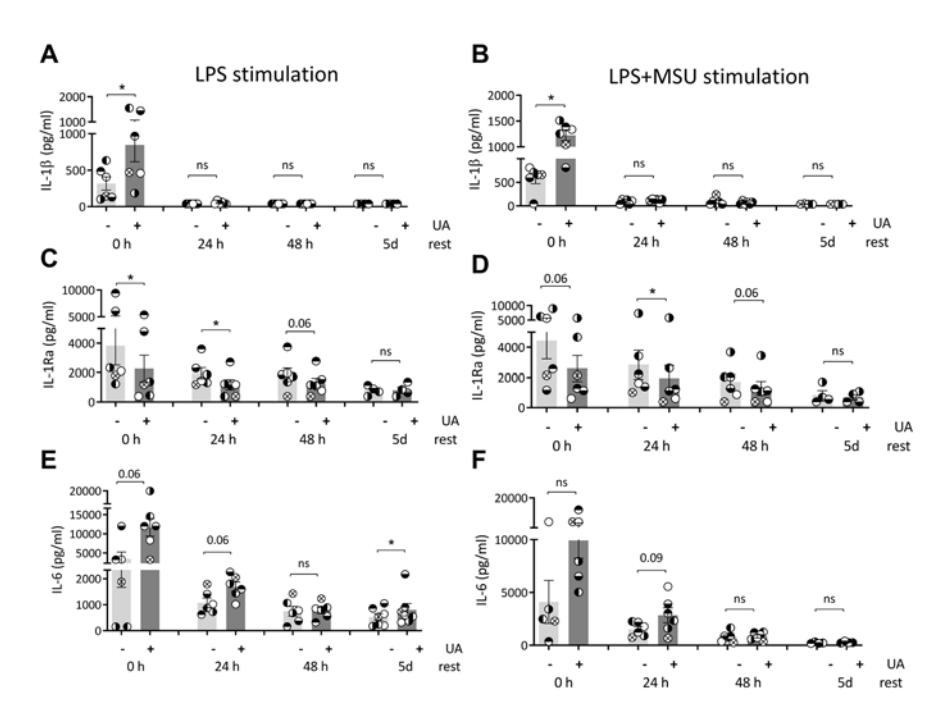


Figure 2 Persistence of urate priming effects in vitro. Freshly isolated PBMCs from 6 healthy volunteers were exposed to culture medium (RPMI 1640 supplemented with 10% human pooled serum) in the presence or absence of urate (UA) 50 mg/dL. After 24 hours, urate was removed, and cells were stimulated with LPS 10 ng/mL in the presence or absence of MSU crystals (300ug/mL). The second stimulation was performed at different times after urate washout: immediately (0 h resting time), or after increasing number of days of resting in 10% serum RPMI (24 hours, 48 hours, 5 days). IL-1β (A-B), IL-1Ra (C-D) and IL-6 (E-F) were measured in the supernatants of cells, data are representative for 3 independent experiments and 6 different volunteers, graphs depict individual values with paired samples shown in identical symbols, bars and error bars represent means+/-SEM. UA, uric acid/urate 50 mg/dL. *, Wilcoxon p<0.05.

Pharmacological inhibition of methyl-transferases inhibits urate effects in an in vivo murine model of gout

The broad protein methyl-transferase inhibitor methylthioadenosine (5'-S-methyl-5'-thioadenosine, MTA) was previously shown to inhibit the cytokine production induced by urate in vitro[21]. To provide validation in an in vivo model, mice were administered exogenous urate in addition to oxonic acid (uricase inhibitor). Acute gout was induced by intraarticular injections with MSU crystals and palmitate (C16:0). Inflammation was significantly enhanced in the oxonic acid group compared with controls as observed by macroscopically scored inflammation (Figure 3A). Addition of MTA inhibited this effect on the enhanced joint inflammation and histology at 24h post intraarticular injections (Figure 3A-C).

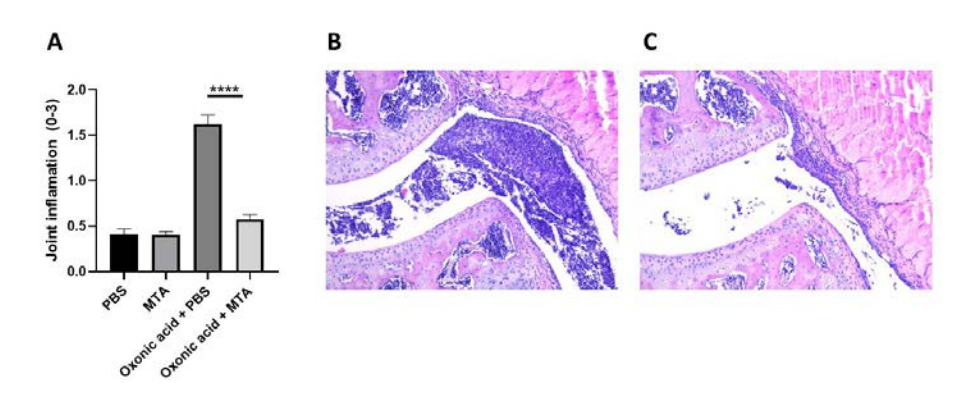


Figure 3 Methyl transferase inhibition limits gout inflammation in mice. Macroscopic (Panel **A**) scores of the knees in mice treated with vehicle control or oxonic acid + urate in the presence or absence of methyl transferase inhibitor MTA (methyl-thio-adenosine) followed by intraarticular injection of MSU+C16:0. Inflammation was scored at 24 h. Histology (H&E staining) of joints treated with MSU+C16:0 in oxonic acid + urate mice (**panel B**) and in the presence of MTA (**panel C**).

Histone 3 Lysine 4 trimethylation (H3K4me3) or Histone 3 Lysine 27 acetylation (H3K27ac) are mildly affected by urate treatment of human monocytes *in vitro*

To test whether specific histone modifications are associated with the persistent effects of urate priming, we used chromatin immunoprecipitation coupled with massively parallel sequencing (ChIP-seq) to profile the enrichment of H3 histones trimethylated at lysine 4 (H3K4me3) and H3 histones acetylated at lysine 27 (H3K27ac), two transcriptionally permissive chromatin modifications previously associated with long-term effects of sterile stimuli[26].

The ChIPseq analysis was based on all dynamic genes that were identified by comparing all samples to each other. After filtering the data based on these cutoffs, no clustering of stimulated samples was evident to indicate that urate induced genome-wide significant differences on these two histone marks (Figure4A-D, Figure S1) Nevertheless, some individual genes, exhibited nominally-significant evidence for variability for H3K4me3 (Table S2) or H3K27ac (Table S3) enrichment at promoter regions. Of these, 12 genes (MED24, CSF3, TAF1C, DNAAF1, HCAR2, ACO73072.5, IDO1, RP11-44K6.2, RP11-370F5.4, RP11-44K6.5, SNRPC, and APOE) displayed variability for both histone modifications in urate-primed cells compared to control conditions (Figure 4E-F).

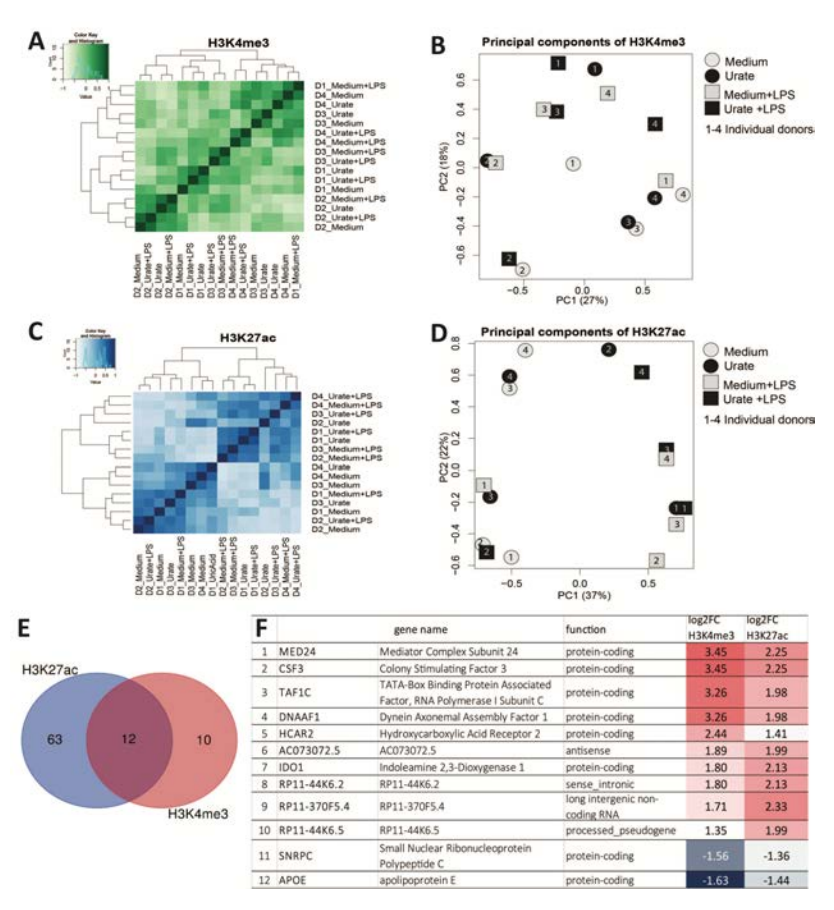


Figure 4 ChIP sequencing in urate-stimulated monocytes reveals no urate-dependent clustering based on phenotype for H3K4 trimethylation and H3K27 acetylation. Cluster and principal component analysis of datasets obtained on ChIP sequencing for H3K4me3 (A and B) or H3K27ac (C and D) in 4 different donors (labeled D1-4) and 4 different conditions (Medium, Urate, Medium+LPS, Urate+LPS). Venn diagram of regions showing differential enrichment of either H3K27ac or H3K4me3 in urate primed cells (E) and list of overlapping genes based on histone marks at promoter regions, including log 2 fold change values for each of the two histone marks (F).

DNA methylation profiling reveals candidates for effects of serum urate levels in vivo in humans

DNA methylation could also function as a basis for urate imprinting as it is a stable epigenetic mark, often associated with long-term gene silencing. In the Aotearoa New Zealand Māori participants, DNA methylation was determined and assessed in whole blood samples of hyperuricemic and normouricemic volunteers. Approximately 850K CpG sites were studied among the two groups and revealed 223 differentially methylated probes (difference in DNA methylation of at least 5%) (Figure 5). 23 regions that exhibited significant differential methylation across the two groups of participants were found both in intergenic or intragenic regions of specific genes, one notable example being *HLA-G* (Figure 5 B-C). Individual differentially methylated probes and differentially methylated regions are listed in Table S4 and Table S5, respectively. An expanded list of candidates was revealed by data analysis of DNA methylation without cell composition correction (detailed information is provided in the supporting information material, Figure S2, Tables S6 and S7).

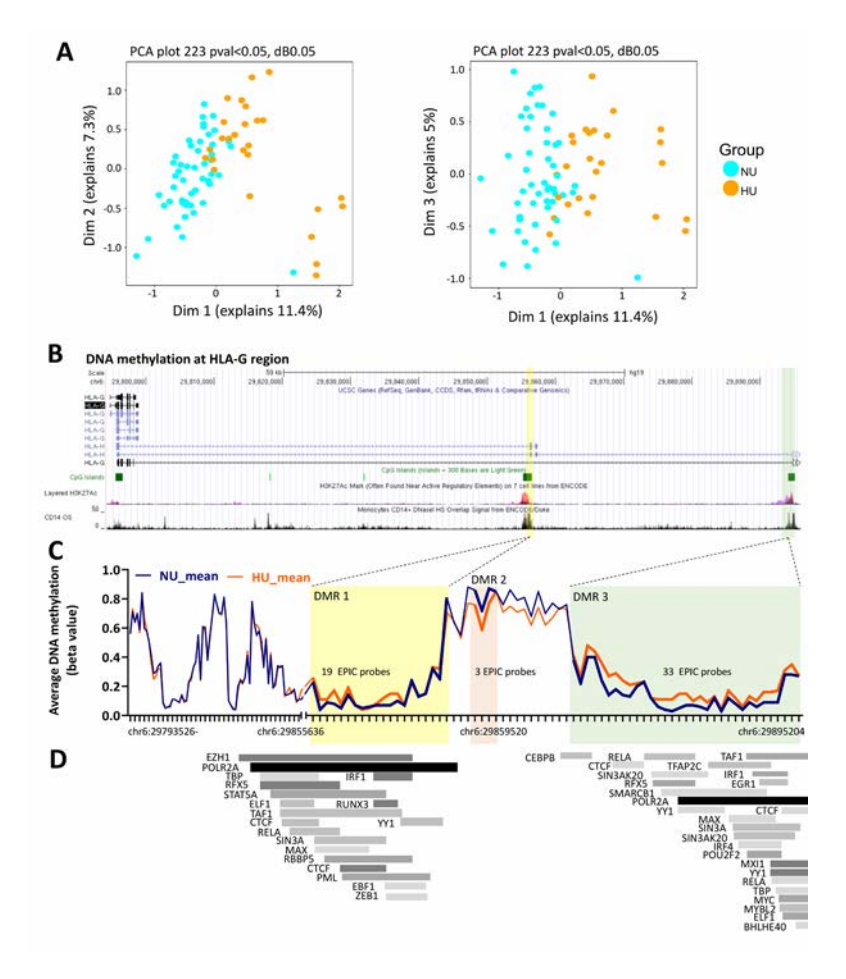


Figure 5 Differential DNA methylation in hyperuricemic versus normouricemic people. Principal component analysis of whole blood DNA methylation data, obtained using Illumina InfiniumMethylationEPIC BeadChips in whole blood of 26 people with hyperuricemia compared to 50 normouricemic individuals **(A)**. Differentially methylated regions (DMRs) at the *HLA-G* locus **(B)** and average DNA methylation levels (beta values) for all CpG probes found within *HLA-G* (ticks on the *x* axis represent individual probes and DNA chromosome position is indicated) **(C)**. Transcription factors known to bind at the highlighted DMR1 and DMR3 regions according to the transcription factor ChIP-seq clusters from ENCODE with factorbook motifs **(D)**.

Discussion

In this study, we assess the effects of exposing PBMCs of 85 healthy participants to soluble urate at concentrations of 10 mg/dL or 50 mg/dL in vitro. We show that both concentrations induce a higher IL-1β release and a lower IL-1Ra production in response to subsequent stimulation with LPS or LPS+MSU crystals (Figure 1). We also describe persistent effects of the treatment with soluble urate in primary myeloid cells that were treated with urate for 24h, followed by medium removal and stimulation for another 24h with LPS or LPS+MSU crystals (in the absence of urate). The behavior of monocytes after priming for 24h with urate has been described previously, demonstrating that the cytokine production capacity of the cells switches to higher IL-1B production and lower IL-1Ra basal concentrations[21], by activating AKT-PRAS40 and inhibiting autophagy[22]. Here, we demonstrate similar effects of urate at 10 mg/dL as high dose urate stimulations (50 mg/dL). Moreover, even after extended resting times between priming and restimulation, modified cytokine levels persisted in primary cells exposed to urate. IL-1Ra remained downregulated after 48h resting time (Figure 2C-D). The increase in IL-6 remained present at all timepoints, although statistically significant differences were only observed after 5 days of rest in between stimulations (Figure 2E-F). This may be due to limited number of donors and high variability. Significant differences have been previously shown for IL-6 in past reports on urate priming, with direct stimulation at the end of the first 24h of urate exposure [33][21]. Other reports have shown that innate immune memory induced by β-glucan, BCG or oxidized LDL particles is best observed after 5 days resting intervals compared to 1 day rest or 3 days rest, possibly in connection with immunometabolism changes (glycolysis induction associated to innate immune memory) [34] IL-1\u03b3 induction upon stimulation was, however, markedly reduced at later incubation time points in all conditions (Figure 1A-B). As opposed to monocytes which express constitutively active caspase-1, in macrophages, the production of IL-1ß is more stringently regulated and needs two signals for active IL-1β release: a PRR signal leading to proIL-1β transcription and translation and an inflammasome activator which leads to the proteolysis of proIL-1\(\beta \) into active IL-1\(\beta \)[35]. Our results are in accordance with the restricted IL-1\(\beta \) production in differentiated macrophages after longer in vitro culture of primary monocytes, due to inflammasome (caspase-1) inactivation[35].

Broad protein methylation inhibitor MTA was shown to reverse the urate effect in vitro[21]. Here we show reversal of inflammation in an in vivo model of gout in mice (Figure 3). The pharmacological inhibition of the uricase enzyme using oxonic acid is a commonly used model to assess hyperuricemia in animal models where the uricase gene functionality is maintained[36, 37]. Previously, we have reported that oxonic acid and urate treatment in mice enhances inflammation triggered by intraarticular injections of palmitate and MSU crystals[22]. In the current study we show that this effect is reversible in mice that were subjected to MTA treatment prior to intraarticular injections, providing evidence that epigenetic modulators could be potential therapeutic agents for the proinflammatory effects associated to urate exposure. Given the broad effects of MTA it cannot be excluded that other processes, such as transcription factor methylation, are at play in urate priming.

To further decipher the involvement of histone marks in urate priming and persistence of effects, a genome-wide approach was undertaken in the pursuit of assessing epigenetic modifications globally. Two histone marks were analysed in the setting of urate priming: trimethylation of lysine 4 of histone 3 (H3K4me3) and acetylation of lysine 27 of histone 3 (H3K27ac). Both marks are associated with activation of gene expression across different cell types[38], have been previously studied in relation to other trained immunity stimuli in recent reports[25, 39], and are known to be present at the promoters of IL1B and IL1RN in monocytes[40]. The ChIPseq data (Figure 4) shows lack of sample clustering based on urate exposure, indicating absence of genome wide effects for H3K4me3 and H3K27ac in this experiment. Nevertheless, given the small number of participants, targeted approaches at validating the hits which showed evidence of variability are likely to provide new understanding of urate-induced epigenetic effects. Target genes that are relevant for urate-mediated effects were identified in the histone modification datasets. The IL1B and IL1A genes encoding the IL-1β and IL-1α proinflammatory cytokines show enrichment of the H3K27ac epigenetic mark, which is consistent with previously shown induction of these cytokines by urate in vitro,[21]. Twelve genes showed concordant variance in both H3K4me3 and H3K27ac (Figure 4 E-F). Enrichment of both histone marks was highest for MED24 (mediator complex subunit 24), CSF3 (colony stimulating factor 3), TAF1C (TATA-box binding protein associated factor, RNA polymerase I subunit C), DNAAF1 (dynein axonemal assembly factor 1), while both marks were downregulated for APOE (apolipoprotein E). APOE has been previously associated to gout and hyperuricemia as a potential link with hypertriglyceridaemia, a common finding in patients with gout[41]. APOE has also been reported to coat MSU crystals and inhibit MSU-induced inflammatory signaling[42], therefore, the finding that urate exposure can lead to a reduction in H3K4me3 and H3K27ac (and, consequently, reduced chromatin accessibility) at the APOE locus, suggests, that this effect could be a point of study for the progression from hyperuricemia to gout. The validation of H3K27ac or H3K4me3 enrichment in response to lower concentrations of urate or in patients with hyperuricemia would

be a useful next step. The fact that no differences are observed for LPS stimulation in our dataset is intriguing and could be attributable to the *in vitro* differentiation of the monocytes into macrophages in the presence of serum-supplemented culture medium. Serum is known to downregulate CD14 expression and to induce the release of CD14 in the extracellular space [43]. Moreover, in vitro culture of monocytes for 24h in standard conditions is reported to lead to the irreversible loss of MD2 activity [44]. Taken together these data suggest that serum-derived macrophages are less responsive to LPS due to CD14 and MD2 downregulation in standard culture conditions, which may explain the lack of significant alteration in the studied histone marks in response to the short 4 h stimulation with LPS.

We also studied the possibility of DNA methylation involvement in the proinflammatory effects associated to hyperuricemia in a sample set of New Zealand Māori ancestry [28]. The Māori population has 2-3-fold higher risk of gout compared to the population of European descent[45], likely contributed to by genetic susceptibility alleles that have increased in prevalence during the Pacific ancestral migrations, through mechanisms that are still debated [46]. By comparing DNA methylation status in hyperuricemic versus normouricemic volunteers within this cohort, 223 differentially methylated probes and 23 differentially methylated regions were identified in the vicinity of genes. Interestingly, three DMRs were found to be present at the HLA-G locus (human leukocyte associated antigen, class I, G) (Figure 5). Two of the HLA-G DMRs coincided with H3K27ac enrichment peaks (Figure 5B), CD14+ monocyte DNAse I accessibility peaks (Figure 5B) and binding sites for several transcription factors (Figure 5D) (www.encodeproject.org), which is indicative of potential functional effects of the DNA methylation variance observed at these sites. HLA-G is a HLA-class Ib molecule with immunomodulatory properties across several tissues, which has recently been suggested to limit the progression of autoimmune and autoinflammatory disorders (extensively reviewed in[47]) and could be a promising target to study in gout.

Other candidates highlighted by the presence of two DMPs in the vicinity of the gene (Table S4) were IFITM3 (Interferon Induced Transmembrane Protein 3) or PRKAB2 (AMP-Activated Protein Kinase Subunit Beta 2, AMPK-β2). Genes in the interferon signaling pathway have previously been reported to be differentially expressed (upregulated) in whole blood of healthy individuals administered rasburicase compared to placebo,[48]. In monocytes pre-treated with urate, transcriptomic analysis revealed downregulation of genes associated to GO term "Influenza A", which includes several interferon signaling related genes[22]. Moreover, type I interferons are known to inhibit STAT1 signalling and inflammasome activation[49], hence, urate-induced downregulation of interferon signaling could play a role in escalating IL-1 production and release. AMPK-β2 is a regulatory subunit of AMP-activated protein kinase (AMPK). AMPK activation was shown to limit MSU crystal-induced IL-1β production and to drive anti-inflammatory macrophage M2 polarisation[50]. DNA hypomethylation at the *PRKAG2* gene body (AMPK Subunit Gamma 2) was reported in gout patients compared to controls [50] Furthermore, PRKAG2 is one of the loci associated with hyperuricemia [12] and gout [51]. Our data suggest that urate exposure could modulate AMPK and interferon signaling pathways via DNA methylation methylation in hyperuricemic people.

This report has the limitation of having studied a small number of donors for the assessment of genome-wide epigenetic modifications (monocytes of 4 donors and stimulations for ChIP sequencing, or 26 versus 50 volunteers for the DNA methylation study). Variation in histone modification or DNA methylation in no gene were found to be experimentally-wide significant between urateexposed and control. Nevertheless, there is evidence of variation correlated to urate exposure for all these epigenetic mechanisms in candidate genes. Further studies using larger sample sizes or targeted approaches based on these initial candidates are needed in order to find statistically significant effects. Since this report describes consequences of higher than normal urate levels, we cannot exclude that any of these effects could also be driven by the precipitated form of urate. For the *in vitro* experiments, using polarized light microscopy, we were not able to observe urate crystals formed during the 24 hours of exposure time for the described experimental conditions. Validating the changes in the histone mark landscape at lower concentrations of urate or in patients with hyperuricemia would be an important next step. Finally, the current study lacks mRNA data to show transcriptional regulation of cytokine genes in response to urate after differential resting periods. A previous report by our group showed that the gene expression of IL1B, IL1RN and IL6 follows the same trend as the protein levels at 24h [22]. Further assessment of the transcriptome of samples at later time-points after the initial encounter with urate would help understand the extent of persistence of the transcriptional programme induced by urate.

Conclusions

We have generated datasets involving epigenomic and functional immunological experiments to investigate potential major mechanisms involved in the urate priming of myeloid cells. Based on complementary methods we show that epigenetic changes are likely to play a role in mediating the persistent effects of urate exposure on innate immune cells. Our study shows that high levels of urate can persistently alter the cytokine production capacity of primary PBMCs in vitro, leading to increased IL-1 beta and IL-6 production and reduced levels of IL-1 receptor antagonist (IL-1Ra). Uricase inhibition in mice led to higher inflammation scores upon intraarticular injection of MSU crystals and palmitate, and this effect was reversed by methyl transferase inhibition. We present here evidence that histone modifications (H3K4me3 or H3K27ac) and DNA methylation show differences in response to high urate exposure and provide potential candidates of differentially regulated targets. The differences in epigenetic regulation may provide new understanding and possibility for intervention in urate-dependent inflammatory responses as well as in the progression from hyperuricemia to gout.

Declarations

Ethics approval and consent to participate

In-vitro experiments were approved by the Ethical Committee of Radboud University Nijmegen (nr. 42561.091.12). The animal experiments were approved by The Institutional Animal Care and Use Committees of the University of Colorado Denver, Aurora, CO (protocol #0035). The DNA methylation study was approved by the New Zealand Lower South Health and Disability Ethics Committee (MEC/05/10/130). All participants provided written informed consent. All experiments were conducted according to the principles of the Declaration of Helsinki.

Consent for publication

Not applicable

Availability of data and material

ChIP-sequencing and cytokine data used for this manuscript will be made available to readers upon request. DNA methylation data cannot be made available due to ethical reasons.

References

- Shi Y, Evans JE, Rock KL (2003) Molecular identification of a danger signal that alerts the immune system to dying cells. Nature 425:516–521
- 2. Kono H, Chen CJ, Ontiveros F, Rock KL (2010) Uric acid promotes an acute inflammatory response to sterile cell death in mice. J Clin Invest. https://doi.org/10.1172/JCI40124
- Mandel NS, Mandel GS (1976) Monosodium Urate Monohydrate, the Gout Culprit. J Am Chem Soc. https://doi.org/10.1021/ja00424a054
- Martinon F, Pétrilli V, Mayor A, Tardivel A, Tschopp J (2006) Gout-associated uric acid crystals activate the NALP3 inflammasome. Nature 440:237–241
- Misawa T, Takahama M, Kozaki T, Lee H, Zou J, Saitoh T, Akira S (2013) Microtubule-driven spatial arrangement of mitochondria promotes activation of the NLRP3 inflammasome. Nat Immunol. https://doi.org/10.1038/ni.2550
- Giamarellos-Bourboulis EJ, Mouktaroudi M, Bodar E, Van Der Ven J, Kullberg BJ, Netea MG, Van Der Meer JWM (2009) Crystals of monosodium urate monohydrate enhance lipopolysaccharideinduced release of interleukin 1 βby mononuclear cells through a caspase 1-mediated process. Ann Rheum Dis. https://doi.org/10.1136/ard.2007.082222
- Mylona EE, Mouktaroudi M, Crisan TO, et al (2012) Enhanced interleukin-1β production of PBMCs from patients with gout after stimulation with Toll-like receptor-2 ligands and urate crystals. Arthritis Res Ther. https://doi.org/10.1186/ar3898
- Joosten LAB, Netea MG, Mylona E, et al (2010) Engagement of fatty acids with toll-like receptor 2 drives interleukin-1β production via the ASC/caspase 1 pathway in monosodium urate monohydrate crystal-induced gouty arthritis. Arthritis Rheum. https://doi.org/10.1002/art.27667
- An LL, Mehta P, Xu L, Turman S, Reimer T, Naiman B, Connor J, Sanjuan M, Kolbeck R, Fung M (2014) Complement C5a potentiates uric acid crystal-induced IL-1β production. Eur J Immunol. https://doi.org/10.1002/eji.201444560
- Dalbeth N, Merriman TR, Stamp LK (2016) Gout. Lancet. https://doi.org/10.1016/S0140-6736(16)00346-9
- 11. Pascual E (1991) Persistence of monosodium urate crystals and low-grade inflammation in the synovial fluid of patients with untreated gout. Arthritis Rheum. https://doi.org/10.1002/art.1780340203
- 12. Köttgen A, Albrecht E, Teumer A, et al (2013) Genome-wide association analyses identify 18 new loci associated with serum urate concentrations. Nat Genet 45:145–154
- Nakatochi M, Kanai M, Nakayama A, et al (2019) Genome-wide meta-analysis identifies multiple novel loci associated with serum uric acid levels in Japanese individuals. Commun Biol. https:// doi.org/10.1038/s42003-019-0339-0
- Boocock J, Leask M, Okada Y, et al (2020) Genomic dissection of 43 serum urate-associated loci provides multiple insights into molecular mechanisms of urate control. Hum Mol Genet. https:// doi.org/10.1093/hmg/ddaa013
- Tin A, Marten J, Halperin Kuhns VL, et al (2019) Target genes, variants, tissues and transcriptional pathways influencing human serum urate levels. Nat Genet. https://doi.org/10.1038/s41588-019-0504-x
- Dalbeth N, Stamp LK, Merriman TR (2017) The genetics of gout: Towards personalised medicine?
 BMC Med. https://doi.org/10.1186/s12916-017-0878-5

- 17. Flynn TJ, Cadzow M, Dalbeth N, Jones PB, Stamp LK, Hindmarsh JH, Todd AS, Walker RJ, Topless R, Merriman TR (2015) Positive association of tomato consumption with serum urate: Support for tomato consumption as an anecdotal trigger of gout flares. BMC Musculoskelet Disord. https:// doi.org/10.1186/s12891-015-0661-8
- 18. Feldman N, Rotter-Maskowitz A, Okun E (2015) DAMPs as mediators of sterile inflammation in aging-related pathologies. Ageing Res Rev. https://doi.org/10.1016/j.arr.2015.01.003
- 19. Athyros VG, Mikhailidis DP (2014) Uric acid, chronic kidney disease and type 2 diabetes: A cluster of vascular risk factors. J Diabetes Complications. https://doi.org/10.1016/j.jdiacomp.2013.11.012
- 20. Eisenbacher JL, Schrezenmeier H, Jahrsdörfer B, et al (2014) S100A4 and Uric Acid Promote Mesenchymal Stromal Cell Induction of IL-10 + /IDO + Lymphocytes. J Immunol. https://doi. org/10.4049/jimmunol.1303144
- 21. Crisan TO, Cleophas MCP, Oosting M, Lemmers H, Toenhake-Dijkstra H, Netea MG, Jansen TL, Joosten LAB (2016) Soluble uric acid primes TLR-induced proinflammatory cytokine production by human primary cells via inhibition of IL-1Ra. Ann Rheum Dis 75:755–762
- 22. Crisan TO, Cleophas MCP, Novakovic B, Erler K, Van De Veerdonk FL, Stunnenberg HG, Netea MG, Dinarello CA, Joosten LAB (2017) Uric acid priming in human monocytes is driven by the AKT-PRAS40 autophagy pathway. Proc Natl Acad Sci U S A. https://doi.org/10.1073/pnas.1620910114
- 23. Netea MG, Quintin J, Van Der Meer JWM (2011) Trained immunity: A memory for innate host defense. Cell Host Microbe. https://doi.org/10.1016/j.chom.2011.04.006
- 24. Quintin J, Saeed S, Martens JHA, et al (2012) Candida albicans infection affords protection against reinfection via functional reprogramming of monocytes. Cell Host Microbe. https://doi. org/10.1016/j.chom.2012.06.006
- 25. Saeed S, Quintin J, Kerstens HHD, et al (2014) Epigenetic programming of monocyte-tomacrophage differentiation and trained innate immunity. Science (80-). https://doi.org/10.1126/ science.1251086
- 26. Bekkering S, Quintin J, Joosten LAB, Van Der Meer JWM, Netea MG, Riksen NP (2014) Oxidized low-density lipoprotein induces long-term proinflammatory cytokine production and foam cell formation via epigenetic reprogramming of monocytes. Arterioscler Thromb Vasc Biol. https:// doi.org/10.1161/ATVBAHA.114.303887
- 27. Van Der Valk FM, Bekkering S, Kroon J, et al (2016) Oxidized phospholipids on Lipoprotein(a) elicit arterial wall inflammation and an inflammatory monocyte response in humans. Circulation. https://doi.org/10.1161/CIRCULATIONAHA.116.020838
- 28. Wang Z, Zhao Y, Phipps-Green A, Liu-Bryan R, Ceponis A, Boyle DL, Wang J, Merriman TR, Wang W, Terkeltaub R (2020) Differential DNA Methylation of Networked Signaling, Transcriptional, Innate and Adaptive Immunity, and Osteoclastogenesis Genes and Pathways in Gout. Arthritis Rheumatol. https://doi.org/10.1002/art.41173
- 29. Li Y, Oosting M, Deelen P, et al (2016) Inter-individual variability and genetic influences on cytokine responses to bacteria and fungi. Nat Med. https://doi.org/10.1038/nm.4139
- 30. Repnik U, Knezevic M, Jeras M (2003) Simple and cost-effective isolation of monocytes from buffy coats. J Immunol Methods. https://doi.org/10.1016/S0022-1759(03)00231-X
- 31. Novakovic B, Habibi E, Wang SY, et al (2016) β-Glucan Reverses the Epigenetic State of LPS-Induced Immunological Tolerance. Cell. https://doi.org/10.1016/j.cell.2016.09.034

- 32. Pidsley R, Zotenko E, Peters TJ, Lawrence MG, Risbridger GP, Molloy P, Van Diik S, Muhlhausler B, Stirzaker C, Clark SJ (2016) Critical evaluation of the Illumina MethylationEPIC BeadChip microarray for whole-genome DNA methylation profiling. Genome Biol. https://doi.org/10.1186/ s13059-016-1066-1
- 33. Crişan TO, Cleophas MCP, Novakovic B, Erler K, van de Veerdonk FL, Stunnenberg HG, Netea MG, Dinarello CA, Joosten LAB (2017) Uric acid priming in human monocytes is driven by the AKT-PRAS40 autophagy pathway. Proc Natl Acad Sci 114:5485-5490
- 34. Bekkering S, Blok BA, Joosten LAB, Riksen NP, Van Crevel R, Netea MG (2016) In Vitro experimental model of trained innate immunity in human primary monocytes. Clin Vaccine Immunol 23:926–933
- 35. Netea MG, Nold-Petry CA, Nold MF, et al (2009) Differential requirement for the activation of the inflammasome for processing and release of IL-1β in monocytes and macrophages. Blood. https://doi.org/10.1182/blood-2008-03-146720
- 36. Dankers ACA, Mutsaers HAM, Dijkman HBPM, van den Heuvel LP, Hoenderop JG, Sweep FCGJ, Russel FGM, Masereeuw R (2013) Hyperuricemia influences tryptophan metabolism via inhibition of multidrug resistance protein 4 (MRP4) and breast cancer resistance protein (BCRP). Biochim Biophys Acta - Mol Basis Dis. https://doi.org/10.1016/j.bbadis.2013.05.002
- 37. Patschan D, Patschan S, Gobe GG, Chintala S, Goligorsky MS (2007) Uric acid heralds ischemic tissue injury to mobilize endothelial progenitor cells. J Am Soc Nephrol. https://doi.org/10.1681/ ASN.2006070759
- 38. Heintzman ND, Hon GC, Hawkins RD, et al (2009) Histone modifications at human enhancers reflect global cell-type-specific gene expression. Nature. https://doi.org/10.1038/nature07829
- 39. Cheng SC, Quintin J, Cramer RA, et al (2014) MTOR- and HIF-1α-mediated aerobic glycolysis as metabolic basis for trained immunity. Science (80-). https://doi.org/10.1126/science.1250684
- 40. Yates A, Akanni W, Amode MR, et al (2016) Ensembl 2016. Nucleic Acids Res. https://doi. org/10.1093/nar/gkv1157
- 41. Moriwaki Y, Yamamoto T, Takahashi S, Tsutsumi Z, Higashino K (1995) Apolipoprotein E phenotypes in patients with gout: Relation with hypertriglyceridaemia. Ann Rheum Dis. https:// doi.org/10.1136/ard.54.5.351
- 42. Terkeltaub RA, Dyer CA, Martin J, Curtiss LK (1991) Apolipoprotein (Apo) E inhibits the capacity of monosodium urate crystals to stimulate neutrophils. Characterization of intraarticular Apo E and demonstration of Apo E binding to urate crystals in vivo. J Clin Invest. https://doi.org/10.1172/ JCI114971
- 43. Ruppert J, Schtitt C, Ostermeier D, Peters JH CD14. 281–286
- 44. Kennedy MN, Mullen GED, Leifer CA, Lee CW, Mazzoni A, Dileepan KN, Segal DM (2004) A complex of soluble MD-2 and lipopolysaccharide serves as an activating ligand for toll-like receptor 4. J Biol Chem 279:34698-34704
- 45. Dalbeth N, Dowell T, Gerard C, Gow P, Jackson G, Shuker C, Te Karu L (2018) Gout in aotearoa New Zealand: The equity crisis continues in plain sight. N. Z. Med. J.
- 46. Gosling AL, Buckley HR, Matisoo-Smith E, Merriman TR (2015) Pacific Populations, Metabolic Disease and "Just-So Stories": A Critique of the "Thrifty Genotype" Hypothesis in Oceania. Ann Hum Genet. https://doi.org/10.1111/ahg.12132
- 47. Morandi F, Rizzo R, Fainardi E, Rouas-Freiss N, Pistoia V (2016) Recent advances in our understanding of HLA-G biology: Lessons from a wide spectrum of human diseases. J Immunol Res. https://doi.org/10.1155/2016/4326495

- 48. Tanaka T, Milaneschi Y, Zhang Y, Becker KG, Zukley L, Ferrucci L (2017) A double blind placebo controlled randomized trial of the effect of acute uric acid changes on inflammatory markers in humans: A pilot study. PLoS One. https://doi.org/10.1371/journal.pone.0181100
- 49. Dasgupta B, Ju JS, Sasaki Y, Liu X, Jung S-R, Higashida K, Lindguist D, Milbrandt J (2012) The AMPK 2 Subunit Is Required for Energy Homeostasis during Metabolic Stress. Mol Cell Biol. https://doi. org/10.1128/mcb.05853-11
- 50. Wang Y, Viollet B, Terkeltaub R, Liu-Bryan R (2016) AMP-activated protein kinase suppresses urate crystal-induced inflammation and transduces colchicine effects in macrophages. Ann Rheum Dis 75:286-294
- 51. Phipps-Green AJ, Merriman ME, Topless R, et al (2016) Twenty-eight loci that influence serum urate levels: Analysis of association with gout. Ann Rheum Dis. https://doi.org/10.1136/ annrheumdis-2014-205877

Supplementary Material

ADDITIONAL FILE 1

MATERIALS AND METHODS

Participants

Venous blood was drawn from the cubital vein of Dutch participants without gout into EDTA tubes. Urate priming experiments were performed in freshly isolated PBMCs of 85 healthy volunteers of Dutch nationality from the 200 Functional Genomics (200FG) cohort in the Human Functional Genomics Project (http://www. humanfunctionalgenomics.org)[1]. Experiments requiring large amounts of cells were performed using cells isolated from buffy coats after overnight storage at room temperature (Sanguin blood bank, Nijmegen, The Netherlands). Stimulation experiments were approved by the Ethical Committee of Radboud University Nijmegen (nr. 42561.091.12) and were conducted according to the principles of the Declaration of Helsinki. The DNA methylation study was approved by the New Zealand Lower South Health and Disability Ethics Committee (MEC/05/10/130). The study included 76 individuals of New Zealand Māori ancestry (Table S1), 38 men and 40 women, with a range of serum urate values (average 0.37 mmol/L, +/- standard deviation 0.12 mmol/L, range 0.6 mmol/L), who for further analysis were segregated into a hyperuricemia group (0.42 mmol/L or higher) (n=26) or a normouricemia (n=50) group. All participants provided written informed consent. Patients or the public were not involved in the design, or conduct, or reporting, or dissemination of our research.

Reagents

Urate, lipopolysaccharide (LPS, *E. coli* serotype 055:B5), and 5'-S-methyl-5'-thioadenosine (methylthioadenosine, MTA) were purchased from Sigma. LPS was subjected to ultra-purification before cell culture experiments. Monosodium urate (MSU) crystals were prepared inhouse as previously described[2]. Pharmacological epigenetic inhibitors were purchased from Tocris, Bio-techne (Table S1).

PBMC and monocyte isolation

Human PBMCs were separated using Ficoll-Paque (Pharmacia Biotech) and suspended in culture medium RPMI (Roswell Park Memorial Institute 1640). Monocytes were enriched using hyperosmotic Percol solution[3] and were subsequently purified by negative selection using the Pan Monocyte Isolation kit (Miltenyi Biotec) according to the manufacturer's instructions. This led to a cell suspension containing monocytes with 85-95% purity.

Stimulation experiments

Experiments were performed in culture medium containing RPMI 1640, supplemented with 50 µg/ml gentamicin, 2 mM L-glutamine, 1 mM pyruvate and 10% human pooled serum following an in vitro urate priming protocol described extensively elsewhere[4]. For ChIP-seq experiments, 5x10^6 human monocytes were seeded in Petri dishes (Corning) and were primed for 20 hours followed by addition of medium or LPS 10 ng/ml for another 4 h. Cells from all donors used for ChIP-seg were also used in a separate experiment conducted in parallel for RNAseg assessment and for control experiments to test if the expected urate priming phenotype was present. The experimental setup, purity of cells and cytokine control experiments were as previously described[4]. For the in vitro experiments, using polarized light microscopy, we were not able to observe urate crystals formed during the 24 hours of exposure time for the described experimental conditions.

Cytokine measurements

Cytokine concentrations were determined in supernatants of cell culture using specific sandwich ELISA kits for interleukin-1ß (IL-1ß), IL-1Ra (receptor antagonist) (R&D Systems), and IL-6 (Sanguin) according to the manufacturer's instructions.

Animal model

Male 10-12 week old C57Bl/6J mice were purchased from Jackson Laboratories (Bar Harbor, Maine, USA), a total of five males were selected per group. The experiments were approved by The Institutional Animal Care and Use Committees of the University of Colorado Denver, Aurora, CO (protocol #0035) and were conducted according to the principles of the Declaration of Helsinki. Uricase was inhibited using oxonic acid and urate was administered in order to increase serum urate levels according to a previously described protocol[4]. At Day 0, mice were given oxonic acid orally 140 mg/kg, 2 times/day (in the morning and in the evening). Each administration was followed after 2 hours by urate 4 mg/kg, intraperitoneally, in the presence of MTA 30 mg/kg or equivalent volumes of vehicle control. At Day 1, the same treatment as Day 0 was performed, together with induction of gouty arthritis at noon. Gouty arthritis was induced by intra-articular injection (i.a.) of 300 µg MSU crystals and 200 µM palmitic acid (C16) in a volume of 10 µl phosphate buffered saline (PBS) as previously described in both the right and left knee joints of each mouse [2-5]. 24h after injection, mice were sacrificed, knees were macroscopically scored for joint thickness after removal of skin resulting in 10 joints in total, 5 mice per group (scores ranging from 0 to 3), followed by harvesting of joints for histology (only the right knee joint of the mice). Histology was performed as previously described[2].

ChIP sequencing preparation and analysis

Immediately after cell isolation and after stimulation, samples were subjected to DNA-histone crosslinking by treatment with 1% formaldehyde for 10 minutes followed by treatment with 1.25 mol/L glycine for another 3 minutes. For cultured cells, floating medium and cells were removed followed by three cycles of scraping and recovering adherent fixated cells (2.4-4.8 x 10^6 cells could be recovered from 5x10^6 plated monocytes). Samples were stored at 4°C in PBS containing complete phosphate inhibitor cocktail until sonicated and subjected to chromatin immunoprecipitation as previously described[6]. Briefly, fixed cell preparations were sonicated using a Diagenode Bioruptor UCD-300 for 3x 10min (30s on; 30s off), 67µl of chromatin (1 million cells) was incubated with 229µl dilution buffer, 3µl protease inhibitor cocktail and 0.5-1ug of H3K27ac or H3K4me3 antibodies (Diagenode) and incubated overnight at 4°C with rotation. Protein A/G magnetic beads were washed in dilution buffer with 0.15% SDS and 0.1% BSA, added to the chromatin/antibody mix and rotated for 60 min at 4°C. Beads were washed with 400µl of buffer for 5min at 4°C with five rounds of washes. Chromatin was eluted using elution buffer for 20min. Supernatant was collected, 8µl 5M NaCl, 3µl proteinase K were added and samples were incubated for 4hr at 65°C. Finally, samples were purified using QIAGEN; Qiaquick MinElute PCR purification Kit and eluted in 20µl EB. Detailed protocols can be found on the Blueprint website (http://www.blueprint-epigenome.eu/ UserFiles/file/Protocols/Histone_ChIP_May2013.pdf).

Illumina library preparation was done as previously described[6], using the Kapa Hyper Prep Kit. Samples were purified using the QIAquick MinElute PCR purification kit and 300bp fragments selected using E-gel. Correct size selection was confirmed by BioAnalyzer analysis. Sequencing was performed using Illumina HiSeg 2000 machines and generated 43bp single end reads. Sequence reads were aligned to human genome assembly hg19 (NCBI version 37) using bwa. Duplicate reads were removed after alignment with Picard tools. For peak calling the BAM files were first filtered to remove the reads with mapping quality less than 15, followed by fragment size modeling (https://code.google.com/archive/p/phantompeakqualtools/) and MACS2 (https://github.com/taoliu/MACS/) was used to call the peaks. For each histone mark dataset, the data were normalized using the R package DESeq2 and then pair-wise comparisons were performed (fold change 3, adjusted p-value < 0.05 and reads per kilo base per million mapped read ≥ 2) to determine the differentially expressed genes per condition. The results from all possible pairwise comparisons (within each condition and similar time points across all conditions per mark) were pooled and merged to define the dynamic set of enriched regions.

DNA methylation analysis

Genomic DNA was isolated from peripheral blood of 76 individuals of New Zealand Māori ancestry with varying serum urate levels. Genome-wide methylation analysis was performed using Illumina InfiniumMethylationEPIC BeadChips (referred to from now as 'EPIC array')[7]. The EPIC array measures DNA methylation level at more than 850,000 CpG sites (referred to as 'EPIC probes'), and covers all gene promoters, gene bodies and ENCODE-assigned distal regulatory elements[8].

Raw IDAT files were processed and analysed using the MissMethyl and minfi packages for R[9, 10], both available from Bioconductor[11]. Samples were checked for quality, with all samples remaining for analysis (all with a mean detection p-value of <0.01). A total of 50 controls and 26 hyperuricemia samples were used for analysis.

Data were normalized for both within and between array technical variation using SWAN (Subset-quantile Within Array Normalization)[12]. A total of 798,740 probes were used for analysis after removal of poor probes, probes that overlap SNPs with MAF>0%, and cross hybridising probes. Cell composition was determined using the estimateCellCounts tool, with the 'Blood' reference data used for adult peripheral blood analysis[13]. Differential methylation analysis by linear regression modelling was performed using limma[14]. Differential methylation analysis with and without cell composition correction was performed.

Differentially methylated probes (DMPs) were identified as those having a p-value of <0.05 and a change in methylation (delta beta or $\Delta\beta$) of \geq 5%. Differentially methylated regions (DMRs) were identified using the DMRcate tool[15].

Statistical analysis

Cytokine data were analyzed using GraphPad Prism version 8. The differences were analysed using Friedmann or Wilcoxon signed rank test after testing for distribution normality. Data were considered statistically significant at a p-value < 0.05. Data is shown as individual or cumulative results of levels obtained in all volunteers (means +/- SEM). ChIP sequencing and DNA methylation data were analyzed using R.

RESULTS

ChIP-Seq analysis in freshly isolated monocytes at day 0 displays a marked clustering feature compared to all stimulated samples obtained at day 1

To assess whether the ChIP-seq data showed differences in freshly isolated monocytes compared to cultured monocytes, samples before and after culturing conditions were included in the analysis. The data was reanalyzed with an extra negative control sample for each of the four donors, which was prepared from freshly isolated monocytes, at day 0, before culture. The analyses performed using day 0 samples and day 1 samples (with the 4 conditions described – RPMI or urate primed cells stimulated with either control medium or LPS) revealed distinct features of the samples obtained at day 0 compared to all samples obtained at day 1.

DNA methylation profiling without cell composition correction reveals an expanded list of candidates for effects of urate in vivo in humans

To obtain additional information regarding the DNA methylation patterns associated to hyperuricemia, DNA methylation data were also analysed without correction for cell composition. This second analysis revealed 676 differentially methylated probes (which consisted of a difference in DNA methylation of at least 5%) and 55 differentially methylated regions (Tables S6 and S7, respectively). The HLA-G locus was consistently identified by both types of analyses. Regions that depicted significant differential methylation over the two groups of patients were found in intergenic or intragenic regions of certain genes, of which a list of candidate genes are shown in Figure 6A. One interesting example with possible roles for the modulation of the IL-1B/IL-1Ra pathway is SOCS3, which exhibited three significantly differentially methylated CpG probes that were found intragenically (FigureS2) and which showed higher methylation in hyperuricemic compared to normouricemic patients (FigureS2 D). Publicly-available data from the ENCODE database show that this region includes transcription factor binding sites that could be influenced by variable methylation and chromatin accessibility (Figure S2 E).

DISCUSSION

Recently, the use of the cell composition correction (Houseman correction,[16]) for whole blood DNA methylation data was challenged due to the possible violation of the no multicollinearity assumption in statistical regression models[17]. This possibility is of particular relevance for studies in which the assessed outcomes are represented by inflammatory phenotypes, because inflammation can be associated to cell-type composition variation[17]. For this reason, in this study, DNA methylation was determined and assessed between hyperuricemic and normouricemic volunteers by using both cell composition correction (as described in the main text of this manuscript) and no correction for cell composition. While this analysis identified 163 differentially methylated probes and 10 differentially methylated regions which were common for the targets identified by the two types of analyses (data not shown), new targets were also revealed. One example is SOCS3 (suppressor of cytokine signaling 3), a regulator of STAT3 signaling with broad roles

in cytokine signaling[18, 19], mostly associated with negative feedback inhibition of proinflammatory cytokines[20, 21]. Our data show higher DNA methylation in hyperuricemic individuals at 3 neighboring SOCS3 intragenic regions (FigureS2). Since the functionality of this higher methylation status is not known, future validation studies are necessary to show whether SOCS3 levels are indeed modified in the context of urate exposure in vitro or in vivo. If SOCS3 levels are diminished, this could typically coincide with less STAT3 inhibition and promotion of proinflammatory cytokines production[20, 21]. However, SOCS3 has been shown to have the dual role of upregulating TLR4 induced cytokines by TGF\$\beta\$ inhibition[22]. Therefore, the possible consequences of SOCS3 regulation in the context of urate priming are an interesting pathway to be tested and further validated in patients.

REFERENCES

- Li Y, Oosting M, Deelen P, et al (2016) Inter-individual variability and genetic influences on cytokine responses to bacteria and fungi. Nat Med. https://doi.org/10.1038/nm.4139
- Joosten LAB, Netea MG, Mylona E, et al (2010) Engagement of fatty acids with toll-like receptor 2. 2 drives interleukin-1ß production via the ASC/caspase 1 pathway in monosodium urate monohydrate crystal-induced gouty arthritis. Arthritis Rheum. https://doi.org/10.1002/art.27667
- Repnik U, Knezevic M, Jeras M (2003) Simple and cost-effective isolation of monocytes from buffy coats. J Immunol Methods. https://doi.org/10.1016/S0022-1759(03)00231-X
- Crisan TO, Cleophas MCP, Novakovic B, Erler K, Van De Veerdonk FL, Stunnenberg HG, Netea MG, Dinarello CA, Joosten LAB (2017) Uric acid priming in human monocytes is driven by the AKT-PRAS40 autophagy pathway. Proc Natl Acad Sci U S A. https://doi.org/10.1073/pnas.1620910114
- Joosten LAB, Crisan TO, Azam T, Cleophas MCP, Koenders MI, Van De Veerdonk FL, Netea MG, Kim S, Dinarello CA (2016) Alpha-1-anti-trypsin-Fc fusion protein ameliorates gouty arthritis by reducing release and extracellular processing of IL-1β and by the induction of endogenous IL-1Ra. Ann Rheum Dis. https://doi.org/10.1136/annrheumdis-2014-206966
- Novakovic B, Habibi E, Wang SY, et al (2016) β-Glucan Reverses the Epigenetic State of LPS-Induced Immunological Tolerance. Cell. https://doi.org/10.1016/j.cell.2016.09.034
- 7. Martino D, Neeland M, Dang T, Cobb J, Ellis J, Barnett A, Tang M, Vuillermin P, Allen K, Saffery R (2018) Epigenetic dysregulation of naive CD4+ T-cell activation genes in childhood food allergy. Nat Commun. https://doi.org/10.1038/s41467-018-05608-4
- Pidsley R, Zotenko E, Peters TJ, Lawrence MG, Risbridger GP, Molloy P, Van Djik S, Muhlhausler B, Stirzaker C, Clark SJ (2016) Critical evaluation of the Illumina MethylationEPIC BeadChip microarray for whole-genome DNA methylation profiling. Genome Biol. https://doi.org/10.1186/ s13059-016-1066-1
- Phipson B, Maksimovic J, Oshlack A (2016) MissMethyl: An R package for analyzing data from Illumina's HumanMethylation450 platform. Bioinformatics. https://doi.org/10.1093/ bioinformatics/btv560
- 10. Aryee MJ, Jaffe AE, Corrada-Bravo H, Ladd-Acosta C, Feinberg AP, Hansen KD, Irizarry RA (2014) Minfi: A flexible and comprehensive Bioconductor package for the analysis of Infinium DNA methylation microarrays. Bioinformatics. https://doi.org/10.1093/bioinformatics/btu049
- 11. Gentleman RC, Carey VJ, Bates DM, et al (2004) Bioconductor: open software development for computational biology and bioinformatics. Genome Biol. https://doi.org/10.1186/gb-2004-5-10-r80
- 12. Maksimovic J, Gordon L, Oshlack A (2012) SWAN: Subset-quantile within array normalization for illumina infinium HumanMethylation450 BeadChips. Genome Biol. https://doi.org/10.1186/gb-2012-13-6-r44
- 13. Houseman EA, Molitor J, Marsit CJ (2014) Reference-free cell mixture adjustments in analysis of DNA methylation data. Bioinformatics. https://doi.org/10.1093/bioinformatics/btu029
- 14. Ritchie ME, Phipson B, Wu D, Hu Y, Law CW, Shi W, Smyth GK (2015) Limma powers differential expression analyses for RNA-sequencing and microarray studies. Nucleic Acids Res. https://doi. org/10.1093/nar/gkv007
- 15. Peters TJ, Buckley MJ, Statham AL, Pidsley R, Samaras K, V Lord R, Clark SJ, Molloy PL (2015) De novo identification of differentially methylated regions in the human genome. Epigenetics and Chromatin. https://doi.org/10.1186/1756-8935-8-6

- 16. Houseman EA, Accomando WP, Koestler DC, Christensen BC, Marsit CJ, Nelson HH, Wiencke JK, Kelsey KT (2012) DNA methylation arrays as surrogate measures of cell mixture distribution. BMC Bioinformatics. https://doi.org/10.1186/1471-2105-13-86
- 17. Barton SJ, Melton PE, Titcombe P, Murray R, Rauschert S, Lillycrop KA, Huang RC, Holbrook JD, Godfrey KM (2019) In Epigenomic Studies, Including Cell-Type Adjustments in Regression Models Can Introduce Multicollinearity, Resulting in Apparent Reversal of Direction of Association. Front Genet. https://doi.org/10.3389/fgene.2019.00816
- 18. Mahony R, Ahmed S, Diskin C, Stevenson NJ (2016) SOCS3 revisited: a broad regulator of disease, now ready for therapeutic use? Cell Mol Life Sci. https://doi.org/10.1007/s00018-016-2234-x
- 19. Yoshimura A, Suzuki M, Sakaguchi R, Hanada T, Yasukawa H (2012) SOCS, inflammation, and autoimmunity. Front Immunol 3:1-9
- 20. Yan C, Ward PA, Wang X, Gao H (2013) Myeloid depletion of SOCS3 enhances LPS-induced acute lung injury through CCAAT/enhancer binding protein δ pathway. FASEB J. https://doi. org/10.1096/fj.12-225797
- 21. Yoshimura A, Yasukawa H (2012) JAK's SOCS: A Mechanism of Inhibition. Immunity. https://doi. org/10.1016/j.immuni.2012.01.010
- 22. Liu X, Zhang Y, Yu Y, Yang X, Cao X (2008) SOCS3 promotes TLR4 response in macrophages by feedback inhibiting TGF-β1/Smad3 signaling. Mol Immunol. https://doi.org/10.1016/j. molimm.2007.08.018
- 23. Ruppert J, Schtitt C, Ostermeier D, Peters JH CD14. 281–286
- 24. Kennedy MN, Mullen GED, Leifer CA, Lee CW, Mazzoni A, Dileepan KN, Segal DM (2004) A complex of soluble MD-2 and lipopolysaccharide serves as an activating ligand for toll-like receptor 4. J Biol Chem 279:34698-34704

Supplemental information

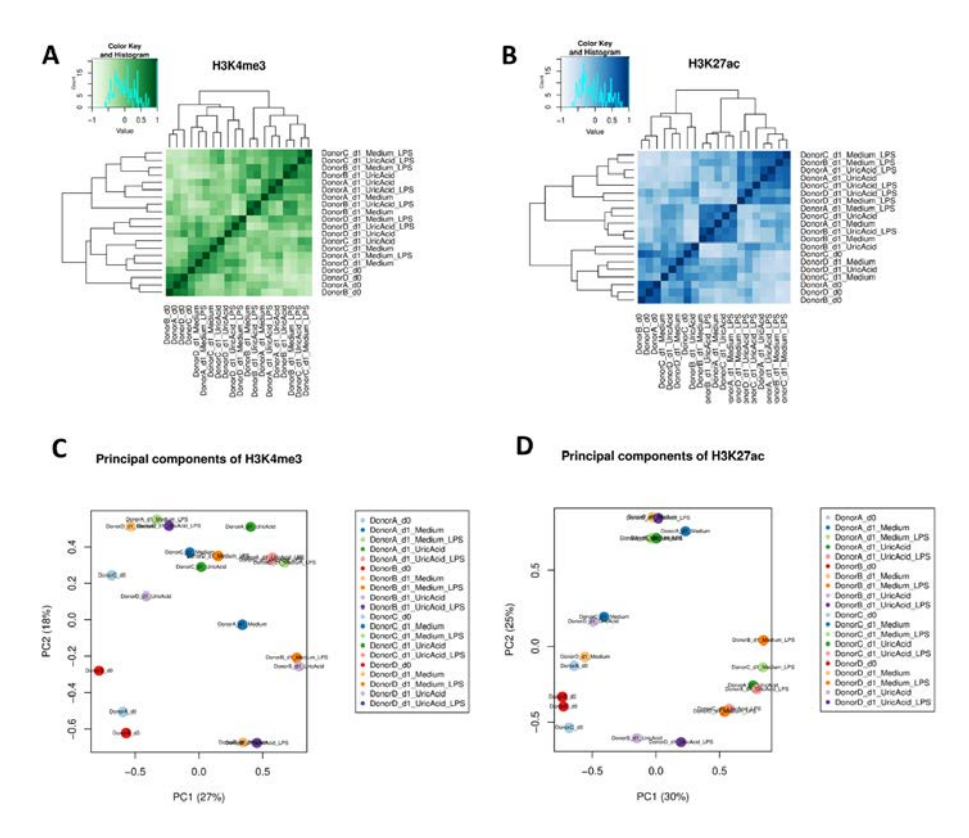


Figure S1 ChIP-Seq analysis in freshly isolated monocytes at day 0 (d0), without culturing, reveals distinct clustering features compared to all stimulated samples obtained at day 1 (d1). Cluster and principal component analysis of datasets obtained on ChIP sequencing for H3K4me3 (**A** and **C**) or H3K27ac (**B** and **D**) in 4 different donors (labeled D1-4) and 4 different conditions (Medium, Urate, Medium+LPS, Urate+LPS).

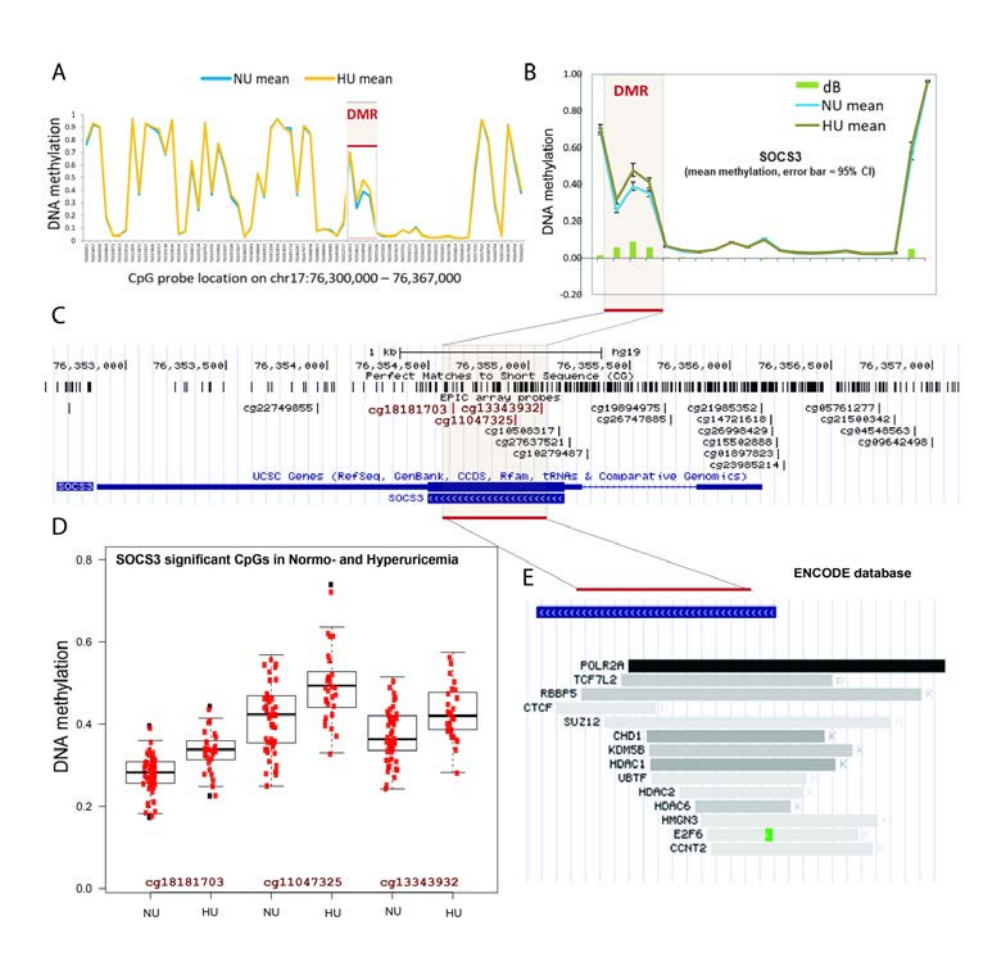


Figure S2 Differential DNA methylation analysis (without cell composition correction) in hyperuricemic versus normouricemic people. DNA methylation levels (A) and absolute change inmean methylation between hyperuricemic (HU) and normouricemic (NU) people (B). UCSC genome browser snapshot of 3 intragenic probes located at the SOCS3 locus (C). Individual methylation levels in NU compared o HU people for the 3 highlighted SOCS3 probes (D). Transcription factors known to bind at the highlighted DMR region according to the transcription factor ChIP-seq clusters from ENCODE with factorbook motifs (E).

Table S1. Patient characteristics for DNA methylation study.

Group	Subjects	Age	Sex	ВМІ	Serum urate	Gout
HU	n = 26	Min.:20.00	F = 7	Min.:30.40	Min.:0.4200	n = 15
		1st Qu.:41.00	M = 19	= 19 1st Qu.:33.92 1st Qu.:0.4425		
		Median :47.50	dian :47.50 Median:37.20 Media		Median :0.4800	
		Mean:47.88		Mean:39.74 Mean:0.4919		
		3rd Qu.:59.50		3rd Qu.:42.06	3rd Qu.:0.5200	
		Max.:70.00		Max.:66.90	Max.:0.6700	
NU	n = 50	Min.:25.00	F = 33	Min.:27.01	Min.:0.0700	n = 14
		1st Qu.:42.25	M = 17	1st Qu.:32.06	1st Qu.:0.2725	
		Median :52.00		Median :35.66	Median :0.3300	
		Mean:51.52		Mean:36.74	Mean:0.3104	
		3rd Qu.:62.00		3rd Qu.:39.66	3rd Qu.:0.3800	
		Max.:83.00		Max.:56.25	Max.:0.4100	

NU=Normouricaemia, HU=Hyperuricaemia; Serum urate levels = mmol/L; NU <0.42mmol/L, HU>0.42mmol/L.

Table S2. Genes showing enrichment of histone modification H3K4me3.

ENSEMBL gene ID	gene name	function	chr	Log 2 Fold change	p-val
ENSG00000008838	MED24	protein_coding	chr17	3,4531	0,0036
ENSG00000108342	CSF3	protein_coding	chr17	3,4531	0,0036
ENSG00000103168	TAF1C	protein_coding	chr16	3,2611	0,0016
ENSG00000154099	DNAAF1	protein_coding	chr16	3,2611	0,0016
ENSG00000182782	HCAR2	protein_coding	chr12	2,7893	0,0035
ENSG00000255398	HCAR3	protein_coding	chr12	2,4391	0,0051
ENSG00000256249	RP11-324E6.6	lincRNA	chr12	2,4391	0,0051
ENSG00000166278	C2	protein_coding	chr6	2,1957	0,0172
ENSG00000179428	AC073072.5	antisense	chr7	1,8949	0,0109
ENSG00000131203	IDO1	protein_coding	chr8	1,7988	0,0162
ENSG00000253838	RP11-44K6.2	sense_intronic	chr8	1,7988	0,0162
ENSG00000171855	IFNB1	protein_coding	chr9	1,7420	0,0444
ENSG00000203364	RP11-370F5.4	lincRNA	chr9	1,7082	0,0317
ENSG00000115009	CCL20	protein_coding	chr2	1,4683	0,0118
ENSG00000229172	AC073065.3	pseudogene	chr2	1,4683	0,0118
ENSG00000253320	KB-1507C5.2	protein_coding	chr8	1,4589	0,0305
ENSG00000237568	RP4-620F22.2	antisense	chr1	1,3998	0,0438
ENSG00000140379	BCL2A1	protein_coding	chr15	1,3622	0,0187
ENSG00000253790	RP11-44K6.5	pseudogene	chr8	1,3460	0,0384
ENSG00000095970	TREM2	protein_coding	chr6	-1,4660	0,0192
ENSG00000124562	SNRPC	protein_coding	chr6	-1,5600	0,0009
ENSG00000130203	APOE	protein_coding	chr19	-1,6253	0,0146

ENSEMBL gene ID	gene name	function	chr	Log 2 Fold change	p-val
ENSG00000240481	Metazoa_SRP	misc_RNA	chr9	2,6607	0,0494
ENSG00000169184	MN1	protein_coding	chr22	2,4834	0,0083
ENSG00000203364	RP11-370F5.4	lincRNA	chr9	2,3311	0,0298
ENSG00000231525	AC002486.2	processed_pseudogene	chr7	2,3170	0,0237
ENSG00000240624	RP11-45P15.2	processed_pseudogene	chr14	2,2890	0,0334
ENSG00000234496	MRPS21P1	processed_pseudogene	chr1	2,2565	0,0380
ENSG00000008838	MED24	protein_coding	chr17	2,2487	0,0314
ENSG00000108342	CSF3	protein_coding	chr17	2,2487	0,0314
ENSG00000238793	SNORD124	snoRNA	chr17	2,2487	0,0314
ENSG00000131203	IDO1	protein_coding	chr8	2,1271	0,0298
ENSG00000253838	RP11-44K6.2	sense_intronic	chr8	2,1271	0,0298
ENSG00000101460	MAP1LC3A	protein_coding	chr20	2,1127	0,0241
ENSG00000101464	PIGU	protein_coding	chr20	2,1127	0,0241
ENSG00000134460	IL2RA	protein_coding	chr10	2,0580	0,0362
ENSG00000251922	SNORA14	snoRNA	chr10	2,0580	0,0362
ENSG00000105855	ITGB8	retained_intron	chr7	2,0193	0,0351
ENSG00000248719	RP11-377G16.2	antisense	chr4	2,0036	0,0298
ENSG00000179428	AC073072.5	antisense	chr7	1,9881	0,0318
ENSG00000188676	IDO2	processed_transcript	chr8	1,9871	0,0482
ENSG00000253790	RP11-44K6.5	processed_pseudogene	chr8	1,9871	0,0482
ENSG00000103168	TAF1C	protein_coding	chr16	1,9753	0,0227
ENSG00000154099	DNAAF1	retained_intron	chr16	1,9753	0,0227
ENSG00000115008	IL1A	protein_coding	chr2	1,9373	0,0193
ENSG00000125538	IL1B	protein_coding	chr2	1,9373	0,0193
ENSG00000221541	AC079753.1	miRNA	chr2	1,9373	0,0193
ENSG00000244104	Metazoa_SRP	misc_RNA	chr12	1,8827	0,0098
ENSG00000234869	RP3-439F8.1	antisense	chr22	1,8560	0,0305
ENSG00000129277	CCL4	protein_coding	chr17	1,8478	0,0370
ENSG00000263488	Metazoa_SRP	misc_RNA	chr17	1,8478	0,0370
ENSG00000264684	MIR4773-2	miRNA	chr2	1,8258	0,0384
ENSG00000234956	RP11-356I2.1	lincRNA	chr6	1,8221	0,0219
ENSG00000232591	RP5-1031D4.2	lincRNA	chr10	1,7670	0,0050
ENSG00000250762	RP1-313L4.4	unprocessed_pseudogene	chr1	1,7670	0,0408
ENSG00000259090	RP11-173D9.5	processed_pseudogene	chr14	1,7077	0,0378
ENSG00000128271	ADORA2A	processed_transcript	chr22	1,6242	0,0166
ENSG00000178803	ADORA2A-AS1	protein_coding	chr22	1,6242	0,0166
ENSG00000258555	SPECC1L	nonsense_mediated_decay	chr22	1,6242	0,0166
ENSG00000168260	C14orf183	protein_coding	chr14	1,5943	0,0289
ENSG00000251792	Y_RNA	misc_RNA	chr14	1,5943	0,0289

Table S3. Continued

ENSEMBL gene ID	gene name	function	chr	Log 2 Fold change	p-val
ENSG00000110047	EHD1	protein_coding	chr11	1,5784	0,0121
ENSG00000226169	RP11-375H17.1	antisense	chr22	1,5761	0,0165
ENSG00000251230	RP11-701P16.5	processed_transcript	chr4	1,5183	0,0464
ENSG00000266698	MIR3945	miRNA	chr4	1,5183	0,0464
ENSG00000235842	RP11-356I2.2	processed_transcript	chr6	1,5052	0,0469
ENSG00000160325	CACFD1	protein_coding	chr9	1,5017	0,0153
ENSG00000160326	SLC2A6	protein_coding	chr9	1,5017	0,0153
ENSG00000227898	RP13-100B2.4	antisense	chr9	1,5017	0,0153
ENSG00000228923	AP000355.2	antisense	chr22	1,4950	0,0496
ENSG00000254693	RP11-58K22.5	antisense	chr11	1,4674	0,0285
ENSG00000227269	RP11-96L7.2	lincRNA	chr9	1,4561	0,0494
ENSG00000240235	Metazoa_SRP	misc_RNA	chr9	1,4561	0,0165
ENSG00000268621	AC006262.5	lincRNA	chr19	1,4445	0,0308
ENSG00000181577	C6orf223	retained_intron	chr6	1,4410	0,0011
ENSG00000238486	snoU13	snoRNA	chr19	1,4326	0,0351
ENSG00000173578	XCR1	protein_coding	chr3	1,4309	0,0429
ENSG00000182782	HCAR2	protein_coding	chr12	1,4093	0,0343
ENSG00000184588	PDE4B	protein_coding	chr1	1,3800	0,0432
ENSG00000169429	IL8	protein_coding	chr4	1,3583	0,0207
ENSG00000228277	AC112518.3	lincRNA	chr4	1,3583	0,0207
ENSG00000101337	TM9SF4	protein_coding	chr20	1,3472	0,0054
ENSG00000232759	AC002480.3	processed_transcript	chr7	-1,3221	0,0487
ENSG00000223009	AL138930.1	miRNA	chr1	-1,3501	0,0027
ENSG00000235007	RP11-344B5.4	lincRNA	chr9	-1,3508	0,0467
ENSG00000124562	SNRPC	protein_coding	chr6	-1,3638	0,0133
ENSG00000232131	RP1-293L8.5	antisense	chr6	-1,4102	0,0082
ENSG00000130203	APOE	protein_coding	chr19	-1,4381	0,0177
ENSG00000267009	RP11-120M18.2	processed_transcript	chr17	-1,4398	0,0217
ENSG00000110079	MS4A4A	protein_coding	chr11	-1,4508	0,0047
ENSG00000260872	RP11-680G24.5	antisense	chr16	-1,4750	0,0065
ENSG00000170323	FABP4	protein_coding	chr8	-1,4973	0,0092
ENSG00000141293	SKAP1	protein_coding	chr17	-1,5263	0,0231
ENSG00000269843	CTC-490E21.10	lincRNA	chr19	-1,5742	0,0419
ENSG00000197849	OR8G7P	unprocessed_pseudogene	chr11	-1,6011	0,0004
ENSG00000255298	OR8G1	unprocessed_pseudogene	chr11	-1,6011	0,0004
ENSG00000204872	AC092653.5	unprocessed_pseudogene	chr2	-1,6486	0,0430
ENSG00000230490	RP11-141M1.3	lincRNA	chr13	-1,6965	0,0169
ENSG00000217746	RP1-303A1.1	processed_pseudogene	chr6	-1,6984	0,0112
ENSG00000235899	RP11-345L23.1	antisense	chr6	-1,9337	0,0001

Table S4. Differentially methylated probes in whole blood of people with hyperuricemia compared to normouricemic people with cell composition correction

Nr.	probe ID	nearest gene (distance in bp)	chr	NU_mean	HU_mean	dB	P.Value
1	cg20482334	FASN (+7677)	chr17	0.715	0.858	0.143	0.0098
2	cg21224286	LRTM2 (-19517)	chr12	0.474	0.611	0.137	0.0016
3	cg12859507	LRTM2 (-19470)	chr12	0.289	0.415	0.126	0.0022
4	cg21022775	AREG (+28658)	chr4	0.685	0.810	0.126	0.0408
5	cg20347269	P2RX1 (+11637)	chr17	0.498	0.623	0.124	0.0003
6	cg18850127	POU6F2 (+152900)	chr7	0.484	0.608	0.124	0.0231
7	cg24751894	HLA-G (+99386)	chr6	0.144	0.266	0.123	0.0071
8	cg18786623	HLA-G (+99295)	chr6	0.239	0.361	0.121	0.0066
9	cg15212455	POU6F2 (+152942)	chr7	0.545	0.662	0.117	0.0153
10	cg15070894	HLA-G (+99407)	chr6	0.180	0.291	0.111	0.0072
11	cg04520169	HLA-G (+99440)	chr6	0.138	0.240	0.103	0.0300
12	cg08951186	ZNF469 (-203509)	chr16	0.531	0.631	0.101	0.0295
13	cg26175789	EVA1A (-25045)	chr2	0.385	0.485	0.100	0.0173
14	cg07973162	UGT2B17 (-1006)	chr4	0.409	0.504	0.095	0.0179
15	cg08231349	HLA-G (+99889)	chr6	0.051	0.146	0.095	0.0043
16	cg03806328	ARHGAP32 (-67539)	chr11	0.588	0.683	0.095	0.0226
17	cg13365324	UGT2B17 (-1229)	chr4	0.427	0.521	0.094	0.0163
18	cg07952421	UGT2B17 (-1357)	chr4	0.525	0.618	0.092	0.0152
19	cg10388667	MRPL53 (+2528)	chr2	0.687	0.779	0.092	0.0049
20	cg24239165	C17orf82 (+7542)	chr17	0.580	0.672	0.091	0.0001
21	cg20302533	POU6F2 (+153166)	chr7	0.266	0.355	0.089	0.0375
22	cg22772380	ZNF12 (-484)	chr7	0.445	0.533	0.088	0.0321
23	cg14381313	ZNF469 (-225540)	chr16	0.493	0.579	0.085	0.0364
24	cg26353469	HLA-G (+61215)	chr6	0.085	0.170	0.085	0.0404
25	cg14904295	PEG3 (+3535)	chr19	0.291	0.375	0.084	0.0262
26	cg03660162	MAF (+721526)	chr16	0.710	0.793	0.083	0.0229
27	cg21332948	AGPAT3 (-21173)	chr21	0.674	0.758	0.083	0.0428
28	cg07346359	OPTC (+26398)	chr1	0.422	0.505	0.083	0.0122
29	cg03995122	HLA-G (+99887)	chr6	0.030	0.113	0.083	0.0183
30	cg21549632	HLA-G (+61532)	chr6	0.066	0.148	0.082	0.0128
31	cg15671450	HLA-G (+100361)	chr6	0.089	0.168	0.079	0.0497
32	cg16302021	HLA-G (+99189)	chr6	0.404	0.481	0.078	0.0230
33	cg00409917	HLA-G (+99924)	chr6	0.074	0.152	0.077	0.0068
34	cg00901687	MYCBPAP (-475)	chr17	0.453	0.529	0.076	0.0250
35	cg23237314	HLA-G (+99442)	chr6	0.130	0.206	0.076	0.0401
36	cg19823512	OPTC (+26455)	chr1	0.305	0.380	0.075	0.0388
37	cg09597767	IFITM3 (-4866)	chr11	0.700	0.772	0.072	0.0036

Table \$4. Continued

Table	Table S4. Continued									
Nr.	probe ID	nearest gene	chr	NU_mean	HU_mean	dB	P.Value			
		(distance in bp)								
38	cg21323039	MATN1 (+3484)	chr1	0.792	0.863	0.072	0.0063			
39	cg01336390	HLA-G (+100304)	chr6	0.087	0.159	0.072	0.0118			
40	cg26028489	LMO3 (+85999)	chr12	0.478	0.550	0.072	0.0297			
41	cg17341345	CCNH (-574)	chr5	0.505	0.575	0.071	0.0151			
42	cg26054541	GSDMC (+815502)	chr8	0.691	0.761	0.070	0.0034			
43	cg22968327	NUP93 (+59405)	chr16	0.258	0.327	0.069	0.0406			
44	cg14449180	HLA-G (+99864)	chr6	0.040	0.109	0.069	0.0293			
45	cg10632656	UGT2B17 (-1349)	chr4	0.274	0.343	0.069	0.0171			
46	cg06223984	UGT2B17 (-7507)	chr4	0.561	0.629	0.068	0.0230			
47	cg13597893	UBE2E3 (-272789)	chr2	0.493	0.561	0.068	0.0121			
48	cg03071500	IFITM3 (-4915)	chr11	0.562	0.629	0.067	0.0012			
49	cg10193107	HSPB1 (-7591)	chr7	0.481	0.547	0.067	0.0378			
50	cg00738934	PKIA (-432095)	chr8	0.487	0.554	0.067	0.0010			
51	cg21665744	POU6F2 (+153516)	chr7	0.631	0.697	0.066	0.0211			
52	cg15931205	HLA-G (+100065)	chr6	0.060	0.126	0.066	0.0121			
53	cg18191116	STON2 (+241)	chr14	0.502	0.568	0.065	0.0475			
54	cg09549987	SPAG11B (+644)	chr8	0.310	0.374	0.064	0.0091			
55	cg22253032	PRSS1 (-37378)	chr7	0.431	0.495	0.063	0.0012			
56	cg21862992	MRPL21 (+12905)	chr11	0.404	0.467	0.063	0.0418			
57	cg15598217	ZZEF1 (+44435)	chr17	0.524	0.587	0.063	0.0237			
58	cg00135841	USP18 (+104683)	chr22	0.762	0.825	0.063	0.0423			
59	cg11440486	MYCBPAP (-529)	chr17	0.462	0.524	0.062	0.0347			
60	cg00186468	CCNH (-393)	chr5	0.248	0.310	0.062	0.0095			
61	cg11449146	GAS2 (+62304)	chr11	0.555	0.617	0.062	0.0034			
62	cg20111217	MYCBPAP (-481)	chr17	0.542	0.604	0.062	0.0171			
63	cg27584762	CCNH (-291)	chr5	0.207	0.269	0.062	0.0202			
64	cg19748509	HLA-G (+116023)	chr6	0.070	0.131	0.061	0.0152			
65	cg01617603	UGT2B17 (+15538)	chr4	0.243	0.304	0.061	0.0116			
66	cg03249561	FCAR (+14427)	chr19	0.674	0.734	0.060	0.0275			
67	cg04815973	STOML1 (+17521)	chr15	0.251	0.311	0.060	0.0453			
68	cg06112835	MRPL21 (+12495)	chr11	0.293	0.352	0.059	0.0399			
69	cg19481811	UGT2B17 (+563)	chr4	0.587	0.646	0.059	0.0314			
70	cg15218522	SBSPON (-75679)	chr8	0.333	0.392	0.059	0.0225			
71	cg21894124	FBRSL1 (-161448)	chr12	0.146	0.205	0.059	0.0018			
72	cg11994053	VEZT (+100370)	chr12	0.740	0.799	0.059	0.0034			
73	cg04184807	GAPVD1 (+207038)	chr9	0.672	0.731	0.059	0.0386			
74	cg17453273	ITSN2 (-61147)	chr2	0.116	0.174	0.059	0.0135			

Table S4. Continued

Nr.	probe ID	nearest gene (distance in bp)	chr	NU_mean	HU_mean	dB	P.Value
75	cg09274344	SOX8 (+46882)	chr16	0.313	0.372	0.059	0.0211
76	cg01062395	HLA-G (+60881)	chr6	0.110	0.169	0.058	0.0212
77	cg09874992	SDC3 (+67000)	chr1	0.372	0.430	0.057	0.0026
78	cg08743428	ROBO2 (+678273)	chr3	0.456	0.513	0.057	0.0070
79	cg18976649	LMX1A (+213468)	chr1	0.718	0.774	0.056	0.0011
80	cg14453346	TSPAN33 (+19652)	chr7	0.807	0.862	0.056	0.0389
81	cg21733854	ZSCAN22 (-615)	chr19	0.517	0.571	0.055	0.0387
82	cg19727165	DHFRL1 (-114061)	chr3	0.608	0.663	0.055	0.0077
83	cg07398106	LDHC (+318)	chr11	0.450	0.505	0.054	0.0182
84	cg20476087	CGREF1 (-126)	chr2	0.117	0.171	0.054	0.0018
85	cg21705926	DNAJB6 (+276978)	chr7	0.483	0.537	0.054	0.0385
86	cg14080482	NONE	chr6	0.383	0.438	0.054	0.0182
87	cg10773881	GGA1 (+15331)	chr22	0.115	0.170	0.054	0.0314
88	cg26942295	PDZD2 (+49191)	chr5	0.494	0.548	0.054	0.0249
89	cg13719529	C11orf44 (+4653)	chr11	0.513	0.567	0.054	0.0379
90	cg19445457	OR52N5 (+451)	chr11	0.531	0.584	0.054	0.0197
91	cg09142843	ARHGAP18 (+389699)	chr6	0.737	0.790	0.053	0.0264
92	cg13910785	HLA-DRB1 (+7776)	chr6	0.283	0.336	0.053	0.0040
93	cg23917496	UACA (+300798)	chr15	0.379	0.432	0.053	0.0416
94	cg15853715	C14orf39 (-2535)	chr14	0.447	0.500	0.053	0.0059
95	cg12884719	SIPA1L2 (+451040)	chr1	0.420	0.473	0.053	0.0053
96	cg22083892	KCNJ8 (-907)	chr12	0.341	0.394	0.053	0.0215
97	cg26637898	PAPD7 (+44310)	chr5	0.804	0.857	0.053	0.0396
98	cg14332815	LDHC (-290)	chr11	0.403	0.456	0.053	0.0267
99	cg13056653	UCP1 (-49011)	chr4	0.519	0.572	0.053	0.0220
100	cg13048967	CXCR1 (+1595)	chr2	0.624	0.676	0.052	0.0150
101	cg03278639	DNAJB8 (+50966)	chr3	0.672	0.724	0.052	0.0003
102	cg23999422	SIRT6 (+9135)	chr19	0.228	0.280	0.052	0.0024
103	cg03518414	TOPAZ1 (-104724)	chr3	0.424	0.476	0.052	0.0270
104	cg07040013	GLRX3 (+164891)	chr10	0.351	0.402	0.052	0.0056
105	cg06012695	TRIM27 (+121173)	chr6	0.296	0.347	0.051	0.0015
106	cg15236555	HS1BP3 (+7072)	chr2	0.319	0.370	0.051	0.0178
107	cg23155965	TTC40 (-22088)	chr10	0.788	0.839	0.051	0.0060
108	cg01521378	ZNRD1 (-40965)	chr6	0.713	0.764	0.051	0.0288
109	cg06902219	HLA-G (+61539)	chr6	0.102	0.152	0.051	0.0144
110	cg15279541	PDCD2 (-142631)	chr6	0.426	0.477	0.051	0.0297
111	cg24931191	STAC (-172977)	chr3	0.264	0.315	0.051	0.0063
112	cq03742947	HLA-G (+61520)	chr6	0.067	0.118	0.051	0.0407

Table S4. Continued

Nr.	probe ID	nearest gene (distance in bp)	chr	NU_mean	HU_mean	dB	P.Value
113	cg21234506	BCL2A1 (+656)	chr15	0.388	0.438	0.051	0.0477
114	cg19107429	FAM86B2 (+21475)	chr8	0.646	0.696	0.050	0.0196
115	cg05707985	PRSS1 (-26980)	chr7	0.294	0.344	0.050	0.0093
116	cg11395062	HS3ST3B1 (-64543)	chr17	0.710	0.760	0.050	0.0388
117	cg13503915	SIGLEC5 (-640)	chr19	0.638	0.588	-0.050	0.0199
118	cg21158434	CLSTN3 (+8365)	chr12	0.700	0.650	-0.050	0.0359
119	cg12709009	DLL1 (+41979)	chr6	0.622	0.571	-0.050	0.0028
120	cg18838701	TNNI3 (+488)	chr19	0.309	0.259	-0.050	0.0094
121	cg17707095	MPC1 (-197056)	chr6	0.653	0.602	-0.051	0.0494
122	cg14222229	HIST2H3PS2 (+262795)	chr1	0.326	0.275	-0.051	0.0111
123	cg15797131	IRS2 (+54603)	chr13	0.547	0.496	-0.051	0.0403
124	cg11524065	ZCCHC8 (+21993)	chr12	0.832	0.781	-0.051	0.0084
125	cg10218876	TNNT1 (+97)	chr19	0.245	0.193	-0.051	0.0007
126	cg04737881	TENM3 (-103639)	chr4	0.326	0.275	-0.051	0.0295
127	cg00143193	SMYD3 (+519171)	chr1	0.753	0.702	-0.051	0.0490
128	cg04161902	BAI2 (+1728)	chr1	0.732	0.681	-0.051	0.0004
129	cg12463722	OR4D1 (+6)	chr17	0.730	0.678	-0.052	0.0225
130	cg24045276	NCF2 (+7621)	chr1	0.654	0.603	-0.052	0.0133
131	cg20212775	SPON2 (+1980)	chr4	0.639	0.587	-0.052	0.0057
132	cg26965779	HLA-G (+59334)	chr6	0.507	0.455	-0.052	0.0088
133	cg12847536	ARHGEF10 (+50045)	chr8	0.636	0.584	-0.052	0.0441
134	cg22027267	COBL (-160023)	chr7	0.751	0.699	-0.052	0.0094
135	cg22898160	NDRG4 (-1339)	chr16	0.662	0.609	-0.053	0.0207
136	cg08121925	FXR1 (-42049)	chr3	0.324	0.271	-0.053	0.0020
137	cg03321588	FAM208A (-70669)	chr3	0.462	0.409	-0.053	0.0398
138	cg20660297	KRR1 (-903)	chr12	0.532	0.479	-0.053	0.0054
139	cg07510085	IL15RA (+18184)	chr10	0.721	0.667	-0.054	0.0079
140	cg05010260	NAT16 (+3266)	chr7	0.610	0.556	-0.054	0.0070
141	cg15324331	SVIL (-60404)	chr10	0.652	0.598	-0.054	0.0054
142	cg20304530	NTRK3 (+297163)	chr15	0.798	0.744	-0.054	0.0158
143	cg01540595	LHX8 (-3159)	chr1	0.468	0.413	-0.054	0.0113
144	cg01799458	HOXB13 (+1736)	chr17	0.569	0.514	-0.055	0.0353
145	cg00590063	B3GNT3 (+12877)	chr19	0.336	0.281	-0.055	0.0457
146	cg11016221	PTGES (+9679)	chr9	0.411	0.356	-0.055	0.0416
147	cg08071329	DLL1 (+43704)	chr6	0.739	0.683	-0.056	0.0096
148	cg19504245	TNNT1 (+102)	chr19	0.294	0.238	-0.056	0.0031
149	cg09810149	NFU1 (-27150)	chr2	0.655	0.599	-0.056	0.0295
150	cg20336352	HERC4 (-13229)	chr10	0.757	0.701	-0.056	0.0032

Table S4. Continued

Nr.	probe ID	nearest gene (distance in bp)	chr	NU_mean	HU_mean	dB	P.Value
151	cg16603012	APRT (-1242)	chr16	0.660	0.604	-0.057	0.0037
152	cg19902553	JPH3 (+49910)	chr16	0.241	0.184	-0.057	0.0394
153	cg08124399	DDX43 (+398)	chr6	0.730	0.672	-0.057	0.0469
154	cg27516945	ZNF528 (-603)	chr19	0.669	0.611	-0.057	0.0010
155	cg08122831	ERBB4 (-294015)	chr2	0.767	0.710	-0.057	0.0356
156	cg06968712	MS4A15 (+10431)	chr11	0.553	0.495	-0.058	0.0024
157	cg18423549	MTRNR2L1 (-278559)	chr17	0.394	0.336	-0.058	0.0050
158	cg09602542	GGT6 (-36137)	chr17	0.840	0.782	-0.058	0.0176
159	cg15199034	ADAMTS1 (-42681)	chr21	0.701	0.642	-0.058	0.0003
160	cg17240725	ABHD11 (+3841)	chr7	0.393	0.335	-0.058	0.0207
161	cg25122629	EML6 (-14857)	chr2	0.360	0.301	-0.059	0.0009
162	cg05176970	GLOD4 (-38693)	chr17	0.654	0.593	-0.060	0.0009
163	cg24441899	FOXK1 (-477568)	chr7	0.561	0.501	-0.060	0.0112
164	cg18503693	FAM155A (+595468)	chr13	0.618	0.557	-0.061	0.0356
165	cg15925527	WRAP73 (+6530)	chr1	0.733	0.672	-0.062	0.0462
166	cg10491108	TST (+6245)	chr22	0.640	0.578	-0.062	0.0352
167	cg22647161	TMPO (-223043)	chr12	0.591	0.529	-0.062	0.0407
168	cg10432947	NAT8L (+1203)	chr4	0.578	0.516	-0.062	0.0000
169	cg09430341	CCDC17 (-481)	chr1	0.762	0.700	-0.062	0.0129
170	cg22871949	NOM1 (-6814)	chr7	0.639	0.577	-0.062	0.0119
171	cg08617160	MIER2 (-520)	chr19	0.542	0.479	-0.062	0.0042
172	cg07442889	SIGLEC5 (-914)	chr19	0.694	0.631	-0.063	0.0029
173	cg21158163	CDH4 (-284904)	chr20	0.809	0.746	-0.063	0.0057
174	cg17014757	CHI3L1 (-221)	chr1	0.393	0.330	-0.064	0.0183
175	cg22526555	KCNJ15 (-49635)	chr21	0.771	0.706	-0.065	0.0002
176	cg19708055	C6orf123 (+151983)	chr6	0.647	0.581	-0.065	0.0174
177	cg16814483	PRKAB2 (+94049)	chr1	0.500	0.435	-0.066	0.0400
178	cg10852875	IRX2 (+214079)	chr5	0.589	0.523	-0.066	0.0000
179	cg10292709	MCPH1 (-435562)	chr8	0.715	0.649	-0.066	0.0065
180	cg14248883	SERP2 (+30700)	chr13	0.736	0.670	-0.066	0.0095
181	cg12159505	DDX56 (+8747)	chr7	0.770	0.704	-0.066	0.0021
182	cg17959580	ELFN2 (-1113)	chr22	0.648	0.581	-0.067	0.0419
183	cg23441030	CACYBP (-59405)	chr1	0.712	0.645	-0.067	0.0089
184	cg15634083	HLA-B (+86056)	chr6	0.204	0.137	-0.067	0.0107
185	cg09189601	UGT2B15 (+22315)	chr4	0.480	0.410	-0.070	0.0264
186	cg20478239	COBL (-159980)	chr7	0.691	0.620	-0.071	0.0010
187	cg16754099	THEM6 (+1615)	chr8	0.560	0.488	-0.072	0.0005
188	cg05056638	NEFM (+30300)	chr8	0.598	0.525	-0.073	0.0411

Table S4. Continued

Nr.	probe ID	nearest gene (distance in bp)	chr	NU_mean	HU_mean	dB	P.Value
189	cg07569483	NLRP9 (-8089)	chr19	0.634	0.558	-0.076	0.0014
190	cg01880147	FCGR3B (-8389)	chr1	0.702	0.625	-0.077	0.0010
191	cg00256329	GLOD4 (-38794)	chr17	0.692	0.614	-0.078	0.0014
192	cg24480926	SFSWAP (-276103)	chr12	0.629	0.550	-0.079	0.0430
193	cg18220841	BANP (+156623)	chr16	0.551	0.472	-0.080	0.0446
194	cg05758861	BAI1 (+50033)	chr8	0.756	0.675	-0.081	0.0117
195	cg22445217	QKI (+585402)	chr6	0.690	0.609	-0.081	0.0020
196	cg18325044	HLA-G (+74145)	chr6	0.812	0.730	-0.081	0.0086
197	cg09105440	THEM6 (+1617)	chr8	0.549	0.468	-0.082	0.0015
198	cg13784004	MYO5B (+24730)	chr18	0.564	0.482	-0.082	0.0069
199	cg03526459	PRKAB2 (+94183)	chr1	0.630	0.546	-0.084	0.0482
200	cg06451157	HLA-G (+73540)	chr6	0.792	0.706	-0.085	0.0169
201	cg10805896	PLXNA4 (-88990)	chr7	0.439	0.350	-0.089	0.0411
202	cg19729930	BOLA3 (+17249)	chr2	0.596	0.506	-0.090	0.0119
203	cg00639946	NONE	chr19	0.499	0.408	-0.091	0.0215
204	cg10804687	HLA-G (+64765)	chr6	0.858	0.765	-0.093	0.0458
205	cg09163930	PDGFRB (+1459)	chr5	0.505	0.409	-0.096	0.0166
206	cg10474018	HLA-G (+65261)	chr6	0.871	0.774	-0.097	0.0043
207	cg01017244	BOLA3 (+17594)	chr2	0.717	0.620	-0.097	0.0097
208	cg26127187	HLA-G (+62040)	chr6	0.807	0.708	-0.099	0.0158
209	cg20891558	BOLA3 (+17270)	chr2	0.565	0.466	-0.099	0.0048
210	cg15514307	PPP2CA (-20989)	chr5	0.743	0.644	-0.099	0.0120
211	cg14018363	HLA-G (+116510)	chr6	0.504	0.404	-0.100	0.0137
212	cg06454464	TSNARE1 (+56622)	chr8	0.833	0.732	-0.101	0.0139
213	cg19077165	TCEB3CL2 (-2555)	chr18	0.744	0.637	-0.106	0.0054
214	cg26649688	HLA-G (+63605)	chr6	0.882	0.774	-0.108	0.0088
215	cg18423635	HLA-G (+75181)	chr6	0.853	0.744	-0.109	0.0345
216	cg24179288	HLA-G (+72530)	chr6	0.860	0.745	-0.115	0.0140
217	cg03395495	GOLGA6L4 (-83129)	chr15	0.706	0.582	-0.124	0.0495
218	cg15825968	SFSWAP (-276155)	chr12	0.614	0.489	-0.125	0.0011
219	cg20381372	ZFP14 (+68693)	chr19	0.571	0.445	-0.126	0.0116
220	cg12046183	HLA-G (+65074)	chr6	0.723	0.594	-0.129	0.0033
221	cg25817503	AFAP1 (+153311)	chr4	0.596	0.463	-0.133	0.0030
222	cg05890377	BOLA3 (+17408)	chr2	0.604	0.465	-0.139	0.0167
223	cg13393919	GPBAR1 (-10899)	chr2	0.788	0.602	-0.187	0.0009

Nr.	nearest gene	DMR chr	DMR start	DMR end	length	probes in dmr
1	HLA-G	chr6	29893273	29895204	1932	33
2	HLA-G	chr6	29855890	29856564	675	19
3	LDHC	chr11	18433500	18434354	855	10
4	DOC2A	chr16	30023028	30024074	1047	10
5	TNNT1	chr19	55660514	55661528	1015	10
6	DLL1	chr6	170553133	170555857	2725	10
7	IRX2	chr5	2537210	2537834	625	8
8	TNNI3	chr19	55667533	55669059	1527	6
9	FXR1	chr3	180587900	180588228	329	6
10	NAT8L	chr4	2061923	2063566	1644	6
11	C6orf123	chr6	168045268	168046457	1190	6
12	MYCBPAP	chr17	48585216	48585470	255	5
13	BOLA3	chr2	74357527	74358223	697	5
14	DLL1	chr6	170557102	170558102	1001	5
15	NOM1	chr7	156735260	156735656	397	5
16	BAI1	chr8	143580770	143581481	712	5
17	UGT2B17	chr4	69435250	69435601	352	4
18	THEM6	chr8	143809371	143810237	867	4
19	FBRSL1	chr12	132904540	132904796	257	3
20	ERBB4	chr2	213697579	213698158	580	3
21	KCNJ15	chr21	39578742	39579277	536	3
22	HLA-G	chr6	29859520	29860016	497	3
23	POU6F2	chr7	39170497	39170763	267	3

Table S6. Differentially methylated probes in whole blood of people with hyperuricemia compared to normouricemic people without cell composition correction

Nr.	probe ID	nearest gene	chr	NU_mean	HU_mean	dB	P.Value
		(distance in bp)					
1	cg07334023	IL2RB (-9994)	chr22	0.487	0.668	0.182	0.0090
2	cg02821156	ANKH (+54827)	chr5	0.566	0.738	0.173	0.0045
3	cg20482334	FASN (+7677)	chr17	0.713	0.857	0.144	0.0011
4	cg21224286	LRTM2 (-19517)	chr12	0.476	0.613	0.137	0.0003
5	cg13632935	RPL12 (+6177)	chr9	0.495	0.624	0.129	0.0413
6	cg07412545	GPR88 (+232)	chr1	0.472	0.599	0.127	0.0256
7	cg12859507	LRTM2 (-19470)	chr12	0.293	0.420	0.127	0.0000
8	cg18850127	POU6F2 (+152900)	chr7	0.479	0.604	0.125	0.0003
9	cg21022775	AREG (+28658)	chr4	0.688	0.813	0.124	0.0035
10	cg20347269	P2RX1 (+11637)	chr17	0.501	0.625	0.124	0.0127
11	cg24751894	HLA-G (+99386)	chr6	0.146	0.269	0.123	0.0037
12	cg26294610	MUT (+158454)	chr6	0.525	0.647	0.122	0.0287
13	cg18786623	HLA-G (+99295)	chr6	0.243	0.363	0.121	0.0025
14	cg16515087	EFCAB6 (-22809)	chr22	0.315	0.435	0.119	0.0000
15	cg12432526	TMEM105 (-50229)	chr17	0.316	0.432	0.117	0.0149
16	cg15212455	POU6F2 (+152942)	chr7	0.551	0.666	0.116	0.0010
17	cg06405219	MTURN (+44710)	chr7	0.267	0.381	0.114	0.0446
18	cg15070894	HLA-G (+99407)	chr6	0.183	0.294	0.111	0.0084
19	cg06223162	GPR88 (-5)	chr1	0.350	0.459	0.109	0.0261
20	cg07297153	REPIN1 (-2012)	chr7	0.655	0.763	0.108	0.0085
21	cg00956193	ZNF770 (-95077)	chr15	0.450	0.557	0.107	0.0054
22	cg13093842	NLRP7 (-23)	chr19	0.600	0.706	0.106	0.0068
23	cg04520169	HLA-G (+99440)	chr6	0.137	0.239	0.102	0.0067
24	cg02249577	SGMS1 (-51036)	chr10	0.682	0.783	0.101	0.0054
25	cg07655261	NANOG (+6526)	chr12	0.490	0.591	0.101	0.0110
26	cg03447150	SEMA5A (+662041)	chr5	0.546	0.646	0.100	0.0244
27	cg08951186	ZNF469 (-203509)	chr16	0.536	0.635	0.100	0.0087
28	cg24680439	TTC40 (-22379)	chr10	0.505	0.604	0.099	0.0260
29	cg26175789	EVA1A (-25045)	chr2	0.391	0.490	0.099	0.0062
30	cg06013395	EPHB3 (+1141)	chr3	0.668	0.766	0.099	0.0072
31	cg18060330	BTNL2 (-1162)	chr6	0.589	0.686	0.097	0.0147
32	cg08778598	LPCAT1 (-70488)	chr5	0.168	0.263	0.096	0.0188
33	cg07973162	UGT2B17 (-1006)	chr4	0.413	0.509	0.096	0.0200
34	cg06221963	KCNN3 (+2943)	chr1	0.298	0.394	0.096	0.0028

Table S6. Continued

Nr.	probe ID	nearest gene (distance in bp)	chr	NU_mean	HU_mean	dB	P.Value
35	cg13166535	LOXL4 (-28710)	chr10	0.459	0.554	0.095	0.0240
36	cg08231349	HLA-G (+99889)	chr6	0.052	0.146	0.095	0.0006
37	cg07748963	LPHN2 (+361581)	chr1	0.316	0.411	0.095	0.0299
38	cg13365324	UGT2B17 (-1229)	chr4	0.431	0.525	0.094	0.0290
39	cg12088417	RPTOR (+55649)	chr17	0.754	0.848	0.094	0.0411
40	cg03806328	ARHGAP32 (-67539)	chr11	0.594	0.687	0.094	0.0015
41	cg07952421	UGT2B17 (-1357)	chr4	0.529	0.622	0.093	0.0183
42	cg24239165	C17orf82 (+7542)	chr17	0.583	0.675	0.092	0.0221
43	cg09359103	KCNN3 (+2847)	chr1	0.240	0.331	0.092	0.0022
44	cg17370981	ATP4B (+918)	chr13	0.445	0.535	0.090	0.0344
45	cg10388667	MRPL53 (+2528)	chr2	0.692	0.782	0.090	0.0171
46	cg06871764	BTNL2 (-1191)	chr6	0.518	0.607	0.089	0.0077
47	cg27219185	BTBD3 (-511455)	chr20	0.453	0.542	0.089	0.0463
48	cg20302533	POU6F2 (+153166)	chr7	0.263	0.352	0.089	0.0004
49	cg27175123	SEL1L (-121914)	chr14	0.617	0.706	0.089	0.0020
50	cg18806707	EPDR1 (+38254)	chr7	0.326	0.414	0.088	0.0122
51	cg22742493	SLC25A38 (-6194)	chr3	0.525	0.613	0.088	0.0276
52	cg22772380	ZNF12 (-484)	chr7	0.450	0.538	0.088	0.0010
53	cg18734446	GDNF (-38184)	chr5	0.653	0.739	0.086	0.0073
54	cg14381313	ZNF469 (-225540)	chr16	0.496	0.581	0.085	0.0098
55	cg26353469	HLA-G (+61215)	chr6	0.086	0.171	0.085	0.0007
56	cg02947374	ZNF469 (-226413)	chr16	0.561	0.645	0.084	0.0208
57	cg15727171	NONE	chr9	0.241	0.325	0.084	0.0019
58	cg04485391	ZMIZ1 (-327344)	chr10	0.526	0.610	0.084	0.0161
59	cg14904295	PEG3 (+3535)	chr19	0.295	0.379	0.083	0.0037
60	cg03660162	MAF (+721526)	chr16	0.713	0.796	0.083	0.0207
61	cg07346359	OPTC (+26398)	chr1	0.427	0.509	0.083	0.0005
62	cg21549632	HLA-G (+61532)	chr6	0.066	0.149	0.083	0.0004
63	cg03995122	HLA-G (+99887)	chr6	0.030	0.112	0.082	0.0008
64	cg13132497	LYSMD4 (-195527)	chr15	0.464	0.544	0.080	0.0321
65	cg00621508	SLC17A2 (+4745)	chr6	0.603	0.684	0.080	0.0250
66	cg20744362	BRD1 (+168288)	chr22	0.473	0.553	0.080	0.0235
67	cg18768136	ASAH2 (-87699)	chr10	0.436	0.516	0.080	0.0009
68	cg07113537	DAZL (+3439)	chr3	0.137	0.217	0.080	0.0001
69	cg25835058	TMEM51 (-71271)	chr1	0.422	0.502	0.080	0.0109

Table S6. Continued

Nr.	probe ID	nearest gene (distance in bp)	chr	NU_mean	HU_mean	dB	P.Value
70	cg00935887	CXXC11 (+32120)	chr2	0.446	0.526	0.079	0.0178
71	cg15671450	HLA-G (+100361)	chr6	0.090	0.170	0.079	0.0107
72	cg06014707	PI15 (-69154)	chr8	0.571	0.650	0.079	0.0028
73	cg10983929	FAM90A1 (+213)	chr12	0.445	0.523	0.079	0.0047
74	cg15681295	TTC40 (-22198)	chr10	0.497	0.575	0.079	0.0070
75	cg08363235	ASAH2 (-168462)	chr10	0.454	0.533	0.078	0.0007
76	cg00413089	WDR60 (+101717)	chr7	0.294	0.372	0.078	0.0223
77	cg16302021	HLA-G (+99189)	chr6	0.409	0.486	0.077	0.0016
78	cg19196320	DEFB115 (-322339)	chr20	0.573	0.650	0.077	0.0158
79	cg00409917	HLA-G (+99924)	chr6	0.074	0.150	0.077	0.0025
80	cg23237314	HLA-G (+99442)	chr6	0.132	0.209	0.076	0.0176
81	cg18896979	CXXC11 (+32294)	chr2	0.455	0.531	0.076	0.0177
82	cg19783563	SPACA7 (-45022)	chr13	0.323	0.399	0.076	0.0022
83	cg19823512	OPTC (+26455)	chr1	0.308	0.383	0.075	0.0011
84	cg14091258	DNAJB6 (+276948)	chr7	0.512	0.587	0.075	0.0067
85	cg05237260	CNTNAP3B (+717097)	chr9	0.291	0.366	0.075	0.0053
86	cg16906964	AJAP1 (-54934)	chr1	0.412	0.487	0.075	0.0040
87	cg00845968	ZMIZ1 (-318760)	chr10	0.578	0.653	0.075	0.0085
88	cg14859874	HAX1 (-6722)	chr1	0.091	0.166	0.075	0.0066
89	cg05181157	SNAPC1 (+47084)	chr14	0.615	0.689	0.075	0.0275
90	cg01918803	PSG2 (-36757)	chr19	0.538	0.613	0.074	0.0013
91	cg02048733	CBLB (-480477)	chr3	0.456	0.530	0.074	0.0016
92	cg01719566	FAM90A1 (-83)	chr12	0.470	0.544	0.074	0.0135
93	cg02033694	NPIPB11 (+118553)	chr16	0.284	0.358	0.074	0.0002
94	cg09928274	ELSPBP1 (+3822)	chr19	0.764	0.837	0.073	0.0313
95	cg17155018	TRAF3IP2 (-25618)	chr6	0.519	0.592	0.073	0.0060
96	cg24236953	FGFR2 (+41563)	chr10	0.496	0.569	0.073	0.0324
97	cg17291189	SLC2A14 (+25003)	chr12	0.346	0.418	0.073	0.0066
98	cg09597767	IFITM3 (-4866)	chr11	0.698	0.770	0.072	0.0037
99	cg13266242	HLA-G (+39740)	chr6	0.551	0.623	0.072	0.0014
100	cg01336390	HLA-G (+100304)	chr6	0.086	0.158	0.072	0.0048
101	cg15532640	GLT1D1 (+216486)	chr12	0.305	0.376	0.071	0.0382
102	cg03410772	ZNRD1 (-59026)	chr6	0.665	0.736	0.071	0.0000
103	cg25539628	ENSG00000182319 (+55525)	chr8	0.300	0.371	0.071	0.0004

Nr.	probe ID	nearest gene	chr	NU_mean	HU_mean	dB	P.Value
104	15700067	(distance in bp)	ala ::1 4	0.500	0.651	0.071	0.0377
104	cg15780967	PPP2R5E (+76068)	chr14	0.580	0.651	0.071	0.0377
105	cg20744163	PPIF (-107393)	chr10	0.665	0.736	0.071	0.0413
106	cg26028489	LMO3 (+85999)	chr12	0.485	0.556	0.071	0.0027
107	cg25877386	DHX37 (-1348)	chr12	0.755	0.825	0.071	0.0361
108	cg17341345	CCNH (-574)	chr5	0.510	0.580	0.071	0.0116
109	cg16223220	HLA-G (+61159)	chr6	0.042	0.112	0.071	0.0017
110	cg09646655	ZFP37 (-2357)	chr9	0.481	0.551	0.070	0.0102
111	cg10632656	UGT2B17 (-1349)	chr4	0.278	0.348	0.070	0.0192
112	cg00661861	GPRIN2 (-3909)	chr10	0.591	0.660	0.069	0.0381
113	cg12038583	ZNF727 (-476334)	chr7	0.484	0.554	0.069	0.0181
114	cg05202858	FGF12 (+352912)	chr3	0.408	0.477	0.069	0.0330
115	cg22968327	NUP93 (+59405)	chr16	0.262	0.331	0.069	0.0178
116	cg14449180	HLA-G (+99864)	chr6	0.039	0.108	0.069	0.0021
117	cg08993878	TMPO (-758029)	chr12	0.355	0.424	0.069	0.0301
118	cg05246613	SH3RF3 (+9250)	chr2	0.302	0.370	0.069	0.0088
119	cg17746638	ENSG00000233024 (-7835)	chr16	0.541	0.609	0.069	0.0219
120	cg09199338	AGA (-311227)	chr4	0.270	0.338	0.069	0.0003
121	cg07318398	NT5C3B (-587)	chr17	0.338	0.406	0.068	0.0043
122	cg03977382	CNTN5 (+672992)	chr11	0.574	0.643	0.068	0.0085
123	cg15411272	HLA-G (+100432)	chr6	0.284	0.352	0.068	0.0392
124	cg01499815	HLA-G (+100319)	chr6	0.087	0.156	0.068	0.0028
125	cg08422420	LPCAT1 (-70642)	chr5	0.145	0.213	0.068	0.0205
126	cg26274304	NCAPG2 (+942)	chr7	0.273	0.341	0.068	0.0042
127	cg24289952	ZNF80 (+14382)	chr3	0.474	0.542	0.068	0.0331
128	cg21963583	MRPL21 (+12452)	chr11	0.399	0.467	0.068	0.0303
129	cg21138405	IRF1 (-1318)	chr5	0.226	0.294	0.068	0.0247
130	cg09801012	ASAH2 (-127080)	chr10	0.644	0.712	0.067	0.0049
131	cg13597893	UBE2E3 (-272789)	chr2	0.498	0.565	0.067	0.0009
132	cg11047325	SOCS3 (+1224)	chr17	0.481	0.548	0.067	0.0042
133	cg14372705	GSC2 (-3235)	chr22	0.490	0.557	0.067	0.0470
134	cg23703303	SPAG11A (+14714)	chr8	0.545	0.611	0.067	0.0107
135	cg03071500	IFITM3 (-4915)	chr11	0.559	0.626	0.067	0.0227
136	cg05187965	TMEM72 (+117)	chr10	0.553	0.619	0.067	0.0142
137	cg15878909	FAM90A1 (-73)	chr12	0.399	0.465	0.066	0.0240

Table S6. Continued

Nr.	probe ID	nearest gene	chr	NU_mean	HU_mean	dB	P.Value
	p	(distance in bp)					
138	cg00255919	IRF1 (-1429)	chr5	0.234	0.300	0.066	0.0153
139	cg25952247	LHX3 (+2131)	chr9	0.413	0.479	0.066	0.0099
140	cg11406274	HLA-G (+61809)	chr6	0.253	0.319	0.066	0.0040
141	cg10621924	POU6F2 (+153473)	chr7	0.692	0.758	0.066	0.0016
142	cg03181300	HIST1H2AD (+3476)	chr6	0.220	0.285	0.066	0.0288
143	cg04034577	AGXT (+28480)	chr2	0.418	0.484	0.066	0.0177
144	cg27149073	LPCAT1 (-70239)	chr5	0.134	0.199	0.066	0.0077
145	cg04972766	NONE	chr5	0.466	0.531	0.066	0.0003
146	cg03607220	HLA-DRB5 (-28200)	chr6	0.564	0.629	0.066	0.0440
147	cg21257293	ZFP37 (-5722)	chr9	0.393	0.459	0.066	0.0484
148	cg08835755	NKX1-1 (-114199)	chr4	0.474	0.540	0.065	0.0191
149	cg08009379	COBL (+125847)	chr7	0.331	0.396	0.065	0.0001
150	cg12744031	WDR60 (+101916)	chr7	0.318	0.383	0.065	0.0460
151	cg15931205	HLA-G (+100065)	chr6	0.060	0.125	0.065	0.0003
152	cg23490161	SDHA (+97)	chr5	0.136	0.201	0.065	0.0240
153	cg21665744	POU6F2 (+153516)	chr7	0.637	0.701	0.065	0.0083
154	cg18191116	STON2 (+241)	chr14	0.508	0.572	0.065	0.0093
155	cg20696345	HS1BP3 (+39466)	chr2	0.415	0.480	0.065	0.0137
156	cg16666458	FAM126A (+72462)	chr7	0.588	0.652	0.065	0.0005
157	cg18146737	GFI1 (+2811)	chr1	0.705	0.769	0.064	0.0432
158	cg05090351	CTBP2 (-134704)	chr10	0.461	0.525	0.064	0.0096
159	cg22253032	PRSS1 (-37378)	chr7	0.436	0.500	0.064	0.0005
160	cg08757828	CPT1A (-28717)	chr11	0.290	0.354	0.064	0.0227
161	cg03877706	NCAM2 (+202000)	chr21	0.544	0.607	0.063	0.0111
162	cg15011775	RARB (+13136)	chr3	0.505	0.569	0.063	0.0020
163	cg06025105	RSPH1 (+21549)	chr21	0.701	0.764	0.063	0.0476
164	cg27421994	NAB1 (+9952)	chr2	0.363	0.426	0.063	0.0027
165	cg02748618	ATPAF2 (+10470)	chr17	0.370	0.433	0.063	0.0016
166	cg19954471	SPACA7 (+66683)	chr13	0.406	0.469	0.063	0.0009
167	cg00186468	CCNH (-393)	chr5	0.250	0.313	0.063	0.0011
168	cg17184855	HLA-G (+595)	chr6	0.607	0.670	0.063	0.0008
169	cg21862992	MRPL21 (+12905)	chr11	0.409	0.471	0.063	0.0432
170	cg10077346	BCKDHB (+104095)	chr6	0.481	0.543	0.063	0.0333
171	cg06752595	ALDH5A1 (-1115)	chr6	0.530	0.592	0.062	0.0464
172	cg27584762	CCNH (-291)	chr5	0.208	0.271	0.062	0.0022

Table S6. Continued

Nr.	probe ID	nearest gene (distance in bp)	chr	NU_mean	HU_mean	dB	P.Value
173	cg05332308	CDH8 (-372226)	chr16	0.439	0.501	0.062	0.0047
174	cg04535902	GFI1 (+2179)	chr1	0.632	0.694	0.062	0.0248
175	cg25897043	ITGB1 (-95701)	chr10	0.511	0.573	0.062	0.0057
176	cg27209610	ST3GAL5 (-102063)	chr2	0.454	0.516	0.062	0.0041
177	cg14223671	GNG13 (-7249)	chr16	0.142	0.205	0.062	0.0065
178	cg15598217	ZZEF1 (+44435)	chr17	0.530	0.592	0.062	0.0058
179	cg01668281	CLDN14 (-62894)	chr21	0.272	0.334	0.062	0.0016
180	cg01324550	HOXB5 (-4777)	chr17	0.355	0.417	0.062	0.0016
181	cg11365170	SEMA6A (+77177)	chr5	0.590	0.652	0.062	0.0015
182	cg27618398	DCLK1 (-27638)	chr13	0.647	0.709	0.062	0.0458
183	cg00135841	USP18 (+104683)	chr22	0.766	0.828	0.062	0.0110
184	cg19748509	HLA-G (+116023)	chr6	0.071	0.133	0.062	0.0014
185	cg03551406	MT1X (-580)	chr16	0.444	0.506	0.062	0.0006
186	cg01617603	UGT2B17 (+15538)	chr4	0.247	0.309	0.062	0.0185
187	cg11449146	GAS2 (+62304)	chr11	0.560	0.622	0.061	0.0026
188	cg00369056	NPIPA7 (+490096)	chr16	0.658	0.719	0.061	0.0223
189	cg19684894	C1orf222 (+11284)	chr1	0.097	0.158	0.061	0.0379
190	cg10031873	ALG10B (-166540)	chr12	0.732	0.793	0.061	0.0003
191	cg27540865	CEP170 (+364418)	chr1	0.189	0.250	0.061	0.0056
192	cg12439472	DNAJC15 (-31940)	chr13	0.497	0.558	0.061	0.0182
193	cg02556954	ETF1 (+30412)	chr5	0.483	0.544	0.061	0.0010
194	cg27119318	WRB (+7405)	chr21	0.171	0.232	0.061	0.0033
195	cg24699985	C1orf174 (-276752)	chr1	0.462	0.522	0.060	0.0024
196	cg16680214	KCNN3 (+2773)	chr1	0.181	0.241	0.060	0.0004
197	cg03249561	FCAR (+14427)	chr19	0.678	0.738	0.060	0.0371
198	cg12545480	SYT14 (-12090)	chr1	0.405	0.465	0.060	0.0309
199	cg23248910	FGFR2 (+87847)	chr10	0.469	0.529	0.060	0.0177
200	cg11351709	TDRP (-333843)	chr8	0.418	0.478	0.060	0.0271
201	cg19061000	GALC (+182752)	chr14	0.560	0.620	0.060	0.0045
202	cg03618918	ITLN1 (-10138)	chr1	0.653	0.713	0.060	0.0004
203	cg16681436	EGFL8 (+2860)	chr6	0.694	0.753	0.060	0.0209
204	cg02447462	CFD (+1619)	chr19	0.403	0.462	0.060	0.0175
205	cg19686152	TMOD3 (-285)	chr15	0.458	0.517	0.060	0.0484
206	cg24960960	LPCAT1 (-70587)	chr5	0.171	0.230	0.059	0.0169
207	cg15218522	SBSPON (-75679)	chr8	0.339	0.398	0.059	0.0137

Table S6. Continued

Table	Table S6. Continued									
Nr.	probe ID	nearest gene (distance in bp)	chr	NU_mean	HU_mean	dB	P.Value			
208	cg02850689	PLCH2 (-7551)	chr1	0.439	0.499	0.059	0.0026			
209	cg21167402	LPCAT1 (-70585)	chr5	0.217	0.277	0.059	0.0214			
210	cg02015053	EIF3J (+24728)	chr15	0.412	0.471	0.059	0.0039			
211	cg22872376	MAGEL2 (-2568)	chr15	0.310	0.369	0.059	0.0015			
212	cg06611532	RASA3 (-1936)	chr13	0.436	0.495	0.059	0.0423			
213	cg03589715	SLC8A3 (-34563)	chr14	0.620	0.679	0.059	0.0256			
214	cg01719179	NPIPB11 (+118657)	chr16	0.221	0.280	0.059	0.0004			
215	cg05037738	ATP13A3 (-1381)	chr3	0.531	0.590	0.059	0.0149			
216	cg21894124	FBRSL1 (-161448)	chr12	0.148	0.207	0.059	0.0006			
217	cg06112835	MRPL21 (+12495)	chr11	0.298	0.357	0.059	0.0296			
218	cg13488542	MPHOSPH6 (+17514)	chr16	0.669	0.728	0.059	0.0152			
219	cg08835956	POU6F2 (+153437)	chr7	0.639	0.698	0.059	0.0086			
220	cg07962847	ACTR3B (+531378)	chr7	0.390	0.449	0.059	0.0233			
221	cg14079719	IPCEF1 (+100117)	chr6	0.420	0.479	0.059	0.0088			
222	cg20370296	ZNF251 (+69043)	chr8	0.352	0.411	0.059	0.0184			
223	cg03785755	HIST1H2AD (+2677)	chr6	0.360	0.419	0.059	0.0038			
224	cg05845204	RBM39 (+12594)	chr20	0.733	0.792	0.059	0.0182			
225	cg09274344	SOX8 (+46882)	chr16	0.315	0.373	0.059	0.0136			
226	cg15111296	CXXC1 (-33327)	chr18	0.545	0.603	0.058	0.0466			
227	cg24126361	SLC25A37 (+12029)	chr8	0.499	0.558	0.058	0.0423			
228	cg01062395	HLA-G (+60881)	chr6	0.111	0.170	0.058	0.0060			
229	cg05875302	CXXC11 (+32901)	chr2	0.695	0.753	0.058	0.0023			
230	cg17590488	NEBL (-132505)	chr10	0.447	0.505	0.058	0.0089			
231	cg26188685	HDC (+17954)	chr15	0.220	0.278	0.058	0.0021			
232	cg20748132	SCARB1 (+130686)	chr12	0.474	0.532	0.058	0.0075			
233	cg11851257	TAC4 (+21973)	chr17	0.579	0.637	0.058	0.0014			
234	cg05636112	KYNU (+47533)	chr2	0.488	0.546	0.058	0.0196			
235	cg11284736	ENSG00000166503 (+50062)	chr15	0.603	0.661	0.058	0.0003			
236	cg09239700	IRF4 (+58348)	chr6	0.604	0.662	0.058	0.0033			
237	cg07872519	ABCB1 (-301)	chr7	0.459	0.517	0.057	0.0021			
238	cg01889129	PDZD8 (-63910)	chr10	0.505	0.562	0.057	0.0063			
239	cg15534755	TAGLN (-2730)	chr11	0.574	0.631	0.057	0.0161			
240	cg05900440	TTC30A (+19814)	chr2	0.441	0.498	0.057	0.0145			
241	cg10814153	ODF3L2 (+10)	chr19	0.578	0.635	0.057	0.0103			

Table S6. Continued

Nr.	probe ID	nearest gene (distance in bp)	chr	NU_mean	HU_mean	dB	P.Value
242	cg09874992	SDC3 (+67000)	chr1	0.376	0.434	0.057	0.0044
243	cg12798157	AKR7A3 (+15025)	chr1	0.185	0.242	0.057	0.0159
244	cg05452645	PRDM8 (+11224)	chr4	0.348	0.405	0.057	0.0426
245	cg14643763	STK35 (+71468)	chr20	0.387	0.444	0.057	0.0146
246	cg13126979	EME2 (+970)	chr16	0.232	0.289	0.057	0.0045
247	cg01876548	ZNF608 (-45746)	chr5	0.560	0.617	0.057	0.0068
248	cg03594447	PLA2G5 (-36957)	chr1	0.292	0.348	0.057	0.0016
249	cg08121845	NONE	chr3	0.261	0.318	0.057	0.0017
250	cg04124281	MTHFS (-747)	chr15	0.229	0.286	0.057	0.0047
251	cg03701930	ADARB2 (-201767)	chr10	0.144	0.200	0.057	0.0014
252	cg07324633	LPCAT1 (-44578)	chr5	0.431	0.488	0.057	0.0012
253	cg23420995	DCLK1 (-2777)	chr13	0.171	0.227	0.057	0.0010
254	cg18181703	SOCS3 (+1537)	chr17	0.307	0.363	0.057	0.0004
255	cg19167230	NONE	chr4	0.344	0.401	0.056	0.0015
256	cg11861562	TAGLN (-2809)	chr11	0.540	0.596	0.056	0.0135
257	cg27029450	BRD1 (+120378)	chr22	0.339	0.396	0.056	0.0013
258	cg18943014	ZNF92 (+89579)	chr7	0.375	0.431	0.056	0.0018
259	cg20681948	ASCL1 (-9167)	chr12	0.373	0.429	0.056	0.0034
260	cg15817705	CAMK1G (-350999)	chr1	0.537	0.594	0.056	0.0018
261	cg16884706	TAS1R2 (+66273)	chr1	0.462	0.518	0.056	0.0011
262	cg07782112	CHAC2 (-887087)	chr2	0.391	0.447	0.056	0.0229
263	cg17309085	CNTN5 (+672975)	chr11	0.681	0.737	0.056	0.0096
264	cg14864167	PDE7A (+3005)	chr8	0.388	0.444	0.056	0.0014
265	cg22872396	SCN9A (+9830)	chr2	0.507	0.562	0.055	0.0150
266	cg11807280	MEIS1 (-7888)	chr2	0.296	0.352	0.055	0.0036
267	cg17361885	MXRA7 (+6038)	chr17	0.669	0.725	0.055	0.0438
268	cg13363596	CLDN14 (-62926)	chr21	0.394	0.449	0.055	0.0036
269	cg10773881	GGA1 (+15331)	chr22	0.118	0.173	0.055	0.0000
270	cg23962358	CPZ (+79985)	chr4	0.402	0.457	0.055	0.0099
271	cg18737081	PPIF (-107427)	chr10	0.624	0.679	0.055	0.0280
272	cg04118610	LPHN3 (+639168)	chr4	0.106	0.161	0.055	0.0309
273	cg00417819	SYT3 (+33140)	chr19	0.579	0.633	0.055	0.0009
274	cg13294652	OBSCN (+20917)	chr1	0.353	0.408	0.055	0.0158
275	cg23299919	DNAJB6 (+276437)	chr7	0.335	0.389	0.055	0.0185
276	cg13470831	SALL3 (-59897)	chr18	0.504	0.558	0.054	0.0058

Table S6. Continued

Nr.	probe ID	nearest gene (distance in bp)	chr	NU_mean	HU_mean	dB	P.Value
277	cg10464773	QKI (+335832)	chr6	0.479	0.534	0.054	0.0121
278	cg20476087	CGREF1 (-126)	chr2	0.115	0.170	0.054	0.0002
279	cg27404186	CXXC11 (+31941)	chr2	0.661	0.716	0.054	0.0133
280	cg08206881	LPIN1 (+499637)	chr2	0.124	0.178	0.054	0.0167
281	cg01176694	MKL2 (+208587)	chr16	0.440	0.495	0.054	0.0009
282	cg12019814	RAD21 (+25858)	chr8	0.376	0.431	0.054	0.0015
283	cg26942295	PDZD2 (+49191)	chr5	0.498	0.552	0.054	0.0125
284	cg02407415	GNG13 (-6722)	chr16	0.207	0.261	0.054	0.0429
285	cg23340194	USP14 (-3299)	chr18	0.484	0.538	0.054	0.0390
286	cg14827090	BEGAIN (+42983)	chr14	0.520	0.574	0.054	0.0233
287	cg25711786	ETF1 (+24486)	chr5	0.417	0.471	0.054	0.0018
288	cg14080482	NONE	chr6	0.389	0.443	0.054	0.0004
289	cg08937153	CEBPD (+146838)	chr8	0.609	0.663	0.054	0.0010
290	cg21705926	DNAJB6 (+276978)	chr7	0.488	0.542	0.054	0.0285
291	cg11124651	NONE	chr19	0.655	0.709	0.054	0.0132
292	cg17565702	KIFC2 (-138)	chr8	0.457	0.511	0.054	0.0029
293	cg19727165	DHFRL1 (-114061)	chr3	0.613	0.667	0.054	0.0436
294	cg14088970	ENGASE (+140423)	chr17	0.342	0.396	0.054	0.0094
295	cg21733854	ZSCAN22 (-615)	chr19	0.523	0.577	0.054	0.0078
296	cg00242965	MRPL21 (+12319)	chr11	0.271	0.325	0.054	0.0396
297	cg18449879	CYP4F11 (+591)	chr19	0.487	0.540	0.054	0.0169
298	cg23917496	UACA (+300798)	chr15	0.383	0.437	0.054	0.0276
299	cg19852147	WWOX (+662174)	chr16	0.311	0.365	0.054	0.0061
300	cg25282559	NONE	chr14	0.468	0.522	0.054	0.0011
301	cg24693741	DYM (+101009)	chr18	0.237	0.290	0.054	0.0009
302	cg12607525	ATXN7L3 (-11412)	chr17	0.559	0.613	0.054	0.0042
303	cg05333568	C1orf65 (+80)	chr1	0.256	0.309	0.053	0.0035
304	cg12884719	SIPA1L2 (+451040)	chr1	0.424	0.477	0.053	0.0066
305	cg10358342	NOBOX (-307)	chr7	0.315	0.368	0.053	0.0004
306	cg19445457	OR52N5 (+451)	chr11	0.536	0.589	0.053	0.0110
307	cg01256539	PRR16 (+2004)	chr5	0.510	0.563	0.053	0.0116
308	cg09142843	ARHGAP18 (+389699)	chr6	0.740	0.793	0.053	0.0448
309	cg13056744	HLA-G (+100185)	chr6	0.118	0.171	0.053	0.0073
310	cg06588529	ECI2 (-18261)	chr6	0.655	0.708	0.053	0.0232
311	cg00666877	CEP112 (+190945)	chr17	0.553	0.606	0.053	0.0028

Table S6. Continued

Nr.	probe ID	nearest gene (distance in bp)	chr	NU_mean	HU_mean	dB	P.Value
312	cg11706815	MBD3L1 (+59748)	chr19	0.396	0.449	0.053	0.0274
313	cg03362483	LDLRAP1 (-23383)	chr1	0.352	0.405	0.053	0.0095
314	cg15853715	C14orf39 (-2535)	chr14	0.452	0.505	0.053	0.0060
315	cg25556464	STOML1 (+17620)	chr15	0.551	0.603	0.053	0.0113
316	cg22083892	KCNJ8 (-907)	chr12	0.347	0.400	0.053	0.0172
317	cg19684207	WRB (+7517)	chr21	0.165	0.217	0.052	0.0050
318	cg03904042	NECAB3 (+6723)	chr20	0.213	0.266	0.052	0.0364
319	cg25220979	IGF2BP1 (+17499)	chr17	0.481	0.533	0.052	0.0002
320	cg18018313	IRS1 (+7283)	chr2	0.322	0.374	0.052	0.0005
321	cg12700863	IRX4 (-244322)	chr5	0.516	0.568	0.052	0.0047
322	cg19318330	SIK1 (+64136)	chr21	0.285	0.338	0.052	0.0059
323	cg13434361	PRSS16 (-18100)	chr6	0.620	0.672	0.052	0.0337
324	cg09125754	POTEF (-8533)	chr2	0.377	0.429	0.052	0.0386
325	cg10130564	TAGLN (-2740)	chr11	0.602	0.654	0.052	0.0456
326	cg23245007	TNK2 (-59895)	chr3	0.580	0.633	0.052	0.0161
327	cg08045932	BHLHE23 (-21594)	chr20	0.419	0.471	0.052	0.0310
328	cg05760951	SPATA31A5 (+453801)	chr9	0.225	0.278	0.052	0.0051
329	cg24531534	R3HCC1 (+16742)	chr8	0.313	0.366	0.052	0.0320
330	cg10609241	MTHFD1 (+29577)	chr14	0.669	0.721	0.052	0.0014
331	cg08975641	COL5A2 (+85053)	chr2	0.500	0.552	0.052	0.0426
332	cg25452172	CYP27B1 (-1718)	chr12	0.568	0.620	0.052	0.0002
333	cg10341310	MTFR1 (+25233)	chr8	0.452	0.503	0.052	0.0053
334	cg16543056	ZFP42 (-236815)	chr4	0.443	0.495	0.052	0.0013
335	cg13343932	SOCS3 (+1097)	chr17	0.440	0.492	0.052	0.0129
336	cg09790280	TMEM229A (-316698)	chr7	0.574	0.625	0.052	0.0076
337	cg11232815	ATP6V0E2 (+176593)	chr7	0.431	0.482	0.052	0.0378
338	cg02830496	SLC25A51 (-25460)	chr9	0.299	0.350	0.052	0.0197
339	cg06012695	TRIM27 (+121173)	chr6	0.300	0.351	0.052	0.0045
340	cg02260461	USH2A (+35690)	chr1	0.467	0.519	0.051	0.0016
341	cg02027518	NDST3 (-201083)	chr4	0.530	0.581	0.051	0.0003
342	cg13048967	CXCR1 (+1595)	chr2	0.629	0.681	0.051	0.0017
343	cg07490070	ANKRD23 (+4307)	chr2	0.159	0.210	0.051	0.0049
344	cg25664381	STX18 (-33719)	chr4	0.228	0.280	0.051	0.0041
345	cg24589936	MTX1 (+2106)	chr1	0.410	0.462	0.051	0.0489
346	cg06531573	GNG13 (-6844)	chr16	0.180	0.232	0.051	0.0220

Table S6. Continued

Nr.	probe ID	nearest gene (distance in bp)	chr	NU_mean	HU_mean	dB	P.Value
347	cg23155965	TTC40 (-22088)	chr10	0.786	0.837	0.051	0.0057
348	cg01124420	EDAR (+310)	chr2	0.401	0.453	0.051	0.0034
349	cg23999422	SIRT6 (+9135)	chr19	0.225	0.276	0.051	0.0005
350	cg12761472	CEP85L (-685)	chr6	0.586	0.637	0.051	0.0014
351	cg20746451	SMARCAD1 (-1059)	chr4	0.593	0.644	0.051	0.0478
352	cg24931191	STAC (-172977)	chr3	0.269	0.319	0.051	0.0044
353	cg08695253	ODF3L2 (+4)	chr19	0.473	0.524	0.051	0.0096
354	cg03742947	HLA-G (+61520)	chr6	0.068	0.119	0.051	0.0080
355	cg25883179	GABRG2 (+256684)	chr5	0.665	0.715	0.051	0.0003
356	cg12552320	SLC25A21 (+176861)	chr14	0.434	0.484	0.051	0.0015
357	cg05707985	PRSS1 (-26980)	chr7	0.299	0.350	0.051	0.0288
358	cg04492858	PPP2R2D (-189169)	chr10	0.244	0.295	0.051	0.0085
359	cg10848692	TCL1A (-121392)	chr14	0.250	0.301	0.051	0.0010
360	cg15441605	TYRP1 (+121209)	chr9	0.538	0.589	0.051	0.0024
361	cg06902219	HLA-G (+61539)	chr6	0.100	0.151	0.051	0.0026
362	cg03307118	MAP1LC3B2 (-41193)	chr12	0.663	0.713	0.051	0.0162
363	cg12219752	FAM189A2 (+56037)	chr9	0.534	0.585	0.051	0.0288
364	cg09775918	NONE	chr9	0.360	0.410	0.051	0.0399
365	cg03226871	MAP3K2 (+17083)	chr2	0.515	0.565	0.051	0.0033
366	cg22499139	HLA-G (-35038)	chr6	0.643	0.693	0.051	0.0065
367	cg22542685	ZNF624 (+36608)	chr17	0.562	0.612	0.051	0.0117
368	cg16875568	ITGBL1 (+68145)	chr13	0.453	0.503	0.050	0.0277
369	cg18087694	RFPL4A (-1134)	chr19	0.319	0.370	0.050	0.0119
370	cg03626024	WSCD2 (-1183)	chr12	0.452	0.502	0.050	0.0019
371	cg21234506	BCL2A1 (+656)	chr15	0.394	0.445	0.050	0.0008
372	cg09680926	CHD2 (-13636)	chr15	0.413	0.464	0.050	0.0005
373	cg09004254	RNF157 (-34042)	chr17	0.578	0.628	0.050	0.0148
374	cg07583744	AUTS2 (+294919)	chr7	0.313	0.363	0.050	0.0254
375	cg05284887	GJA5 (+12178)	chr1	0.527	0.578	0.050	0.0046
376	cg22943590	MEIS1 (-13735)	chr2	0.458	0.508	0.050	0.0387
377	cg15221739	GPR98 (+381941)	chr5	0.267	0.318	0.050	0.0027
378	cg20787634	UQCRB (+7604)	chr8	0.592	0.642	0.050	0.0128
379	cg09906620	CCNB2 (-21939)	chr15	0.786	0.736	-0.050	0.0063
380	cg00919702	C1QL3 (+2653)	chr10	0.719	0.669	-0.050	0.0231
381	cg23223755	LHFPL4 (-1364)	chr3	0.625	0.575	-0.050	0.0024

Table S6. Continued

Nr.	probe ID	nearest gene (distance in bp)	chr	NU_mean	HU_mean	dB	P.Value
382	cg02512888	CAMK1D (+66264)	chr10	0.637	0.587	-0.050	0.0007
383	cg26985140	SLC23A2 (-848)	chr20	0.710	0.660	-0.050	0.0019
384	cg14222229	HIST2H3PS2 (+262795)	chr1	0.322	0.272	-0.050	0.0115
385	cg09166973	PRDM9 (-151)	chr5	0.707	0.656	-0.050	0.0146
386	cg05250352	POR (+27235)	chr7	0.695	0.645	-0.050	0.0010
387	cg27019757	PDCD4 (+18771)	chr10	0.715	0.665	-0.050	0.0041
388	cg11541587	TPGS2 (-123951)	chr18	0.779	0.728	-0.051	0.0014
389	cg13795666	DDX59 (+20818)	chr1	0.685	0.634	-0.051	0.0075
390	cg24821564	KIR2DL1 (-591)	chr19	0.774	0.723	-0.051	0.0270
391	cg04161902	BAI2 (+1728)	chr1	0.736	0.686	-0.051	0.0043
392	cg00804338	TFDP1 (+179)	chr13	0.166	0.115	-0.051	0.0038
393	cg10085053	NARS2 (-5329)	chr11	0.692	0.641	-0.051	0.0105
394	cg09886641	SPESP1 (+180)	chr15	0.741	0.690	-0.051	0.0018
395	cg00496389	OTOP1 (+88771)	chr4	0.748	0.697	-0.051	0.0139
396	cg23609713	TRIM27 (+153477)	chr6	0.585	0.534	-0.051	0.0045
397	cg11524065	ZCCHC8 (+21993)	chr12	0.834	0.783	-0.051	0.0402
398	cg10218876	TNNT1 (+97)	chr19	0.243	0.192	-0.051	0.0443
399	cg12463722	OR4D1 (+6)	chr17	0.734	0.682	-0.051	0.0002
400	cg23492448	RPL38 (-113727)	chr17	0.598	0.547	-0.051	0.0134
401	cg06820102	ZBTB38 (-2263)	chr3	0.665	0.614	-0.051	0.0003
402	cg15547703	CSTB (+3154)	chr21	0.590	0.539	-0.051	0.0018
403	cg10556772	HLA-G (+679)	chr6	0.406	0.354	-0.051	0.0065
404	cg24836607	ASZ1 (-176)	chr7	0.679	0.627	-0.051	0.0096
405	cg26259926	LRRC24 (-3573)	chr8	0.655	0.604	-0.051	0.0294
406	cg03203155	SCAND3 (-154692)	chr6	0.681	0.630	-0.052	0.0152
407	cg10082647	C12orf23 (-645)	chr12	0.690	0.638	-0.052	0.0049
408	cg14841443	RGS9 (+92958)	chr17	0.543	0.492	-0.052	0.0457
409	cg02109003	HSBP1 (-106440)	chr16	0.552	0.500	-0.052	0.0051
410	cg24045276	NCF2 (+7621)	chr1	0.658	0.606	-0.052	0.0035
411	cg20212775	SPON2 (+1980)	chr4	0.643	0.591	-0.052	0.0008
412	cg09598512	XYLB (-17726)	chr3	0.602	0.550	-0.052	0.0254
413	cg20050113	SLC9A2 (+696)	chr2	0.387	0.334	-0.052	0.0092
414	cg17623013	FAM81B (+81020)	chr5	0.856	0.804	-0.052	0.0172
415	cg08121925	FXR1 (-42049)	chr3	0.319	0.267	-0.052	0.0009
416	cg23522194	CABP5 (-17880)	chr19	0.786	0.734	-0.052	0.0452

Table S6. Continued

Nr.	probe ID	nearest gene (distance in bp)	chr	NU_mean	HU_mean	dB	P.Value
417	cg02675179	ACSM1 (+16505)	chr16	0.518	0.466	-0.052	0.0093
418	cg12847536	ARHGEF10 (+50045)	chr8	0.641	0.589	-0.052	0.0147
419	cg22898160	NDRG4 (-1339)	chr16	0.666	0.614	-0.052	0.0018
420	cg08087268	CHGA (+16658)	chr14	0.619	0.567	-0.052	0.0218
421	cg26209990	LEP (+29922)	chr7	0.682	0.630	-0.052	0.0289
422	cg13518079	EBF4 (+1549)	chr20	0.438	0.386	-0.052	0.0205
423	cg17241353	CBLN4 (+712513)	chr20	0.672	0.620	-0.052	0.0026
424	cg02663317	ARNTL2 (-40043)	chr12	0.671	0.619	-0.053	0.0018
425	cg18193195	SUOX (-10774)	chr12	0.709	0.657	-0.053	0.0237
426	cg22027267	COBL (-160023)	chr7	0.749	0.696	-0.053	0.0047
427	cg11546683	CPPED1 (+187159)	chr16	0.787	0.734	-0.053	0.0140
428	cg22079902	PRDM9 (-80)	chr5	0.592	0.539	-0.053	0.0193
429	cg19162470	FAN1 (-3185)	chr15	0.663	0.610	-0.053	0.0170
430	cg22762992	DDX18 (+44152)	chr2	0.657	0.604	-0.053	0.0384
431	cg09209787	PROX1 (-10179)	chr1	0.519	0.466	-0.053	0.0015
432	cg03971051	KLHL35 (-11281)	chr11	0.816	0.762	-0.053	0.0280
433	cg01066472	LHX8 (-3090)	chr1	0.431	0.378	-0.053	0.0216
434	cg24920126	RPP40 (-82986)	chr6	0.693	0.639	-0.053	0.0167
435	cg15846771	ZDHHC11 (-4165)	chr5	0.542	0.488	-0.053	0.0039
436	cg07531550	FRG1 (-209348)	chr4	0.661	0.607	-0.053	0.0402
437	cg21556998	STRBP (+44032)	chr9	0.686	0.632	-0.054	0.0003
438	cg20304530	NTRK3 (+297163)	chr15	0.801	0.747	-0.054	0.0018
439	cg13476778	FRMD6 (-1261)	chr14	0.555	0.501	-0.054	0.0191
440	cg14771877	C17orf99 (-1396)	chr17	0.712	0.658	-0.054	0.0133
441	cg18211633	RHOF (+26559)	chr12	0.669	0.615	-0.054	0.0081
442	cg20660297	KRR1 (-903)	chr12	0.538	0.484	-0.054	0.0169
443	cg09053901	SHANK2 (+8174)	chr11	0.821	0.767	-0.054	0.0041
444	cg05010260	NAT16 (+3266)	chr7	0.615	0.561	-0.054	0.0054
445	cg27585222	ACTR3 (+90194)	chr2	0.649	0.595	-0.054	0.0108
446	cg04678955	DEFB115 (-321336)	chr20	0.512	0.458	-0.054	0.0336
447	cg00561395	ATXN10 (+46358)	chr22	0.693	0.638	-0.054	0.0045
448	cg17850273	KIF21A (+74994)	chr12	0.649	0.595	-0.054	0.0049
449	cg01540595	LHX8 (-3159)	chr1	0.474	0.420	-0.054	0.0071
450	cg03779490	SNX9 (-174754)	chr6	0.551	0.496	-0.055	0.0162
451	cg00590063	B3GNT3 (+12877)	chr19	0.332	0.277	-0.055	0.0255

Table S6. Continued

Nr.	probe ID	nearest gene (distance in bp)	chr	NU_mean	HU_mean	dB	P.Value
452	cg03499324	PSMD5 (-858)	chr9	0.741	0.686	-0.055	0.0352
453	cg00105415	EGR2 (-3162)	chr10	0.669	0.615	-0.055	0.0021
454	cg09048334	FGD2 (+39218)	chr6	0.432	0.377	-0.055	0.0455
455	cg23425970	HS6ST1 (-244)	chr2	0.242	0.187	-0.055	0.0172
456	cg15620114	SLC16A12 (-1145)	chr10	0.768	0.713	-0.055	0.0053
457	cg01799458	HOXB13 (+1736)	chr17	0.573	0.518	-0.055	0.0048
458	cg25890575	DNAJB6 (+240283)	chr7	0.788	0.733	-0.055	0.0343
459	cg02655397	TMEM262 (-3138)	chr11	0.731	0.675	-0.056	0.0009
460	cg11016221	PTGES (+9679)	chr9	0.415	0.359	-0.056	0.0123
461	cg05874329	CYP11B1 (+17565)	chr8	0.625	0.569	-0.056	0.0018
462	cg13375654	DOC2A (-1283)	chr16	0.454	0.398	-0.056	0.0084
463	cg05663294	DUSP10 (-236921)	chr1	0.594	0.538	-0.056	0.0027
464	cg16506114	EPHA6 (-37633)	chr3	0.638	0.581	-0.057	0.0020
465	cg14551984	SGOL2 (+8923)	chr2	0.726	0.669	-0.057	0.0018
466	cg05208483	CSPG4 (+30148)	chr15	0.797	0.740	-0.057	0.0362
467	cg11206167	SEPP1 (-112187)	chr5	0.767	0.710	-0.057	0.0328
468	cg08310558	SLFN13 (-10935)	chr17	0.851	0.794	-0.057	0.0233
469	cg05343328	ING1 (+98215)	chr13	0.649	0.593	-0.057	0.0172
470	cg16603012	APRT (-1242)	chr16	0.658	0.602	-0.057	0.0195
471	cg20336352	HERC4 (-13229)	chr10	0.761	0.704	-0.057	0.0157
472	cg08145067	PIP5K1C (+12301)	chr19	0.329	0.272	-0.057	0.0112
473	cg03264585	MTRNR2L1 (-229467)	chr17	0.646	0.589	-0.057	0.0031
474	cg02996355	STON2 (+14373)	chr14	0.278	0.221	-0.057	0.0105
475	cg00816676	MTRNR2L7 (-78458)	chr10	0.731	0.674	-0.057	0.0018
476	cg02661831	PHF3 (+41346)	chr6	0.676	0.619	-0.057	0.0105
477	cg26137217	TAF4 (+309977)	chr20	0.600	0.543	-0.057	0.0090
478	cg08122831	ERBB4 (-294015)	chr2	0.770	0.713	-0.057	0.0002
479	cg18844029	TRIM27 (+6749)	chr6	0.753	0.696	-0.057	0.0131
480	cg08124399	DDX43 (+398)	chr6	0.733	0.676	-0.057	0.0257
481	cg10831285	B3GNT3 (+13009)	chr19	0.319	0.261	-0.058	0.0009
482	cg11643285	OXNAD1 (+104962)	chr3	0.814	0.757	-0.058	0.0042
483	cg24727089	TXNL1 (+46082)	chr18	0.663	0.606	-0.058	0.0082
484	cg27516945	ZNF528 (-603)	chr19	0.673	0.616	-0.058	0.0114
485	cg14361252	ING1 (+98129)	chr13	0.593	0.536	-0.058	0.0223
486	cg05275595	TEX101 (-47774)	chr19	0.374	0.316	-0.058	0.0430

Table S6. Continued

Nr.	probe ID	nearest gene (distance in bp)	chr	NU_mean	HU_mean	dB	P.Value
487	cg07938212	BICD1 (+13201)	chr12	0.637	0.579	-0.058	0.0007
488	cg06968712	MS4A15 (+10431)	chr11	0.558	0.500	-0.058	0.0059
489	cg15199034	ADAMTS1 (-42681)	chr21	0.705	0.647	-0.058	0.0024
490	cg09602542	GGT6 (-36137)	chr17	0.839	0.780	-0.059	0.0025
491	cg18423549	MTRNR2L1 (-278559)	chr17	0.398	0.339	-0.059	0.0210
492	cg06650819	ACTL6A (+2784)	chr3	0.495	0.436	-0.059	0.0309
493	cg04272684	OVCH1 (-21212)	chr12	0.676	0.617	-0.059	0.0173
494	cg27393610	TMEM116 (+6954)	chr12	0.889	0.831	-0.059	0.0015
495	cg17240725	ABHD11 (+3841)	chr7	0.398	0.339	-0.059	0.0110
496	cg16294255	MMEL1 (+1855)	chr1	0.507	0.448	-0.059	0.0057
497	cg03116837	ZNF596 (+34320)	chr8	0.453	0.394	-0.059	0.0257
498	cg20493661	KIR3DL1 (+15456)	chr19	0.590	0.531	-0.059	0.0093
499	cg02878510	SERTAD4 (-32407)	chr1	0.654	0.595	-0.059	0.0063
500	cg03218402	TAS2R13 (+26087)	chr12	0.818	0.759	-0.059	0.0196
501	cg06015275	HSBP1 (-66549)	chr16	0.603	0.544	-0.059	0.0175
502	cg27427514	HES1 (+68104)	chr3	0.199	0.139	-0.060	0.0083
503	cg25122629	EML6 (-14857)	chr2	0.366	0.306	-0.060	0.0045
504	cg13729548	CHGA (+16513)	chr14	0.742	0.682	-0.060	0.0204
505	cg04601780	ENSG00000264813 (+10162)	chr17	0.474	0.413	-0.060	0.0182
506	cg06520296	ZNF703 (-202288)	chr8	0.569	0.509	-0.060	0.0155
507	cg14554415	SPESP1 (+150)	chr15	0.636	0.576	-0.060	0.0107
508	cg06513015	ERV3-1 (+7785)	chr7	0.784	0.723	-0.060	0.0016
509	cg07256649	HOPX (+68186)	chr4	0.828	0.768	-0.060	0.0408
510	cg08030235	EEPD1 (-95569)	chr7	0.726	0.665	-0.060	0.0104
511	cg05471900	IL1F10 (-1191)	chr2	0.704	0.643	-0.061	0.0035
512	cg00167275	GLUD1 (+35)	chr10	0.165	0.104	-0.061	0.0008
513	cg10846356	CALCB (-726)	chr11	0.643	0.581	-0.061	0.0042
514	cg15936068	DDX43 (+407)	chr6	0.751	0.689	-0.061	0.0312
515	cg18503693	FAM155A (+595468)	chr13	0.623	0.561	-0.062	0.0131
516	cg10491108	TST (+6245)	chr22	0.645	0.583	-0.062	0.0384
517	cg22647161	TMPO (-223043)	chr12	0.595	0.533	-0.062	0.0017
518	cg26111308	TVP23B (+14743)	chr17	0.524	0.462	-0.062	0.0173
519	cg00464738	HLA-G (+35493)	chr6	0.784	0.722	-0.062	0.0009
520	cg10432947	NAT8L (+1203)	chr4	0.583	0.521	-0.062	0.0061

Table S6. Continued

521		(distance in bp)					P.Value
JZ 1	cg09430341	CCDC17 (-481)	chr1	0.766	0.703	-0.063	0.0054
522	cg08617160	MIER2 (-520)	chr19	0.537	0.475	-0.063	0.0058
523	cg22871949	NOM1 (-6814)	chr7	0.641	0.578	-0.063	0.0007
524	cg22545206	DDX18 (+45274)	chr2	0.523	0.460	-0.063	0.0084
525	cg07442889	SIGLEC5 (-914)	chr19	0.698	0.635	-0.063	0.0207
526	cg12060669	R3HCC1 (+33863)	chr8	0.323	0.259	-0.064	0.0443
527	cg17014647	GMPR (+192496)	chr6	0.603	0.539	-0.064	0.0011
528	cg22599254	BCAR3 (+126150)	chr1	0.863	0.799	-0.064	0.0027
529	cg09419670	PSMD5 (-405)	chr9	0.215	0.151	-0.064	0.0388
530	cg06940110	DDX18 (+44205)	chr2	0.498	0.434	-0.064	0.0201
531	cg11092486	RPP40 (-83324)	chr6	0.547	0.482	-0.064	0.0252
532	cg17014757	CHI3L1 (-221)	chr1	0.398	0.334	-0.064	0.0256
533	cg15838333	PCNXL4 (-4189)	chr14	0.684	0.619	-0.065	0.0211
534	cg05915609	PRSS22 (+3716)	chr16	0.650	0.585	-0.065	0.0105
535	cg22526555	KCNJ15 (-49635)	chr21	0.774	0.709	-0.065	0.0026
536	cg26011615	BATF3 (+34020)	chr1	0.692	0.627	-0.065	0.0003
537	cg19708055	C6orf123 (+151983)	chr6	0.644	0.578	-0.065	0.0027
538	cg14248883	SERP2 (+30700)	chr13	0.739	0.674	-0.065	0.0053
539	cg10852875	IRX2 (+214079)	chr5	0.586	0.521	-0.066	0.0030
540	cg08219700	IMPAD1 (-149624)	chr8	0.485	0.419	-0.066	0.0201
541	cg10292709	MCPH1 (-435562)	chr8	0.719	0.653	-0.066	0.0091
542	cg00073565	ZFPM2 (+131789)	chr8	0.562	0.496	-0.066	0.0279
543	cg03994477	FKBP4 (-75225)	chr12	0.556	0.489	-0.066	0.0007
544	cg27565337	RASA3 (+42024)	chr13	0.543	0.476	-0.067	0.0274
545	cg04580344	KIAA0408 (-16487)	chr6	0.728	0.661	-0.067	0.0053
546	cg06068545	SMYD2 (+81413)	chr1	0.161	0.094	-0.067	0.0219
547	cg15634083	HLA-B (+86056)	chr6	0.203	0.136	-0.067	0.0041
548	cg23441030	CACYBP (-59405)	chr1	0.716	0.648	-0.067	0.0001
549	cg06143315	CXXC11 (+138431)	chr2	0.769	0.702	-0.067	0.0201
550	cg19097082	ZBTB44 (-16742)	chr11	0.732	0.664	-0.068	0.0024
551	cg10907232	FAM49B (+44722)	chr8	0.790	0.722	-0.068	0.0012
552	cg16048001	PPP1R12B (+30298)	chr1	0.787	0.719	-0.068	0.0017
553	cg10756719	NKX6-1 (+118018)	chr4	0.736	0.668	-0.068	0.0001
554	cg08557536	ZNF112 (-689)	chr19	0.516	0.447	-0.069	0.0045
555	cg09798387	DEFB115 (-321358)	chr20	0.382	0.313	-0.069	0.0059

Table S6. Continued

Nr.	probe ID	nearest gene (distance in bp)	chr	NU_mean	HU_mean	dB	P.Value
556	cg04974804	HTR1D (-594)	chr1	0.733	0.664	-0.070	0.0022
557	cg02603861	NONE	chr14	0.418	0.348	-0.070	0.0053
558	cg00783857	SYT2 (+104642)	chr1	0.782	0.712	-0.070	0.0015
559	cg18174881	MIS18BP1 (-749)	chr14	0.710	0.640	-0.070	0.0006
560	cg02825122	ZHX2 (-97192)	chr8	0.784	0.714	-0.071	0.0139
561	cg20478239	COBL (-159980)	chr7	0.696	0.625	-0.071	0.0044
562	cg12011299	ADH4 (-99)	chr4	0.609	0.537	-0.071	0.0121
563	cg11494091	GH2 (-233)	chr17	0.711	0.640	-0.072	0.0156
564	cg03804706	SYT2 (+115163)	chr1	0.775	0.703	-0.072	0.0007
565	cg00191853	SPAG1 (+7078)	chr8	0.506	0.434	-0.072	0.0277
566	cg27562174	ADH4 (+2)	chr4	0.740	0.667	-0.073	0.0203
567	cg06083423	RHOU (+244657)	chr1	0.690	0.617	-0.073	0.0112
568	cg05056638	NEFM (+30300)	chr8	0.595	0.522	-0.073	0.0026
569	cg05697751	DUSP16 (+4582)	chr12	0.786	0.713	-0.073	0.0056
570	cg17765025	SUCLG1 (+581435)	chr2	0.747	0.674	-0.073	0.0027
571	cg24008280	PLD5 (-288775)	chr1	0.643	0.569	-0.073	0.0213
572	cg09027495	TBC1D2B (+210643)	chr15	0.735	0.661	-0.073	0.0022
573	cg04603290	TNFSF14 (+9947)	chr19	0.624	0.550	-0.074	0.0017
574	cg06489993	CALM3 (-21497)	chr19	0.640	0.566	-0.074	0.0190
575	cg21720175	MAF (-53056)	chr16	0.537	0.462	-0.074	0.0343
576	cg14393316	CAMSAP1 (+86740)	chr9	0.780	0.705	-0.075	0.0010
577	cg13912224	MCM3 (-22449)	chr6	0.497	0.422	-0.075	0.0386
578	cg18325044	HLA-G (+74145)	chr6	0.814	0.739	-0.076	0.0051
579	cg16270721	EXOSC5 (-9704)	chr19	0.401	0.325	-0.076	0.0361
580	cg11061773	TSC22D2 (-156570)	chr3	0.760	0.683	-0.076	0.0188
581	cg11685843	ADAM29 (+509663)	chr4	0.628	0.551	-0.076	0.0015
582	cg07569483	NLRP9 (-8089)	chr19	0.638	0.562	-0.076	0.0388
583	cg01813171	HLA-G (-32746)	chr6	0.720	0.643	-0.077	0.0173
584	cg08414882	BCMO1 (-15730)	chr16	0.595	0.517	-0.077	0.0095
585	cg03911306	DAZL (-1998)	chr3	0.727	0.650	-0.077	0.0021
586	cg01880147	FCGR3B (-8389)	chr1	0.706	0.628	-0.078	0.0264
587	cg22629375	OSCAR (+6096)	chr19	0.539	0.461	-0.078	0.0362
588	cg10661558	LIPI (+136111)	chr21	0.732	0.654	-0.078	0.0002
589	cg24480926	SFSWAP (-276103)	chr12	0.633	0.555	-0.078	0.0002
590	cg24213669	DDX18 (+44351)	chr2	0.472	0.393	-0.079	0.0029

Table S6. Continued

Nr.	probe ID	nearest gene (distance in bp)	chr	NU_mean	HU_mean	dB	P.Value
591	cg16324669	CDK11A (-8318)	chr1	0.847	0.768	-0.079	0.0448
592	cg17056703	SYCP2L (+65575)	chr6	0.792	0.712	-0.079	0.0133
593	cg07753967	DEFB115 (-233815)	chr20	0.287	0.208	-0.080	0.0401
594	cg03787837	HLA-DQA1 (+252)	chr6	0.477	0.397	-0.080	0.0306
595	cg20811988	DEFB115 (-233543)	chr20	0.273	0.193	-0.080	0.0118
596	cg18220841	BANP (+156623)	chr16	0.553	0.473	-0.080	0.0236
597	cg22223119	STK24 (+78568)	chr13	0.542	0.462	-0.080	0.0080
598	cg07195891	CLEC4C (+1997)	chr12	0.729	0.648	-0.080	0.0117
599	cg10871684	PLB1 (-44639)	chr2	0.859	0.779	-0.081	0.0147
600	cg22445217	QKI (+585402)	chr6	0.695	0.614	-0.081	0.0104
601	cg05758861	BAI1 (+50033)	chr8	0.754	0.673	-0.081	0.0001
602	cg22744079	PLRG1 (+60727)	chr4	0.614	0.532	-0.081	0.0009
603	cg15563854	TLE1 (-59)	chr9	0.200	0.118	-0.082	0.0004
604	cg20390711	KIAA0408 (-16148)	chr6	0.733	0.651	-0.083	0.0009
605	cg14079463	KIAA0408 (-16454)	chr6	0.563	0.481	-0.083	0.0227
606	cg09829303	CALD1 (-44627)	chr7	0.674	0.591	-0.083	0.0004
607	cg09516963	DYRK2 (-56)	chr12	0.320	0.237	-0.083	0.0017
608	cg22457256	AZGP1 (-1085)	chr7	0.662	0.579	-0.083	0.0010
609	cg22032020	MEF2A (+15666)	chr15	0.721	0.637	-0.083	0.0420
610	cg13469777	ZNRD1 (-50410)	chr6	0.676	0.591	-0.085	0.0141
611	cg06451157	HLA-G (+73540)	chr6	0.795	0.709	-0.085	0.0013
612	cg02783661	KDM5A (-3573)	chr12	0.614	0.529	-0.085	0.0117
613	cg24433124	IER3 (-43638)	chr6	0.611	0.524	-0.086	0.0383
614	cg04692312	DEFB115 (-326651)	chr20	0.278	0.191	-0.087	0.0028
615	cg18349077	TMEM87B (+30103)	chr2	0.524	0.436	-0.088	0.0122
616	cg23904161	ING1 (+98212)	chr13	0.542	0.452	-0.090	0.0135
617	cg27286337	NKX6-2 (+44276)	chr10	0.607	0.518	-0.090	0.0327
618	cg19729930	BOLA3 (+17249)	chr2	0.599	0.509	-0.090	0.0096
619	cg10805896	PLXNA4 (-88990)	chr7	0.444	0.354	-0.090	0.0033
620	cg13139335	C8orf37 (-333487)	chr8	0.465	0.374	-0.091	0.0173
621	cg11581472	SLC25A12 (+83511)	chr2	0.767	0.675	-0.091	0.0014
622	cg20926353	TLE1 (+862)	chr9	0.299	0.206	-0.093	0.0007
623	cg10804687	HLA-G (+64765)	chr6	0.860	0.766	-0.094	0.0061
624	cg00063654	OXNAD1 (+106372)	chr3	0.712	0.618	-0.094	0.0003
625	cg22425359	IRX2 (+335898)	chr5	0.810	0.716	-0.095	0.0061

Table S6. Continued

Nr.	probe ID	nearest gene (distance in bp)	chr	NU_mean	HU_mean	dB	P.Value
626	cg22945019	RASGRP3 (-174836)	chr2	0.739	0.644	-0.095	0.0263
627	cg01966510	ZSCAN2 (-68809)	chr15	0.619	0.523	-0.096	0.0007
628	cg01017244	BOLA3 (+17594)	chr2	0.720	0.624	-0.096	0.0037
629	cg10892585	ZNF138 (+43878)	chr7	0.773	0.676	-0.097	0.0012
630	cg23024343	DUS4L (-2653)	chr7	0.605	0.508	-0.097	0.0321
631	cg12060786	HSPA1B (+8207)	chr6	0.267	0.170	-0.097	0.0184
632	cg10474018	HLA-G (+65261)	chr6	0.873	0.775	-0.098	0.0011
633	cg00399683	DPP6 (-640390)	chr7	0.698	0.600	-0.098	0.0027
634	cg15514307	PPP2CA (-20989)	chr5	0.746	0.647	-0.099	0.0185
635	cg20891558	BOLA3 (+17270)	chr2	0.569	0.470	-0.099	0.0141
636	cg21717724	PSMD5 (+748)	chr9	0.604	0.504	-0.099	0.0138
637	cg26127187	HLA-G (+62040)	chr6	0.810	0.710	-0.100	0.0008
638	cg11955727	SUCLG1 (+581058)	chr2	0.783	0.683	-0.100	0.0007
639	cg06454464	TSNARE1 (+56622)	chr8	0.834	0.733	-0.101	0.0288
640	cg19899561	BDH2 (-38226)	chr4	0.832	0.731	-0.102	0.0213
641	cg14018363	HLA-G (+116510)	chr6	0.509	0.407	-0.102	0.0044
642	cg15482884	PNO1 (+38423)	chr2	0.576	0.474	-0.103	0.0198
643	cg12949927	ZNF138 (+43874)	chr7	0.750	0.647	-0.103	0.0009
644	cg00157199	DEFB115 (-293845)	chr20	0.439	0.336	-0.104	0.0037
645	cg26844603	TMEM87B (+30108)	chr2	0.631	0.528	-0.104	0.0107
646	cg14815891	DEFB115 (-233564)	chr20	0.290	0.186	-0.104	0.0217
647	cg20578893	HLA-G (+75305)	chr6	0.774	0.669	-0.105	0.0005
648	cg04057469	RFTN1 (+82369)	chr3	0.710	0.604	-0.106	0.0001
649	cg19077165	TCEB3CL2 (-2555)	chr18	0.747	0.640	-0.107	0.0002
650	cg26649688	HLA-G (+63605)	chr6	0.883	0.776	-0.107	0.0004
651	cg26964592	HLA-DMB (+4226)	chr6	0.566	0.457	-0.109	0.0046
652	cg18423635	HLA-G (+75181)	chr6	0.855	0.746	-0.109	0.0003
653	cg09104915	SHANK2 (-8851)	chr11	0.632	0.520	-0.112	0.0020
654	cg03126799	R3HCC1 (+33566)	chr8	0.657	0.545	-0.112	0.0254
655	cg24819596	ST3GAL5 (-18877)	chr2	0.765	0.649	-0.116	0.0008
656	cg09670175	KCNA6 (+5127)	chr12	0.734	0.618	-0.116	0.0230
657	cg12182020	NONE	chr3	0.415	0.298	-0.117	0.0297
658	cg15228509	CEP170 (+343635)	chr1	0.573	0.454	-0.119	0.0008
659	cg24179288	HLA-G (+72530)	chr6	0.866	0.747	-0.119	0.0002
660	cg00151744	AKAP13 (-32444)	chr15	0.576	0.456	-0.120	0.0012

Nr.	probe ID	nearest gene (distance in bp)	chr	NU_mean	HU_mean	dB	P.Value
661	cg03395495	GOLGA6L4 (-83129)	chr15	0.709	0.586	-0.123	0.0000
662	cg15825968	SFSWAP (-276155)	chr12	0.618	0.494	-0.125	0.0000
663	cg12927252	UPP2 (+18697)	chr2	0.715	0.590	-0.126	0.0305
664	cg20381372	ZFP14 (+68693)	chr19	0.574	0.448	-0.127	0.0266
665	cg17232014	HEBP1 (+14)	chr12	0.310	0.183	-0.127	0.0006
666	cg00727777	MYOM2 (+344659)	chr8	0.612	0.485	-0.128	0.0048
667	cg12046183	HLA-G (+65074)	chr6	0.727	0.597	-0.130	0.0013
668	cg13149459	PPP1R12B (+107853)	chr1	0.753	0.622	-0.131	0.0005
669	cg25817503	AFAP1 (+153311)	chr4	0.599	0.466	-0.133	0.0054
670	cg25343008	SYT2 (+142351)	chr1	0.701	0.564	-0.137	0.0004
671	cg05890377	BOLA3 (+17408)	chr2	0.601	0.461	-0.140	0.0014
672	cg13685349	STON2 (+14501)	chr14	0.736	0.586	-0.151	0.0047
673	cg17939448	FAM47E-STBD1 (-26347)	chr4	0.517	0.360	-0.157	0.0043
674	cg26919182	SYT2 (+90349)	chr1	0.720	0.541	-0.179	0.0004
675	cg13393919	GPBAR1 (-10899)	chr2	0.791	0.605	-0.186	0.0000
676	cg04462931	ZNF138 (+45259)	chr7	0.690	0.502	-0.188	0.0006

Table S7. Differentially methylated regions in whole blood of people with hyperuricemia compared to normouricemic people without cell composition correction

Nr.	nearest gene	DMR chr	DMR start	DMR end	Length	probes in dmr
1	HLA-G	chr6	29855325	29858360	3036	34
2	HLA-G	chr6	29893273	29895204	1932	33
3	HLA-B	chr6	31238388	31239411	1024	16
4	HLA-G	chr6	29910525	29911550	1026	14
5	FAM90A1	chr12	8380001	8381021	1021	11
6	SPACA7	chr13	112984602	112986285	1684	11
7	LPCAT1	chr5	1594021	1595048	1028	11
8	C1orf65	chr1	223566268	223567002	735	10
9	CLDN14	chr21	37915044	37915391	348	10
10	WRB	chr21	40759534	40760975	1442	10
11	PRDM9	chr5	23507243	23507752	510	10
12	CCNH	chr5	86708832	86709603	772	10
13	TLE1	chr9	84303358	84304983	1626	10
14	HLA-G	chr6	29795350	29795595	246	9
15	GLUD1	chr10	88853608	88854588	981	8
16	SPESP1	chr15	69222400	69223368	969	8
17	MTHFS	chr15	80189694	80190344	651	8
18	KIAA0408	chr6	127796287	127797286	1000	7
19	PLCH2	chr1	2390701	2391837	1137	6
20	FBRSL1	chr12	132903921	132904796	876	6
21	BCL2A1	chr15	80263132	80263923	792	6
22	IGF2BP1	chr17	47091521	47092272	752	6
23	SOCS3	chr17	76354621	76355288	668	6
24	SUCLG1	chr2	84105169	84105744	576	6
25	ANKRD23	chr2	97505275	97505787	513	6
26	DDX18	chr2	118616155	118617230	1076	6
27	FXR1	chr3	180587900	180588228	329	6
28	HLA-G	chr6	29868295	29870060	1766	6
29	POU6F2	chr7	39170497	39171113	617	6
30	DNAJB6	chr7	157405965	157406737	773	6
31	EGR2	chr10	64579032	64579646	615	5
32	BOLA3	chr2	74357527	74358223	697	5
33	USP16	chr21	30395808	30396586	779	5
34	C6orf123	chr6	168045268	168045888	621	5
35	ZNF12	chr7	6746799	6747037	239	5

Table S7. Continued

Nr.	nearest gene	DMR chr	DMR start	DMR end	Length	probes in dmr
36	NOM1	chr7	156735260	156735656	397	5
37	BAI1	chr8	143580770	143581481	712	5
38	CEP170	chr1	243053673	243054071	399	4
39	MTRNR2L7	chr10	37969553	37970316	764	4
40	TAGLN	chr11	117069849	117070046	198	4
41	NPIPB11	chr16	29296186	29296797	612	4
42	HOXB5	chr17	46675892	46676375	484	4
43	NOBOX	chr7	144107418	144107626	209	4
44	CNTNAP3B	chr9	44401998	44402433	436	4
45	KCNN3	chr1	154839813	154839983	171	3
46	TTC40	chr10	134778286	134778648	363	3
47	CALCB	chr11	15094338	15094382	45	3
48	SFSWAP	chr12	131919527	131919784	258	3
49	B3GNT3	chr19	17918795	17919173	379	3
50	ERBB4	chr2	213697579	213698158	580	3
51	CXXC11	chr2	242843821	242844174	354	3
52	BRD1	chr22	50098074	50098317	244	3
53	NAT8L	chr4	2062392	2063036	645	3
54	HIST1H2AD	chr6	26196580	26196794	215	3
55	HLA-G	chr6	29859520	29860016	497	3



Chapter 7

Trained immunity and inflammation in rheumatic diseases

Orsolya Gaal *, Medeea Badii *, Radu A. Popp¹, Tania O. Crişan#, Leo A.B. Joosten#

*These authors contributed equally to this work.

#These authors share senior authorship

Abstract

Background

Rheumatic diseases include a variety of autoimmune and autoinflammatory conditions that are characterised by musculoskeletal involvement and systemic disease. Both innate and adaptive immunity can contribute to the complex inflammatory processes that take part in the pathogenesis of these debilitating disorders.

Findings

Over the past decade, studies have led to a paradigm-shift around the concept of immune memory, generating the knowledge that cells of the innate immune system can develop a *de facto* memory mediated by epigenetic reprograming and metabolic changes (trained immunity). Here we provide an overview of current data that describe features of trained immunity in rheumatic diseases. We link evidence on inflammatory mediators and cytokine production, immunometabolism and epigenetic regulation of immunological programs, and outline the fact that trained immunity could play mechanistic roles in rheumatic diseases such as gout, rheumatoid arthritis, systemic lupus erythematosus or systemic sclerosis.

Conclusion

This review describes recent findings in several important rheumatic disorders and emphasizes changes in the functional program of innate immune cells that are reminiscent of a trained immune phenotype. Further assessment of trained immunity in rheumatic disease can provide targetable mechanisms that could potentially alter the disease symptomatology and evolution.

Introduction

Innate immune memory has been increasingly studied over the past decade. Features of immunological memory have been described in organisms that lack an adaptive immune system, such as plants or invertebrates, raising the hypothesis that innate immune memory is also present in vertebrates [1]. Studies in mammals have pointed out to a cross-protection between infections with different pathogens that is mediated by the activation of nonspecific innate immune mechanisms [1]. In humans, epidemiological studies have demonstrated beneficial effects of vaccines, such as Bacillus-Calmette-Guérin (BCG), measles, or oral polio vaccine against infections with pathogens other than the ones targeted by the vaccine itself [1]. In the last decade, the study of innate immune memory has been significantly moved forward as the concept of "trained immunity" was proposed by Netea et al. [2]. Trained immunity is currently defined as the long-term adaptation of myeloid cells, natural killer (NK) cells, and innate lymphoid cells (ILCs), mediated by metabolic rewiring and epigenetic reprogramming that follow an encounter with inflammatory triggers, infections or vaccinations. This functional reprogramming leads to an increased innate immune response to subsequent challenges [1][2].

Trained immunity is initiated in response to Pathogen-associated molecular patterns (PAMPs) or Damage-associated molecular patterns (DAMPs). DAMPs are endogenous molecules capable of inducing inflammatory responses under sterile conditions by modulation of inflammatory gene expression and inflammasome activation. Interleukin 6 [1], TNF- α [3] but also members of the IL-1 family such as interleukin 1 beta (IL-1β) [4], are among the proinflammatory cytokines involved in the immune responses of trained cells. We can note an increase in cytokine production when human monocytes are primed or trained in-vitro with microbial stimuli (such as beta-glucan or BCG)[5], but also with endogenous molecules such as oxidized low-density lipoprotein(oxLDL) [6], oxidized phospholipids (oxPAPC) [7], or urate [8]. These stimuli bind to Pattern Recognition Receptors (PRRs) on myeloid cells leading to the release of effector molecules and subsequent increased response to second stimulation (Figure 1) [1]. The increase in proinflammatory cytokines such as IL-6,, and IL-1\beta is present up to 3 months post-BCG vaccination in humans [9]. But how does this memory persist in time, considering that, in humans, both the non-classical and classical monocytes are short-lived? (11). It is now known that the innate immune memory is formed and maintained at the level of myeloid progenitor cells in the bone marrow [9] [10].

Innate immune memory, as opposed to adaptive memory, is a consequence of the functional adaptation of innate immune cells induced by epigenetic changes, such as alterations of chromatin marks, and by modifications in cellular metabolism, including a shift towards increased glycolysis and decreased oxidative phosphorylation (Figure 1). Histone modifications accumulate in response to training in monocytes, such as H3K4me3 at gene promoters, or H3K4me1 and H3K27ac at enhancer regions, and some of them persist even after the initial stimuli have been removed (e.g. H3K4me1) [11]. More recently, the inhibition of lysine methyltransferase G9a in BCG-trained monocytes resulted in a decrease of H3K9me2 marks at the promoters of pro-inflammatory genes, emphasizing the potential role of H3K9me2 in trained immunity [12].

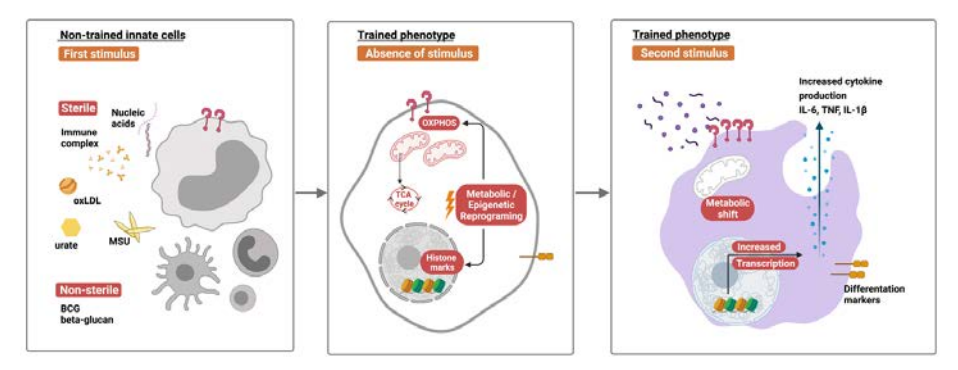


Figure 1 Schematic representation of innate immune memory development. Upon a first encounter of innate immune cells with a Pathogen Associated Molecular Pattern (e.g., BCG, beta-glucan)/or Damage Associated Molecule Pattern (e.g., urate, oxLDL, immune complexes), the down-stream signaling via Pattern Recognition Receptors (PRRs) promotes metabolic changes (e.g., altered glycolysis or OXPHOS) and epigenetic modifications (e.g., histone modifications, DNA methylation) which persist after the initial triggers have been removed. Consequently, on a subsequent stimulation, the cells exhibit faster and stronger inflammatory responses facilitated by the pre-existent epigenetic marks which allow for increased gene expression, giving rise to hyper-inflammatory responses.

Another hallmark of trained innate immune cells is metabolic rewiring. Proinflammatory cytokines or PRR ligands promote different metabolic pathways in monocytes and modulate the mammalian target of rapamycin (mTOR), which is a central metabolic regulator of immunity. Classical induction of trained immunity by beta-glucan leads to a shift of cellular metabolism from oxidative phosphorylation (OXPHOS) towards aerobic glycolysis via the mTOR/HIF1a/Akt pathway [13]. LPS-derived macrophages express a strong glycolysis signature known as the Warburg effect, associated with increased pro-inflammatory cytokine production. Mannose, natural C-2 epimer of glucose, prevents LPS-induced macrophage activation by impairing *ll1B* gene expression and therefore attenuating inflammation. Such effect results from inhibition of glucose metabolism and suppression of succinate-mediated HIF-1α activation [14]. Along with increased glycolysis, beta-glucan-trained monocytes display an increased activity of the cholesterol synthesis pathway and elevated mevalonate, which in turn amplifies the inflammatory response through an IGF1R-mTOR mediated pathway [15]. Treatment with fumarate, a TCA (tricarboxylic acid) cycle metabolite, leads to increased TNF-α production upon LPS stimulation in monocytes, along with ultrastructural changes of the mitochondria and elevated membrane potential that could propose mitochondrial activation. [3]. Moreover, itaconate, a metabolite that can alter the TCA cycle, contributes to immune tolerance and has been associated with the prevention of immunopathology during Mycobacterium tuberculosis infection [16]. Taken together, these processes indicate that cells displaying a trained innate immune phenotype show alterations in the cellular metabolism and that metabolic changes can directly impact the immune response of the cell.

As mentioned above, trained immunity can have a beneficial role when referring to cross-protection in the case of infection with various pathogens, but it can also contribute to the worsening of autoimmune or autoinflammatory diseases by contributing to chronic inflammation. We posit that trained immunity is a process that takes place in cells of patients with autoinflammatory or autoimmune rheumatic diseases, potentially predisposing to persistent inflammation and exacerbation of symptoms (Figure 2). An extensive review of the literature is beyond the scope of this report, as it has been elaborated in more detail elsewhere [17], instead we focus here on recent studies that contribute to our knowledge on epigenetic and metabolic changes in innate immune cells revealing the potential roles of innate immune training in several rheumatic disorders.

Gout

Gout is a chronic inflammatory arthritis generally affecting middle-aged men and the elderly population caused by monosodium urate (MSU) crystal deposition and inflammation within joints and periarticular structures. The MSU crystals form when serum urate concentrations surpass the solubility threshold, leading to precipitation into needle-shaped crystals. Serum urate above physiological levels(0.36 mmol/l or 6 mg/dl), is defined as hyperuricemia [18] [19]. The IL-1 family members play an important role in gout, particularly IL-1β released by MSU-stimulated monocytes and macrophages which further contribute to the pathogenesis of the flares. MSU crystals trigger gout flares by activating the NLRP3 inflammasome [20]. The gout flare is characterized by secretion of pro-inflammatory cytokines such as IL-1 β by the resident macrophages, neutrophilic infiltration in the synovial tissue and fluid, redness and swelling in the affected area [21]. In contrast, IL-1Ra has a counterbalancing role, binding to IL-1 receptor type 1 and competitively inhibiting further IL-1β signalling [22].

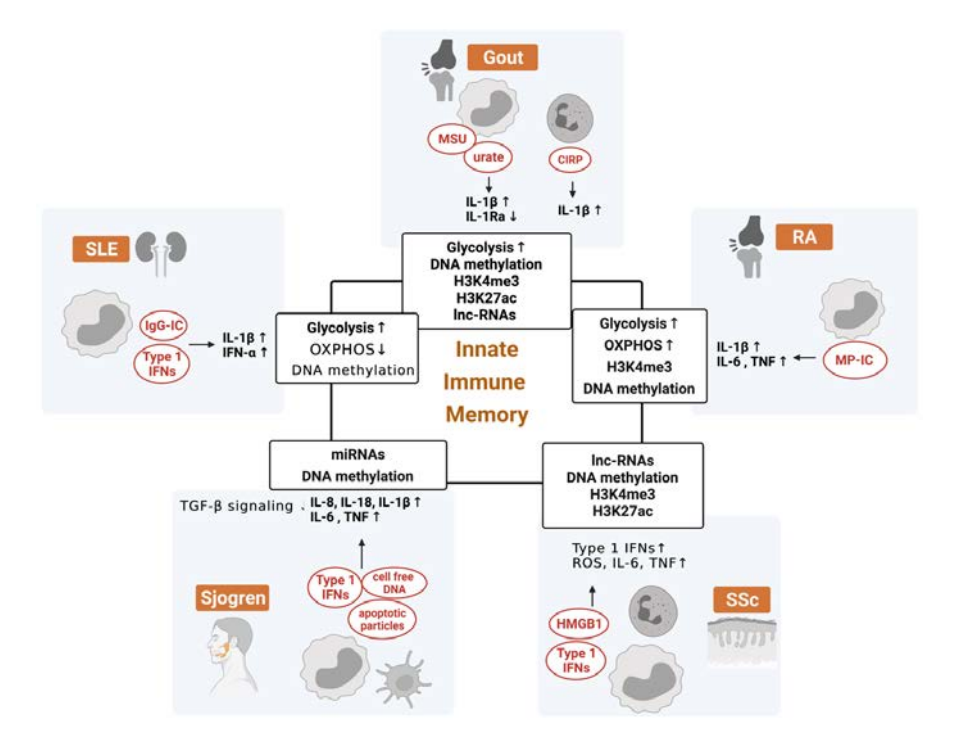


Figure 2 Potential mediators of innate immune memory in rheumatic disorders. Innate immune memory formation follows through epigenetic and metabolic rewiring of the myeloid cells. Certain endogenous or exogenous stimuli initiate inflammatory responses and alterations in the metabolic pathways (e.g., enhanced glycolysis) or changes in the epigenetic blueprint (e.g., hyper/hypo methylation of DNA regions, histone modifications) that will further affect how the cells respond (e.g., increased transcription of inflammatory genes) contributing to the induction, maintenance, or even worsening of the symptoms in rheumatic disorders. In gout, MSU-treated macrophages reveal a GLUT1-mediated glucose uptake and subsequent enhanced glycolysis to promote IL-1 β production. Additionally, soluble urate primes circulating monocytes towards an elevated production of IL-1β and reduced IL-1Ra. Hyperuricemia correlated with changes in DNA methylation patterns or differential enrichment of histone modifications H3K4me3 and H3K27ac at promoters of genes. Moreover, the NLRP3 inflammasome in neutrophils of gout patients could be primed by the cold-inducible RNAbinding protein (CIRP) to produce increased levels of IL-1β on a later stimulation with MSU crystals. PBMCs of gout patients show differential expression of several LncRNAs. In RA, common increased proinflammatory mediators are IL-6, TNF and IL-1β. The elevated cytokine responses could be attributed to an altered epigenetic landscape such as histone modifications (H3K4me3) at the promoter region of RANK-L in monocytes. Immune complexes MP-IC can drive monocytes towards a M1-like phonotype differentiation with increased IL-1β, IL-6 and TNF production. LPS-stimulated monocytes from RA patients display altered cellular metabolism, in particular increased glycolysis and OXPHOS. Genes in RA might be differentially expressed via DNA methylation. The type 1 interferon (IFN1) gene signature is one of the hallmarks of SLE in myeloid cells and DNA methylation is a possible epigenetic mechanism by which these genes are regulated. Additionally, over-production of autoantibodies and further immune complex formation stimulate monocyte-derived-macrphages and kidney macrophages to results in an altered cell metabolism along with elevated levels of pro-inflammatory mediators such as IL-1ß or IFN-a. In primary Sjögren syndrome (pSS), apoptotic particles stimulate dendritic cells to

support autoinflammation by production of IL-6, TNF and IL-8. Additionally, cell free-DNA present in the serum of pSS patients primes the NLRP3 inflammasome of monocytes for increased IL-1β and IL-18 (ref52). miRNAs were found associated to pSS by supressing the TGFβ signalling pathway. IFN1 genes in pSS might be regulated by DNA methylation. HMGB1, released from activated platelets of patients with SSc, promotes fibrosis while modulating the activity of monocytes and neutrophils as to maintain the vasculopathy associated with the disease (increased pro-inflammatory cytokines, increased ROS). Changes in histone marks H3K4me3 and H3K27ac, IncRNAs and DNA methylation could explain how IFN1 genes are regulated in patients with SSc.

MSU crystals are an important characteristic of the gout pathogenesis and act as DAMPS to activate the NLRP3 inflammasome. The elevated levels of IL-1B and increased expression of NLRP3 inflammasome in response to MSU stimulation in macrophages are accompanied by a GLUT1-mediated glucose uptake and a cellular metabolic shift towards upregulated glycolysis [23]. Recently, it has been shown that soluble urate can also activate the inflammasome [24], while other investigations argue that the precipitation of urate into crystals is required for the activation of NLRP3 [25]. In addition, inflammasome-independent effects of MSU were also reported in macrophages, and this was shown to be mediated by JNK phosphorylation and subsequent translocation of the transcription factor JUN to gene regions that regulate inflammation and metabolism [26].

Another described DAMP that might contribute to the gout pathogenesis is the cold-inducible RNA-binding protein (CIRP), which, through the priming of the NLRP3 inflammasome in neutrophils, leads to an increase of cleaved IL-1ß levels after a subsequent stimulation with MSU crystals [27].

Notably, in-vitro treatment of human monocytes with soluble urate primes the cells to a production of increased IL-1\beta, and decreased IL-1Ra following a subsequent LPS stimulation, and this effect on cytokine production is observed at the level of gene transcription. These changes are mediated by activation of the AKT–PRAS40 pathway and inhibition of autophagy, which leads to IL-1 mediated inflammation [28]. This facilitated state of IL-1β production is long lived, and the imprinting seems to be mediated by epigenetic reprogramming, because inhibitors of histone methyl transferases abolished the "reprogramming" effect of urate [29]. Moreover, in human monocytes, urate treatment resulted in enrichment of histone modifications H3K4me3 and H3K27ac at promoters of genes such as MED24, CSF3, TAF1C, DNAAF1, and downregulation at APOE promoter. In addition, the assessment of whole blood DNA of hyperuricemic individuals revealed several differentially methylated regions in comparison to normouricemic individuals (e.g. HLA-G, IFITM3, PRKAB2), suggesting that urate induced inflammatory responses might be epigenetically regulated [8].

When monocytes of gout patients were investigated for DNA methylation, results revealed differentially methylated sites associated with IL-1 β signalling and with gouty inflammation, suggesting that DNA methylation might be an important regulator of cytokine production in monocytes. [30]. In addition, PBMCs of gout patients show differentially methylated regions in known gout risk genes (e.g., *SLC2A9, ABCC9*), together with transcription factors that have enriched motifs for genes involved in osteoclast and T helper cell differentiation (e.g. (*NFATC2, MEF2C*), indicating that epigenetic changes might take place in both innate and adaptive immunity pathways. [31]. Long non-coding RNAs are emerging as novel biomarkers in various disorders, and a first such study performed on samples from gout patients reveals differentially expressed Inc-RNAs in acute and intercritical phase that associated with inflammatory markers in these patients [32].

The altered cytokine profile observed in immune cells, both at protein and gene level, along with the epigenetic changes, enforce the hypothesis that trained immunity might be present in myeloid cells of patients with gout.

Rheumatoid arthritis (RA)

Rheumatoid arthritis (RA), a chronic systemic autoimmune disease which primarily affects women, is defined by persistent synovial inflammation in small diarthrodial joints, progressive cartilage and bone destruction along with autoantibody production [33]. The cause of cartilage and bone destruction present in RA is mainly caused by macrophages via the production of cytokines and chemokines and by the regulation of osteoclast activity [34]. The role of the innate immune system is gaining much attention in the development of RA, and indications that innate immune memory could be relevant to this disease have been observed.

Cytokines play a crucial role in the pathogenesis of the disorder, with TNF or IL-6 having an important role in the induction of osteoclasts, which may contribute to joint destruction [35]; IL-1ß is proven to have stimulatory effects on osteoclastogenesis [36], which can be accompanied by initiation of synovial cell proliferation and matrix metalloproteinase induction by chondrocytes, together contributing to bone destruction [37]. The presence of autoantibodies is another important hallmark of RA. Extracellular vesicles, like microparticles (MP), can form immune complexes with autoantibodies (MP-IC) and further promote the proinflammatory differentiation of macrophages to an M1-like profile while supporting B-cell survival [38]. *in vitro* data on monocyte-derived macrophages from patients with RA and healthy controls in the presence of MP-IC shows a more proinflammatory M1-like phenotype which could not be completely reversed by IL-4 treatment [38].

Monocytes from RA patients seem to be more prone to metabolic reprogramming with LPS for sustained induction of pro-inflammatory responses. The cells display significantly higher baseline OCR, maximal respiratory capacity and ATP synthesis compared to LPS-activated healthy monocytes [39]. Enhanced glycolysis, as indicated by high concentrations of lactate and distinctly low concentrations of glucose, is observed in the inflamed joint of patients with RA [40]. These metabolic changes are suggestive of a trained immunity phenotype.

Epigenetic modifications, such as histone acetylation was shown to be involved in the regulation of chemokine C-C motif ligand 2 (CCL2), also known as monocyte chemoattractant protein-1 (MCP1), associated with disease activity in RA. LPSstimulated THP-1 cells show increased histone acetylation of H3 and H4 in the CCL2 promoter region [41]. While analysing PBMCs from patients with RA, the gene expression of activation marker histone variant H3.3 encoded by H3F3A was increased in patients with RA in comparison with healthy controls [42]. In addition, there is also evidence of hypomethylation at the TNF-a promotor in CD4+T-cells along with differential expression of 3 cytokines (IL-21, IL-34 and RANKL). Although most DNA methylation changes are seen in T-cells, monocytes also have some differentially methylated genes in RA [43].

Surprisingly however, TNF has been recently reported to also be able to serve as a critical downregulator of CD14+ monocyte differentiation into osteoclasts in homeostatic conditions [44]. TNF inhibited osteoclastogenesis and was associated to a reduction in H3K4me3 enrichment at the promoter region of RANK-L, which plays a key role in the osteoclast formation and activity [44]. At the same time, a population of circulating non-monocyte osteoclast precursors were epigenetically preconditioned to neglect TNF-mediated signalling (32, 40). Interestingly, monocytes from a subset of patients with active RA were shown to have altered epigenetic states which made them resistant to the homeostatic pathway of TNFdependent inhibition of osteoclast differentiation. This suggests that previous epigenetic processes could aggravate erosive processes in different subsets of patients and that alternative mechanisms may be at play in the progression of RA. The cause of such initial epigenetic reprogramming is yet unknown, but addressing the possibility of trained immunity occurring and contributing to the pathogenesis and response to therapy in RA is worthwhile.

Systemic Lupus Erythematosus (SLE)

SLE is a complex autoimmune disease affecting females more frequently than males, characterized by over-production of autoantibodies, multi-organ involvement and extreme variability in patient phenotype. The main cause remains elusive and to date there is not a cure available, but innate immune cells are described to be involved in the pathogenesis of the disease. CD16+ monocytes play an important role in the pathogenesis of SLE and exhibit a proinflammatory phenotype with elevated CD80, CD86, HLA-DR, and CX3CR1 expression on the cell surface. This cell subset is enriched in SLE and has an exacerbated capacity to promote CD4+ T cell polarization into a Th17 phenotype. CD16+ monocytes can also drive CD19+ B cells to differentiate into plasma B cells and regulatory B cells with more lg production [45]. Transcriptomic assessment of hematopoietic stem and progenitor cells (HSPC) in mice and patients with SLE revealed a strong myeloid signature which correlated to transcriptional activation of cytokines and chemokines [46]. This indicates that priming of the immune cells in SLE could already happen in the bone marrow in a similar manner as seen in trained immunity scenarios [46].

The type 1 interferon (IFN1) gene signature is one of the hallmarks of SLE [47]. Moreover, prior exposure to IFNα results in enhanced IFNα-producing capacity of monocytes [48]. TNF is important in the pathogenesis of SLE and crosstalk signalling between TNF and IFN1 can reshape the chromatin in order to work as an "integration node" that regulates transcriptional output and reprograms the inflammatory responses induced by TLR4 ligands. On the one hand, TNF extensively reprogrammed human macrophages in response to LPS tolerization and almost abolished TLR4 signalling in these cells. On the other hand, IFN1 effectively ended TNF-induced cross-tolerance by priming chromatin to enable strong transcriptional responses to weak signals and to prevent the silencing of T cell genes. This suggests that IFN1 is able to regulate chromatin at distinct sets of genes that encode for inflammatory mediators, in addition to canonical ISGs [49].

The role of IgG-immune complexes (IC) has widely been described in SLE but the mechanisms by which they trigger organ inflammation have long remained unresolved. Jing C. *et al* have found that stimulation of monocyte-derived-macrphages and of kidney macrophages during antibody-mediated nephritis with IgG-ICs results in a altered cell metabolism with elevated glycolisis and reduced OXPHOS and fatty acid metabolism. This shift is mediated by the HIF1 α /mTOR pathway, necessary for the induction of ROS production and proinflammatory mediators such as IL-1 β and PG2E. Furthermore, glycolysis inhibition with 2-Deoxy-D-glucose significantly diminished tissue inflammation, underlining its therapeutic potential in treating in lupus nephritis [50]. This immunometabolic profile is reminiscent of the metabolic shift observed in cells trained with β -glucan [51]. In addition to this, T cells and neutrophils in patients with SLE manifest increased

levels of reactive oxygen species (ROS) and inhibiting mitochondrial ROS (mtROS) and oxidative stress can mitigate certain aspects of autoimmune disease and organ damage in lupus-predisposed mice [52]. Role of NET formation by neutrophils in sterile inflammation remains largely unresolved, but the mitochondria might play an important role in the generation of NETs via ROS production and release of oxidized mtDNA [53].

Several studies have focused on epigenetic modification such as DNA methylation to answer the question on how certain genes are regulated in SLE. Whole-genome transcription and DNA methylation analysis of peripheral blood mononuclear cells identified differential gene regulation in pathways involving IFN, TLR, accompanied by abnormal DNA methylation and elevated cytokine production (e.g., IL-17A, IP-10, bFGF, TNF, IL-6, IL-15, GM-CSF, IL-1Ra, IL-5, and IL-12p70) in SLE patients compared to healthy individuals [54]. Also, in a paediatric SLE (pSLE) genomewide DNA methylation analysis, the DNAm signature comprised 21 CpG sites that point to differential loss of DNAm across the major immune cell lineages of pSLE patients. Epigenetic reprogramming of type I interferon-related genes is a widespread phenomenon in blood cells of pSLE patients, which can occur in the haematopoietic stem cells [55]. Furthermore, H3K4me3 is a major chromatin mark regulating gene transcription and histone modifications in SLE across different cell types. Differential H3K4me3 enrichment was observed in monocytes at promoters and enhancers of genes related to inflammatory response such as CCL2, CCL7, CCR1, CXCR1, IL-1R1, and TRIM1 and TNF signaling.

Finally, transcriptomic profiling in patients with the disease reveals no differences when comparing active and inactive SLE. These results suggest that immune cells from inactive SLE patients maintain a transcriptomic profile resembling that of active SLE, despite favourable treatment [56]. Based on these results, it is tempting to speculate that these effects could be mediated by persistent epigenetic changes in trained immune cells.

Sjögren syndrome

Primary Sjögren syndrome (pSS) is a chronic autoimmune disease, most commonly present in middle aged women, associated with lymphocytic infiltration or immune complex deposition at exocrine glands, causing dryness of mucosal surfaces [57]. pSS often accompanies other systemic autoimmune diseases such as RA or SLE.

Several reports indicate that pSS patients depict elevated levels of cytokines, such as IL-6, IL-7, IL-18, IL-22 produced by epithelial cells, and TNF or IFN-y generated by regulatory B cells [58]. The secretion of proinflammatory cytokines in pSS was recently shown to be induced by epithelial cell-derived apoptotic particles which carry autoantigens and adjuvant nucleic acids [59]. These apoptotic particles are considered danger signals that stimulate plasmacytoid dendritic cells (pDCs) via TLR-7 and TLR-9, favouring the autoantibody production and autoinflammation [59]. Additionally, the NLRP3 inflammasome activation by monocytes in pSS patients is triggered due to build-up of proinflammatory cell free-DNA from pyroptotic macrophages in the blood circulation and the further infiltration into salivary gland tissues [60]. STAT1 phosphorylation following IFN-γ stimulation of PBMCS of pSS patients is significantly enhanced compared to controls, suggesting an important role for STAT1-mediated gene responses in patients with pSS [61]. Moreover, the expression of *SOCS1* and *SOCS3* mRNA is increased in pSS patients, indicating increased sensitivity of immune cells from patients with pSS to STAT1-activating signals, partly explaining the IFN signature observed in pSS [62].

Epigenetic modifications, such as DNA methylation, play an important role in the pathological process of the disease [63]. IFN1 inducible genes *IFI44L*, *MX1*, *PAARP9*, *EPSTI1* and *IFITM1* are among the genes that are hypomethylated in circulating monocytes isolated from patients with pSS [63]. In addition, miRNAs were also associated to pSS by supressing the TGFβ signalling pathway [64]. TGFβ1 plays an important role in the induction of fibrotic processes via the activation of the SMAD signalling pathway and it is observed to be an essential component in the transition phase from salivary gland inflammation to salivary gland fibrosis [64]. Yet, mir-146a is one of the miRNAs discovered to have higher expression in mouse primary macrophages, dendritic cells and neutrophils in the presence of TLR agonists, besides having a role in macrophage activation and control of proinflammatory cytokine production. In line with this, it is reported as being overexpressed in PBMCs from pSS patients and proven to activate the IL23/IL23R signalling pathway and promote Th17 cell differentiation *in vitro*[65].

These observations provide clues that epigenetic regulation in response to inflammatory triggers could alter the inflammatory signalling and contribute to the deregulation of immune processes in pSS. Albeit coincidental, these findings suggest that the study of innate immune training in both circulating and epithelial cells would be an interesting future research step in pSS.

Systemic sclerosis (SSc)

SSc is an autoimmune connective tissue disease consisting in immune dysfunction, fibrosis and vasculopathy, ultimately leading to multi-system involvement [66].

Innate immune cells play a major role in SSc pathophysiology, with mononuclear inflammatory cells infiltrating the perivascular and dermal areas at a very early stage of the disease [67]. Moreover, macrophages are presented as modulators of fibroblast activation as well as drivers of fibrosis. Interestingly, TGFβ, IL-6, and CCL2 are elevated in SSc macrophages and cannot be further induced by LPS under basal conditions. The basal release and synthesis of IL-6 in macrophages of patients with SSc drives STAT3 phosphorylation and immune activation [68].

Stimuli initiating inflammatory responses in SSc are still the subject of research. Microparticles released from activated platelets are abundant in the blood of patients with SSc and express the damage-associated molecular pattern (DAMP) HMGB1 [69]. HMGB1 promotes fibrosis while coordinating the actions of monocytes and neutrophils in deep vein thrombosis, sustaining the vasculopathy associated to the disease [69]. Another DAMP proposed lately in the literature is the tenascin-C, an endogenous TLR4 ligand with a likely pathogenetic role in SSc, being an essential promoter of tissue fibrosis [70]. Skin biopsies of SSc patients reveals tenascin-C as a highly upregulated matricellular protein associated with both TLR4 and IL-6 expression and the deposition of this protein might contribute to the progression of skin and lung fibrosis [70].

The effects of trained immunity in SSc inflammation and fibrosis were addressed in murine models and in co-culture models of macrophage-(HOCI)-fibroblasts using macrophages previously trained with BCG or low dose LPS. Depending on initial stimulus, trained macrophages exhibited different immunomodulatory properties in vitro and in vivo: training with BCG promoted T and B cell activation along with cytokine production and subsequent fibrosis, whereas low dose LPS promoted tolerance and diminished the fibro-inflammatory phenotype [67]. This indicates that trained immunity can be therapeutically targeted in SSc and also that trained immunity stimuli that are not directly related to the SSc pathogenesis could aggravate or dampen the inflammation and fibrosis observed in SSc.

Similarly to SLE or pSS, there is a strong type I IFN signature in SSc as well. Type I IFN pathway is dysfunctional at the epigenetic level in SSc patients, being associated to a hypomethylation status and upregulation of type I IFNassociated genes IFI44L, IFITM1, EIF2AK2, MX1, and PARP9 both in CD4+ and CD8+ T cells [71]. Recently, it has been shown that IFN\(\beta \) stimulation induces epigenetic changes (acquisition of chromatin marks such as altered histone H3.3 and H3K36 trimethylation) and transcriptional memory at interferon inducible genes Mx1, Ifit1, Oas1a granting faster and prominent transcription upon restimulation in mouse embryonic fibroblasts (MEFs) and bone marrow (BM)-derived macrophages. [72]. Moreover, transcriptome analysis of monocyte-derived macrophages of patients with SSc show enrichment of genes involved in increased metabolic rates (glycolysis, hypoxia and mammalian target of rapamycin (mTOR) signalling), all of which being linked with a proinflammatory activation profile [76].

Based on all evidence at the level of epigenetic profile, and considering the indications of immunometabolic changes, trained immunity might play a role in the pathogenesis and progression of SSc and holds promise for targeted immunotherapies.

Conclusions

The incidence of auto-inflammatory and auto-immune diseases is expected to increase in the near future, especially in developed and industrialized countries, highlighting the importance of finding novel therapeutic approaches in which trained immunity might constitute a relevant target. In this review, we present recent findings supporting the concept that trained immunity may be present in several autoinflammatory and autoimmune rheumatic diseases (Figure 2) and that it could contribute to the induction, maintenance, or even worsening of the symptoms. The main characteristics of innate immune memory are epigenetic modifications, altered cellular metabolism along with higher cytokine production. Here we provide an overview of recent findings which suggest that these trained immunity features are observed in rheumatic diseases, nevertheless, further studies are required to establish the precise mechanisms that underlie these processes in each of these examples. In addition to this, trained immunity may be an inflammatory process which can predispose individuals with rheumatic diseases to chronic secondary pathologies, such as atherosclerosis and cardiovascular disease risk in patients with RA or SLE, associated comorbidities like metabolic syndrome in gout or risk of lymphoma in pSS. Together, these results underpin the possible involvement of trained immunity in rheumatic diseases and their longterm complications and open new avenues for targetable mechanistic discoveries.

References

- [1] Netea MG, Domínguez-Andrés J, Barreiro LB, et al. Defining trained immunity and its role in health and disease. Nat Rev Immunol 2020; 20: 375;88.
- [2] Netea MG, Quintin J, Van Der Meer JWM. Trained immunity: A memory for innate host defense. Cell Host Microbe 2011; 9: 355;61.
- [3] Pérez-Hernández CA, Kern CC, Butkeviciute E, et al. Mitochondrial Signature in Human Monocytes and Resistance to Infection in C. elegans During Fumarate-Induced Innate Immune Training. Front Immunol 2020: 11: 1751.
- [4] Moorlag SJCFM, Röring RJ, Joosten LAB, Netea MG. The role of the interleukin-1 family in trained immunity. Immunol Rev 2018: 281: 28:39.
- Moorlag SJCFM, Khan N, Novakovic B, et al. β-Glucan Induces Protective Trained Immunity against Mycobacterium tuberculosis Infection: A Key Role for IL-1. Cell Rep 2020; 31: 107634.
- Groh LA, Ferreira A V, Helder L, et al. oxLDL-Induced Trained Immunity Is Dependent on Mitochondrial Metabolic Reprogramming. Immunometabolism 2021; 3: e210025.
- [7] Di Gioia M, Spreafico R, Springstead JR, et al. Endogenous oxidized phospholipids reprogram cellular metabolism and boost hyperinflammation. Nat Immunol 2020; 21: 42;53.
- Badii M, Gaal OI, Cleophas MC, et al. Urate-induced epigenetic modifications in myeloid cells. Arthritis Res Ther 2021; 23: 1;11.
- [9] Cirovic B, de Bree LCJ, Groh L, et al. BCG Vaccination in Humans Elicits Trained Immunity via the Hematopoietic Progenitor Compartment. Cell Host Microbe 2020; 28: 322;34.e5.
- [10] Mitroulis I, Ruppova K, Wang B, et al. Modulation of Myelopoiesis Progenitors Is an Integral Component of Trained Immunity. Cell 2018; 172: 147;61.e12.
- [11] Fanucchi S, Domínguez-Andrés J, Joosten LAB, Netea MG, Mhlanga MM. The Intersection of Epigenetics and Metabolism in Trained Immunity. Immunity 2021; 54: 32;43.
- [12] Mourits VP, van Puffelen JH, Novakovic B, et al. Lysine methyltransferase G9a is an important modulator of trained immunity. Clin Transl Immunol 2021; 10: e1253.
- [13] Arts RJW, Carvalho A, La Rocca C, et al. Immunometabolic Pathways in BCG-Induced Trained Immunity. Cell Rep 2016; 17: 2562;71.
- [14] Torretta S, Scagliola A, Ricci L, et al. D-mannose suppresses macrophage IL-1ß production. Nat Commun 2020; 11: 1;12.
- [15] Bekkering S, Arts RJW, Novakovic B, et al. Metabolic Induction of Trained Immunity through the Mevalonate Pathway. Cell 2018; 172: 135;46.e9.
- [16] Domínguez-Andrés J, Novakovic B, Li Y, et al. The Itaconate Pathway Is a Central Regulatory Node Linking Innate Immune Tolerance and Trained Immunity. Cell Metab 2019; 29: 211;20.e5.
- [17] Arts RJW, Joosten LAB, Netea MG. The potential role of trained immunity in autoimmune and autoinflammatory disorders. Front Immunol 2018; 9: 6;9.
- [18] Bardin T, Richette P. Definition of hyperuricemia and gouty conditions. Curr Opin Rheumatol 2014; 26: 186:91.
- [19] Bardin T. Hyperuricemia starts at 360 micromoles (6mg/dL). Joint Bone Spine 2015; 82: 141;3.
- [20] Dalbeth N, Merriman TR, Stamp LK. Gout. The Lancet 2016; 388: 2039;52.
- [21] Dalbeth N, Choi HK, Joosten LAB, et al. Gout. Nat Rev Dis Primers 2019; 5: 69.
- [22] Klück V, Liu R, Joosten LAB. The role of interleukin-1 family members in hyperuricemia and gout. Jointt Bone Spine 2021; 88: 105092.

- [23] Renaudin F, Orliaguet L, Castelli F, et al. Gout and pseudo-gout-related crystals promote GLUT1-mediated glycolysis that governs NLRP3 and interleukin-1β activation on macrophages. Ann Rheum Dis 2020: 79: 1506:14.
- [24] Braga TT, Forni MF, Correa-Costa M, et al. Soluble Uric Acid Activates the NLRP3 Inflammasome. Sci Rep 2017; 7: 1;14.
- [25] Alberts BM, Barber JS, Sacre SM, et al. Precipitation of soluble uric acid is necessary for *in Vitro* activation of the NLRP3 inflammasome in primary human monocytes. J Rheumatol 2019; 46: 1141;50.
- [26] Cobo I, Cheng A, Murillo-saich J, et al. Monosodium Urate Crystals regulate a unique JNK-dependent macrophage metabolic and inflammatory response. bioRxiv 2021 doi: https://doi.org/10.1101/2021.04.14.439881.
- [27] Fujita Y, Yago T, Matsumoto H, et al. Cold-inducible RNA-binding protein (CIRP) potentiates uric acid-induced IL-1β production. Arthritis Res Ther 2021; 23: 1;9.
- [28] Crişan TO, Cleophas MCP, Oosting M, et al. Soluble uric acid primes TLR-induced proinflammatory cytokine production by human primary cells via inhibition of IL-1Ra. Ann Rheum Dis 2016; 75: 755;62.
- [29] Crişan TO, Cleophas MCP, Novakovic B, et al. Uric acid priming in human monocytes is driven by the AKT-PRAS40 autophagy pathway. Proc Natl Acad Sci U S A 2017; 114: 5485-5490.
- [30] Tseng CC, Liao WT, Wong MC, et al. Cell lineage-specific methylome and genome alterations in gout. Aging (Albany NY) 2021; 13: 3843;63.
- [31] Wang Z, Zhao Y, Phipps-Green A, et al. Differential DNA Methylation of Networked Signaling, Transcriptional, Innate and Adaptive Immunity, and Osteoclastogenesis Genes and Pathways in Gout. Arthritis Rheumatol 2020; 72: 802;14.
- [32] Qing YF, Zheng JX, Tang YP, et al. LncRNAs Landscape in the patients of primary gout by microarray analysis. PLoS One 2021; 16: 1;17.
- [33] Sparks JA. Rheumatoid arthritis. Ann Intern Med 2019; 170: ITC1–ITC15.
- [34] Horwood NJ. Macrophage Polarization and Bone Formation: A review. Clin Rev Allergy Immunol 2016; 51: 79;86.
- [35] Yokota K, Sato K, Miyazaki T, et al. Characterization and Function of Tumor Necrosis Factor and Interleukin-6–Induced Osteoclasts in Rheumatoid Arthritis. Arthritis Rheumatol 2021; 73:1145;54.
- [36] Shiratori T, Kyumoto-Nakamura Y, Kukita A, et al. IL-1β Induces Pathologically Activated Osteoclasts Bearing Extremely High Levels of Resorbing Activity: A Possible Pathological Subpopulation of Osteoclasts, Accompanied by Suppressed Expression of Kindlin-3 and Talin-1. J Immunol 2018; 200: 218;28.
- [37] Dayer JM. The pivotal role of interleukin-1 in the clinical manifestations of rheumatoid arthritis. Rheumatology 2003; 42: 3;10.
- [38] Burbano C, Villar-Vesga J, Vásquez G, et al. Proinflammatory differentiation of macrophages through microparticles that form immune complexes leads to T-and B-cell activation in systemic autoimmune diseases. Front Immunol 2019; 10: 1;18.
- [39] McGarry T, Hanlon MM, Marzaioli V, et al. Rheumatoid arthritis CD14+ monocytes display metabolic and inflammatory dysfunction, a phenotype that precedes clinical manifestation of disease. Clin Transl Immunol 2021; 10: 1;18.
- [40] Qiu J, Wu B, Goodman SB, et al. Metabolic Control of Autoimmunity and Tissue Inflammation in Rheumatoid Arthritis. Front Immunol 2021; 12: 1;17.
- [41] Lin YC, Lin YC, Huang MY, et al. Tumor necrosis factor-alpha inhibitors suppress CCL2 chemokine in monocytes via epigenetic modification. Mol Immunol 2017; 83: 82;91.

- [42] Asadipour M, Hassan-Zadeh V, Aryaeian N, Shahram F, Mahmoudi M. Histone variants expression in peripheral blood mononuclear cells of patients with rheumatoid arthritis. Int J Rheum Dis 2018: 21: 1831:7.
- [43] Pitaksalee R, Burska AN, Ajaib S, et al. Differential CpG DNA methylation in peripheral naïve CD4+ T-cells in early rheumatoid arthritis patients. Clin Epigenetics 2020; 12: 1;16.
- [44] Ansalone C, Cole J, Chilaka S, et al. TNF is a homoeostatic regulator of distinct epigenetically primed human osteoclast precursors. Ann Rheum Dis 2021; 80: 748;57.
- [45] Zhu H, Hu F, Sun X, et al. CD16+ monocyte subset was enriched and functionally exacerbated in driving T-cell activation and B-cell response in systemic lupus erythematosus. Front Immunol 2016; 7: 1;15.
- [46] Grigoriou M, Banos A, Filia A, et al. Transcriptome reprogramming and myeloid skewing in haematopoietic stem and progenitor cells in systemic lupus erythematosus. Ann Rheum Dis 2019: 242:53.
- [47] Herrada AA, Escobedo N, Iruretagoyena M, et al. Innate immune cells' contribution to systemic lupus erythematosus. Front Immunol 2019; 10: 1;9.
- [48] Murayama G, Chiba A, Kuga T, et al. Inhibition of mTOR suppresses IFNa production and the STING pathway in monocytes from systemic lupus erythematosus patients. Rheumatol (United Kingdom) 2020; 59: 2992;3002.
- [49] Park SH, Kang K, Giannopoulou E, et al. Type i interferons and the cytokine TNF cooperatively reprogram the macrophage epigenome to promote inflammatory activation. Nat Immunol 2017; 18: 1104;16.
- [50] Jing C, Castro-Dopico T, Richoz N, et al. Macrophage metabolic reprogramming presents a therapeutic target in lupus nephritis. Proc Natl Acad Sci U S A 2020; 117: 15160;71.
- [51] Kumar V, Giamarellos-bourboulis EJ, Martens JHA, et al. mTOR/HIF1α-mediated aerobic glycolysis as metabolic basis for trained immunity. Science 2014; 345: 1;18.
- [52] Fortner KA, Blanco LP, Buskiewicz I, et al. Targeting mitochondrial oxidative stress with MitoQ reduces NET formation and kidney disease in lupus-prone MRL- lpr mice. Lupus Sci Med 2020; 7: e000387.
- [53] Lood C, Blanco LP, Purmalek MM, et al. Neutrophil extracellular traps enriched in oxidized mitochondrial DNA are interferogenic and contribute to lupus-like disease. Nat Med 2016; 22: 146;53.
- [54] Zhu H, Mi W, Luo H, et al. Whole-genome transcription and DNA methylation analysis of peripheral blood mononuclear cells identified aberrant gene regulation pathways in systemic lupus erythematosus. Arthritis Res Ther 2016; 18: 1;17.
- [55] Yeung KS, Lee TL, Mok MY, et al. Cell lineage-specific genome-wide DNA methylation analysis of patients with paediatric-onset systemic lupus erythematosus. Epigenetics 2019; 14: 341;51.
- [56] Panousis NI, Bertsias GK, Ongen H, et al. Combined genetic and transcriptome analysis of patients with SLE: distinct, targetable signatures for susceptibility and severity. Ann Rheum Dis 2019; 78: 1079;89.
- [57] Brito-Zerón P, Baldini C, Bootsma H, et al. Sjögren syndrome. Nat Rev Dis Prim 2016; 2: 1;20.
- [58] Srivastava A, Makarenkova HP. Innate immunity and biological therapies for the treatment of sjögren's syndrome. Int J Mol Sci 2020; 21: 1;45.
- [59] Ainola M, Porola P, Takakubo Y, et al. Activation of plasmacytoid dendritic cells by apoptotic particles – mechanism for the loss of immunological tolerance in Sjögren's syndrome. Clin Exp Immunol 2018; 191: 301;10.

- [60] Vakrakou AG, Boiu S, Ziakas PD, et al. Systemic activation of NLRP3 inflammasome in patients with severe primary Sjögren's syndrome fueled by inflammagenic DNA accumulations. J Autoimmun 2018: 91: 23:33.
- [61] Pertovaara M, Silvennoinen O, Isomäki P. Cytokine-induced STAT1 activation is increased in patients with primary Sjögren's syndrome. Clin Immunol 2016; 165: 60;7.
- [62] Yoshimoto K, Suzuki K, Takei E, Ikeda Y, Takeuchi T. Elevated expression of BAFF receptor, BR3, on monocytes correlates with B cell activation and clinical features of patients with primary Sjögren's syndrome. Arthritis Res Ther 2020; 22: 1;10.
- [63] Luo X, Peng Y, Chen Y-Y, et al. Genome-wide DNA methylation patterns in monocytes derived from patients with primary Sjogren syndrome. Chin Med J (Engl) 2021; 134: 1310;6.
- [64] Sisto M, Lorusso L, Ingravallo G, et al. The TGF-β1 signaling pathway as an attractive target in the fibrosis pathogenesis of Sjögren's syndrome. Mediators Inflamm 2018; 2018: 5;7.
- [65] Wang X, Xin S, Wang Y, et al. MicroRNA-146a-5p enhances T helper 17 cell differentiation via decreasing a disintegrin and metalloprotease 17 level in primary sjögren's syndrome. Bioengineered 2021; 12: 310;24.
- [66] Wells AU. Systemic sclerosis. ERS Monogr 2019; 2019: 90;105.
- [67] Jeljeli M, Riccio LGC, Doridot L, et al. Trained immunity modulates inflammation-induced fibrosis. Nat Commun 2019; 10: 1;15.
- [68] Bhandari R, Ball MS, Martyanov V, et al. Profibrotic Activation of Human Macrophages in Systemic Sclerosis. Arthritis Rheumatol 2020; 72: 116;9.
- [69] Maugeri N, Capobianco A, Rovere-Querini P, et al. Platelet microparticles sustain autophagy-associated activation of neutrophils in systemic sclerosis. Sci Transl Med 2018; 10: eaao3089.
- [70] Bhattacharyya S, Wang W, Morales-Nebreda L, et al. Tenascin-C drives persistence of organ fibrosis. Nat Commun 2016: 7: 1:14.
- [71] Ding W, Pu W, Wang L, et al. Genome-Wide DNA Methylation Analysis in Systemic Sclerosis Reveals Hypomethylation of IFN-Associated Genes in CD4+ and CD8+ T Cells. J Invest Dermatol 2018; 138: 1069;77.
- [72] Kamada R, Yang W, Zhang Y, et al. Interferon stimulation creates chromatin marks and establishes transcriptional memory. Proc Natl Acad Sci U S A 2018; 115: E9162;71.
- [73] Mariotti B, Servaas NH, Rossato M, et al. The long non-coding RNA NRIR drives IFN-Response in monocytes: Implication for systemic sclerosis. Front Immunol 2019; 10: 1;16.
- [74] Servaas NH, Mariotti B, van der Kroef M, et al. Characterization of long non-coding rnas in systemic sclerosis monocytes: A potential role for psmb8-as1 in altered cytokine secretion. Int J Mol Sci 2021; 22: 4365.
- [75] Van Der Kroef M, Castellucci M, Mokry M, et al. Histone modifications underlie monocyte dysregulation in patients with systemic sclerosis, underlining the treatment potential of epigenetic targeting. Ann Rheum Dis 2019; 78: 529;38.
- [76] Moreno-Moral A, Bagnati M, Koturan S, et al. Changes in macrophage transcriptome associate with systemic sclerosis and mediate GSDMA contribution to disease risk. Ann Rheum Dis 2018; 77: 596;601.



Chapter 8

Summary and general discussion

Gout is a form of arthritis with records dating back to thousand of years, the ancient Egyptians being the first to document the symptoms of it (1), being associated with a luxurious lifestyle, often reffered to as the "disease of kings". Today, gout is recognized as a chronic condition, curently affecting cca. 4% of the adult population in Western countries (2,3), requiring long-term management. It is already known that gout is a disease caused by the sustained levels of serum urate which then leads to the formation and deposition of MSU crystals in joints and periarticular structures. In addition, there seems to be a significant overlap that trigger gout flares and the common environmental influences, such as diet (4), medications (5), and stress (6), which affect epigenetic markers like DNA methylation, histone modifications, and non-coding RNA (7–9).

More recently, genome-wide genetic and epigenetic studies have elucidated new pathways involved in the inflammatory processes in gout, including links between genetic factors and epigenetic regulators. Thereafter, our understanding of the molecular mechanisms driving gout has improved by translating genetic associations into precise molecular pathways. Furthermore, genome-wide association studies of gout, assert the significance of epigenomic pathways, indicating that epigenetic reprogramming of innate immune cells by soluble urate heightens their sensitivity to monosodium urate crystals. Moreover, these studies have uncovered multiple loci (eq. SLC2A9, SLC22A12, ABCG2, SLC22A11, SLC17A1, SLC16A9, PDZK1, GCKR, INHBC, HNF4A, MAF), contributing to risk of gout via their implications for hyperuricemia. The genetic factors that contribute to both hyperuricemia and gout mostly include genes that encode transporters, transcriptional factors along with signaling receptors and enzymes, shedding light on the complex genetic landscape that underlies susceptibility to these inflammatory conditions. Such genetic studies shed light not only on the importance and involvement of pathways such as urate metabolism and transportation in the transition from hyperuricemia to clinically manifested gout, but on genes encoding innate immune cytokines and receptors as well. Therefore, the need for further exploration of the GWAS signals into molecular mechanisms and identifying new candidate molecules for therapeutic purposes remain to be elucidated.

In the current thesis, we seeked to explore the variation in gout and urate-associated inflammation caused by genetic differences and epigenetic modifications thereby identifying possible gene variants the transition from hyperuricemia to gout. This chapter summarizes our findings and provide future perspectives for future research.

Advances in our knowledge

In Chapter 2 of this thesis we described a newly identified region IL1RN-IL1F10 in gout, representing well characterized molecules directly connected to IL-1ß induced inflammation. IL-1 family cytokines and their receptors have crucial roles in innate and partly adaptive immunity, therefore their implications in the pathogenesis of gout is highly recognized. Interleukin IL-1\beta is the essential inflammatory cytokine in gout, which is antagonized by IL-1 Receptor antagonist (IL-1Ra), both of which are known to be modulated in gout and urate-driven inflammation. IL-1Ra operates as an acute-phase protein, its expression being strongly induced by LPS, IL-1α and IL-1β, and interferon (IFN)-β. The balance between IL-1 and IL-1Ra is critical for the development of adaptive immune responses and for the regulation of innate immunity. IL-1F10 (IL-38) is another anti-inflammatory member of the IL-1 family that shares 41% sequence homology with IL-1Ra (10) and is known to suppress inflammation. Moreover, variation at the IL1RN-IL1F10 region is believed to have possible roles in the inflammatory aspects of transition from asymptomatic hyperuricemia to gout. Therefore, we showed in two independent cohorts, that the G allele of the gout lead SNP IL1RN rs9973741 variant associates with lower circulating concentrations of IL-1Ra, lower IL-1Ra production in PBMC assays and elevated IL-1β production in PBMCs challenged with C16+MSU crystals. Our data indicated that the genetic signal that associates with gout at IL1RN-IL1F10 region (or locus) revealed to alter the expression of both IL1RN and IL1F10 resulting in modified cytokine profiles, leading to elevated bioactive IL-1\u00ed. Therefore, we propose IL-1Ra as a potent inhibitor of IL-1R1 signaling

In Chapter 3, we aimed to further explore the genetic control of gout inflammatory pathways. In particular, we focused on the effect of the IGF1R rs6598541 urate locus and its association with the inflammatory capacity of mononuclear cells. IGF-1 is an important growth factor with signaling roles in numerous cell types, including monocytes (11), macrophages (12) and chondrocytes (13). The protein binds with high affinity to the Insulin Like Growth Factor 1 Receptor (IGF1R) (14). IGF1R is one of the loci associated with both urate levels and gout susceptibility in GWAS to date, while IGF-1/IGF-1R signaling is known to be implicated in urate control. To investigate this in the context of of gouty inflammation, we tested the gout and urate-associated IGF1R rs6598541 polymorphism for association with the inflammatory capacity of mononuclear cells.

In our approach in assessing the IGF-1/IGF1R signaling in urate priming using primary PBMCs we observed that IGF-1 does not contribute to urate-induced inflammation and blocking IGF1R did not influence the inflammatory responses triggered by urate. The expression of *IGF1R* itself is not modulated *in vitro* by urate in PBMCs from healthy donors nor *in vivo* in PBMCs from gout patients. However, we noticed that gout patients are presented with an increased steady-state mRNA expression of *IGF1R* compared to hyperuricemic individuals or normouricemic controls.

Several studies suggest that *IGF1R* genetic variants are potentially functionally relevant in gout and hyperuricemia, since the genetic control of urate levels and risk of gout at the *IGF1R* locus also colocalizes with genetic control of *IGF1R* expression data (15). Intriguingly, in our study, when assessing freshly isolated PBMCs from patients with gout or controls we did not observe association of *IGF1R* gene expression with rs6598541 SNP. Moreover, the fact that the ex vivo cytokine production of freshly isolated PBMCs challenged with certain stimuli was not associated with our SNP of interest, this might indicate that this SNP may exert relevant functional roles in gouty inflammation, but they may be tissue specific and mononuclear cells do not show IGF1R expression patterns nor inflammatory cytokine production capacity in relationship to this SNP. All in all, this study suggest that a role of IGF1R in gout may be more relevant for the control of urate levels rather than on the inflammatory process.

In Chapter 4, we continued to explore the genetic control of the progression from hyperuricemia to gout. In particular, in this chapter we focus on another newly identified locus from the latest GWAS study published by Major et al. (16), namely IL1R1. It was the first time this locus being associated with gout, none of the goutor urate- related GWAS studies have reported it before. To do so, we studied the proposed locus in two independent cohorts, one is the HINT Cluj-Napoca study groups of gout, hyperuricemia and normouricemic controls, while the other one is the 500FG cohort from the Netherlands. As many studies document that Interleukin IL-1β is the central inflammatory cytokine in gout (17,18) and its effects are mediated through signalling via IL1 receptor type I (IL1R1) (18). Thereafter, the binding of IL-1β to IL1R1 prompts downstream signaling pathways which are then promoting inflammation by producing more cytokines, chemokines, and the recruitment of neutrophils to the site of inflammation (19). In this way, studying genetic variants in inflammatory genes such as IL1R1, seems to be a valid point, as they might be responsbile for the shift from having asymptomatic hyperuricemia to developing gout. In our attempt to explore the importance of the IL1R1 locus when assessing the steady-state mRNA expression levels in individuals with hyperuricemia, gout and normouricemic controls from the HINT Clui-Napoca study group, we could observe that the gene is highly upregulated in PBMCs from hyperuricemic persons

in comparison to normouricemic controls or gout. It is tempting to assume that this locus presents a urate-specific effect, reinforcing the recognition of urate as an important activator of inflammatory pathways. By combining genetic data with, for instance, gene expression data and stimulation-induced cytokine responses helps pinpointing useful potential therapeutic targets. However, we were not able to demonstrate in both of the studied groups the association of the newly proposed gout-related IL1R1 SNP neither with altered gene expression, nor with increased cytokine response, indicating that pleiotropy was more likely than causality. Therefore, the possible mechanism of how the risk variant at this locus could contribute to progression from asymptomatic hyperuricemia to gout pathogenesis needs further assessment.

While we focused the first part of this thesis on associating genetic loci on the pathogenesis from hyperuricemia to gout, in the last two chapters we tried to elucidate one the mechanism involved in urate iduced inflammation. In Chapter 6, we assessed the epigenetic processess associated to urate-mediated hyperresponsiveness. Based on previously cited reports, high urate concentrations excerted a priming effect on PBMCs, where a shift in IL-1B and IL-1Ra production was observed (20). These findings prompted the basis for our aim to study urate and its exercited proinflammatory effects from the epigenetic point of view. To do so, we used complementary approaches aimed to establish the molecular basis of urate-mediated proinflammatory status of human monocytes. In our experimental setup, we were able to demonstrate similar effects of urate both at high (50mg/ dl urate) or at concentrations similar to in vivo hyperuricemia (10 mg/dL), namely modified cytokine levels (higher IL-1β release and a lower IL-1Ra production in response to subsequent stimulation with LPS or LPS+MSU crystals). As a next step, we tested the broad protein methyl-transferase inhibitor methylthioadenosine (5'-S-methyl-5'-thioadenosine, MTA) on an in vivo mice model for gout. With this approach we were able to provide validation for the already described evidence on MTA inhibiting the cytokine production induced by urate in vitro (21). Therefore, MTA was able to inhibit the joint inflammation and histology at 24h post intraarticular injections. This providing evidence that epigenetic modulators could be potential therapeutic agents for the proinflammatory effects associated to urate exposure. However, given the broad effects of MTA, it cannot be excluded that other processes, such as transcription factor methylation, are at play in urate priming. To further decipher the involvement of histone marks in urate priming, two histone marks were analyzed in the setting of urate priming: trimethylation of lysine 4 of histone 3 (H3K4me3) and acetylation of lysine 27 of histone 3 (H3K27ac). For instance, both histone marks have been previously studied in relation to other trained immunity stimuli in several reports (22,23). We were able to confirm the presence of histone modifications in response to high urate exposure, however he validation of H3K27ac or H3K4me3 enrichment in response to lower concentrations of urate or in patients with hyperuricemia would be a useful next step.

Taking the advantage of having access to a sample set of Aotearoa Study with encompassing of individuals with New Zealand Māori ancestry (24) we were able to study the possibility of DNA methylation involvement in the proinflammatory effects associated to hyperuricemia. Whole blood samples of hyperuricemic and normouricemic volunteers was assessed and the analysis revealed 223 differentially methylated probes (difference in DNA methylation of at least 5%). Worth mentioning are the three DMRs which were found to be present at the HLA-G locus, which is known for its immunomodulatory properties across several tissues. Therefore this molecule, might represent a promising target to further study in gout having described evidence that it is having a role in limiting the progression of autoimmune and autoinflammatory disorders. Finally, we suggested that urate alters the epigenetic landscape in selected human monocytes or whole blood of people with hyperuricemia compared to normouricemia.

Lastly, Chapter 7 provides and extensive literature overview on the current knowledge and describes recent findings in several important rheumatic disorders and emphasizes changes in the functional program of innate immune cells that are reminiscent of a trained immune phenotype. Trained immunity has been extensively studied and linked to many inflammatory and rheumatic diseases, for that reason this chapter tried to support the concept that trained immunity may be present in diseases such as gout, rheumatoid arthritis (RA), systemic lupus erythematosus (SLE), primary Sjögren syndrome (pSS) and systemic sclerosis (Ssc). As the main characteristics of innate immune memory are epigenetic modifications, altered cellular metabolism along with higher cytokine production we could provide enough evidence that that these trained immunity features are observed in rheumatic diseases. In addition to this, trained immunity may be an inflammatory process which can predispose individuals with rheumatic diseases to chronic secondary pathologies, such as atherosclerosis and cardiovascular disease risk in patients with RA or SLE, associated comorbidities like metabolic syndrome in gout or risk of lymphoma in pSS. Based on the reviewed data, we propose that Both innate and adaptive immunity can contribute to the complex inflammatory processes that take part in the pathogenesis of these debilitating disorders.

Closing remarks

Gout is a form of arthritis which continues to represent an important health issue worldwide in the middle-aged men and elderly population, eventhough its presence is known since ancient egyptian times. Despite ongoing efforts done to address the issues related to gout, research into pathogenesis is still limited, as a consequence the disease progression and clinical manifestation lacks full understanding. By investigating the genetic profile in relation to gout and hyperuricemia based on the functional association could reveal whether gene variants in key factors might associate with the inflammatory processes previously linked to disease susceptibility and towards disease progression. As the use of anti-IL-1 injectables for the use in patients with gout has not been broadly adopted because the production of them is extremely costly, therefore this poses the need for the development of new, targeted and cost-effective treatment options. Thereafter, our approach to combine genetic data with gene expression data and stimulation-induced cytokine responses helps in identifying clinically useful and targetable gene-phenotype associations. Moreover, such approaches may help in identifying useful therapeutic targets and to optimize treatment for individuals with hyperuricemia and gout based on personalized strategies. Additionally, we propose that urate represent such a danger signal capable of inducing epigenetic reprogramming of the innate immune cells while this mechanism representing a promising therapeutic target in autoinflammatory rheumatic diseases.

References

- 1. Schwartz SA. Disease of distinction. Explore (NY). 2006;2(6):515–9.
- 2. Dehlin M, Jacobsson L, Roddy E. Global epidemiology of gout: prevalence, incidence, treatment patterns and risk factors. Nat Rev Rheumatol. 2020 Jul;16(7):380–90.
- Branco JC, Rodrigues AM, Gouveia N, Eusébio M, Ramiro S, Machado PM, et al. Prevalence of rheumatic and musculoskeletal diseases and their impact on health-related quality of life, physical function and mental health in Portugal: results from EpiReumaPt

 – a national health survey. RMD Open [Internet]. 2016 Jan 1;2(1):e000166. Available from: http://rmdopen.bmj.com/ content/2/1/e000166.abstract
- Choi HK, Atkinson K, Karlson EW, Willett W, Curhan G. Purine-rich foods, dairy and protein intake, and the risk of gout in men. N Engl J Med. 2004 Mar;350(11):1093–103.
- 5. Bruderer S, Bodmer M, Jick SS, Meier CR. Use of diuretics and risk of incident gout: a population-based case-control study. Arthritis Rheumatol (Hoboken, NJ). 2014 Jan;66(1):185–96.
- Helget LN, Mikuls TR. Environmental Triggers of Hyperuricemia and Gout. Rheum Dis Clin North Am. 2022 Nov;48(4):891–906.
- 7. Tseng CC, Liao WT, Wong MC, Chen CJ, Lee SC, Yen JH, et al. Cell lineage-specific methylome and genome alterations in gout. Aging (Albany NY). 2021;13(3):3843–63.
- 8. Qing YF, Zheng JX, Tang YP, Dai F, Dong ZR, Zhang QB. LncRNAs Landscape in the patients of primary gout by microarray analysis. PLoS One. 2021;16(2 February):1–17.
- Badii M, Gaal Ol, Cleophas MC, Klück V, Davar R, Habibi E, et al. Urate-induced epigenetic modifications in myeloid cells. Arthritis Res Ther. 2021;23(1):1–11.
- 10. Bensen JT, Dawson PA, Mychaleckyj JC, Bowden DW. Identification of a novel human cytokine gene in the interleukin gene cluster on chromosome 2q12-14. J Interf Cytokine Res. 2001;21(11):899–904.
- 11. Ge RT, Mo LH, Wu R, Liu JQ, Zhang HP, Liu Z, et al. Insulin-like growth factor-1 endues monocytes with immune suppressive ability to inhibit inflammation in the intestine. Sci Rep. 2015;5:1–7.
- 12. Gow DJ, Sester DP, Hume DA. CSF-1, IGF-1, and the control of postnatal growth and development. J Leukoc Biol. 2010;88(3):475–81.
- 13. Schalkwijk J, Joosten LAB, Van Den Berg WB, Van Wyk JJ, Van Putte LAD. Insulin-like growth factor stimulation of chondrocyte proteoglycan synthesis by human synovial fluid. Arthritis Rheum. 1989;32(1):66–71.
- 14. Rosenzweig SA, Pharmacology M, Therapeutics E. The Continuing Evolution of Insulin-like Growth Factor Signaling [version 1; peer review: 4 approved]. 2020;9:1–10.
- 15. Boocock J, Leask M, Okada Y, Matsuo H, Kawamura Y, Shi Y, et al. Genomic dissection of 43 serum urate-associated loci provides multiple insights into molecular mechanisms of urate control. Hum Mol Genet. 2020;
- Major TJ, Takei R, Matsuo H, Leask MP, Topless RK, Shirai Y, et al. A genome-wide association analysis of 2,622,830 individuals reveals new pathogenic pathways in gout. medRxiv [Internet]. 2022 Jan 1;2022.11.26.22281768. Available from: http://medrxiv.org/content/early/2022/11/29/2022.11.26.22281768.abstract
- 17. Narang RK, Dalbeth N. Pathophysiology of Gout. Semin Nephrol. 2020 Nov;40(6):550–63.
- 18. Klück V, Liu R, Joosten LAB. The role of interleukin-1 family members in hyperuricemia and gout. Jt Bone Spine. 2021;88(2).

- 19. Dinarello CA. How interleukin-1β induces gouty arthritis. Vol. 62, Arthritis and rheumatism. United States; 2010. p. 3140-4.
- 20. Crişan TO, Cleophas MCP, Novakovic B, Erler K, Van De Veerdonk FL, Stunnenberg HG, et al. Uric acid priming in human monocytes is driven by the AKT-PRAS40 autophagy pathway. Proc Natl Acad Sci U S A. 2017;
- 21. Crisan TO, Cleophas MCP, Oosting M, Lemmers H, Toenhake-Dijkstra H, Netea MG, et al. Soluble uric acid primes TLR-induced proinflammatory cytokine production by human primary cells via inhibition of IL-1Ra. Ann Rheum Dis. 2016;
- 22. Saeed S, Quintin J, Kerstens HHD, Rao NA, Aghajanirefah A, Matarese F, et al. Epigenetic programming of monocyte-to-macrophage differentiation and trained innate immunity. Science (80-). 2014;
- 23. Kumar V, Giamarellos-bourboulis EJ, Martens JHA, Rao NA, Aghajanirefah A, Manjeri GR, et al. mTOR/HIF1q-mediated aerobic glycolysis as metabolic basis for trained immunity. Science (80-). 2014;345(6204):1-18.
- 24. Wang Z, Zhao Y, Phipps-Green A, Liu-Bryan R, Ceponis A, Boyle DL, et al. Differential DNA Methylation of Networked Signaling, Transcriptional, Innate and Adaptive Immunity, and Osteoclastogenesis Genes and Pathways in Gout. Arthritis Rheumatol. 2020;



Appendix

Nederlandse samenvatting
English Summary
PhD portfolio
List of publications
Acknowledgements
Curriculum Vitae

Nederlandse samenvatting

Jicht is een veelvoorkomende auto-inflammatoire ziekte, veroorzaakt door MSUkristallen en gekenmerkt door acute of chronische gewrichtsontsteking. Patiënten beschrijven het vaak als een zeer pijnlijke acute gewrichtsontsteking. De pathogenese van jicht begint met hyperurikemie, verhoogde uraatconcentraties in het bloed. De kans op het ontwikkelen van jicht is gecorreleerd met de serum uraatconcentraties op een dosisafhankelijke manier. Hyperurikemie kan worden veroorzaakt door overproductie van uraat, zoals bij purinerijke diëten, myeloproliferatieve ziekten of andere aandoeningen die gepaard gaan met een hoge cellulaire omzet, evenals verminderde excretie zoals bij nierfunctiestoornissen of gebruik van bepaalde diuretica. Aangeboren afweercellen, voornamelijk macrofagen en monocyten, herkennen MSU-kristallen wat leidt tot de productie van IL-1β door de activering van het NLRP3-inflammasoom, een intracellulaire sensor voor gevaarsignalen. Dit veroorzaakt de ontstekingsreactie die leidt tot een acute gewrichtsontsteking. De huidige behandelingsstrategieën voor jicht volgen een "treat to target"-benadering met uraatverlagende therapie, gericht op het oplossen van MSU-kristallen, met een therapeutische streefwaarde van serum uraatconcentraties onder 0.36 mmol/l.

Recente studies suggereren dat verhoogd uraat een vorm van immuungeheugen in aangeboren afweercellen kan induceren, bekend als getrainde immuniteit. Getrainde immuniteit verwijst naar het vermogen van aangeboren afweercellen, zoals monocyten en macrofagen, om een eerdere blootstelling aan een stimulus zoals hyperurikemie te "onthouden" en bij hernieuwde blootstelling agressiever te reageren. Deze getrainde immuniteit omvat epigenetische en metabolische herprogrammering van aangeboren afweercellen, wat leidt tot een verhoogde ontstekingsreactie die in de tijd kan aanhouden. Dit kan bijdragen aan chronische ontsteking bij aandoeningen zoals asymptomatische hyperurikemie en jicht. Genetische factoren spelen ook een belangrijke rol in de variatie van serum uraat en de inflammatoire toestand van het individu. Genome Wide Association (GWAS)studies hebben het belang aangetoond van uraatexcretie als een mechanisme waarmee het lichaam probeert de serum uraat te beheersen, waarbij de darmen, nieren en lever als belangrijke regelcentra fungeren.

Ondanks de vooruitgang in onderzoek blijft de vraag waarom sommige individuen nooit jicht ontwikkelen, ondanks verhoogde uraatconcentraties, een aanhoudend raadsel in dit veld. De complexiteit van jicht lijkt beïnvloed te worden door een combinatie van genetische en omgevingsfactoren en de interactie met tussen deze twee.

Het doel van deze thesis is daarom om de variatie van inflammatoire reacties bij jicht en hyperurikemie te onderzoeken. Daarnaast hebben we mechanismen onderzocht die bijdragen aan ontsteking geïnduceerd door hoge uraatconcentraties.

Na een algemene introductie hebben we in **Hoofdstuk 2** een nieuw jichtgerelateerd gebied beschreven in het DNA, IL1RN (coderend voor IL-1Ra) -IL1F10 (ook bekend als IL-38), bestaande uit goed gekarakteriseerde moleculen die rechtstreeks verband houden met IL-1β-geïnduceerde ontsteking. Cytokinen uit de IL-1-familie en hun receptoren spelen cruciale rollen in de aangeboren en gedeeltelijk in de adaptieve immuniteit, daarom zijn hun implicaties in de pathogenese van jicht algemeen erkend. Interleukine (IL)-1β is de essentiële inflammatoire cytokine bij jicht, geantagoneerd door de IL-1-receptorantagonist (IL-1Ra). De genetische variatie in het IL1RN-IL1F10-gebied speelt mogelijk een rol in de inflammatoire aspecten van de overgang van asymptomatische hyperurikemie naar jicht. We hebben in twee onafhankelijke cohorten aangetoond dat het G-allel van de single nucleotide polymorfism (SNP) IL1RN rs9973741, geassocieerd met jicht, verband houdt met lagere circulerende concentraties van IL-1Ra, verminderde IL-1Ra-productie in menselijke perifere mononucleaire bloedcellen PBMC-testen en verhoogde IL-1βproductie in PBMCs blootgesteld aan palmitaat met MSU-kristallen (jichtrelevante costimulatiecocktail voor TLR2-binding en NLRP3-inflammasome-activering). We vonden dat het met jicht geassocieerde genetische signaal in de IL1RN-IL1F10regio de expressie van beide genen, IL1RN en IL1F10, veranderde, wat leidde tot andere cytokineprofielen en een toename van bioactieve IL-1\u00e3.

In Hoofdstuk 3, hebben we de genetische regulatie van jichtgerelateerde inflammatie verder verkend. We richtten ons op het effect van het IGF1R rs6598541gebied en de associatie ervan met de inflammatoire capaciteit van mononucleaire cellen. IGF-1 is een belangrijke groeifactor met een signaalfunctie in verschillende celtypen, waaronder monocyten, macrofagen en chondrocyten. Het IGF-1 eiwit bindt met hoge affiniteit aan de insuline-achtige groeifactor 1-receptor (IGF1R). IGF1R is een van de loci die tot nu toe geassocieerd is met zowel serum uraat als jicht in GWAS. Het is bekend is IGF-1/IGF-1R-signaaltransductie betrokken is bij uraatcontrole. Om te onderzoeken of IGF1R ook een rol speelt in de context van jichtontsteking, testten we de IGF1R rs6598541-polymorfisme op de associatie met de inflammatoire capaciteit van mononucleaire cellen. We observeerden we dat IGF-1 niet bijdroeg aan uraat-geïnduceerde ontsteking en dat IGF1R-blokkade geen invloed had op door uraat-geïnduceerde ontstekingsreacties. IGF1R-expressie zelf werd in vitro niet gemoduleerd door uraat in PBMCs van gezonde donoren, noch in vivo in PBMCs van jichtpatiënten. We observeerden echter wel dat jichtpatiënten een verhoogde IGF1R-mRNA-expressie vertoonden in steady-state vergeleken met hyperurikemische individuen of normourikemische controles. Dit onderzoek suggereert daarom dat IGF1R een grotere rol speelt bij regulatie van serum uraat dan bij het ontstekingsproces in jicht.

In **Hoofdstuk 4**, richtten we ons op een andere nieuw geïdentificeerde locus uit de GWAS-studie gepubliceerd, namelijk IL1R1. Dit was de eerste keer dat deze locus werd geassocieerd met jicht. We onderzochten deze locus in twee onafhankelijke cohorten. IL-1ß is de centrale inflammatoire cytokine is bij jicht, en de effecten ervan worden gemedieerd via signalering via de type I IL-1-receptor (IL-1R1). Het combineren van genetische gegevens met bijvoorbeeld genexpressiegegevens en cytokineresponsen, helpt bij het identificeren van nuttige potentiële therapeutische doelen. We konden echter in beide onderzochte groepen geen associatie aantonen tussen de IL1R1 SNP en gewijzigde genexpressie of verhoogde cytokinerespons.

In **Hoofdstuk 5**, leveren we bewijs voor de ontsteking door serum uraat in vivo. We beschrijven een sterk en breed ontstekingpatroon die geassocieerd is met asymptomatische hyperurikemie. Deze correleerde met de waargenomen verschillen bij patiënten met jicht en hyperurikemie vergeleken met jichtpatiënten met normaal serum uraat. De door ons geïdentificeerde eiwitten werden ook geassocieerd met klinisch relevante fenotypen bij jicht, zoals de aanwezigheid en ernst van aanvallen of tophi. Belangrijk is dat de verhoogde expressie van deze eiwitten gedeeltelijk omkeerbaar is door uraatverlagende therapie, wat pleit voor het causale effect van uraat in de verschillen die waargenomen zijn voor deze eiwitten bij hyperurikemische personen. Onze bevindingen vormen een basis voor toekomstig functioneel onderzoek om de mechanistische relaties van deze inflammatoire eiwitten bij jicht en hyperurikemie te onderzoeken, hun potentieel als klinisch relevante biomarkers van de ziekte te verkennen en therapieën te ontwikkelen die gericht zijn op asymptomatische hyperurikemie als een strategie om cardiometabole ziekten te voorkomen.

In **Hoofdstuk 6**, hebben we datasets gegenereerd die epigenetisch en functionele immunologische experimenten omvatten om mogelijke belangrijke mechanismen te onderzoeken die betrokken zijn bij de priming van uraat op myeloïde cellen. Op basis van aanvullende methoden tonen we aan dat epigenetische veranderingen waarschijnlijk een rol spelen bij het mediëren van de blijvende effecten van uraatblootstelling op aangeboren afweercellen. Onze studie toont aan dat hoog serum uraat de cytokineproductiecapaciteit van primaire PBMCs in vitro blijvend kunnen veranderen, wat leidt tot een verhoogde productie van IL-1β en IL-6 en

*

minder IL-1 receptor antagonist (IL-1Ra). Inhibitie van uricase (een enzym dat uraat afbreekt) bij muizen leidde tot hogere ontstekingsscores na intra-articulaire injectie van MSU-kristallen en palmitaat, en dit effect werd omgekeerd door remming van methyltransferase. We presenteren hier bewijs dat histonmodificaties (H3K4me3 of H3K27ac) en DNA-methylering verschillen als reactie op hoge uraat concentraties. Verschillen in epigenetische regulatie geven een nieuw inzicht en bieden potentieel een mogelijkheid tot interventie in uraat-geïnduceerde ontsteking en de progressie van hyperurikemie naar jicht.

Tot slot biedt **Hoofdstuk 7** een uitgebreid overzicht van de wetenschappelijke literatuur over de huidige kennis in verschillende belangrijke reumatische aandoeningen wat betreft getrainde immuniteit in afweercellen van het aangeboren immuunsysteem. Getrainde immuniteit is uitgebreid bestudeerd en in verband gebracht met vele inflammatoire en reumatische ziekten, daarom probeert dit hoofdstuk het concept te ondersteunen dat getrainde immuniteit aanwezig kan zijn in ziekten zoals jicht, reumatoïde artritis (RA), systemische lupus erythematosus (SLE), primair Sjögren-syndroom (pSS) en systemische sclerose (SSc). We vonden de belangrijkste kenmerken van getrainde immuniteit bij verschillende reumatische ziekten: epigenetische veranderingen, veranderde cellulaire stofwisseling en verhoogde cytokineproductie zijn. Daarnaast kan getrainde immuniteit een ontstekingsproces zijn dat personen met reumatische aandoeningen vatbaar maakt voor secundaire chronische ziekten, zoals atherosclerose en hart- en vaatziekten bij patiënten met RA of SLE, het metabool syndroom bij jicht of een lymfoom bij pSS. Op basis van de gevonden literatuur stellen we voor dat zowel het aangeboren als het adaptieve immuunsysteem bijdragen aan de complexe ontstekingsprocessen die een rol spelen in de pathogenese van reumatische aandoeningen.

English Summary

Gout is a common auto-inflammatory disease caused by the deposition of MSU crystals and characterized by acute or chronic inflammation and joint involvement. Patients often describe it as a very painful acute inflammatory arthritis. The pathogenesis of gout begins with hyperuricemia, and the likelihood of developing gout is correlated with serum urate concentrations in a dose-dependent manner. Hyperuricemia can be caused by factors that promote the overproduction of uric acid, such as purine-rich diets, myeloproliferative diseases, or other conditions associated with high cellular turnover, as well as excretion-related defects such as kidney dysfunction or certain diuretics. Innate immune cells, primarily macrophages and monocytes, recognize MSU crystals as a damage-associated molecular pattern (DAMP), triggering an inflammatory cascade that leads to IL-1β production through activation of the NLRP3 inflammasome, an intracellular danger signal sensor. Current treatment strategies for gout follow a "treat to target" approach with urate-lowering therapy aimed at dissolving MSU crystals, with a therapeutic target of serum urate concentrations below 0,36 mmol/l.

Recent studies suggest that uric acid may induce a form of immune memory in innate immune cells known as **trained immunity**. Trained immunity refers to the ability of innate immune cells, such as monocytes and macrophages, to "remember" a previous exposure to a stimulus like uric acid and respond more aggressively upon re-exposure. This trained immunity involves **epigenetic and metabolic reprogramming** of innate immune cells, leading to a heightened inflammatory response that can persist over time. This can contribute to chronic inflammation in conditions such as asymptomatic hyperuricemia and gout.

Genetic factors also play an important role in the variation of serum urate levels and the individual's inflammatory state. Genome Wide Association studies (GWAS) have demonstrated the importance of urate excretion as a mechanism by which the body attempts to control serum urate concentrations, with the intestines, kidneys, and liver acting as major regulatory centers.

Despite research progress, the question of why some individuals never develop gout despite elevated urate concentrations remains a persistent puzzle in this field. Although significant progress has been made in understanding the pathophysiology of gout, the complexity of its manifestation remains difficult to fully grasp. The complexity of gout appears to be influenced by a combination of genetic and environmental factors, and the interaction with lifestyle and environmental factors further deepens the complexity of this disease.

The aim of this thesis is therefore to investigate the variation in inflammatory responses in gout and hyperuricemia associated genetic and epigenetic changes. Additionally, we have explored mechanisms that could contribute to inflammation induced by high urate concentrations.

After a general introduction, in Chapter 2 we described a new gout-related region, IL1RN (encoding for IL-1Ra) -IL1F10 (also known as IL38), consisting of wellcharacterized molecules directly related to IL-1β-induced inflammation. Cytokines from the IL-1 family and their receptors play crucial roles in innate and partially in adaptive immunity, and therefore their implications in the pathogenesis of gout are widely recognized. Interleukin (IL)-1β is the key inflammatory cytokine in gout, antagonized by the IL-1 receptor antagonist (IL-1Ra), both known for their modulation in gout and urate-induced inflammation. The variation in the IL1RN-IL1F10 region may play a role in the inflammatory aspects of the transition from asymptomatic hyperuricemia to gout. In two independent cohorts, we demonstrated that the G allele of the SNP (single nucleotide polymorphism) IL1RN rs9973741, associated with gout, is linked to lower circulating concentrations of IL-1Ra, reduced IL-1Ra production in human peripheral blood mononuclear cells (PBMC) assays, and increased IL-1ß production in PBMCs exposed to palmitate with MSU crystals (C16.0+MSU) (gout relevant costimulation cocktail for TLR2 binding and NLRP3 inflammasome activation). Our data indicated that the gout-associated genetic signal in the IL1RN-IL1F10 region altered the expression of both genes, IL1RN and IL1F10, leading to altered cytokine profiles and an increase in bioactive IL-1\u00ed.

In **Chapter 3**, we further explored the genetic regulation of gout-related inflammatory pathways. We focused on the effect of the IGF1R rs6598541 region and its association with the inflammatory capacity of mononuclear cells. IGF-1 is an important growth factor with signaling roles in various cell types, including monocytes, macrophages, and chondrocytes. The protein binds with high affinity to the insulin-like growth factor 1 receptor (IGF1R). IGF1R is one of the loci associated with both urate levels and susceptibility to gout in GWAS, while IGF-1/IGF1R signaling is known to be involved in urate control. To investigate this in the context of gout inflammation, we tested the gout- and urate-associated IGF1R rs6598541 polymorphism for association with the inflammatory capacity of mononuclear cells. In our approach to assess IGF-1/IGF1R signaling in urate priming using primary PBMCs, we observed that IGF-1 did not contribute to urate-induced inflammation and that IGF1R blockade had no effect on urate-induced inflammatory responses. IGF1R expression itself was not modulated by urate *in vitro* in PBMCs from healthy donors, nor *in vivo* in PBMCs from gout patients. However, we did observe that

gout patients had increased IGF1R mRNA expression in steady state compared to hyperuricemic individuals or normouricemic controls. This research therefore suggests that the role of IGF1R in gout may be more relevant to the management of serum urate concentrations than to the inflammatory process.

In **Chapter 4**, we focused on another newly identified locus from the latest GWAS study published by Major et al. (16), namely *IL1R1*. This was the first time that this locus was associated with gout, as none of the previous GWAS studies related to gout or urate had identified it. To do this, we examined the proposed locus in two independent cohorts. Many studies document that IL-1 β is the central inflammatory cytokine in gout, and that its effects are mediated through signaling via the type I IL-1 receptor (IL-1R1). Combining genetic data with, for example, gene expression data and cytokine responses induced by stimulation helps in identifying useful potential therapeutic targets. However, we were unable to demonstrate an association between the newly proposed gout-associated *IL1R1* SNP and altered gene expression or increased cytokine response in either of the studied groups.

In **Chapter 5**, we provide evidence for the inflammatory consequences of urate exposure *in vivo*. We describe a strong and broad inflammatory signature associated with asymptomatic hyperuricemia, which correlated with the observed differences in gout patients with hyperuricemia compared to normouricemic gout. The proteins we identified were also associated with clinically relevant phenotypes in gout, such as the presence and severity of attacks or tophi. Importantly, the increased expression of these proteins is partially reversible with urate-lowering therapy, supporting the causal effect of urate in the significant enrichment observed for these proteins in hyperuricemic individuals. Our findings form a basis for future functional research to explore the mechanistic relationships of these inflammatory proteins in gout and hyperuricemia, explore their potential as clinically relevant biomarkers of the disease, and develop therapies targeting asymptomatic hyperuricemia as a strategy to prevent cardiometabolic diseases.

In **Chapter 6**, we generated datasets involving epigenomic and functional immunological experiments to investigate possible major mechanisms involved in urate priming of myeloid cells. Based on complementary methods, we show that epigenetic changes are likely to play a role in mediating the lasting effects of urate exposure on innate immune cells. Our study demonstrates that high urate levels can persistently alter the cytokine production capacity of primary PBMCs *in vitro*, leading to increased production of IL-1beta and IL-6 and decreased levels of the IL-1 receptor antagonist (IL-1Ra). Inhibition of uricase (an enzyme in mammals,

facilitating the efficient elimination of uric acid) in mice led to higher inflammation scores following intra-articular injection of MSU crystals and palmitate, and this effect was reversed by methyltransferase inhibition. We present evidence here that histone modifications (H3K4me3 or H3K27ac) and DNA methylation differ in response to high urate exposure, and we provide possible candidates for differentially regulated targets. Differences in epigenetic regulation may provide new insight and intervention possibilities in urate-dependent inflammatory responses and the progression from hyperuricemia to gout.

Finally, Chapter 7 provides a comprehensive review of the scientific literature on current knowledge and describes recent findings in several major rheumatic disorders, highlighting changes in the functional program of innate immune cells reminiscent of a trained immunity phenotype. Trained immunity has been extensively studied and linked to many inflammatory and rheumatic diseases, and this chapter therefore attempts to support the concept that trained immunity may be present in diseases such as gout, rheumatoid arthritis (RA), systemic lupus erythematosus (SLE), primary Sjögren's syndrome (pSS), and systemic sclerosis (SSc). Since the key features of innate immune memory are epigenetic changes, altered cellular metabolism, and increased cytokine production, we were able to provide sufficient evidence that these features of trained immunity are observed in rheumatic diseases. Moreover, trained immunity may be an inflammatory process that predisposes individuals with rheumatic diseases to secondary chronic pathologies, such as atherosclerosis and the risk of cardiovascular diseases in patients with RA or SLE, associated comorbidities such as metabolic syndrome in gout, or the risk of lymphoma in pSS. Based on the reviewed data, we propose that both innate and adaptive immunity may contribute to the complex inflammatory processes involved in the pathogenesis of these debilitating disorders.

Research Data Management

The data obtained during this PhD are archived according to Findable, Accesible, Interoperable and Reusable (FAIR) principles Raw and processed data for Chapters 2, 3, 4, 5 and 6 are stored on the private server of the department of Medical Genetics University of Pharmacy and Medicine "Iuliu Hatieganu" Cluj-Napoca.

The human studies described in **Chapter 2, 3, 4, 5, 6** were conducted according to the principles of the declaration of Helsinki and were approved by the Medical Ethics Committee of the University of Pharmacy and Medicine "Iuliu Hatieganu" Clui-Napoca. All participants gave written informed consent upon enrolling in the studies. The study in Chapter 2, 3, 4, 5 and 6 was approved by the Ethics Committee of "Iuliu Hatieganu" University of Medicine and Pharmacy (approval number 425/2016), the Medical Ethics Committee of the Radboud University Medical Centre (approval numbers: nr. 42561.091.12) and by the New Zealand Lower South Health and Disability Ethics Committee (MEC/05/10/130).

Data for **Chapters 2, 3, 4, 5 and 6** was obtained through laboratory experiments involving pseudonymized human materials.

The animal study in **Chapter 6**, was approved by The Institutional Animal Care and Use Committees of the University of Colorado Denver, Aurora, CO (protocol #0035).

Data generated in this thesis are part of published articles and files are available upon request.

PhD portfolio of Ildikó-Orsolya Gaál

Department: Internal Medicine PhD period: 31/08/2019 - 25/03/2025 **PhD Supervisor(s):** Prof. L.A.B. Joosten, M.G. Netea

PhD Co-supervisor(s): Dr T.O. Crişan

Training activities	Hours
Courses	
Radboudumc - Scientific integrity (2024)	20.00
Medical Biotechnology UMF "Iuliu Hatieganu" Cluj-Napoca	40.00
Evidence-based medicine UMF "Iuliu Hatieganu" Cluj-Napoca	8.00
Poster communication - rules, solutions UMF "Iuliu Hatieganu" Cluj-Napoca	4.00
Scientific research methodology UMF "Iuliu Hatieganu" Cluj-Napoca	80.00
Ethics in scientific research UMF "Iuliu Hatieganu" Cluj-Napoca	20.00
European legislation in research UMF "Iuliu Hatieganu" Cluj-Napoca	16.00
 Publication norms and ethics of scientific publishing UMF "Iuliu Hatieganu" Cluj-Napoca 	16.00
Scientific documentation UMF "Iuliu Hatieganu" Cluj-Napoca	16.00
Grant writing and management UMF "Iuliu Hatieganu" Cluj-Napoca	16.00
 Power point presentations UMF "Iuliu Hatieganu" Cluj-Napoca 	8.00
Handling of laboratory animals used in biomedical	32.00
research UMF "Iuliu Hatieganu" Cluj-Napoca	
 Theoretical foundations of in vitro and in vivo experiments - cell 	8.00
cultures and organoids UMF "Iuliu Hatieganu" Cluj-Napoca	
 Cell cultures in experimental medicine UMF "Iuliu Hatieganu" Cluj-Napoca 	8.00
Functional genomics in oncology UMF "Iuliu Hatieganu" Cluj-Napoca	100.00
Conferences	
 New Frontiers in Innate Immunity and Inflammation (2018) * 	24.00
European Crystal Network Workshop -Paris (2019) *	16.00
Gout, Hyperuricemia and Crystal-associated Disease	16.00
Network Conference- ATLANTA (2019) *	
 2019 American College of Rheumatology/The Association of 	40.00
Rheumatology Professionals (ACR/ARP) Annual Meeting (2019) *	
European Crystal Network Workshop -Paris (2020) *	16.00
Gout, Hyperuricemia and Crystal-associated Disease	16.00
Network Conference - Washington USA (2022) ^	
European Crystal Network Workshop -Paris (2023) *	16.00
Gout, Hyperuricemia and Crystal-associated Disease	
Network Conference - San Diego USA (2023) ^	16.00
European Crystal Network Workshop -Paris (2023)	16.00
Gout, Hyperuricemia and Crystal-associated Disease	16.00
Network Conference – Washington USA (2024)	
Other	
• Cytokine meeting (2019 – 2024, weekly) ^	150.00
Teaching activities	
Lecturing Workshop trainer (2019)	6.00
Workshop trainer (2018)	
Total	738.00

^{^:} oral presentation

^{*:} poster presentation

List of publications

- 1: Gaal Ol, Leask M. Nica V. Cabău G. Badii M. Hotea I. de Graaf DM, Zhang Z. Li Y. Pamfil C. Rednic S. Merriman TR, Crisan TO, Joosten LAB, Gout-associated SNP at the IL1RN-IL1F10 region is associated with altered cytokine production in PBMCs of patients with gout and controls. Arthritis Res Ther. 2024 Nov 20;26(1):205. doi: 10.1186/s13075-024-03436-0. PMID: 39568029.
- 2: Gaal OI, Liu R, Marginean D, Badii M, Cabău G, Hotea I, Nica V, Colcear D; HINT Consortium; Pamfil C, Merriman TR, Rednic S, Popp RA, Crisan TO, Joosten LAB. GWAS-identified hyperuricemiaassociated IGF1R variant rs6598541 has a limited role in urate mediated inflammation in human mononuclear cells. Sci Rep. 2024 Feb 12;14(1):3565. doi: 10.1038/s41598-024-53209-7. PMID: 38347000.
- 3: Badii M*, Gaal O*, Popp RA, Crişan TO, Joosten LAB. Trained immunity and inflammation in rheumatic diseases. Joint Bone Spine. 2022 Jul;89(4):105364. doi: 10.1016/j.jbspin.2022.105364. Epub 2022 Feb 24. PMID: 35219890.
- 4: Badii M*, Gaal OI*, Cleophas MC, Klück V, Davar R, Habibi E, Keating ST, Novakovic B, Helsen MM, Dalbeth N, Stamp LK, Macartney-Coxson D, Phipps-Green AJ, Stunnenberg HG, Dinarello CA, Merriman TR, Netea MG, Crisan TO, Joosten LAB. Urate-induced epigenetic modifications in myeloid cells. Arthritis Res Ther. 2021 Jul 28;23(1):202. doi: 10.1186/s13075-021-02580-1. PMID: 34321071.
- 5: Cabău G, Gaal O, Badii M, Nica V, Mirea AM, Hotea I; HINT-consortium; Pamfil C, Popp RA, Netea MG, Rednic S, Crisan TO, Joosten LAB. Hyperuricemia remodels the serum proteome toward a higher inflammatory state. iScience. 2023 Sep14;26(10):107909. doi: 10.1016/j.isci.2023.107909. PMID: 37810213.
- 6: Major TJ, Takei R, Matsuo H, Leask MP, Sumpter NA, Topless RK, Shirai Y, Wang W, Cadzow MJ, Phipps-Green AJ, Li Z, Ji A, Merriman ME, Morice E, Kelley EE, Wei WH, McCormick SPA, Bixley MJ, Reynolds RJ, Saag KG, Fadason T, Golovina E, O'Sullivan JM, Stamp LK, Dalbeth N, Abhishek A, Doherty M, Roddy E, Jacobsson LTH, Kapetanovic MC, Melander O, Andrés M, Pérez-Ruiz F, Torres RJ, Radstake T, Jansen TL, Janssen M, Joosten LAB, Liu R, Gaal OI, Crişan TO, Rednic S, Kurreeman F, Huizinga TWJ, Toes R, Lioté F, Richette P, Bardin T, Ea HK, Pascart T, McCarthy GM, Helbert L, Stibůrková B, Tausche AK, Uhlig T, Vitart V, Boutin TS, Hayward C, Riches PL, Ralston SH, Campbell A, MacDonald TM; FAST Study Group; Nakayama A, Takada T, Nakatochi M, Shimizu S, Kawamura Y, Toyoda Y, Nakaoka H, Yamamoto K, Matsuo K, Shinomiya N, Ichida K; Japan Gout Genomics Consortium; Lee C; Asia Pacific Gout Consortium; Bradbury LA, Brown MA, Robinson PC, Buchanan RRC, Hill CL, Lester S, Smith MD, Rischmueller M, Choi HK, Stahl EA, Miner JN, Solomon DH, Cui J, Giacomini KM, Brackman DJ, Jorgenson EM; GlobalGout Genetics Consortium; Liu H, Susztak K; 23andMe Research Team; Shringarpure S, So A, Okada Y, Li C, Shi Y, Merriman TR. A genome-wide association analysis reveals new pathogenic pathways in gout. Nat Genet. 2024 Nov;56(11):2392-2406. doi: 10.1038/s41588-024-01921-5. Epub 2024 Oct 15. Erratum in: Nat Genet. 2024 Nov;56(11):2577. doi: 10.1038/s41588-024-02017-w. PMID: 39406924.

- 7: Badii M, Klück V, Gaal O, Cabău G, Hotea I, Nica V, Mirea AM, Bojan A, Zdrenghea M; HINT Consortium; Novakovic B, Merriman TR, Liu Z, Li Y, Xu CJ, Pamfil C, Rednic S, Popp RA, Crişan TO, Joosten LAB. Regulation of SOCS3-STAT3 in urate-induced cytokine production in human myeloid cells. Joint Bone Spine. 2024 May;91(3):105698. doi: 10.1016/j.jbspin.2024.105698. Epub 2024 Feb 1. PMID:38309518.
- 8: Badii M, Nica V, Straton AR, Kischkel B, Gaal O, Cabău G, Klück V, Hotea I; HINT Consortium; Novakovic B, Pamfil C, Rednic S, Netea MG, Popp RA, Joosten LAB, Crişan TO. Downregulation of type I interferon signalling pathway by urate in primary human PBMCs. Immunology, 2024 Oct 1. doi: 10.1111/imm.13858. Epub ahead of print. PMID: 39354748.
- 9: Cruceriu D, Balacescu L, Baldasici O, Gaal OI, Balacescu O, Russom A, Irimia D, Tudoran O. Gene expression-phenotype association study reveals the dual role of TNF-α/TNFR1 signaling axis in confined breast cancer cell migration. Life Sci. 2024 Oct 1;354:122982. doi: 10.1016/j. lfs.2024.122982. Epub 2024 Aug 14. PMID: 39151886.
- 10: Röring RJ, Li W, Liu R, Bruno M, Zhang B, Debisarun PA, Gaal O, Badii M, Klück V, Moorlag SJCFM, van de Veerdonk F, Li Y, Joosten LAB, Netea MG. Epigenetic, transcriptional, and functional characterization of myeloid cells in familial Mediterranean fever. iScience. 2024 Feb 29;27(4):109356. doi:10.1016/j.isci.2024.109356. PMID: 38510149.
- 11: Cabău G, Badii M, Mirea AM, Gaal OI, van Emst L, Popp RA, Crişan TO, Joosten LAB. Long-Lasting Enhanced Cytokine Responses Following SARS-CoV-2 BNT162b2 mRNA Vaccination. Vaccines (Basel). 2024 Jul 3;12(7):736. doi: 10.3390/vaccines12070736. PMID: 39066374.
- 12: de Graaf DM, Teufel LU, de Nooijer AH, van Gammeren AJ, Ermens AAM, Gaál IO, Crişan TO, van de Veerdonk FL, Netea MG, Dinarello CA, Joosten LAB, Arts RJW; Radboudumc Center for Infectious Diseases COVID-19 Study Group. Exploratory analysis of interleukin-38 in hospitalized COVID-19 patients. Immun Inflamm Dis. 2022 Nov;10(11):e712. doi: 10.1002/iid3.712. PMID: 36301025.
- 13: Szabo I, Badii M, Gaál IO, Szabo R, Popp RA, Joosten LAB, Crişan TO, Rednic S. Enhanced Innate and Acquired Immune Responses in Systemic Sclerosis Primary Peripheral Blood Mononuclear Cells (PBMCs). Int J Mol Sci. 2023 Sep 22;24(19):14438. doi: 10.3390/ijms241914438. PMID: 37833885.
- 14: Szabo I, Badii M, Gaál IO, Szabo R, Sîrbe C, Humiţă O, Joosten LAB, Crişan TO, Rednic S. Immune Profiling of Patients with Systemic Sclerosis through Targeted Proteomic Analysis. Int J Mol Sci. 2023 Dec 18;24(24):17601. doi: 10.3390/ijms242417601. PMID: 38139427.

Acknowledgements

"If you want to go fast, go alone. If you want to go far, go together."

This timeless wisdom perfectly captures the journey I have undertaken during this unique experience. I am deeply grateful and profoundly humbled by the many individuals who have walked alongside me, offering their guidance, support, and encouragement. The list is long and cherished—comprising supervisors, colleagues, friends, and family—each playing a vital role in helping me navigate this path and achieve more than I could have ever imagined alone.

First and foremost, I would like to thank my PhD supervisors, prof. Leo Joosten and prof. Mihai Netea.

Leo, your expertise and insights have not only shaped my research but have also profoundly influenced my professional development. Thank you for being there with insightful advice, encouragement whenever I needed it. Your words, "Veeery nice," this always created a very positive and collaborative atmosphere for discussing and improving our research. Thank you for helping me becoming the scientist I am today.

Mihai, I highly value your enthusiastic perspective on research. Your presence makes every reserach team a very motivating place to do reserach. Thank you for providing such a wealth of knowledge.

Dear Tania, thank you for your endless support, guidance and mentorship during my PhD. You truly shaped my professional career in the best ways possible. I am grateful for many conversations with you after which I felt confident in my abilities. You are a great scientific role model that I look up to \approx.

The chapters of this thesis could not have existed without collaborative work, therefore thank you to my collaborators, Tony and Megan for their contribution and work as well as the pleasant collaboration.

Thank you to all my lab mates especially Georgiana and Medeea — who have supported me throughout the years. Thank you for all the moments of shared struggle and success, the nice conference trips and all the late Elisa parties. I will always cherish the memories of celebrating my 30th birthday together with you in New York, especially waking up to your surprise birthday cake 👛 . What a memorable day!

Valentin, thank you for the many transcriptome analysis \bigcirc and SNP arrays....also, It was always fun talking about life's big problems.

Anca, we shared not just many lab hours and scientific meetings but some memorable airbnb rooms while going to conferences abroad...hehe : Cheers to Sonic 1.

To my friends who always supported me. Thank you for being my unpaid therapist. I am so glad you exist!

To my dear parents, Csabi and Gyöngyi, for their infinite love, support and constant belief in me. Your encouragement has been my foundation through every challenge and triumph. Köszönöm, hogy vagytok nekem 💚. Erőt adtok, hogy az álmaimat követni meriem.

Last but certainly not least, to my husband, Atti. Your belief in me and your partnership in this journey called life are more appreciated than words can express. You and me, my favorite team <3. Atti, nélküled nemcsak nehezebb, de sokkal unalmasabb is lett volna ez az út.

To the \rightarrow and back.

Curriculum Vitae

Ildikó Orsolya Gaál was born in 1992, Zalau, Romania. She embarked on her academic journey at the University of Agricultural Sciences and Veterinary Medicine of Cluj-Napoca. During her undergraduate years, she cultivated a deep interest in molecular biology and genetics, which flourished during her Erasmus exchange program at the Georg August University of Göttingen.

It was there that she had the transformative opportunity to work independently on her first research project, applying Next-Generation Sequencing (NGS) techniques. This experience not only fined her technical skills but also instilled in her the confidence and curiosity to pursue innovative scientific questions. Her time in Göttingen was pivotal, laying the foundation for her future in research.

Motivated by her growing enthusiasm for genomics, she returned to Cluj-Napoca and joined her internship at the Research Center for Functional Genomics, Biomedicine, and Translational Medicine at the Iuliu Hatieganu University of Medicine and Pharmacy. This environment of discovery inspired her to take the next step in her career: pursuing a PhD focused on her own research project related to functional genetic assessment in order to understand gout pathophysiology.

Now she continues to explore the complex world of genetics driven by a commitment to unraveling complex biological mechanisms and contributing to the advancement of genomic medicine.

